

**GEOCHEMICAL CHARACTERIZATION OF SUBSURFACE
SEDIMENTS IN THE NETHERLANDS**

Promotor:

Prof. S.B. Kroonenberg

Hoogleraar in de geologie aan de Faculteit voor Technische Aardwetenschappen van de Technische Universiteit Delft

Co-Promotoren:

Dr G.Th. Klaver

Nederlands Instituut voor Toegepaste Geowetenschappen (NITG- TNO) in Haarlem

Dr. Ir. A. Veldkamp

Universitair Docent Geomorfologie aan de Vakgroep Bodemkunde en Geologie van de Landbouw Universiteit Wageningen

1998-1999

GEOCHEMICAL CHARACTERIZATION OF SUBSURFACE SEDIMENTS IN THE NETHERLANDS

D.J. HUISMAN

Proefschrift
ter verkrijging van de graad van
doctor in de landbouw- en milieuwetenschappen,
op gezag van de rector magnificus,
Dr. C.M. Karssen,
in het openbaar te verdedigen
op woensdag 25 maart 1998
des namiddags te half twee in de Aula
van de Landbouwuniversiteit te Wageningen

WU 953830

BIBLIOTHEEK
LANDBOUWUNIVERSITEIT
WAGENINGEN

Voorwoord en Dankbetuiging

Dit proefschrift bevat de resultaten van vier jaar werk aan het zogenaamde GEOBON-project. Dit project werd gezamenlijk gefinancierd door de Rijks Geologische Dienst (RGD; tegenwoordig NITG-TNO), het Rijks Instituut voor Volksgezondheid en Milieu (RIVM) en de vakgroep (tegenwoordig Laboratorium) Bodemkunde en Geologie van de Landbouw Universiteit in Wageningen, met als een doel een begin te maken met een systematische karakterisering van de geochemische samenstelling van de Nederlandse ondergrond.

Een belangrijk deel van het plezier waarmee ik aan dit onderzoek heb gewerkt komt door de prettige manier waarmee ik met verschillende mensen heb kunnen samenwerken. Het is jammer dat zowel in Wageningen als in Haarlem deze samenwerkingen geregeld werden verstoord door reorganisaties. Ik denk daarbij vooral aan de inkrimping van vakgroep bodemkunde en geologie, het opheffen van de leerstoel geologie in Wageningen en de fusie van de RGD en TNO.

Ik wil in de eerste plaats Salle Kroonenberg, mijn promotor, bedanken voor zijn ondersteuning en zijn inspirerend enthousiasme bij nieuwe resultaten. Ik vind het jammer dat onze samenwerking zich na de afbraak van de geologie-leerstoel in Wageningen op grotere afstand (Delft) heeft moeten afspelen. Gerard Klaver wil ik bedanken voor alle eerlijke kritiek, discussies, en steun bij veldwerk, analyses, interpretatie en publicatie. Ik wil Tom Veldkamp bedanken voor de dagelijkse begeleiding, die hij op zich genomen heeft na het vertrek van Salle Kroonenberg naar Delft. Zowel aan de inhoudelijke discussies met hem als aan zijn kritieken op concept-papers heb ik veel gehad. Zowel Gerard Klaver als Tom Veldkamp hebben mij veel geleerd, niet alleen over geochemie, geomorfologie en analysetechnieken maar ook over hoe de wetenschappelijke wereld werkt. Ik hoop in de toekomst weer met net zoveel plezier met hun te kunnen samenwerken als in de afgelopen jaren.

Wat betreft de mileukundige implicaties van mijn resultaten en met name de papers over de diagenetisch geochemie heb ik veel baat gehad bij de kritieken van en discussies met Bertil van Os. Ik heb veel hulp gehad van Toine Jongmans bij de interpretatie van verschillende series slijpplaten en SEM-analyses. Jan Jaap van Dijke heeft geholpen met het programmeerwerk voor het bevragen van de zware mineralen database. Ik wil Admin Prüftert en collega's van het Geologisch Landesamt Nordrhein-Westfalen bedanken voor het beschikbaar stellen van de boringen Schalbruch en Erkelnz.

Ik ben mijn (ex-)collega's op en rond Duivendaal 10 dankbaar voor de goede werksfeer en voor alles wat mijn AIO-tijd aangenaam heeft gemaakt.

Dit onderzoek was onmogelijk geweest zonder steun uit de districtskantoren Zuid en West van NITG-TNO. Patrick Kiden heeft veel ondersteuning gegeven bij het onderzoek in Brabant, terwijl Wim Westerhoff een belangrijke bijdrage heeft geleverd aan het onderzoek in Limburg. Henk Zwaan en Wim de Gans gaven ondersteuning bij het werk in Zuid-Holland. Ik heb bij het database-werk waardevolle hulp gehad van Lydia Dijkshoorn en Jean Weijers van NITG-TNO

afdeling Heerlen. Meindert van den Berg stelde zijn breukenkaarten beschikbaar, en gaf mij een serie geïnterpreteerde boorbeschrijvingen van kaartblad 60.

Het moge duidelijk zijn dat een onderzoek als dit drijft op grote hoeveelheden goede kwaliteit laboratorium analyses. Frans Vermeulen en James Baker van NITG-TNO waren verantwoordelijk voor de XRF-analyses. Jan van Doesburg (LUW) voerde de XRD-analyses uit. Corg-analyses werden gedaan door Frans Lettink (LUW) en later door Johan Wit (NITG-TNO). Nicolai Walraven en Bertil van Os voerden de ICP-MS analyses en een deel van de destructies uit. Slijpplaten werden gemaakt door Arie van Dijk, terwijl SEM-EDAX en -WDAX analyses werden uitgevoerd door respectievelijk Anke Clerckx (IPO-DLO Wageningen) and Jack Voncken (TUD). Zware mineralen preparaten werden gemaakt door Erik van Vilsteren, en geteld en mede geïnterpreteerd door Adri Burger.

Ik wil Kees Kasse en Peter van Rossum (VU) bedanken omdat zij mij de kleigroeve in groeve Beerse toonden, en geochemische analyses beschikbaar stelden van verschillende monsters uit die groeve. Daarnaast stelde Kees Kasse mij ook een deel van zijn zware mineralen data uit Brabant en België beschikbaar. E. Broers van de Waterleiding Maatschappij Noord-West Brabant en D. Edelman van de Tilburgse Waterleiding Maatschappij wil ik bedanken voor het beschikbaar stellen van grondwater analyses.

Verschillende doctoraal studenten uit Wageningen en Amsterdam hebben in het kader van afstudeervakken en stages in meer of mindere mate bijgedragen aan dit onderzoek. Gerben Mol heeft in het eerste stadium van dit project enthousiast meegewerkt aan het bemonsteren en analyseren van de boringen Reusel en Sprundel. Zijn resultaten zijn verwerkt in hoofdstuk 3.1 over de geochemische variatie in de Brabantse ondergrond. Freek Schouten bestudeerde de effecten van pyrietoxidatie in zanden van de formatie van Tegelen op de grondwaterchemie in een door hemzelf opgezet project. De resultaten zijn niet opgenomen in dit proefschrift, maar hebben wel bijgedragen aan de beeldvorming over de processen die zorgen voor anomalieën in organische lagen. Niels Hartog heeft met veel energie de boringen uit Zuid Holland bemonsterd en geanalyseerd, en concentreerde zich op de herkomst van hoge As-waardes in venen. Zijn werk heeft bijgedragen aan de hoofdstukken over anomalieën in organische lagen (4.2) en aan het ruimtelijk modelleren van de geochemie in de Kedichem formatie (6). Margo Steehouwer analyseerde een aantal secties in Limburg, en bestudeerde de effecten van sediment herkomst en vertering. Erik van Gelder maakte een zeer gedetailleerde studie van de geochemie en kleimineralogie van de sectie BTAB. Hun resultaten zijn verwerkt in het hoofdstuk over de geochemie van de Limburgse kleipakketten (3.2). Rienk Smittenberg bestudeerde de genese van sideriet in Onder- en Boven-Pleistocene afzettingen. Zijn bijdrage is in aangepaste vorm als hoofdstuk 4.1 in dit proefschrift opgenomen.

Ik wil Simon Vriend bedanken voor het beschikbaar stellen en het voor mijn data aanpassen van het programma FUZZY voor fuzzy C-means cluster analyse.

Een aantal reviewers heeft meegeholpen aan dit proefschrift door hun kritieken op eerder versies van manuscripten, waarvoor mijn dank.

Stellingen, behorende bij het proefschrift "Geochemical characterization of subsurface sediments in the Netherlands" van ir. D.J. Huisman.

- 1 Hogere Na gehalten in Rijnsedimenten rond de overgang Pliocéen-Pleistoceen reflecteren de aansluiting van de Alpen op het stroomgebied van de Rijn.
- 2 Hoge gehalten aan TiO_2 in siliciklastische sedimenten zijn niet noodzakelijk een indicatie voor een sterke verweringsgraad, maar kunnen ook veroorzaakt zijn door sorterings-processen.
- 3 De aanwezigheid van specifieke diagenetische mineralen als pyriet en sideriet kan alleen worden gebruikt om paleo-afzettingssmilieus te reconstrueren als, door middel van bijvoorbeeld micromorfologische studies, wordt aangetoond hoe de vorming van deze mineralen is gekoppeld aan de afzettingsgeschiedenis van het omliggende sediment.
- 4 Menselijke activiteiten als waterwinning, ondergronds bouwen en opslag van afval kunnen resulteren in een zodanige verstoring van het ondergrondse geochemische milieu dat de kwaliteit van grond - en drinkwater wordt bedreigd.
- 5 De grondsoortcorrectie van de streef- en interventiewaardes voor zware metalen in de Nederlandse bodem kan beter plaatsvinden op basis van gehalten aan Al dan op basis van de nu gebruikelijke percentages aan klei en organisch stof.
- 6 De praktijk van het toekennen van bonussen aan onderzoeksgroepen voor iedere promotie en het straffen van onderzoeksgroepen als een AIO-onderzoek niet resulteert in een promotie werkt een devaluatie van de Nederlandse doctorstitel in de hand.
- 7 Any boring technique may result in loss of concentration.
- 8 Handel in aandelen dient te vallen onder de wet op de kansspelen.
- 9 Verlanglijstjes verkleinen de kans op het geven en krijgen van ongewenste cadeaus. Het is echter de vraag of dat opweegt tegen vermindering van de kans dat een cadeau echt verrassend is.

- 10 De gebieden die middels “nature building” (“natuurbouw”) aangepast zijn aan de recente trends in landschapsarchitectuur worden ten onrechte natuurgebieden genoemd.

- 11 Bonzai-mountains weigh many, many very small tons.
Terry Pratchett, “Small Gods”

Wageningen, februari 1998

Contents

Voorwoord en dankbetuiging	I
Contents	III
1 Introduction	1
2 Materials and methods	3
3 Regional geochemical studies	
3.1 A geochemical record of Late Cenozoic sedimentation history in the Southern Netherlands.....	13
3.2 Geochemical compositional changes of the Pliocene- Pleistocene transition in fluviodeltaic deposits in the southeastern Netherlands.....	41
4 Specific diagenetic processes	
4.1 Siderite, syn- or postdepositional? A comparison of Early and Late Pleistocene deposits in the Netherlands.....	67
4.2 Trace element and REE anomalies in Quaternary organic-rich deltaic deposits.....	83
5 A geological interpretation of heavy metal concentrations in soils and sediments in the southern Netherlands	105
6 Spatial prediction of the geochemical variability of Early Pleistocene subsurface sediments in the Netherlands	123
7 Synthesis and conclusions	151
Summary	157
Samenvatting	161
Literature Cited	165
Curriculum Vitae	175

Some of the Chapters are already published or are in press:

Chapter 3.1: Geologie en Mijnbouw (*in press*)

Chapter 5 Journal of Geochemical Exploration 59 (1997) 163-174

Chapters 3.2, 4.1, 4.2 and 6 are or will be submitted for publication.

1 Introduction

Traditionally, the Netherlands' subsurface is mainly used to obtain good quality drinking and industrial waters from the different aquifers. Due to the lack of space on the surface, increasing environmental problems and demand for energy, the subsurface will be used increasingly for other activities than providing the nations' drinking water. These activities vary from large underground infrastructural projects like tunnels, railways and parking places to underground storage of waste (chemical, nuclear) and greenhousegasses (CO₂) to the use of the underground storage capacity for the energy sector (natural gas and heat exchange projects).

Because of the conflicting nature of these activities, a regional and spatial planning for the use of the subsurface is under consideration. In order to evaluate the effects of the underground activities, detailed knowledge about the subsurface sediments is required. The geochemical composition of the subsurface sediments and the associated mineralogy forms an important part of the information needed to make decisions where and under what restrictions the different activities in the subsurface can best be planned.

As is indicated by a number of detailed studies, the subsurface sediments act as a source or sink for heavy metals. Other studies have shown that due to microbial processes, organic pollutants break down to less hazardous components (so-called natural attenuation). Finally, if the proper minerals or organic matter are available the input of anthropogenic nitrate will be buffered. On the other hand, due to intensive pumping of oxygenated water through pyrite-bearing anoxic zones, heavy metal concentrations in the pumped water may rise to levels far above the allowed concentrations.

These examples demonstrate that it is important to have detailed knowledge about the chemical characteristics of the subsurface in order to evaluate heavy metal behavior and the results of pollution on the quality of drinking water. Moreover, the effects of changing groundwater levels can only be evaluated if enough geochemical and associated mineralogical data are available.

Apart from that, as the chemical composition of most soils in the Netherlands is influenced by anthropogenic activities, subsurface sediment composition may be used as a proxy for natural background values for heavy metals. In recent geochemical mapping campaigns, preindustrial sediments were regarded as pristine, without anthropogenic influences (Hindell et al., 1996; De Vos et al., 1996). The background values for heavy metals that are in use now for legislative purposes however, are based on samples from topsoils (cf. Edelman, 1984) which in the Netherlands almost by definition have anthropogenic influence. The use of subsurface sediments as a proxy for natural background values of soil material however, neglects possible heavy metal accumulation by geochemical cycling processes (leaching, organic decay, plant growth) that may affect topsoils.

Previous studies on the bulk geochemistry of Dutch subsurface sediments (Moura and Kroonenberg (1990) and Hakstege et al. (1993)) indicated that the most important factors that determine the geochemical composition of Dutch subsurface sediments are grain size and sediment provenance. However, these studies were of a too limited scale to be directly applicable for large-scale characterization programs.

In order to meet the demand for information on the geochemical composition of the Dutch subsurface sediments, the GEOBON project (**GEO**chemische karakterisering van **Bodem** en

Ondergrond in Nederland; Geochemical mapping of soil and subsoil in the Netherlands) was started in cooperation between the Geological Survey of the Netherlands (RGD; presently NITG-TNO), the National Institute for Environmental protection and Public health (RIVM) and the Wageningen Agricultural University (WAU). The goals of this project were first to develop adequate means for the characterization of subsurface sediments, and second to determine the most important factors that influence its geochemical properties. This thesis contains the first results of the GEOBON-project:

The first stage of the GEOBON-project consisted of regional geochemical studies that encompassed several geological formations. Geochemical variation was described as a function of specific mineralogy, sediment provenance, grain size, sorting and diagenetic processes, based on the relations and ratios between key elements. Interpretation was supported by analyses of the clay mineralogy and by micromorphological studies. Chapter 2 described the methods employed for the analyses. Chapter 3.1 and 3.2 contain the results of the two regional mapping campaigns in Brabant and Limburg respectively. In order to study specific subsurface diagenetic processes, additional micromorphological and submicroscopical analyses were done. Chapter 4 contains the results of two such studies: Chapter 4.1 describes the genesis of secondary Fe-carbonates, whereas Chapter 4.2 studies the origin of anomalous organic-related enrichments of heavy metals, REE, Y and U.

Knowledge and experience from these studies subsequently was applied on environmental applications of the data and on spatial modeling of the subsurface geochemical composition: In Chapter 5, concentrations of heavy metals and their relations with major element concentrations are discussed in the light of environmental implications. Chapter 6 contains the results of a model study in which the geochemical variation of a single formation (Kedichem) in its total could be characterized. This model study provides data that form the basis to set up a nation-wide geochemical database. The thesis is concluded by a short general discussion in Chapter 7.

2 Materials and Methods

Sampling and pretreatment

As standard characterization procedure, samples were taken from borings of the Geological Survey of the Netherlands (presently NITG-TNO), from borings of the Geological survey of Nordrhein-Westphalen, and from clay pits. The sampled borings usually consisted of cores with a diameter of 7 or 10 cm. However, in two cases (Reusel and Sprundel) only Bailer-bore samples were present of the coarser-grained sections (sand and shells). In clay pits we sampled using zinc boxes of 30 x 2 cm which were pushed in to the quarry face. These boxes were subsequently dug out, and sampled in the laboratory. Our sampling strategy was aimed at incorporating as much of the geochemical variation as possible, so usually representative samples were taken of each distinct sedimentary unit, and at least once per meter. Sample densities therefore can vary from one to fifty per meter. Flush- or counterflushborings were not incorporated in this research as it is unknown to what extent the sediment composition may alter (loss of micas or clay) as a result of the boring technique. In our experience, geochemical characterization of sediments requires such precise sampling on visible phenomena, that both flush and bailer-bore samples are hardly suitable. Further information on sampling strategies can be found in the relevant chapters.

Samples were dried at 40-60 °C or freeze-dried, where necessary sieved through a 2 mm copper or stainless steel sieve, and stored. Of all these samples, subsamples were taken for XRF-analyses. The remaining samples were in some cases later on used for ICP-MS, grain size or mineralogical analyses. From some sections, additional samples were taken to prepare thin sections.

Geochemical analyses

XRF

For XRF-analyses, a 10 g subsample was ground and subsequently pressed with wax into pressed-powder tablets. We tried three different grinding methods (see table 2.1): The first series of approximately 300 samples (Borings Reusel and Sprundel) was ground with an agate-swing mill, and additional subsamples were ground in a sialon mill. The agate mill proved to have two major disadvantages: Firstly, coarse-grained samples were not ground to sufficiently small grain sizes which can cause increased uncertainties in analyses of especially light elements. Secondly, the procedure proved to be time-consuming. The sialon mill produced finely enough ground material, but it was as time-consuming as the agate mill, and additionally caused contamination by Y. No data produced with sialon are used in this report. The rest of the samples was ground using a Tungsten-carbide mill in an automated grinding- and pressing machine (Herzog HSM-HTP). Grinding was satisfactory, producing small enough grain sizes, and it was considerably less time-consuming. However, contamination with Co occurred. Moreover, an overcorrection for W in the calibration caused errors in the Cu, Ni and Zn-measurements part of the measurements, but this

problem was solved later. We decided that the increased speed of analyses was more important than the Co-contamination, and therefore we used this grinding method for all subsequent samples.

Table 2.1: Comparison of grinding methods used for XRF-analyses

Grinding method	Advantages	Disadvantages
Agate swing-mill (NITG-TNO)	No contamination	Time-intensive Bad performance
Sialon (WAU)	Good performance	Time-intensive Y-contamination
Tungsten-carbide (NITG-TNO)	Time-extensive Good performance	Co-contamination

The tablets were analyzed for major and trace elements by X-ray spectroscopy, using an ARL8410 spectrometer with a Rh tube, with full matrix correction for major elements (SiO₂, TiO₂, Al₂O₃, Fe₂O₃, MnO, MgO, CaO, Na₂O, K₂O, P₂O₅, S) and Compton scatter method for trace elements (As, Co, Cr, Cu, Ni, Pb, V, Zn, Ba, Ga, Nb, Rb, Sr, Y, Zr). The XRF was calibrated using approximately 100 certified Geological reference samples. Three reference samples were added to each batch of 50 samples to determine precision (0.5-1 % relative standard deviation) and accuracy (1-5 % relative standard deviation). The accuracy of S may be worse, however, because of the lack of certified S-rich Geological samples, and a slight S-contamination because of the presence of S in the pressing wax. No Fe-speciation was determined, so all Fe is reported as Fe₂O₃.

XRF-analyses from the sediments and a pyrite-nodule at Beerse were provided by Peter van Rossum (Free University, Amsterdam). They were measured with the same techniques as described above.

ICP-MS

ICP-MS analyses were performed on a series of selected samples in order to measure the contents of those elements that could not be measured by XRF (Cd, Se, Mo, REE). We first compared two types of destruction, to wit boiling Aqua Regia (HCl, HNO₃) and a total destruction involving repeated boiling with concentrated HF, HNO₃ and HClO₄. In a later stage, we used a total destruction involving concentrated HF, HNO₃ and HClO₄ at elevated pressure and temperature (240 °C) using a Milestone Microwave 1200 Mega. The sample size was usually 0.25 grams, but in a few cases not enough material was left, and sample sizes were smaller.

Measurements were performed on a Fisons Plasmaquad PQ 2+ ICP-MS, calibrated usage

two multi-element standards prepared from 1000 ppm stock dilutions from Merck, Alfa and Aldrich and a blank.

For most elements a good agreement exists of the ICP-MS analyses with XRF-measurements of the same samples (Fig. 2.1). However, there are several cases in which these analyses do not agree:

1 Ti, Cr, Rb, Nb, Ba, Ga and Pb are lower in ICP-MS analyses after aqua regia-destruction. This problem is, except for Cr and Zr, not present in ICP-MS analyses after total destruction. This indicates that aqua regia destruction is incomplete. The lower values of Zr and Cr of after total destruction at elevated temperatures and pressure indicates that even this method is not capable to dissolve the mineral phases that contain significant amounts of Zr and Cr.

2 The two outliers with anomalously elevated concentrations of Cr, Pb and Zn are very small samples. Their small sample size makes them extra vulnerable to sample inhomogenities and laboratory contamination.

3 The anomalously high As-contents measured for As in Aqua-Regia destruates is probably caused by insufficient correction of the high contents of Cl as a result of the use of HCl in the destruction.

4 The Rb- and Th-measurements do not correlate well. As the ICP-MS analyses on the Rb-content of standard samples is also way off, the error must be sought in the ICP-MS measurements. The problem with Rb is probably that it forms insoluble complexes with the HClO_4 used in the destruction agent. For Th, the cause for the bad correlation lies probably in the XRF-measurements being too close to the detection limit.

Because of the apparent problems with aqua regia destruction, we use in the rest of this thesis (Chapter 4.2), only the ICP-MS measurements after total destruction.

C-analyses

For the sections BTAB, Reusel and Sprundel, additional subsamples were taken for Corg analysis. The Corg-analyses of the borings Reusel and Sprundel were performed according to the method of Nieuwenhuize et al. (1993).

In order to discern organic C and the C present in various carbonate fractions like siderite-calcite and dolomite, we measured the C-output while heating a sample stepwise. We used a Strohlein C-mat 5500, which measures the CO_2 -output with IR-adsorption, while heating approximately 0.1g of the sample. Organic matter was burned out after 4 minutes at 400°C , after which the sample was heated from 400 to 1000°C at a speed of 7000°C . Siderite-C was released around 550°C , whereas Calcite and Dolomite-C were determined around 800°C .

The Corg-analyses from the BTAB section were done using a Strohlein CSmat 5500 by measuring the CO_2 -output while heating at 400°C .

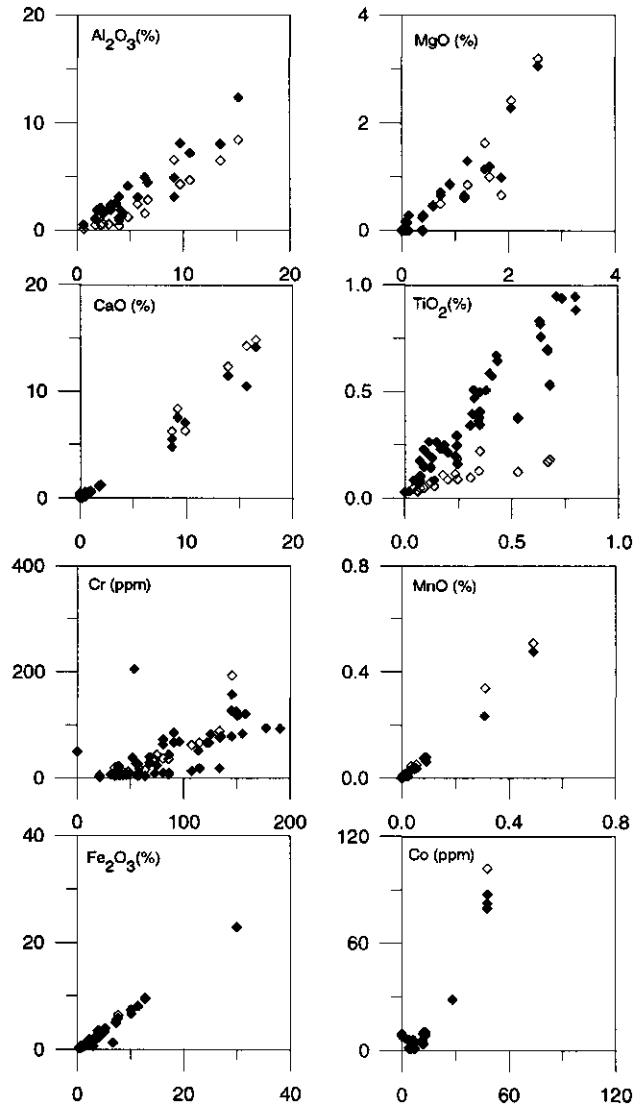


Figure 2.1 Scatterplots to compare XRF (x-axis) and ICP-MS (y-axis) analyses. Open diamonds represent ICP-MS analyses after aqua regia destruction, filled diamonds after total destruction. Note that the analyses for Ti, Cr, Rb, Nb, Ba, Ga and Pb are lower after aqua regia than after total destructions. The relatively high ICP-MS results of the encircled samples in the Pb- and Zn-plots are probably related to the small sample sizes (see text).

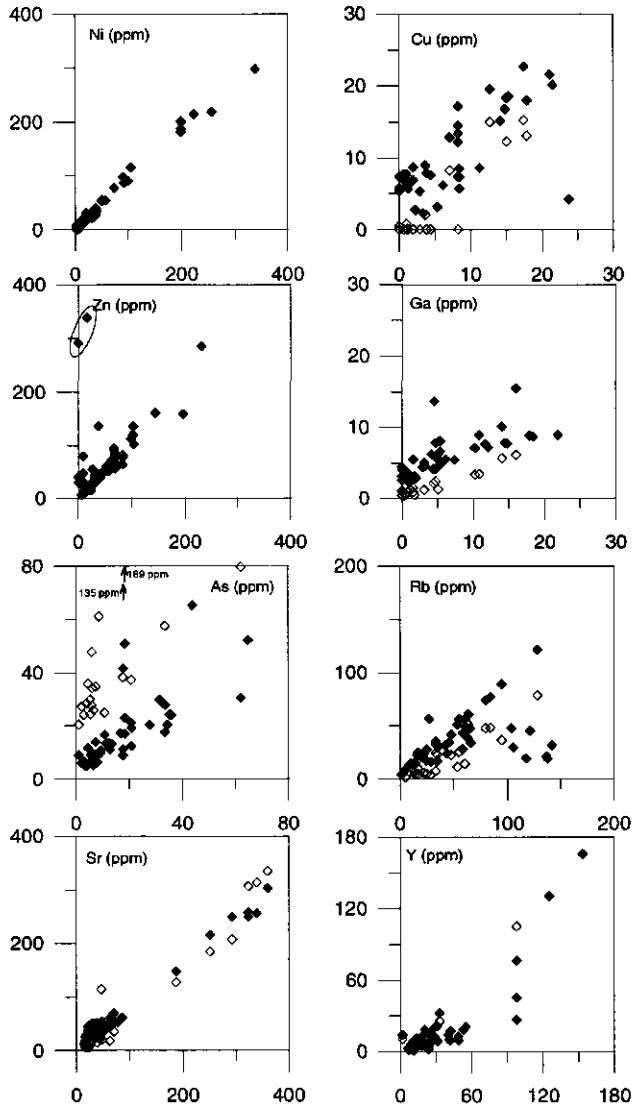


Figure 2.1 (Continued)

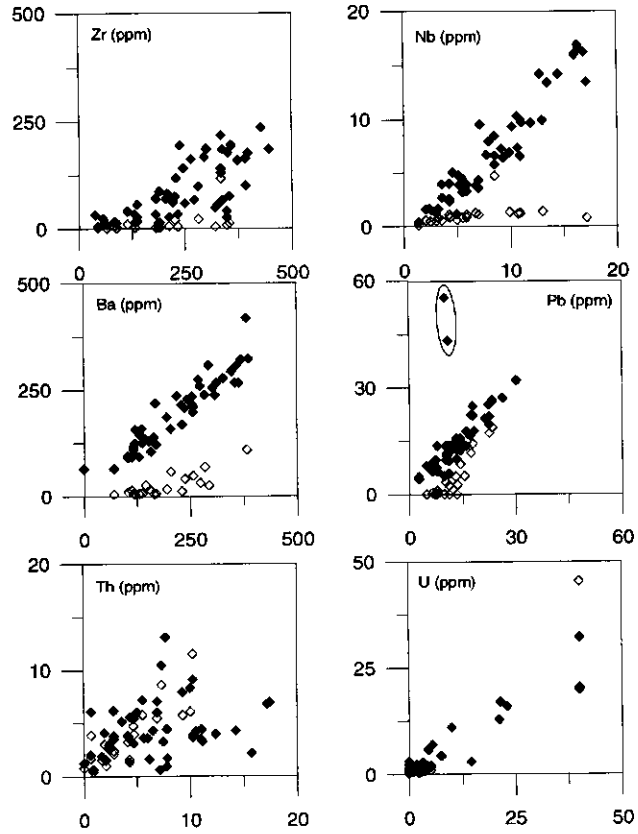


Figure 2.1 (Continued)

Grain size analysis

Grain size distribution was determined using a Malvern-X laser grain sizer for samples from the Reusel and Sprundel borings.

Mineralogical analyses

XRD

Standard powder X-ray diffraction (XRD) analyses were performed on selected freeze-dried or air-dried samples. Clay mineralogy was determined by first treating the samples with Na-acetate, H₂O₂ and Na-dithionite to remove carbonates, organic matter and Fe and Mn (hydr)oxides. Subsequently, clay size was separated by pipetting after settling, and X-ray diffractograms were made of oriented samples. The diffractograms were digitized by hand. Peaks heights were measured to compare the (semi-quantitative) XRD diffractograms and reported in % of total peak height. The presence and relative degree of Al-hydroxy interlayering was determined by stepwise heating of K-treated samples. Both for standard powder XRD and for clay mineralogical analyses, a Philips PW1820/PW1710 diffractometer was used, using a Co X-ray tube at 40kV and 30mA, with a focussing monochromator. The divergence slit was set at 1°, the receiving slit at 0.2 mm, and the anti-scatter slit at 1°.

TGA

Thermal Gravimetric Analysis was used to study and identify various carbonates. Freeze-dried samples were analyzed using a DuPont 951 Thermogravimetric Analyzer, which measured from 20°C to 1000°C at a speed of 10°C/min and with an air flow of 50 ml/min. Organic matter, siderite and calcite were discerned by comparing the weight loss below 400°C, at 450°C and between 700 and 800°C respectively.

Heavy mineral counts

For some additional samples from boring Rucphen 2, heavy-mineral counts were performed. The samples were treated with Na-acetate, H₂O₂ and Na-dithionite to remove carbonates, organic matter and Fe and Mn (hydr)oxides. The fraction 63-500µm was separated by sieving, and was mounted on a microscopical slide. The counting was performed by A. Burger of NITG-TNO (formerly Geological Survey of the Netherlands).

(Sub)microscopical techniques

Undisturbed (8 x 8 cm) samples were taken in cardboard boxes for micromorphological research. Thin sections were made following the method of Fitzpatrick (1970) and examined with an Olympus petrographic microscope in plane and polarized light, and in incident light with a Leitz

petrographic microscope. The micromorphological description follows the terminology of Bullock et al. (1985). Uncovered thin sections (4x2 cm) were made and studied with a Philips 535 Scanning Electron Microscope (SEM) and analyzed with a 9900 Energy Dispersive X-ray Analyzer (EDAX), at IPO-DLO in Wageningen, and by SEM with Wavelength Dispersive Analytical X-ray (WDAX) at the Institute for Applied Earth Sciences of the Technical University Delft using a JXA-8800M Electronprobe Microanalyzer. Rough surfaces of undisturbed pieces were also studied with SEM-EDAX.

3 Regional Geochemical Studies

3.1 A geochemical record of Late Cenozoic sedimentation history in the Southern Netherlands

D.J. Huisman
P. Kiden

Abstract

A geochemical study was performed on unconsolidated Upper Cenozoic siliclastic sediments from an area in the south of the Netherlands. Glauconite-rich sediments (Breda Formation) show anomalously high K contents and low Ba/K ratios. Major shifts in sediment composition as a result of changes in the Rijn system and shifts between Rijn and Schelde provenance, as known from heavy-mineral studies, are also recorded in changes in the grain-size-dependent variations between Al, Na and K. Pleistocene Rijn sediments (Tegelen Formation) show higher Na contents than Pliocene Rijn sediments (Oosterhout and Kiezeloöliet Formations) and Schelde-derived material (Kedichem Formation), probably as a result of larger contents of sodic plagioclase. Schelde-derived sediments show low K/Al ratios as a result of a smectite-dominated clay-mineralogical composition and low contents of micas, whereas Rijn-derived sediments have high K/Al ratios which reflect an illite-kaolinite-dominated clay composition and higher contents of muscovite.

The presence of siderite causes high Fe-contents in the Tegelen formation in the east of the area. Increased Mg contents in the siderite-bearing sections from the Tegelen formation and in parts of the Oosterhout and Kiezeloöliet Formation are probably caused by the presence of minor amounts of dolomite. Localized high (pyrite-) S-concentrations are not only found in the marine Oosterhout and estuarine Tegelen Formations, but also in the fluvial Kiezeloöliet and Kedichem Formations, which may indicate minor marine transgressions during their deposition.

Introduction

In 1993 a project was started for a nation-wide characterization of the geochemical variation in Dutch unconsolidated subsurface sediments. Geochemical data from these sediments are still scarce, but from two Dutch regional investigations (Moura and Kroonenberg, 1990; Hakstege et al., 1993) and from several other larger-scale studies (Bhatia, 1983; Roser and Korsch, 1986; Kroonenberg, 1992; Cox et al., 1995; Tebbens et al., 1996) we know that grain size, provenance-related variations in mineralogy, weathering and diagenetic processes are the major factors that determine the geochemical composition of sediments. As a start of our mapping project we wanted to determine to what extent and in which ways these factors influence the geochemical composition of the sediments, which mainly consist of mature siliclastic material. For this purpose, we sampled and analyzed 14 borings from the central-southern Netherlands. Two borings, Reusel and Sprundel, were selected because they contain a more or less complete representative sequence of Late Cenozoic deposits, with major variations in provenance, grain size, lithology and depositional environment. Other borings contain only Early Pleistocene

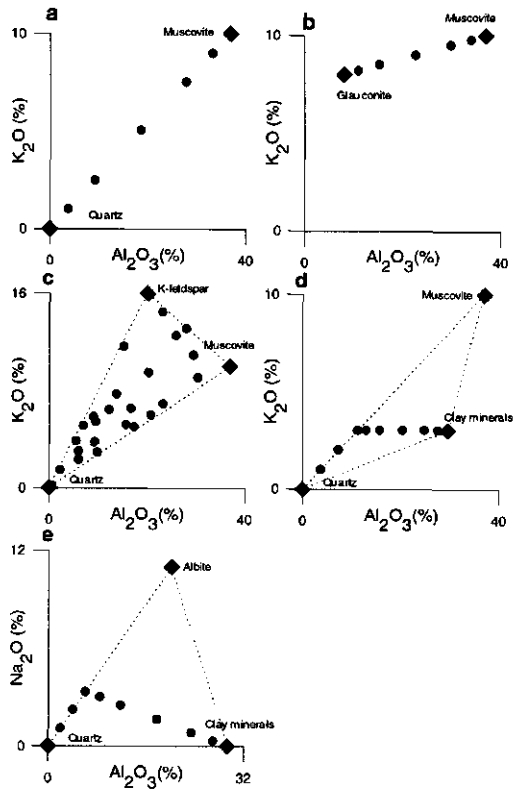


Figure 3.1.1 Theoretical mixing ranges. **A** gives the theoretical contents of Al and K in samples, consisting of mixture of pure quartz and muscovite. **B** Shows the composition of mixtures of glauconite and muscovite. **C** and **D** give a three-component model, with samples consisting of a mixture of quartz, muscovite and K-feldspar. **C** shows a random mixture, whereas **D** shows the effects of grain size sorting of a mixture of (coarse) quartz, (medium) muscovite and (fine) clay on the K- and Al-contents. **E** demonstrates the effects of grain size sorting of a mixture of (coarse) quartz, (medium) albite and (fine) clay on the Na- and Al-contents.

deposits, and are especially relevant for studying lateral variations in these deposits. In this paper we will study how these known variations are reflected in the bulk geochemical composition.

Establishing the relation between chemical composition and sedimentation history requires consideration of the relation between chemistry and mineralogy, and ways to portray these relations graphically. Provided that a sediment consists of only a limited number of monocrystalline mineral species, its mineralogical composition can be inferred from geochemical data alone by combining patterns that emerge in bivariate plots of major and trace element concentrations without having to perform extensive mineralogical analyses (Argast and Donnelly, 1987). Hypothetical mixtures consisting of varying proportions of two minerals plot on a straight line between the data points of the pure minerals as is shown in K_2O/Al_2O_3 diagrams (Fig. 3.1.1a,b). Random mixtures of three minerals plot in a triangle with the chemical compositions of each pure mineral as corners (Fig. 3.1.1c). In a situation where the sediment consists of three minerals which are preferentially sorted, this triangle will be only partially filled. A set of samples, derived by grain size sorting from a mixture of coarse quartz, fine muscovite and clay (with 33% illite, 33% smectite and 33% kaolinite) would show mixing of predominantly quartz and muscovite in the coarse-grained samples, and of muscovite and clay in the finer-grained samples (Fig. 3.1.1d). A Na_2O/Al_2O_3 diagram of mixtures of coarse quartz, medium-sized albite and fine clay minerals shows basically the same pattern (Fig. 3.1.1e), but here Na_2O correlates negatively with Al_2O_3 in the fine samples as albite contents drop with higher contents of clay minerals. Grain size-induced relations in element contents, like the ones in Figs. 3.1.1d and 3.1.1e, can be used to deduce mineralogical properties of sedimentary units, provided the samples encompass sufficient variation in grain size. Variations in these inter-element relations indicate changes in overall mineralogical composition, effectively recording changes in provenance and degree of weathering.

In this study we will compare variations in these inter-element relations with stratigraphical data. The Dutch Pliocene-Pleistocene stratigraphy is based on a combination of lithology, heavy-mineral composition and palynology (Zagwijn and Van Staaldunin, 1975). The heavy-mineral subdivision employs variations in the contents of the various sand-sized transparent heavy minerals that can be distinguished optically (polarizing microscope). A major distinction made is between associations of so-called stable and unstable minerals. Typical stable minerals are zircon and tourmaline, whereas typical unstable minerals include garnet, epidote, hornblende and alterite. Note that in this heavy-mineral stratigraphy the heavy minerals are defined only by their optical properties and that some, e.g. alterite, would not be distinguished on the basis of chemistry or crystallography (cf. Van Andel, 1950, 1958). The only published research on light minerals in the Netherlands (Van Baren, 1934) shows that in general high contents of unstable heavy minerals are associated with high contents of feldspars.

Geological setting

The study area is situated on the southern edge of the North Sea Basin, west of the Roer Valley Graben Fig. 3.1.2 and table 3.1.1 give an overview of the borings investigated. The sedimentary record in this area shows a general regression with smaller-scale fluctuations during the Late Cenozoic, with sediment supplied alternately by the Rijn, Maas and Schelde river systems (Fig. 3.1.3) (Zagwijn and Van Staaldunin, 1975; Kasse, 1988).

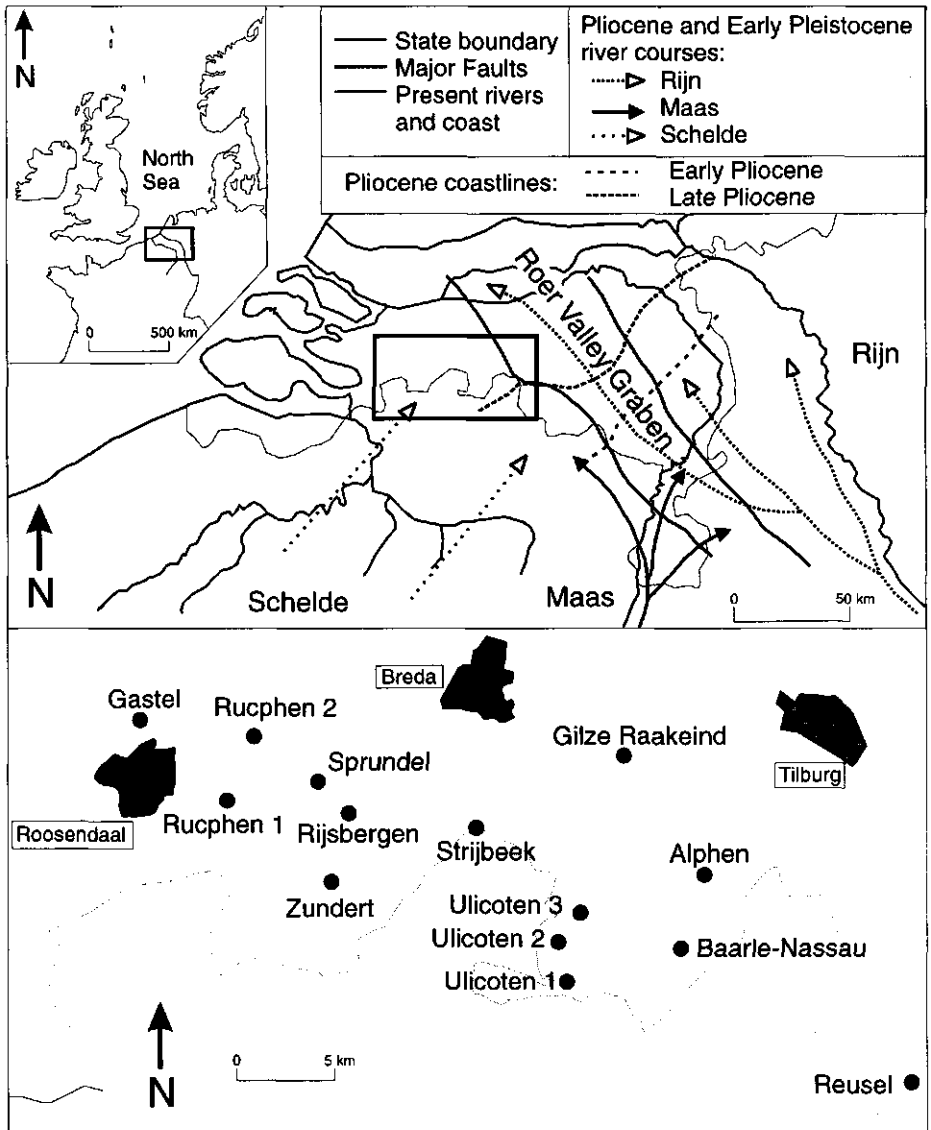


Figure 3.1.2 Study area and position of borings listed in Table 3.1.1

Table 3.1.1: Borings, codes, X- and Y-coordinates, depth reached and number of samples:

Boring	RGD-code	X	Y	Depth (m)	# Core samples	# Bailer samples
Gastel	49F423	91.450	397.540	11	43	
Rucphen 1	49F418	96.850	392.570	20	24	
Rucphen 2	49F424	98.480	396.520	11	50	
Sprundel	50A337	102.450	393.750	113	72	83
Rijsbergen	50A336	104.330	391.785	21	57	
Zundert	50A338	103.255	387.585	9	31	
Strijbeek	50B339	112.130	390.900	11	27	
Ulicoten 1	50D34	117.695	381.450	10	34	
Ulicoten 2	50D35	117.150	383.890	6	30	
Ulicoten 3	50D36	118.505	385.680	7	39	
Gilze	50E368	121.175	395.320	22	55	
Alphen	50E367	126.120	388.005	21	56	
Baarle-Nassau	50G90	124.675	383.485	24	63	
Reusel	50H74	138.830	375.290	98	53	73

The oldest sediments investigated belong to the Miocene marine Breda Formation, according to the stratigraphic nomenclature of Zagwijn and Van Staaldouin (1975). They were only recovered from the Reusel boring, where they consist of glauconiferous sands with phosphorite nodules. Glauconite is a K- and Fe-rich mica of marine diagenetic origin (Deer et al., 1992; Porrenga, 1967). In our samples, the glauconite is present as coarse black-green grains. The Pliocene Oosterhout Formation consists predominantly of shell-bearing sands with clayey intercalations and is locally glauconiferous. It records a general regression with some smaller oscillations, related to uplift south of the area studied in the Ardennes and the Brabant Massif, as well as to climatic cooling. The formation is distinguished from the Breda formation by its higher content of shells and lower content of glauconite (Fig. 3.1.3; Zagwijn, 1960, 1989; Zagwijn and Doppert, 1978). The Oosterhout Formation was recovered from the Reusel and Sprundel borings. In the Reusel boring it is overlain by the Kiezeloöliet Formation, which is its continental equivalent and which is distinguished from it by the absence of marine shells. The Pliocene Oosterhout and Kiezeloöliet Formations are overlain by the Early Pleistocene Tegelen Formation. The base of the latter is typically marked by a transition from a stable (zircon, tourmaline) to an unstable (epidote, alterite, hornblende) heavy-mineral association (Zagwijn and Van Staaldouin, 1975; Boenigk, 1970). This break is interpreted as a change in sediment provenance from reworked regional weathered deposits to fresh Alpine sources caused by the headward extension of the Rijn system into the Alps, combined with the onset of the first glaciations (Fig. 3.1.3; Gibbard, 1988) and increased tectonic activity (Tebbens et al., 1995; Van den Berg and Veldkamp, 1993).

The Tegelen Formation in the area consists of micaceous sands and finely laminated clays which were deposited in a fresh to brackish tidal environment and locally contains siderite and

pyrite enrichments (Kasse, 1988). Heavy-mineral counts show that most of the formation has a Rijn provenance, but locally Schelde-derived material is found. Sediments with Schelde provenance seem to be more frequent in the lowermost units (Merksplas Sands) and to the west of the study area (Woensdrecht and Hoogerheide Members; Kasse, 1988). The borings Reusel and Sprundel are the only ones which contain a complete Tegelen section. In the Sprundel boring the lowermost parts of the Tegelen Formation are calcareous and interfinger with sands of the Maassluis Formation which is characterized by the presence of abundant shells. In the Reusel boring the Maassluis Formation is lacking. In the other borings where the Tegelen Formation is reached, it consists of homogeneous or laminated clay which often is organic-rich near the top.

The Kedichem Formation overlying the Tegelen Formation consists of fluvial sands of Early Pleistocene (Menapien to Bavelien) age, with local clay and peat intercalations. It is distinguished from the Tegelen formation by its low mica contents and on other lithostratigraphic features. By virtue of their very stable heavy-mineral association, the sands seem to be derived from the Schelde river system, which supplied reworked Paleocene and Eocene sediments, whereas its gravels suggest a Maas provenance (Kasse, 1988).

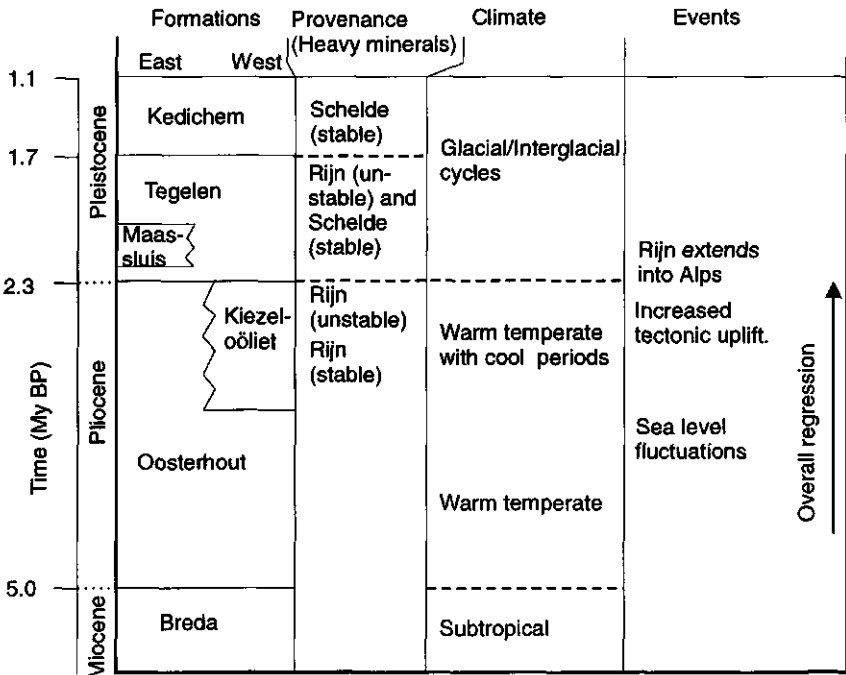


Figure 3.1.3 Summary of stratigraphy, heavy-mineral provenance and geological history of Late Cenozoic sediments in the Southern Netherlands.

In the east of the study area, a thin cover of Middle Pleistocene fluvial gravel, belonging to the Sterksel Formation, occurs locally on top of the Kedichem Formation. Most profiles are overlain by Upper Pleistocene cover sands of the Nuenen Group. Neither the Sterksel Formation nor the Nuenen Group will be considered in this study.

Results

Effects of grain size and specific mineralogy

In order to study the expected relations of Al_2O_3 and SiO_2 with the fine grain size fractions, the bivariate plots of both oxides versus the percentage of the fraction $< 16 \mu\text{m}$ were made for the Reusel and Sprundel borings. In these plots, Al_2O_3 shows a clear positive correlation with this fraction, while SiO_2 shows a negative correlation (Fig. 3.1.4). Therefore either of these oxides can be used as a general proxy for grain size, but Al_2O_3 seems much better suited. The variability of SiO_2 is mainly related to the quartz-content which correlates negatively with the contents of clays and carbonates. Most detrital variability between sediments, however, is related to varying contents of feldspars, micas and clay minerals, in which the ratio between Al_2O_3 and other oxides such as K_2O and Na_2O plays a major role (Bhatia, 1983; Roser and Korsch, 1986; Argast and Donnelly, 1987; Moura and Kroonenberg, 1990; Hakstege et al., 1993; Cox et al., 1995). From the total of bivariate plots made for all element combinations the $\text{Ba}/\text{K}_2\text{O}$ plot was the best to discriminate for the presence of the macroscopically visible coarse-grained glauconite. Most of the other measured elements (Ti, Co, Cr, Cu, Ni, Pb, V, Zn, Ga, Nb, Rb and Y) show linear relations with the Al_2O_3 content in all formations as they occur in clay minerals and micas in constant ratios to Al_2O_3 (cf. Chapter 5). As these elements do not show clear differences between the formations, they cannot be used for classification. Sr shows a strong linear correlation with CaO content, as does Mn with Fe_2O_3 . Since Fe_2O_3 , CaO, MgO and S do not only occur in clays and micas but also in oxides, carbonates, sulfides and sulfates, we made plots and depth profiles of

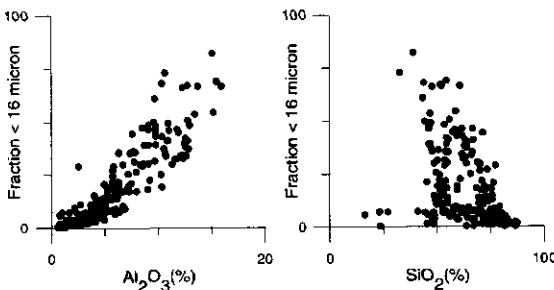


Figure 3.1.4 Scatterplots of Al_2O_3 and SiO_2 versus the contents of grain size fraction $< 16 \mu\text{m}$; borings Reusel and Sprundel, 284 samples. There is positive correlation between the contents of Al_2O_3 - and of the fraction $< 16 \mu\text{m}$. The correlation of the fraction $< 16 \mu\text{m}$ with SiO_2 is negative.

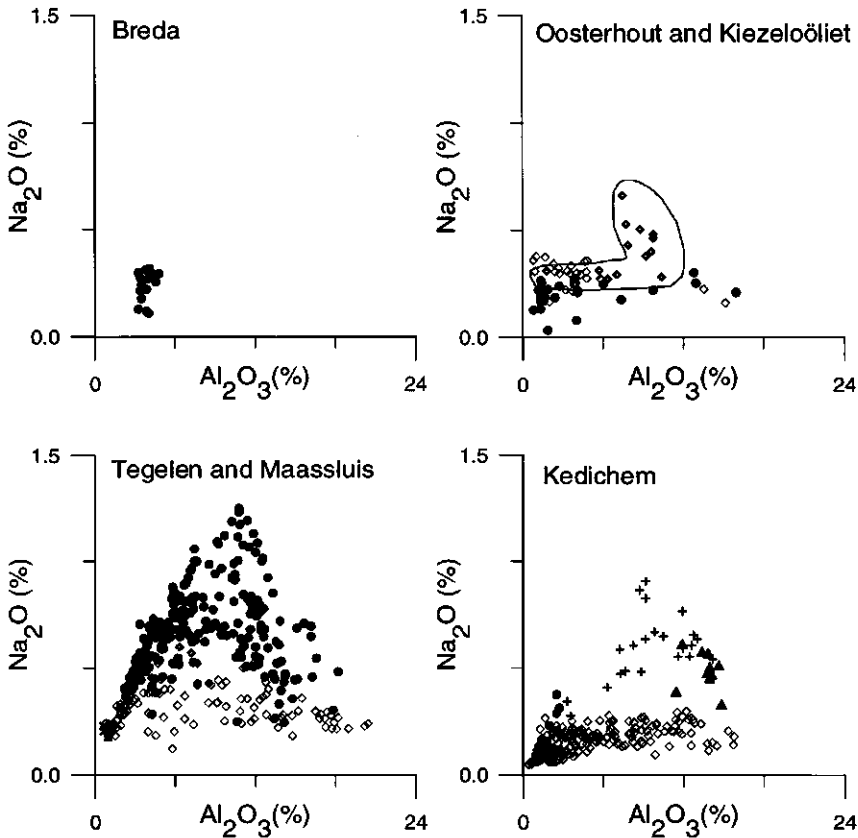
these elements or oxides versus Al_2O_3 to study possible diagenetic controls on the bulk geochemical composition. In order to study the detrital and the diagenetic chemistry, we plotted the geochemical variation separately for each of the four main (groups of) formations: Breda, Oosterhout and Kiezeloöliet, Tegelen and Maassluis, and Kedichem. To facilitate the discussion a further division was made, based on the $\text{Na}_2\text{O}/\text{Al}_2\text{O}_3$ diagrams. This division is presented in the next paragraph, and used in the subsequent paragraphs where the major geochemical variations in our dataset are presented. A mineralogical and sedimentological interpretation of these geochemical variations follows in the Discussion.

The $\text{Na}_2\text{O}/\text{Al}_2\text{O}_3$ diagrams

In bivariate $\text{Na}_2\text{O}/\text{Al}_2\text{O}_3$ diagrams of the Breda, Kiezeloöliet and Oosterhout Formations the data points show a wide scatter around 0.25% Na_2O , irrespective of Al_2O_3 content (Fig. 3.1.5). Only a few samples from the top part of the Oosterhout Formation in boring Sprundel show elevated Na_2O contents. Sediments from the Tegelen Formation show a steeply increasing Na_2O content with increasing Al_2O_3 content until about 10 % Al_2O_3 . At higher Al_2O_3 contents, Na_2O drops again. The Kedichem Formation generally shows a scatter in low Na_2O -contents without a relation to Al_2O_3 , similar to the Breda and Oosterhout Formations.

In both the Tegelen and Kedichem Formations exceptions to the general $\text{Na}_2\text{O}/\text{Al}_2\text{O}_3$ trends occur. The samples from the lower halves of the Tegelen Formation in the Reusel and Sprundel borings show a scatter between 0.25 and 0.5 % Na_2O , irrespective of Al_2O_3 . The same is true for the Tegelen Formation in the borings Ulicoten 2 and 3 and in the upper few meters of the Tegelen Formation in borings Gastel and Gilze. The section of Tegelen Formation intercalated between the Maassluis and Oosterhout Formations in the Sprundel boring shows elevated Na_2O contents which are in the same range as those of the directly underlying top part of the Oosterhout Formation. The upper few meters of Kedichem Formation in the Gilze and Rijsbergen borings, and the lower half of this Formation in Rucphen 2 show higher Na_2O contents than the rest of the formation. These variations in $\text{Na}_2\text{O}/\text{Al}_2\text{O}_3$ trends can be used to subdivide the Kedichem and Tegelen Formation.

Further in this paper, we will use a subdivision based on these $\text{Na}_2\text{O}/\text{Al}_2\text{O}_3$ trends (Fig. 3.1.5). We distinguish within the Oosterhout formation the high-Na group in the formation's top part in the Sprundel section from the low-Na groups in the other parts of this formation. Within the Tegelen formation we distinguish the low-Na sections in the Ulicoten 2 and 3, Gilze and Gastel borings and in the lower parts of the Reusel and Sprundel borings from the high-Na parts of the other Tegelen sections. In addition we discern the section of Tegelen Formation with intermediate Na contents between the Maassluis and Oosterhout Formations in the Sprundel boring. In the low-Na Kedichem formation we plot the high-Na sections of Gilze, Rijsbergen and Rucphen 2 separately.



Legend for Figures 5–9 (in brackets: number of samples):

Kiezeloöliet and Oosterhout Fms:

- Kiezeloöliet (16)
- ◇ Top Oosterhout section Sprundel (14)
- ◇ Rest Oosterhout (28)

Kedichem Fms

- ▲ Top Kedichem section Gilze (10)
- Top Kedichem section Rijsbergen (8)
- + Lower Kedichem section Rucphen 2 (9)
- ◇ Rest Kedichem (237)

Maassluis and Tegelen Fm:

- ◇ Tegelen between Maassluis and Oosterhout (10)
- ◇ Lower Tegelen sections Reusel (43) and Sprundel (20), Tegelen sections Ulicoten 2 (10) and Ulicoten 3 (10), Top Tegelen sections Gilze (10) and Gastel (10)
- Rest Tegelen (231)
- × Maassluis (10)

Figure 3.1.5 Scatterplots of Na_2O versus Al_2O_3 for all samples per formation investigated. The samples can be grouped into a high-Na and a low-Na group. This division roughly follows the stratigraphic subdivision, with high Na-values in the Tegelen formation and low Na-values in the other formations, but exceptions are also indicated. Samples with high Na_2O -contents probably contain abundant sodic plagioclase, whereas it is absent in low-Na samples.

The K₂O/Al₂O₃ diagrams

Bivariate K₂O/Al₂O₃ diagrams show that the samples from the Breda Formation are strikingly different from those of the other formations. The Breda samples show a scatter around 4 % Al₂O₃, while K₂O contents vary between 1 and 3 % (Fig. 3.1.6). The K₂O/Al₂O₃ ratios of the samples with low K₂O contents fall in the range of published values for muscovite, while they approach the K₂O/Al₂O₃ ratio of glauconite in the high-K₂O samples (Newman and Brown, 1987).

The other formations show in general a positive correlation between K₂O and Al₂O₃. In the Oosterhout Formation, K₂O shows a steep increase with increasing Al₂O₃ in the range from 0 to 4%, and a less steep increase above 4% Al₂O₃. The K₂O/Al₂O₃ ratio in the high-Al₂O₃ range varies considerably. The Kiezeloëliet Formation has a constant slope of the mixing line with K₂O/Al₂O₃ ratios comparable to the lowest ratios of the Oosterhout Formation. The Tegelen Formation shows a similar pattern as the Oosterhout Formation, with a high K₂O/Al₂O₃ ratio between 0 and 4% Al₂O₃ which decreases above 4% Al₂O₃, but here the absolute K₂O/Al₂O₃ ratios reach higher values. In the Kedichem Formation, the K₂O/Al₂O₃ ratio shows considerably more scatter, and is often lower than in the other formations. In organic-rich layers in the Kedichem and Tegelen Formations, a drop in the K₂O/Al₂O₃ ratio can often be observed. The samples with lowest K₂O/Al₂O₃ ratios in the Kedichem formation are all organic-rich, as indicated in Fig. 3.1.6. A similar drop can furthermore only be observed in the Ba/Al₂O₃ ratio, but not in any of the other ratios of elements or oxides to Al₂O₃.

The samples from the Tegelen Formation that show low Na contents in the Na₂O/Al₂O₃ diagrams also have lower K₂O/Al₂O₃ ratios (compare Figs. 3.1.5 and 3.1.6). In the Kedichem Formation, the high-Na samples show no clear distinction in K₂O/Al₂O₃ ratio.

The Ba/K₂O diagrams

The Ba/K₂O diagrams show a decrease in Ba content with increasing K₂O for the glauconiferous Breda Formation, whereas the Ba contents increase with increasing K₂O in the Oosterhout, Tegelen and Kedichem Formations (Fig. 3.1.7). The Ba/K₂O ratios are lower in the Oosterhout Formation than in the Kiezeloëliet Formation. The Ba/K₂O ratios of the Tegelen and Kedichem Formations fall in the same range as those of the Kiezeloëliet Formation.

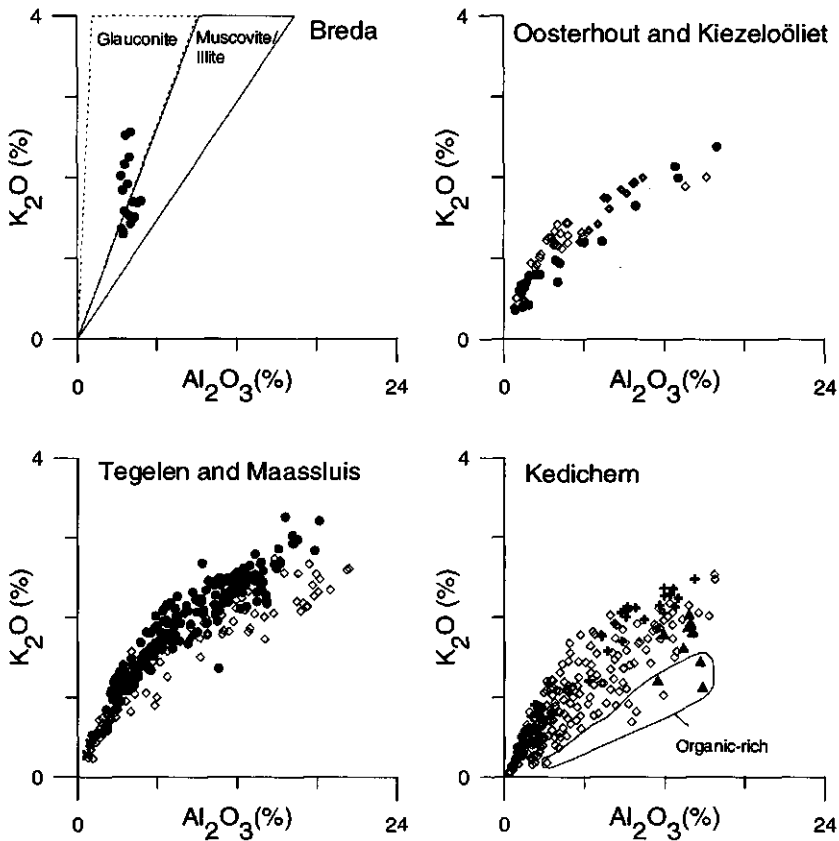


Figure 3.1.6 Scatterplots of K_2O versus Al_2O_3 ; all samples. For the Breda Formation a range of literature values of K_2O/Al_2O_3 ratios for muscovite/illite and glauconite are plotted (Newman and Brown, 1987). The high K_2O -contents in sediments from the Breda formation can be attributed to the presence of abundant glauconite. In the other formations, variations in the K_2O to Al_2O_3 relation can be attributed to variations in the contents of muscovite and illite. For the Kedichem Formation a group of organic-rich samples with extremely low K_2O/Al_2O_3 ratios that are probably due to *in situ* weathering processes are indicated. Legend in Fig. 3.1.5.

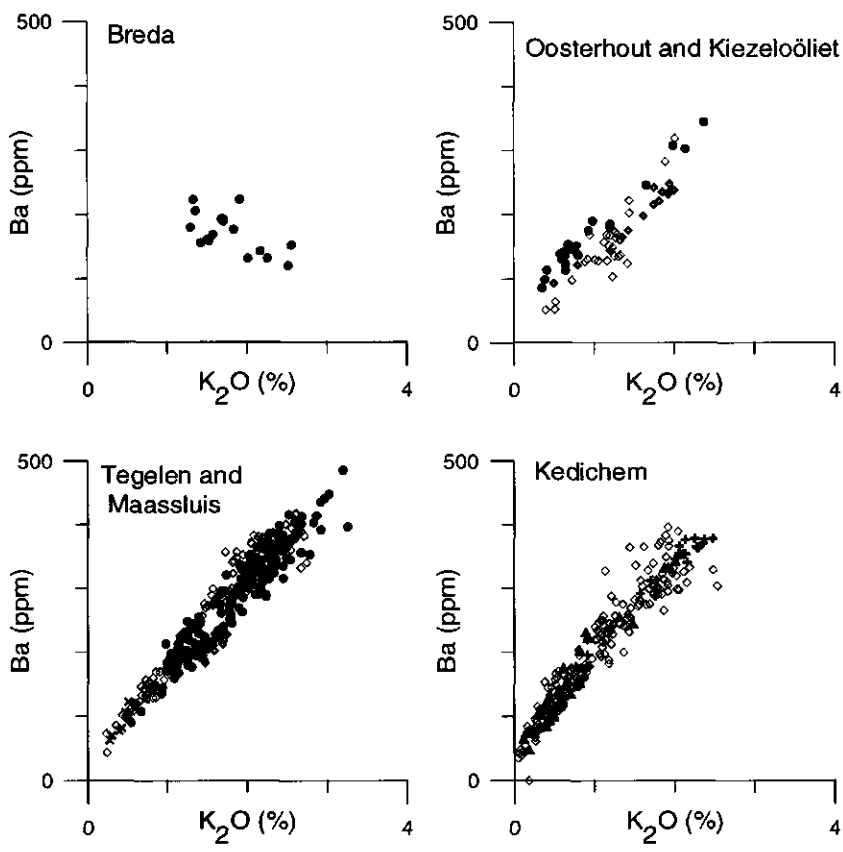


Figure 3.1.7 Scatterplots of Ba versus K₂O; all samples. Note the relatively low Ba/K₂O ratio in the Breda samples, which is attributed to the presence of abundant glauconite. The variation in Ba/K₂O in the Oosterhout formation suggests that locally also glauconite is present. Legend in Fig. 3.1.5.

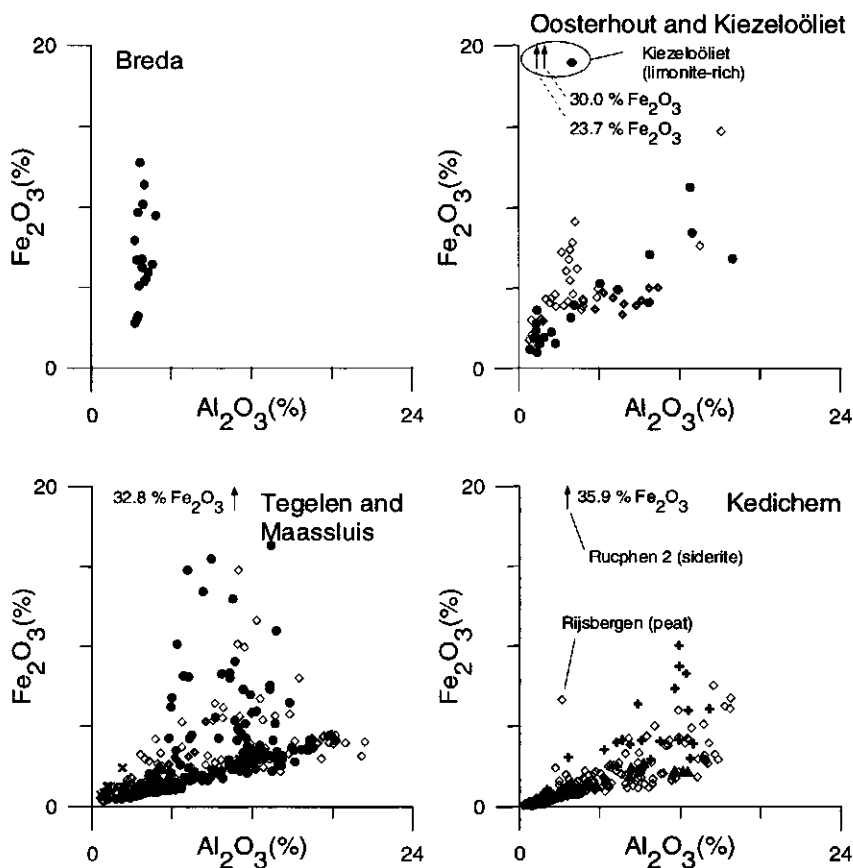


Figure 3.1.8 Scatterplots of Fe_2O_3 versus Al_2O_3 ; all samples. There appears to be a background with an $\text{Fe}_2\text{O}_3/\text{Al}_2\text{O}_3$ -ratio of 1/4. Higher Fe_2O_3 -contents are related to the presence of glauconite (in Breda), siderite, Fe(hydr)oxides and pyrite. Legend in Fig. 3.1.5.

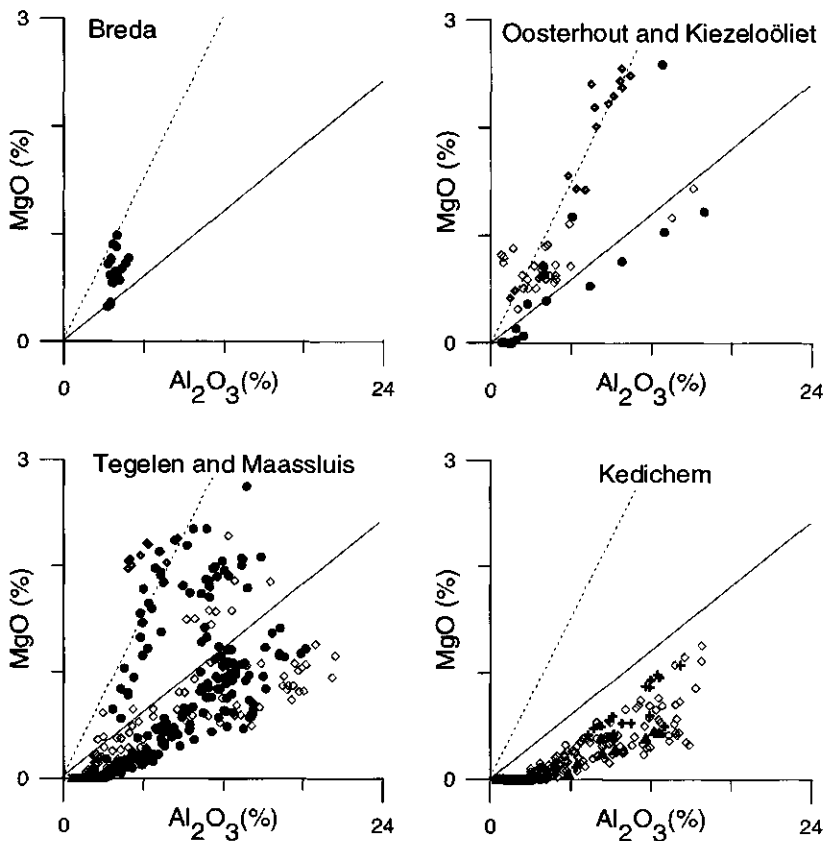


Figure 3.1.9 Scatterplots of MgO versus Al₂O₃; all samples. There appears to be a background with a MgO/Al₂O₃-ratio at or below 1/10 (the solid lines indicate the 1/10 ratio). MgO-contents that exceed this ratio can be linked to the presence of glauconite (in Breda) and dolomite. In the Oosterhout and Kiezeloöliet formations, samples with elevated MgO contents appear to have a MgO/Al₂O₃-ratio around 1/4 (indicated by dashed line). Legend in Fig. 3.1.5.

The Fe₂O₃/Al₂O₃ diagrams

In all formations with the exception of the Breda Formation, there is a basic linear correlation, with an Fe₂O₃ /Al₂O₃ ratio of approximately 0.25, with groups of high-Fe₂O₃ outliers rising up to 35% (Fig. 3.1.8). Note that all Fe, including FeCO₃ is reported as Fe₂O₃. The group of three high outliers in the Kiezeloöliet Formation are from limonite-crusts at the boundary with the Oosterhout Formation. In the Tegelen Formation, the high-Fe₂O₃ (> 0.25 Al₂O₃) group does not relate to the subdivision based on Na₂O/Al₂O₃ diagrams, but is restricted to the borings Gilze, Alphen and Reusel in the east of the study area. In the Kedichem Formation, the sample with ca. 35 % Fe₂O₃ is from a 2-cm-thick siderite layer in a clay layer clay in Rucphen 2. Other high-Fe₂O₃ outliers in this formation are from a peat layer in Rijsbergen, and from the lower half of Rucphen 2.

The MgO/Al₂O₃ diagrams

In the MgO/Al₂O₃ diagrams of the Oosterhout and Kiezeloöliet Formations, two groups can be distinguished which both show a linear correlation between MgO and Al₂O₃ (Fig. 3.1.9). One group, consisting of parts of the Kiezeloöliet and of the Oosterhout sections has MgO/Al₂O₃ ratios of ca. 1:4. The other samples have a ratio of ca. 1:10. In the Tegelen Formation, a similar distinction can be made, but here the high-MgO/Al₂O₃ group shows more variation. There is no correlation between the subdivision in high and low-MgO/Al₂O₃-groups and in high and low-Na₂O groups. The high-MgO/Al₂O₃ group however is only found in the high-Fe₂O₃ sections of the borings Gilze, Alphen and Reusel (cf. Fig. 3.1.10), and in the calcareous Tegelen deposits between the Oosterhout and Maassluis Formations in the Sprundel boring. The MgO/Al₂O₃ contents of all the samples from the Kedichem Formation are comparable to those of the 1:10 groups in the Tegelen, Oosterhout and Kiezeloöliet Formation.

The sulfur-contents

In all formations the S-content is low (< 0.5%) with sporadic isolated peaks (Fig. 3.1.11 a,b). These are often but not exclusively related to organic-rich layers. Taken the Reusel and Sprundel borings together, these S-peaks are highest in the Oosterhout, the Kiezeloöliet and lower half of the Tegelen Formation (10000-12000 ppm) and decrease upwards in the upper parts of the Tegelen Formation and in the Kedichem Formation. In boring Rucphen 2, however, the lower half of the Kedichem section shows increased S contents up to 15000 ppm throughout (Fig. 3.1.11 c), and in the peat layer of the Kedichem section in boring Rijsbergen the highest S content of the study area is found: 49000 ppm. All of these S peaks coincide with increases in As content (see also Chapter 5).

A comparison of the S profiles with the Fe₂O₃ profiles shows that most of the Fe₂O₃ peaks do not show elevated S contents and vice versa (Figs. 11a-c).

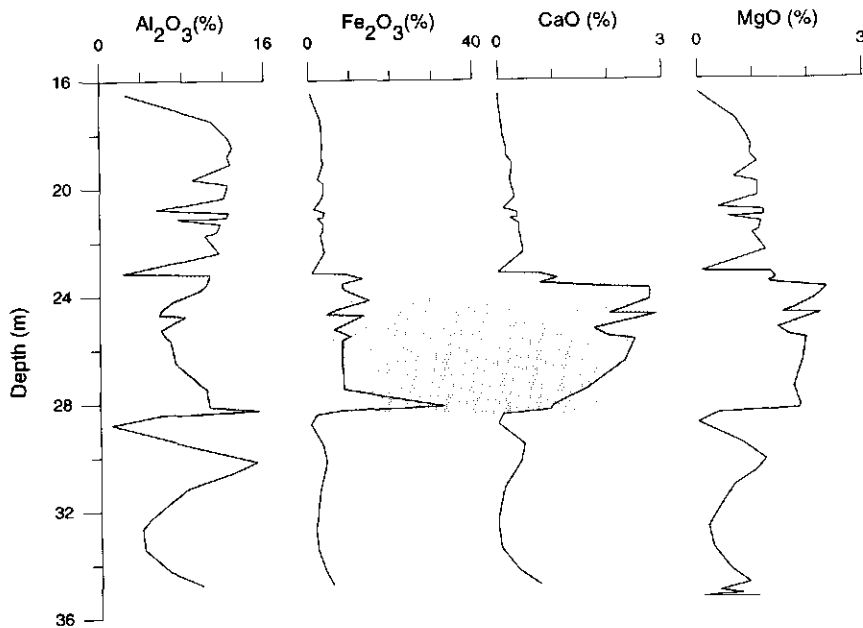
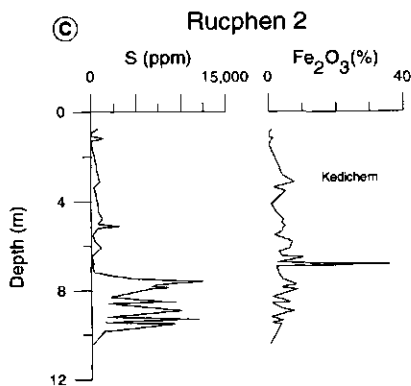


Figure 3.1.10 Boring Reusel, Tegelen Formation 16-36 m. Depth profiles of Al_2O_3 , Fe_2O_3 , CaO and MgO . The shaded area marks a section with increased Fe_2O_3 , CaO , and MgO contents as a result of the presence of siderite, calcite and dolomite.



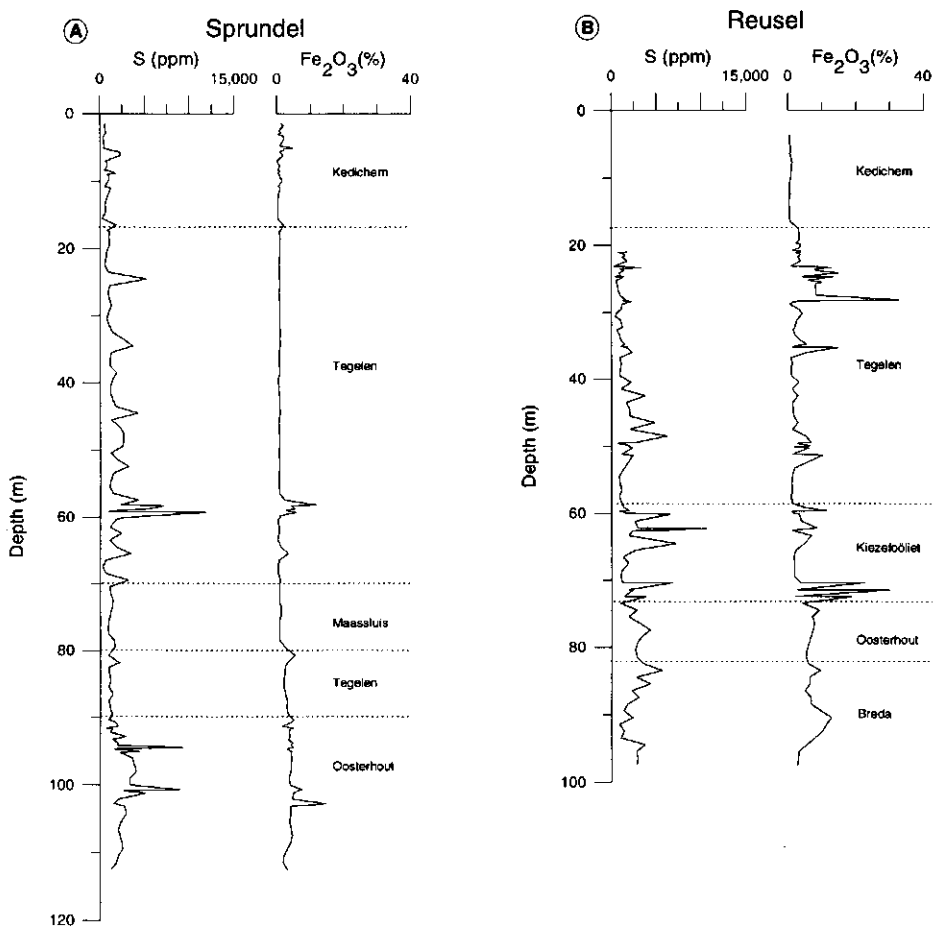
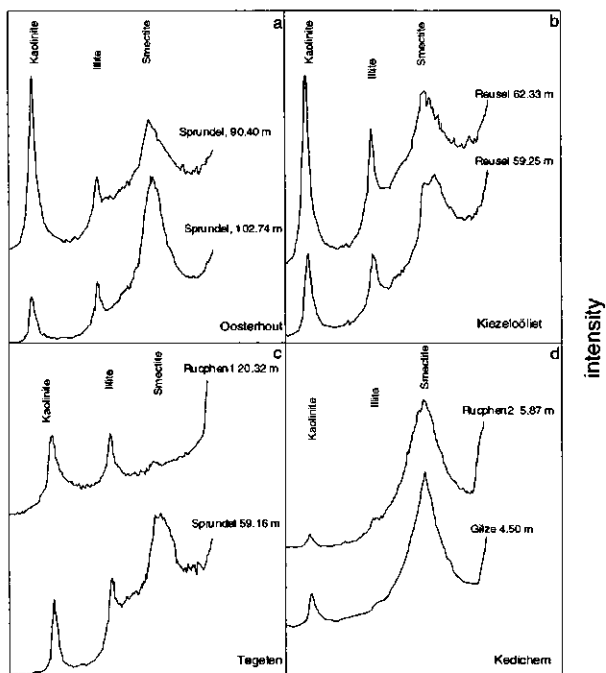


Figure 3.1.11 Depth profiles of S and Fe₂O₃ in borings Sprundel (A), Reusel (B) and Rucphen 2 (C; previous page). S-contents are indicative for the presence of pyrite, whereas the Fe₂O₃-contents are related to pyrite or siderite. The elevated Fe-contents in boring Reusel between 70 and 73 m depth, however, are related to the presence of Fe(hydr)oxides. Note enlarged depth scale of Rucphen 2. Formation names are indicated.



26

Figure 3.1.12 X-ray diffractograms of samples with clay mineralogy typical for the Oosterhout (A), Kiezeloöliet (B), Tegelen (C) and Kedichem (D) Formations. Horizontal axis: 2θ , vertical axis: intensity. ‘Kaolinite’, ‘Illite’ and ‘Smectite’ at respectively 7, 10 and 14 Å.

Clay mineralogy

The samples for clay-mineral analyses were chosen so that enough representative analyses were obtained from the Oosterhout, Kiezeloöliet, Tegelen, and Kedichem Formations (no clay-rich samples were recovered from the Maassluis and Breda Formations). As illustration, two representative samples of each of the four formations are presented in Fig. 3.1.12.

The the Kiezeloöliet and the Oosterhout Formations are characterized by a mixture of moderately to well-crystallized smectite, with illite and kaolinite (Fig. 3.1.12 a,b). The kaolinite content varies greatly. In the lower units of the Tegelen Formation (such as Sprundel; 59.16 m), the clay composition is dominated by well-crystallized smectite with illite and kaolinite. In the upper units of the formation (such as Rucphen 1; 20.32 m) the clay is dominated by illite and kaolinite (Fig. 3.1.12c). The smectite contents in these units are low and variable and the smectite itself is poorly crystallized. In organic-rich layers, the illite content tends to decrease whereas that of smectite is higher. The clays of the Kedichem Formation in general show high contents of well-

crystallized smectite with some additional kaolinite (Fig. 3.1.12d). Locally they are illite-kaolinite dominated with low contents of poorly crystallized smectite.

Heavy minerals

The heavy-mineral profile of boring Rucphen 2 was studied to assess whether the variations in geochemistry ($\text{Na}_2\text{O}/\text{Al}_2\text{O}_3$) and clay mineralogy which do not coincide with a formation boundary could be linked to provenance-change. The heavy-mineral profile of the Kedichem Formation in this boring (Fig. 3.1.13) shows an upper unit with an extremely stable composition, whereas the lower unit has a mixed heavy-mineral composition (cf. Kasse, 1988; Woensdrecht and Hoogerheide Members of the Tegelen Formation). This change is consistent with the above-mentioned change in Na_2O_3 - Al_2O_3 -trend. A few decimeters below the change in the Na_2O - Al_2O_3 -trend, the clay mineralogical composition changes from smectite-dominated to an illite-kaolinite-smectite mixture.

Discussion

Interpretation of $\text{Na}_2\text{O}/\text{Al}_2\text{O}_3$ diagrams

The relation between Na_2O and Al_2O_3 seems to be controlled by mineralogical properties. The samples with low Al_2O_3 content are generally coarse-grained because of the abundance of quartz in the coarse fractions, whereas samples high in Al_2O_3 are clay-rich (Fig. 3.1.4). The characteristic peak in the Na_2O - Al_2O_3 trend in the upper layers of the Tegelen Formation (Fig. 3.1.5; 'Rest Tegelen') falls around 10 % Al_2O_3 . Samples with these percentages of Al_2O_3 are silts and very fine sands. As sodic plagioclase is the only major Na-bearing mineral in Dutch Upper Cenozoic sediments (Van Baren, 1934), this suggests that sodic plagioclase is common in the silt and very fine sand fraction of these layers. The positive correlation in the low- Al_2O_3 range reflects a mixing range of relatively fine-grained sodic plagioclase with coarse quartz. In this range, increasing Na_2O content is caused by increasing contents of sodic plagioclase. The fact that the $\text{Na}_2\text{O}/\text{Al}_2\text{O}_3$ ratio is much lower than that of a pure albite-quartz mixing line (cf. Fig. 3.1.1) is probably caused by the presence of additional Al_2O_3 in the micas in the fine sand fraction (see below). As the CaO content does not show increased values in the fine sandy and silty samples it is unlikely that significant amounts of Ca-rich, Na-poor plagioclase are present. The negative correlation in the high- Al_2O_3 range corresponds with dilution of sodic plagioclase with Na-poor clay in the very fine grain size classes.

The elevated but lower Na_2O contents in the top part of the Oosterhout Formation in boring Sprundel suggest that these sediments also contain sodic plagioclase in the fine sand fraction in abundancies comparable to those of the Tegelen-sediments intercalated between the Maassluis and Oosterhout Formation in the same boring. The low Na_2O contents in the Kedichem Formation indicate that sodic feldspar is absent or rare. The sporadic occurrences of elevated Na_2O -contents point to localized sodic plagioclase rich sediments.

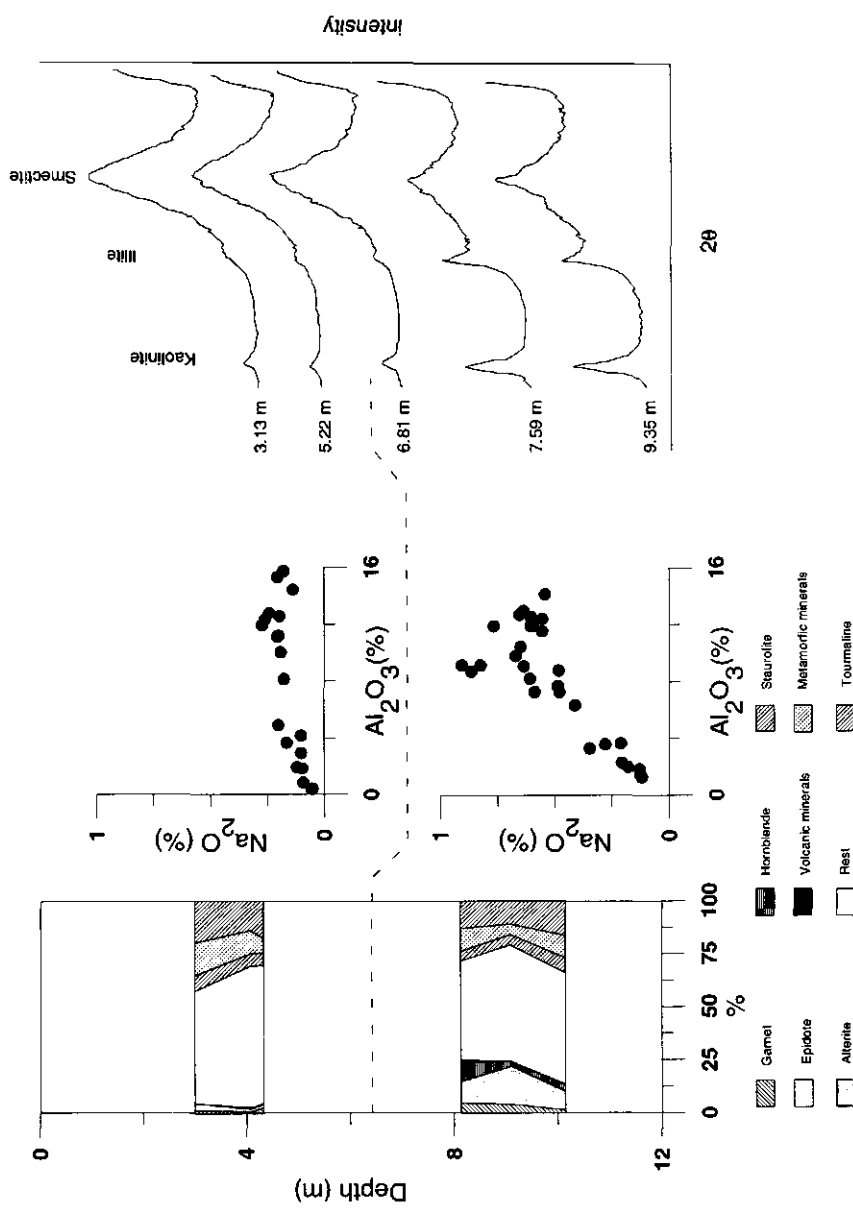


Figure 3.1.13 Heavy mineralogy, Na/Al relation and clay mineralogy of the Kedicheh Formation in boring Rucphen 2. See 'Introduction' for heavy-mineral names. Dashed line indicates boundary between high and low Na_2O contents. High Na_2O contents correlate with a mixed heavy mineral composition, whereas low Na_2O -contents correlate with a stable heavy-mineral suite. Somewhat below the boundary between high and low Na_2O -contents, the clay mineralogy shifts from smectite-dominated to kaolinite-illite-dominated.

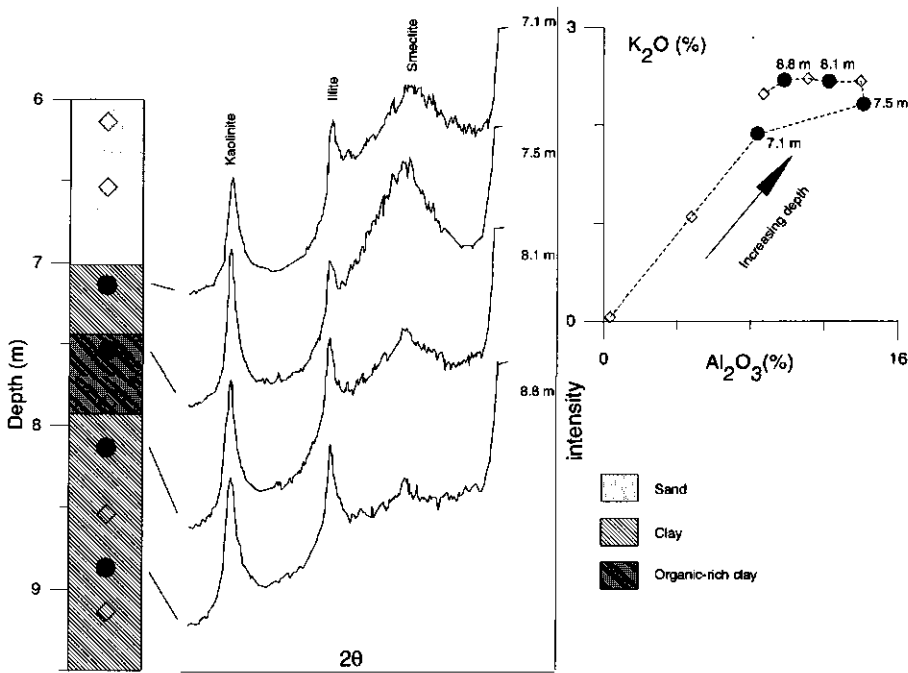


Figure 3.1.14 K-Al relation and clay mineralogy around an organic-rich clay layer in boring Rijsbergen. The ratio K_2O/Al_2O_3 decreases in the organic-rich layer.

Interpretation of K_2O/Al_2O_3 diagrams

On the basis of the K_2O/Al_2O_3 diagrams, the sediments can be subdivided into a number of groups: one (1) with a positive correlation between K_2O and Al_2O_3 and a characteristic change in K_2O/Al_2O_3 ratio around 4% Al_2O_3 (Tegelen and Oosterhout Formations), one (2) with a lower K_2O/Al_2O_3 ratio and lacking the characteristic knickpoint at 4% Al_2O_3 (Kiezeloöliet), one (3) with a large spread in K_2O/Al_2O_3 ratios but still with a positive K-Al correlation and a knickpoint at 4% Al_2O_3 (Kedichem), and one (4) with high K_2O contents and no correlation between K_2O and Al_2O_3 (Breda Formation) (Fig. 3.1.6).

The characteristic change in K_2O/Al_2O_3 ratio around 4% Al_2O_3 in the Kedichem, Tegelen and Oosterhout Formations can be explained by grain size related variations in the mineralogy. Between 0 and 4% Al_2O_3 , the sediment is coarse-grained and the K_2O/Al_2O_3 ratio falls in the range of quartz-muscovite mixtures. Above 4% Al_2O_3 the material is finer and contains more clay, consisting of mixtures of illite, kaolinite and smectite, resulting in a lower K_2O/Al_2O_3 ratio.

The variation in K_2O/Al_2O_3 ratios in the Oosterhout Formation can probably be attributed to variations in the kaolinite content of the clay (cf. Fig. 3.1.12 a). It is not clear however why a

similar difference in kaolinite content in the Kiezeloöliet Formation does not seem to affect the K_2O/Al_2O_3 ratio. The lack of the bend at 4% Al_2O_3 in the Kiezeloöliet may be attributed to lower contents of micas in the sand fraction when compared to the Oosterhout Formation.

The high K_2O/Al_2O_3 ratio in the Tegelen Formation if compared to the Oosterhout and Kedichem Formation can be linked to the macroscopic observations of relatively large amounts of micas, and to the dominance of illite in the clay fraction (Fig. 3.1.12). There are two groups of occurrences of relatively lower K_2O/Al_2O_3 ratios in the Tegelen Formation. In the first group these ratios coincide with lower Na_2O contents (Reusel, Sprundel, Gastel, Gilze and Ulicoten 2 and 3). This group increased contents of well-crystallized smectite which apparently lowered the K_2O/Al_2O_3 ratio through dilution. As this indicates major mineralogical changes in both the sand and the clay fraction, it suggests a change in sediment provenance. The second group consists of localized drops in K_2O/Al_2O_3 ratio in organic-rich layers. Usually, these drops are accompanied by an increase in the contents of poorly crystallized smectite and a decrease in illite in the clay fraction (Fig. 3.1.14). This indicates that in these organic-rich layers illite is weathered to smectite, probably as a result of attack by organic acids, resulting in a net loss of K_2O from the clay fraction.

The, in general, lower K_2O/Al_2O_3 ratios in the Kedichem Formation can be attributed to the high contents of smectite in the clay fraction, although also here local decreases in K_2O/Al_2O_3 ratio occur in organic-rich layers. Typical Kedichem clays with high contents of well-crystallized smectite have a K_2O/Al_2O_3 ratio of ca. 1:12. The samples with the highest K_2O/Al_2O_3 ratios have higher illite and kaolinite contents. The samples distinguished by their high Na_2O contents are not significantly different from the rest of the Kedichem Formation, but high Na_2O contents in general correlate with high K_2O/Al_2O_3 ratios, which strengthens the argument for mineralogical change.

The trend in the Breda Formation is not comparable to those in the Oosterhout, Tegelen and Kedichem Formations because Al_2O_3 is constant, but K_2O varies considerably. The variations in K_2O content can be linked to the macroscopically observed variations in glauconite content.

Interpretation of Ba/ K_2O diagrams

In general, Ba and K_2O show a linear correlation, indicating that Ba substitutes for K in most K-bearing minerals. However, if K-bearing minerals are formed in an environment where no Ba is available, no Ba will substitute for K_2O . Of the sediments under consideration, all formations show a linear correlation Ba/ K_2O with the exception of the Breda Formation where Ba is negatively correlated with K_2O (Fig. 3.1.7). This indicates that the major K-bearing minerals in this formation, viz. glauconite, were formed in a Ba-poor environment. Glauconite is formed in a marine depositional environment by biological activity (Hillier, 1995), where Ba is unavailable as a result of scavenging by microorganisms and subsequent immobilization by the formation of barite ($BaSO_4$; Van Santvoort and de Lange, 1996; Deer et al., 1992). The lack of substitution of Ba for K therefore can be attributed to the unavailability of Ba during the formation of glauconite. This also suggests that generally the Ba/ K_2O relation indicates the presence of glauconite. Therefore the relatively low Ba-contents in relation to K_2O in part of the Oosterhout Formation could indicate the presence of glauconite, which is indeed not uncommon in the Oosterhout Formation (Zagwijn and Van Staaldin, 1975).

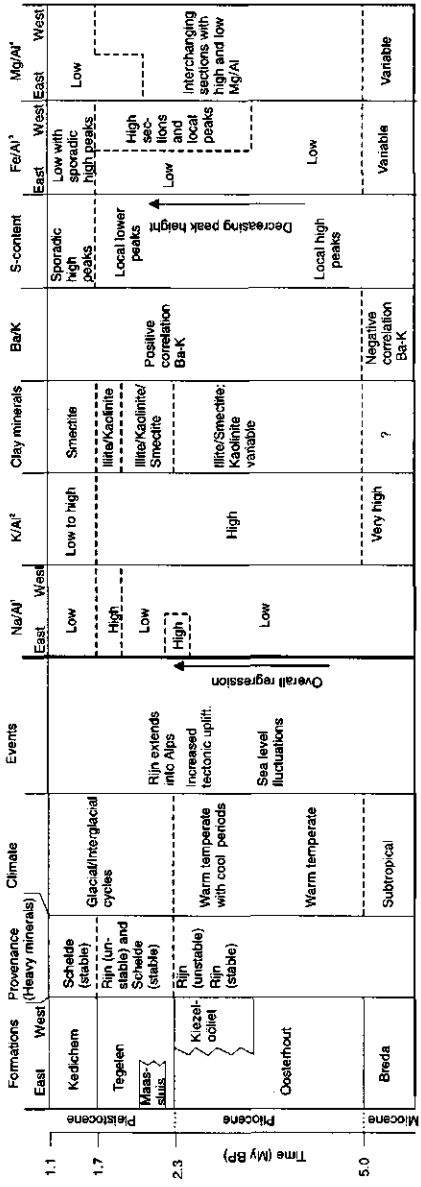
Interpretation of the Fe₂O₃/Al₂O₃ and S diagrams.

The background Fe₂O₃ /Al₂O₃ ratio of approximately 0.25 lies close to the ratio generally regarded as normal for detrital siliclastic sediments, and represents the Fe-content of phyllosilicates (e.g. Dellwig et al., 1996). The Fe-contents in the Breda Formation exceed this background as a result of the relative abundance of glauconite. In the other formations, Fe-contents can exceed the 0.25 Fe₂O₃ /Al₂O₃ ratio as a result of diagenetic processes which led to neoformation of secondary minerals.

The presence of peaks of S and associated As as recorded in the Oosterhout, Kiezeloëliet, Tegelen and Kedichem Formations indicates the presence of pyrite. This is confirmed by a series of XRD and micromorphological observations (Chapters 3.2 and 4.2). On the whole, there is a lack of correlation between S and Fe₂O₃ peaks (Fig. 3.1.11) because the vast variation in carbonate- and oxide-derived Fe₂O₃ dwarfs the pyrite-Fe content. This shows that most of the Fe is present in non-sulfidic Fe-minerals. XRD and micromorphological observations show that in the Tegelen Formation most of the Fe-enrichments are in the form of siderite (FeCO₃). In the Kiezeloëliet Formation, the major part of the Fe is present as (hydr)oxides. The localized high S-values in the Kedichem Formation (Rucphen 2, Fig. 3.1.11 c and the Rijsbergen-peat) are probably pyritic, but in the latter case the XRD analyses show that gypsum is present also.

Interpretation of MgO/Al₂O₃ diagrams

In the Tegelen Formation, the striking division in high-MgO/Al₂O₃ and low-MgO/Al₂O₃ can be linked to the presence of carbonates. All siderite-rich sections show elevated MgO/Al₂O₃ ratios, as does the calcareous Tegelen section between the Oosterhout and Maassluis Formations in the Sprundel boring. The Mg could be partly present as minor substituent for Ca and Fe in calcite and siderite respectively, but XRD-measurements and SEM-analyses (Chapter 4.1) show also the presence of minor amounts of dolomite in some of the samples from siderite-rich sections. Therefore it is likely that the division in high-MgO/Al₂O₃ and low-MgO/Al₂O₃ sections in the Tegelen Formation is in fact a division in relatively dolomite-rich and dolomite-poor sediments. The presence of high and low-MgO/Al₂O₃ sections in the Oosterhout and Kiezeloëliet Formations suggests that here also dolomite-bearing sections occur.



¹Low: Na₂O = 0 - 0.4 %
 High: Na₂O = 0-1.2 %

²Low: K₂O/Al₂O₃ = 0.33 - 0.06
 High: K₂O/Al₂O₃ = 0.33 - 0.11
 Very high: K₂O/Al₂O₃ = 0.67 - 0.33

³Low: Fe₂O₃/Al₂O₃ = 0.2 - 0.3
 High: Fe₂O₃/Al₂O₃ > 0.3

⁴Low: MgO/Al₂O₃ < 1:10
 High: MgO/Al₂O₃ > 1:10

Figure 3.1.15 Correlation of geological history with geochemistry and clay mineralogy in the study area.

Geochemistry and sedimentation history

The geochemistry and sedimentation history of the Late Cenozoic in the study area are summarized in Fig. 3.1.15. The marine character of the Breda Formation is clearly illustrated by the combination of high contents of K_2O , MgO and Fe_2O_3 and low Ba/K_2O -ratios, which characterizes the presence of glauconite.

The marine depositional environment of the Oosterhout Formation is reflected by the presence of shells or shell debris, causing high CaO -contents. Apart from that, the relatively low Ba/K_2O ratio in part of the Oosterhout sediments probably glauconite formed in a marine environment. The differences in Ba/K_2O ratio that occur in the clays of the Oosterhout Formation indicate that glauconite formation did not occur uniformly throughout the formation. As in modern deltas this K_2O -enrichment increases with increasing distance from the river mouth (Porrenga, 1967), lack of diagenetic enrichment of K_2O could suggest a more littoral depositional environment locally in the Oosterhout Formation. The shifts between deeper marine and more littoral environments in the Oosterhout Formation can be interpreted as an expression of one of the regressional and transgressional cycles during the Pliocene (Van den Berg, 1996). The overall large-scale regression or delta progradation is reflected in the sequence from the marine sediments of the Oosterhout Formation, to the littoral or continental Kiezeloëliet deposits in the Reusel boring.

The stratigraphical deepest occurrences of Na_2O -rich sediment in the studied sections are in the top part of the Oosterhout Formation and in the overlying Tegelen Formation, indicating a transition from plagioclase-poor to plagioclase-rich deposits. The shift towards plagioclase-rich sediments coincides with the change from stable to unstable heavy minerals around the Pliocene-Pleistocene boundary which marks the change in the provenance of Rijn sediments from regional to Alpine. As sodic plagioclase is easily weathered, its presence in sedimentary deposits indicates that the material is relatively fresh. The lack of sodic plagioclase in the Breda, Oosterhout and Kiezeloëliet Formations, as deduced from the low Na -contents, is consistent with prolonged weathering in the warm, humid climate during the Miocene and Pliocene (Zagwijn, 1960; Buurman, 1972). The increase in Na -content thus reflects the input of fresh sediment by the headward extension of the Rijn into the Alps, the onset of glaciations and increased tectonic activity around the Plio-Pleistocene transition.

The $Na_2O-Al_2O_3$ diagrams of the Pleistocene deposits show an overall succession from plagioclase-poor (lower sections Tegelen Formation) to plagioclase-rich (upper sections Tegelen Formation) to plagioclase-poor (Kedichem Formation). Similar successions can be observed in the K_2O/Al_2O_3 diagrams and the clay mineralogy. The K_2O/Al_2O_3 ratios rise somewhat from the lower to the upper half of the Tegelen Formation and subsequently decrease and become more variable in the Kedichem Formation. The clay mineralogy shifts from illite-kaolinite-smectite to illite-kaolinite to smectite-dominated. This reflects the succession in the sand provenance from Schelde (Merksplas Sands) to Rijn (Turnhout and Rijkevorsel Members) and back to Schelde (Gilze Member) as described on the basis of heavy minerals by Kasse (1988). Apparently sediments of Schelde provenance have low Na_2O contents, relatively low K_2O/Al_2O_3 ratios and a clay

mineralogy dominated by well-crystallized smectite, whereas Rijn sediments have high Na₂O contents, high K₂O/Al₂O₃ ratios and a clay mineralogy dominated by illite and kaolinite.

Low Na₂O contents, low K₂O/Al₂O₃ ratios and smectite-rich clays in the Tegelen sections in the borings Ulicoten 2 and 3 and in the top parts of the borings Gilze and Gastel, and elevated Na₂O-contents in the lower section of the Kedichem Formation in Rucphen 2 (Fig. 3.1.13) indicate that the transition from Rijn to Schelde provenance locally does not coincide with the lithological and sedimentological formation boundary between the Tegelen and Kedichem Formations. This could be due to localized sediment supply or reworking of Schelde material during deposition of the Tegelen Formation, and of Rijn material during deposition of the Kedichem Formation. The elevated Na₂O contents in the top part of the Kedichem Formation in Gilze and Rijsbergen can be due either to reworking of Tegelen material or to increased Rijn influence.

It is striking that the siderite-rich sections in the Tegelen Formation are concentrated in the east of the study area (Gilze, Alphen, Reusel). Siderite can only be formed in a reducing environment without sulfate, as the presence of (sea-water) sulfate would cause the formation of pyrite (e.g. Postma, 1982). Therefore the occurrence of localized S peaks in siderite-rich sections in the Oosterhout, Kiezeloöliet and especially the Tegelen Formations could indicate a fresh-water depositional environment with small marine incursions. However, high S-contents are also known from methanogenic organic-rich settings (see Chapter 4.1). The concentration of siderite-rich sections in the east of the area suggests a decreasing marine influence from west to east. In the easternmost area there was not sufficient S to form a major pyritic phase, and instead siderite was formed (cf. Postma, 1982). Kasse (1988) interpreted the presence of siderite underneath a pyrite-bearing peat in quarry Ravels, south of Baarle-Nassau, as an indicator for a transition from a fresh-water to a brackish or saline depositional environment in the top part of the Tegelen Formation. Pyrite formation, however, depends not only on the Fe and sulfate availability but also on sedimentation rates, biological activity and the availability and degradability of organic matter. Several cases have been described recently where siderite was formed alongside pyrite in marine coast-near settings (Aller and Michalopoulos, 1996; Haese et al., 1997). Therefore the presence of siderite or the absence of pyrite on their own are not diagnostic for continental depositional environments. The way the formation of siderite is linked to that of calcite and dolomite is investigated further in Chapter 4.1.

The presence of considerable amounts of S in the Kiezeloöliet Formation and locally in the Kedichem section of Rucphen 2 and in the peat of the same formation in Rijsbergen are indications for at least localized marine influences during deposition, and can be interpreted as resulting from minor marine transgressions over coast-near fluvial deposits.

Conclusion

The observations and interpretations in the foregoing Discussion as summarized in Figure 3.1.15. show that grain size related variations in concentrations and ratios of Al₂O₃, K₂O, Na₂O and Ba in scatter diagrams provide information about the contents of light minerals like muscovite, glauconite and sodic plagioclase, and about the clay-mineralogical composition in a sedimentary unit. This information correlates well with macroscopical observations and XRD-measurements and indirectly with heavy-mineral counts. The scatter diagrams therefore can be used to determine boundaries between sedimentary units with provenance-related mineralogical differences.

Diagenetic processes which are indicative for depositional environments can be identified by using scatter diagrams and depth profiles of Al, Fe, Ca, Mg and S. In this way, sediment geochemistry combined with a few representative mineralogical analyses can be used to trace transgressions and regressions, major shifts in provenance and the impact of weathering.

3.2 Geochemical compositional changes of the Pliocene-Pleistocene transition in fluviodeltaic deposits in the southeastern Netherlands.

D.J. Huisman
G. Th. Klaver
A. Veldkamp
B.J.H. van Os

Abstract

At the Pliocene-Pleistocene transition, the sediment composition of Rijn-derived sediments changes from a stable to an unstable heavy-mineralogy. This change has previously been attributed to a decrease in weathering intensity due to climatic cooling, and to a change in the Rijn sediment provenance from local to Alpine-derived.

We studied the geochemistry of several sections with Pliocene and Early Pleistocene Rijn deposits, and one section (BTAB) in more detail using clay mineralogical and micromorphological techniques to study the exact nature and the cause of this change, and associated changes in sedimentary setting. We found a general increase in Na₂O- contents at the local to Alpine provenance shift, which can be attributed to the Alpine source supplying fresh, sodic plagioclase-rich material in stead of the local, strongly weathered sediments. There is a general trend of increasing K₂O/Al₂O₃ from the Pliocene to the Early Pleistocene that can be attributed to a similar decrease in degree of weathering. However, this trend is disturbed by the loss of K from clay minerals during post-depositional *in situ* weathering in organic-rich layers. In the Upper Pliocene BTAB section, we found a clear transition from kaolinite and high TiO₂/Al₂O₃-ratios to smectite-rich material with lower TiO₂/Al₂O₃ that coincides with the local to Alpine provenance shift. However, Early Pleistocene sediments have TiO₂/Al₂O₃-ratios that are similar to the ones before the transition so this effect is not consistent. Local high TiO₂-anomalies, caused by preferential sorting and concentration of especially rutile in placer-like deposits are found in most Pliocene sections, but they are absent in the Upper Pliocene and Lower Pleistocene Alpine-derived deposits. Overall, the detrital geochemical variation in these deposits are primarily controlled by the source of the sediment, and hence the large-scale tectonic setting, whereas climatic control is limited

The Pliocene organic-rich layers were originally formed in a fresh-water fluvial environment. Nevertheless they show high concentrations of S due the presence of abundant pyrite. The pyrite was formed as a result of inundation by saline water during short-termed flooding events like spring tides or storm floods, after or alternating with one or more desiccation phases.

Introduction

Sediment composition is determined by source rock composition, nature and intensity of weathering processes, hydrodynamic sorting and the diagenetic depositional environment during and after deposition (Johnsson, 1993; Nesbitt et al., 1996; Nesbitt et al., 1997; Roser and Korsch, 1986). The composition of the source rock determines the range of possible compositions in the

sediment derived from it: Ideally, the composition of immature sediments that consist mainly of rock fragments will be proportional to the relative contribution of each source rock, independent of grain size (cf. Veldkamp and Kroonenberg, 1993). However, the composition of most siliclastic sediments has been severely altered as a result of weathering processes before and during transport (Kroonenberg, 1992; Cox et al., 1995; Nesbitt et al., 1996). The strongest weathering occurs in areas with warm, moist climates and small erosion rates through little tectonic uplift. Weathering causes first the breakdown of plagioclase-feldspar and, to a lesser extent, K-feldspar, and the formation of clay minerals. Nesbitt and Young (1996) consider the association of clay-mineral-rich muds and quartz sands in the lower reaches of major river systems as proof that weathering was the major factor in removing feldspars from the original source mineral-suite. As a result of the removal of feldspars by weathering and the formation of clay minerals, the bulk chemical composition of the weathered sediments will be depleted in Na and (subsequently) K, and enriched in Al. As a result of mixing and sorting processes in a fluvial system, however, Al will be concentrated in the clay fraction, whereas the sand fraction will consist mainly of (quartz-)Si. Presence of plagioclase and K-feldspar minerals together with quartz in the sand fractions indicates therefore that these sediments did not undergo severe chemical weathering, but most likely suffered mainly mechanical breakdown. Prolonged and/or more intensive weathering would deplete Si and K by transforming 2:1 clay minerals (smectite, illite) and micas to 1:1 clays (kaolinite) and dissolution of quartz. Al and Ti contents rise due to residual enrichment of detrital Al, Ti-rich minerals and neoformation of kaolinite, gibbsite and anatase (Milnes and Fitzpatrick, 1989; Righi and Meunier, 1995; Tebbens et al., 1996). However, high contents of Ti do not necessarily result from severe weathering. Firstly, Ti occurs as a minor element in clays. As a result of this, clay will have higher Ti-contents (up to approx. 1% TiO₂) than sand. Secondly, winnowing and sorting processes may concentrate heavy minerals, including Ti-oxides, resulting in elevated Ti-contents. K can be depleted after deposition by the transformation of illite to smectite under the influence of organic acids in organic-rich layers (see Chapter 3.1).

Depositional environment can be recorded in the effects of low-temperature diagenetic processes. Pyrite is most abundant in deposits influenced by saline or brackish water as a result of which marine sediments may show combined enrichments of Fe and S (Casagrande, 1987; Cohen et al., 1984). Siderite is mostly confined to high-Fe, low-S continental sediments (cf. Postma, 1982; see also Chapter 4.1). Note that pyrite-rich sediments need not be deposited in a marine environment, but that short-termed flooding (e.g. during spring-tides or storms) of terrestrial organic-rich sediments with saline or brackish water may cause significant accumulations of pyrite (see Chapter 4.1 and Wright et al., 1997).

In this Chapter we want to study the bulk geochemical effects of a major change in provenance and climate that occurred in the Rijn system at the Pliocene-Pleistocene boundary, and the relative importance of source area, weathering, sorting and diagenesis in determining sediment composition. We chose to study the contents of Al, K, Ti, Na, Fe and S as they are most likely to show variations as a result of these changes: Al is representative of clay contents and is used as grain size indicator. Elements like V, Ga, Y, Rb and the heavy metals are generally well correlated with Al because they also occur mainly in phyllosilicates. Na and K represent plagioclase, K-feldspar and micas/illite which are destroyed by weathering processes (Roser and Korsch, 1986; Cox et al., 1995; Chapter 3.1). The contents Ba are in general linearly correlated with K contents.

Ti is concentrated in primary heavy minerals (ilmenite, rutile, anatase) and can be enriched during severe weathering as secondary anatase or through residual enrichment. It shows a close correlation with the Nb-content. To distinguish effects of weathering, provenance, etc. from grain size effects, we use plots of K, Na and Ti against Al, with Al serving as a representation of the clay content. Fe and S contents reflect the depositional environment, where we interpret that higher contents of Fe and S are indicative for deposits influenced by sulfate reduction due to marine influence. Low S- and high Fe-contents apparently did not experience significant sulfate reduction processes, and are regarded as continental deposits.

In Huisman et al. (1996) and Van Os et al. (1996) we presented a general trend of increasing K- and Na-contents and decreasing Ti-contents with time from Brunssumian to Reuverian to Tiglian sediments, and interpreted this trend as resulting mainly from the general climatic cooling during this period. These results were based mainly on two sections from the Limburg area; one (Maalbeek 2) containing Reuver and Tegelen clays, the other (Brunssum) only Brunssum clay. In this study we first present a detailed study of one section in the Reuver clay in order to assess what processes are responsible for the geochemical variation, and how the geochemical variation in this section compares with the results published earlier. We focus in this study especially on the effects of pre- and postdepositional weathering and diagenesis, and the role of organic layers. We chose for this study the section Brachter Ton Abbau (BTAB in Boenigk (1970); also known as section Brachterwald in Zagwijn (1960). Apart from bulk geochemistry we used mineralogical, optical and in situ microscopical techniques to support our interpretations. Subsequently, we present the results of geochemical studies of several other sections in the Tegelen-, Reuver- and Brunssum clays to determine how consistent the differences between these deposits are, and how they can be related to tectonic, climatic and diagenetic variations.

Geological Setting

The research area is situated in the western part of the Lower Rijn Embayment, which forms the southern edge of the North Sea Basin and is bounded on the south by Paleozoic Rocks of the Rhenish Massive (Fig. 3.2.1). The studied sections are of Pliocene and Early Pleistocene age, and are located on the eastern part of the Peel Blocks, a tectonically uplifted area, and along the southern edge of the Roer Valley Graben, a tectonically subsiding part of the Lower Rijn Embayment. The sections Hoher Stahl and BTAB are equivalent to sections studied by Zagwijn (1960) and Boenigk (1970).

The sediments studied consists of mature siliclastic material deposited by the Rijn river system during the Pliocene and Early Pleistocene in a fluvial lowland area. These fluvial deposits consist of sequences of gravel and sand in which three main clay seams have developed. The lower two are formed during the Pliocene and palynologically respectively dated as Brunssumian and Reuverian (Fig. 3.2.2). The upper clay seams are of Tiglian (Early Pleistocene) age (Zagwijn, 1960). The Pliocene clays are often rich in organic matter due to the development of browncoal. In the Tegelen area, the Reuver clay is characterized by a typical blue color and the occurrence of two and sometimes three browncoallayers in its upper part (Boenigk, 1970; Zagwijn, 1960; Zagwijn and Van Staaldunin, 1975).

Pollen records show a gradual cooling down from warm temperate climatic conditions during the Brunssumian towards temperate conditions in the Tegelen. However, superimposed

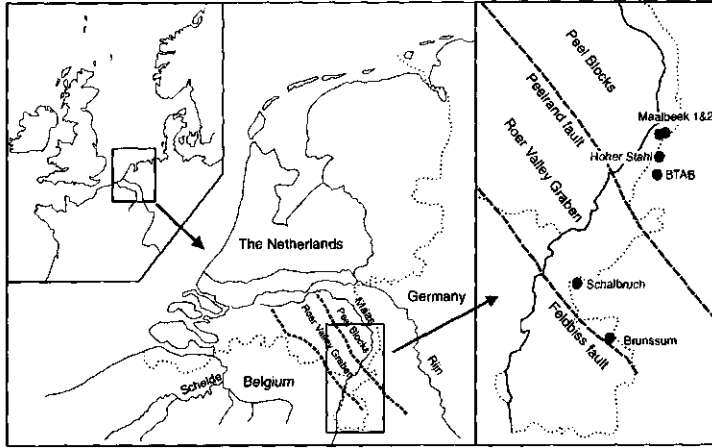


Figure 3.2.1 Study area and sampling locations

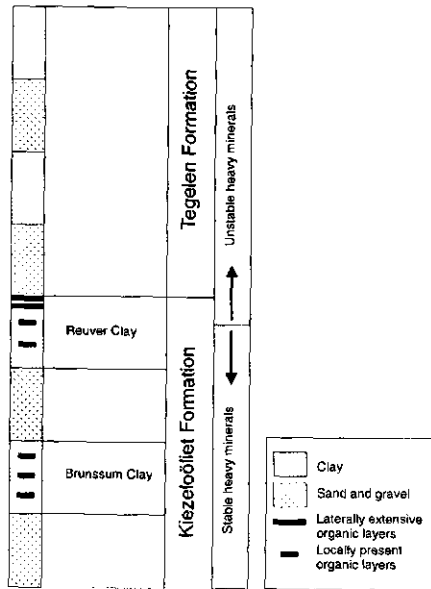


Figure 3.2.2 Schematic stratigraphic overview.

on this general trend cooler phases exist already during the Late Pliocene, while the Pleistocene starts with a cold/glacial phase, the Praetiglian (Fig. 3.2.3). Temperate conditions prevail during the Tiglian, but there are several cooler and even a cold phase registered (Kasse, 1988; Van den Berg, 1996).

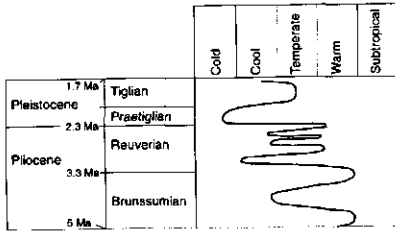


Figure 3.2.3 Climatic record based on pollen from Brunssumian to Tiglian (after Van den Berg, 1996).

Heavy-mineral-counts show a shift from a stable (zircon-tourmaline) to an unstable (garnet, epidote, alterite, hornblende) association, either in the top of the upper Pliocene deposits, or at the Pliocene-Pleistocene transition. This transition is linked with the extension of the Rijn drainage area into the Alps (Boenigk, 1970; Klostermann, 1992; Zagwijn, 1960) and, on a larger scale, the increase in tectonic activity in North-Western Europe at that time (Van den Berg and Veldkamp, 1993). The (Early) Pliocene stable heavy-mineral suite is a reflection of local sources with a high degree of weathering. The Pleistocene unstable heavy minerals originate from the Alps or the Alpine foothills, and are less weathered. The effects of these changes on the bulk sediment composition were studied by Huisman et al. (1996) and Van Os et al. (1996). These workers presented Al-corrected variations in the contents of Ti, K and Na. These variations were thought to be caused mainly by the climatic fluctuations whereas the major change in sediment provenance and speed of tectonic uplift (Van den Berg and Veldkamp, 1993) were considered less important.

Materials and Methods

Samples were taken from two cores from the Geological Survey of the Netherlands (Maalbeek 1 (58E 269) and Maalbeek 2 (58E284)), the Geological Survey of Nordrhein-Westfalen (Schalbruch (4901-KB1); see Stritzke (1997) and Wefels (1995) and from the clay pits at Hoher Stahl, Brachterwald (BTAB) and Brunssum (Fig.3.2.1). Most of the sections show the general interchanging of homogeneous sand layers with clay layers with especially in the Pliocene sections intercalations of browncoal. The Reuver Clay at the top of fluvial sands from the Kiezeloöliet formation was recovered from all sections except Brunssum. In Hoher Stahl and both Maalbeek sections the Reuver clay is overlain by fluvial gravel and sand from the Tegelen formation, which again are covered by clay which forms part of the Tegelen Clay members. Brunssum Clay was only recovered from sections Schalbruch and Brunssum. Our stratigraphic classification of the Schalbruch boring is based on lithostratigraphic interpretation of surrounding borings, and deviates from the Brunssumian-Susterian (Upper Miocene) datings given by Stritzke

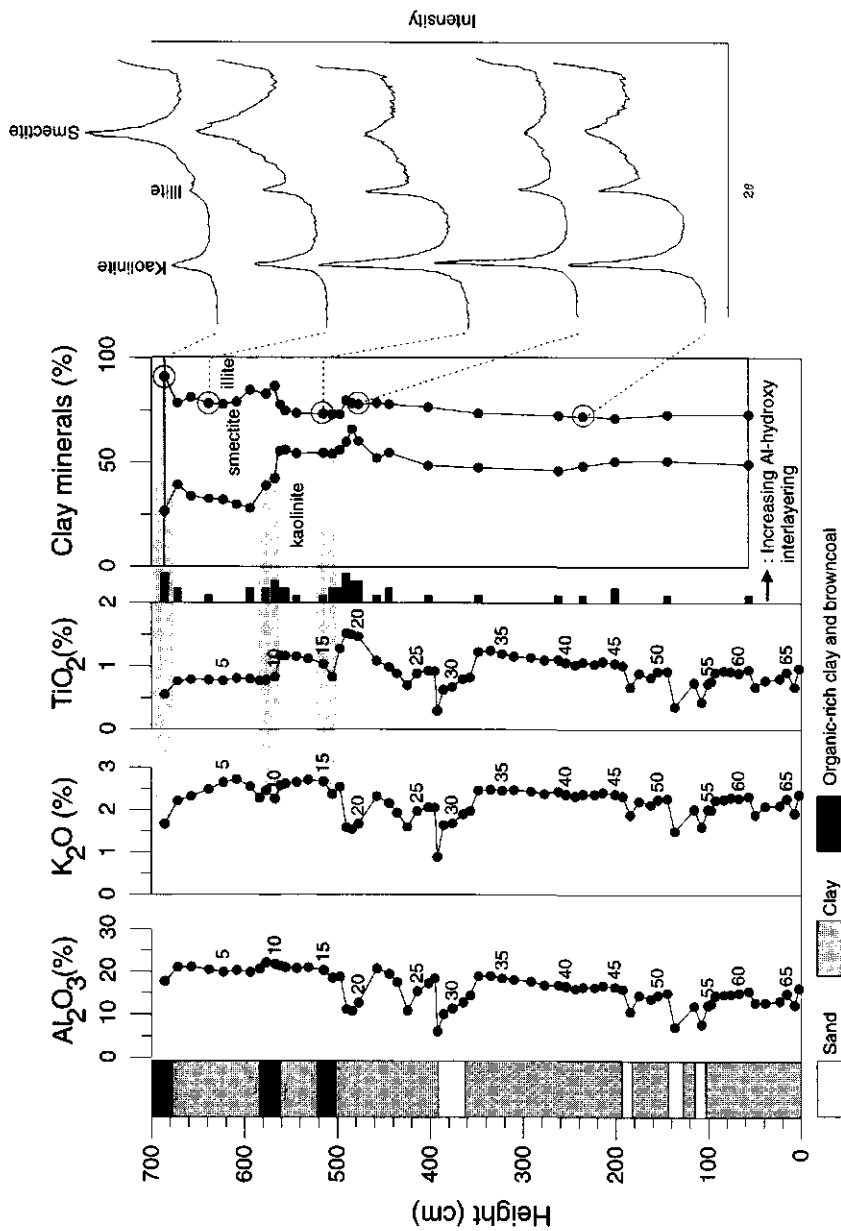


Figure 3.2.4 Depth profiles of Al_2O_3 , K_2O and TiO_2 -contents and clay mineralogical properties of section BTAB. Figures indicate sample numbers (referred to in text). Degree of Al-hydroxy interlayering is a qualitative scale. Clay mineral percentages are based on relative peak heights. The diffractograms of five representative samples are given, with “kaolinite”, “illite” and “smectite” at 7, 10 and 14Å respectively. The clay above the middle organic-rich layer is smectite-rich, whereas the clay below it shows higher contents of kaolinite and TiO_2 . TiO_2 and kaolinite contents are further elevated immediately below the lower organic-rich layer. K_2O -contents drop in all three organic-rich layers, and there is an increase in Al-hydroxy interlayering.

(1997) on the basis of pollenanalyses. We first analyzed the section BTAB and, to a lesser extent, Hoher Stahl in more detail using clay mineralogical analyses, micromorphology, submicroscopy (SEM-EDAX) and XRD to investigate the mechanisms behind the observed geochemical differentiation and link our data with literature (Zagwijn, 1960; Boenigk, 1970), and used these findings to interpret the results from the other sections. The clay mineralogical composition was determined of a selection of samples from Hoher Stahl and BTAB. See Chapter 2 for a description of sampling practice and of the various analytical methods.

Results and discussion

Detailed study of section BTAB

The BTAB-section consists of about 7 m clay. In the lower few meters, a few thin sand layers are intercalated in the clay. In the top, three organic-rich layers occur. The top organic layer consists of browncoal, the lower two are organic-rich clay bands. The clay underneath the lower organic layer has a light color and seems bleached, whereas the rest of the clay has blue to dark brown colors. One of the reasons to choose the BTAB-section for a detailed study on the geochemistry, clay mineralogy and the micromorphology is that this bleached layer may be caused by soil formation and, and therefore may reveal the effects of post-depositional weathering. Apart from that, Boenigk (1970) found sand with an unstable heavy-mineral composition in the top of the BTAB section, whereas the rest had a stable heavy-mineral composition, which indicates that the lower part of the section was deposited prior to the shift from local to Alpine mineralogy in the Rijn system, and the upper part after that.. This means that this section gives the possibility to study the effects of this transition on the sediment geochemistry. We first present shortly the clay mineralogical observations, and proceed then with the geochemistry, supported with microscopical techniques.

Clay mineralogy The major clay minerals present are illite, kaolinite and smectite. In the lower part of the section (below the middle organic layer) kaolinite is the most abundant mineral, and there is little variation in the contents of all three clay minerals (see Fig.3.2.4). The only exception is just below the organic layer at 500 cm, where the kaolinite contents show a peak. In the upper part of the section, i.e. above the middle organic layer, kaolinite contents drop, and smectite contents rise. Illite contents are fairly constant throughout the section, but illite contents seem to drop and smectite contents rise in especially the upper two organic layers. In or slightly below the organic layers, Al-hydroxy interlayering occurs.

Ti and Al Ti and Al show a general positive correlation, with high Ti-contents coinciding with high Al-contents. There is a distinct abrupt change in the Ti-Al relation at the middle organic layer, with lower Ti-contents and high Al-contents in the upper part of the section (samples 1-10; Fig. 3.2.4 and 3.2.5) and higher Ti contents in the lower part. Directly underneath the lower organic layer the light-colored section of 40 cm shows typical anomalously high Ti-concentrations (samples 18-20). The changes in the content of kaolinite in the clay fraction coincide with the variations in Ti-contents described above (Fig. 3.2.4): The kaolinite content increases below the

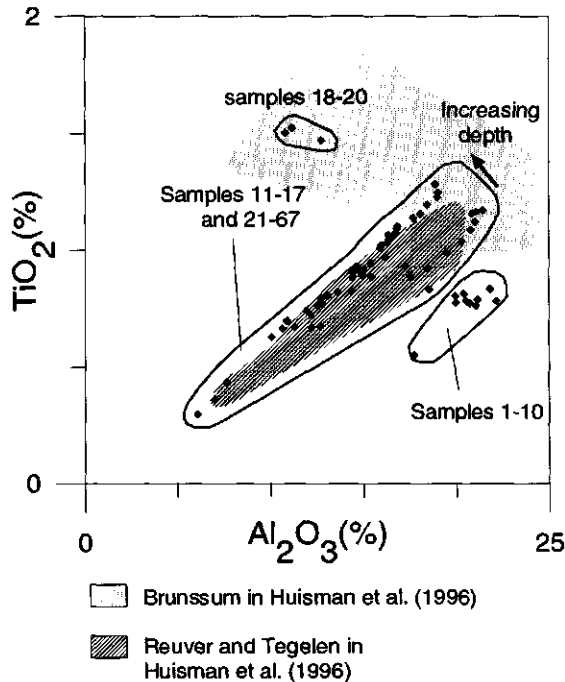


Figure 3.2.5 Scatterplot of TiO_2 versus Al_2O_3 for section BTAB. Samples 1-10 have anomalously low, and samples 18-20 anomalously high $\text{TiO}_2/\text{Al}_2\text{O}_3$ -ratios. The other samples show an overall trend of increasing $\text{TiO}_2/\text{Al}_2\text{O}_3$ -ratios. Shaded fields indicate previously published TiO_2 and Al_2O_3 contents.

middle organic layer, just as Ti/Al. Furthermore, the layer with anomalously high Ti-contents shows also further increased kaolinite contents.

As high Al-contents coincide with high clay contents, the overall relation between Al and Ti indicates that Ti is mainly present in clay minerals. Variations in the overall Ti/Al ratio then would represent variations in Ti-contents in the clays. However, the samples with anomalously high Ti-contents below the lower organic layer (nrs. 18-20) fall outside the positive Ti-Al correlation and seem to show a negative correlation between Al and Ti (Fig. 3.2.5). This indicates that the Ti here is not present in the clay minerals, but as separate minerals which are not enriched in the clay fraction. Micromorphological observations show increased amounts of small (10-30 μ), lath-shaped strongly birefringent heavy minerals in the Ti-enriched layer (see Fig. 3.2.6). SEM-EDAX analysis shows that most of these consist of Ti-oxide (Fig. 3.2.7). They can be identified as rutile, the most common Ti-oxide in soils (Milnes and Fitzpatrick, 1989), on the basis of their morphology. This is corroborated by the close correlation of Ti with Nb in these sediments (cf. Deer et al., 1992)

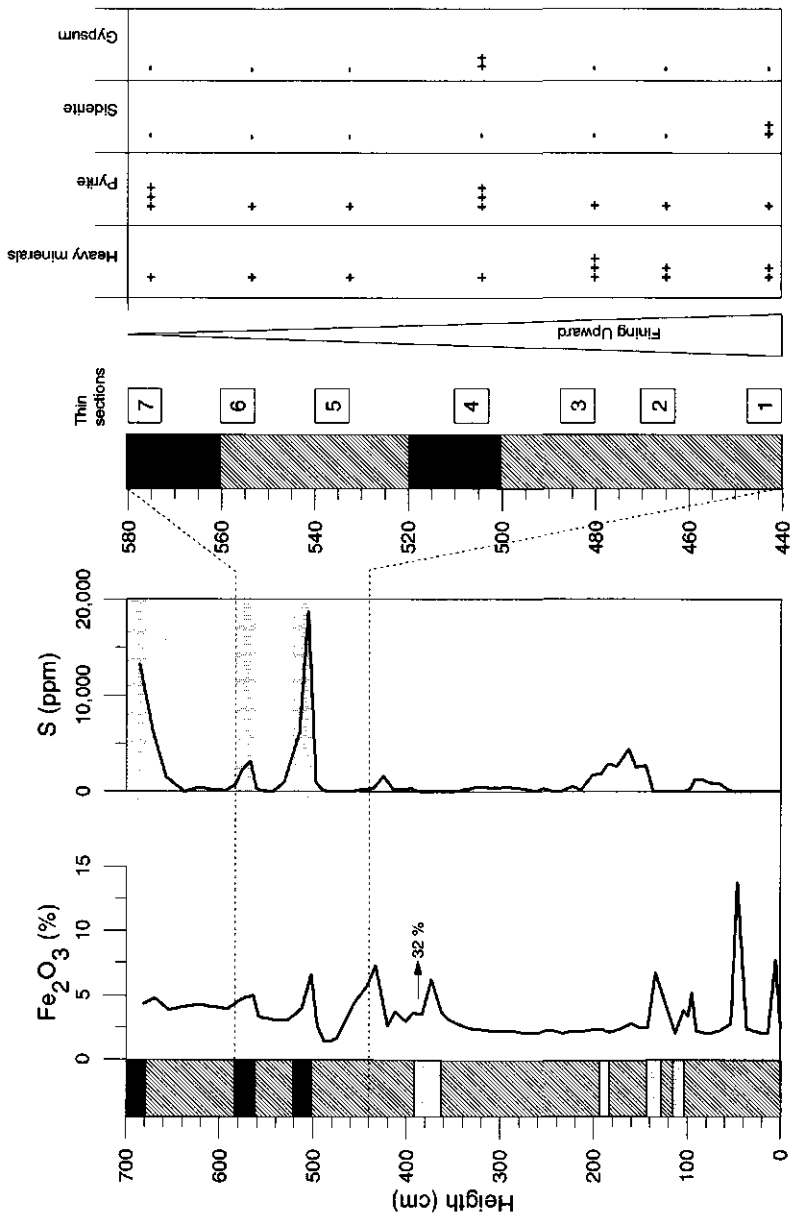


Figure 3.2.6 Depth profile of Fe- and S-contents (section BTAB). Part of the section is enlarged to indicate the and micromorphological observations. S-contents are elevated in the organic layers due to the presence of pyrite. Fe₂O₃-contents show a large amounts of local elevations, related to the presence of pyrite (in the organic layers) and (hydr)oxides.



Figure 3.2.7 SEM-photograph of TiO_2 -mineral, probably rutile, from thin section 3.

K and Al The K-contents show a positive correlation with Al, but in the lower part of the section (samples 33-67), the K/Al are higher and less variable than in the upper part of the section (Figs. 3.2.4 and 3.2.8). Furthermore, there is a drop in K-contents in the organic-rich layers. Al-contents drop also, but the K/Al ratio is lower than outside the organic layers (samples 1-3 and 8-10). There is no change in the K-Al relation that can be correlated to the changes in Ti/Al

The general positive correlation between K and Al is probably a reflection of the occurrence of K in clay minerals and micas (illite and muscovite in particular). The higher K/Al-ratio in the lower part of the BTAB-section suggests higher contents of illite or muscovite. This is supported by the frequent drops in illite contents above 400 cm depth (Fig. 3.2.4). The decrease in K in organic-rich layers correlates with decreased illite- and increased smectite-contents and increased levels of Al-hydroxy interlayering. The formation Al-hydroxy interlayered clays in soils is favored by oxidizing conditions and frequent wetting and drying cycles (Barnhisel and Bertsch, 1989). Therefore it is likely that after deposition weathering processes occurred, during which illite was transformed in situ to (partly Al-hydroxy interlayered) smectite and, as a result K was

lost. This process is probably enhanced by organic acids derived from the organic matter, and probably occurred before burial during repeated wetting and drying.

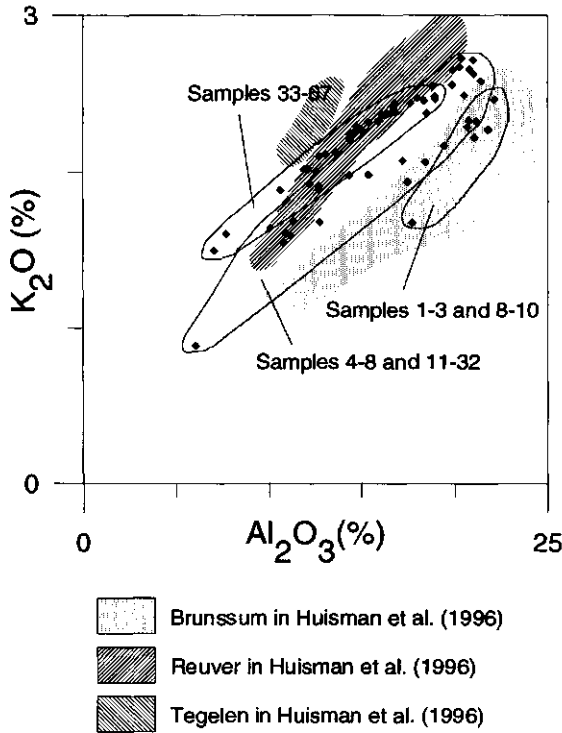


Figure 3.2.8. Scatterplot of K_2O versus Al_2O_3 for section BTAB. Samples from organic-rich layers (1-3 and 8-10) show a drop in K_2O/Al_2O_3 -ratios. In the other samples this ratio seems to increase with increasing depth. Shaded fields indicate previously published TiO_2 and Al_2O_3 contents.

Reflection of provenance change The clay mineralogical composition of the BTAB section can be divided into two major groups (Fig. 3.2.9) with a clear transition at the middle organic layer. One, occurring between the two topmost organic layers, is dominated by moderately to well crystallized smectite with additional illite and kaolinite. The second group, occurring below the middle organic layer, is characterized by low contents of moderately to badly crystallized smectite and higher contents kaolinite and shows increased contents of Ti.

The overall succession from a smectite-poor, kaolinite-rich to a smectite-rich, kaolinite-poor clay mineralogy is consistent with the decrease in kaolinite and increase in smectite+chlorite contents during the Pliocene described by Brinkman (1976). It coincides with the shift in heavy

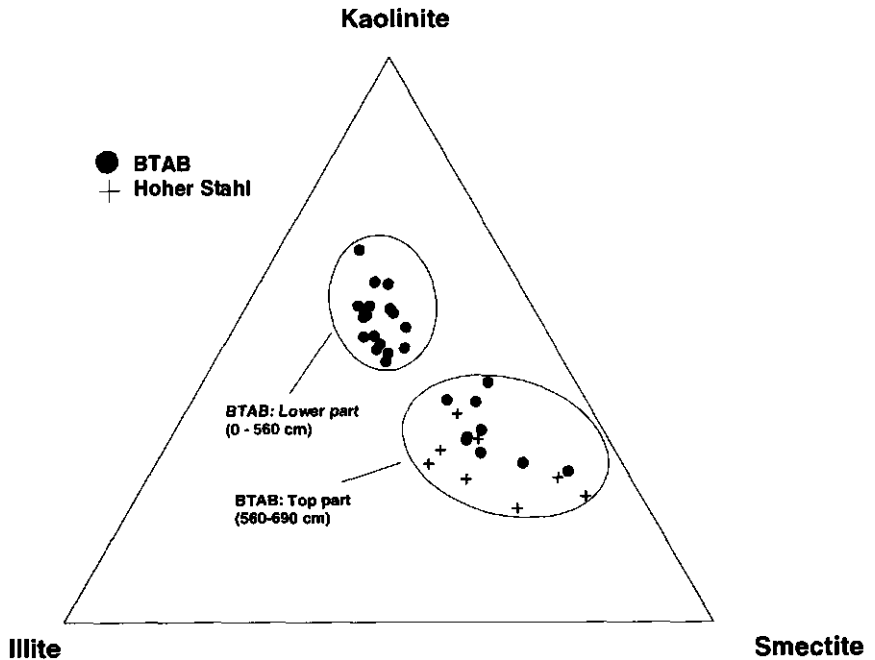


Figure 3.2.9 Triangular graph of the clay mineralogical composition of sections BTAB and Hoher Stahl. Clay mineral percentages based on relative peak height. The clay from the top of the BTAB section can be discerned clearly from the lower part of the section. The clay from Hoher Stahl has a similar mineralogy as the upper part of the BTAB section.

mineralogy from a general stable composition (zircon-tourmaline) to an unstable (garnet-epidote-alterite) one as described for this section by Boenigk (1970). This indicates that the shift from local to Alpine mineralogy in the Rijn sediments at the transition Pliocene-Pleistocene as recorded in the heavy-mineralogy, is also reflected in the clay mineralogy by increased smectite and decreased kaolinite contents. This correlation between clay and heavy-mineralogy is consistent with the observations from Hoher Stahl: The clay mineralogical composition of all samples studied from this section is have low kaolinite and high smectite contents similar to that in the upper part of BTAB. Heavy-mineralogy studies describe for Hoher Stahl an unstable composition (garnet-epidote-alterite), which indicates an Alpine Rijn sediment provenance (Boenigk, 1970; Burger, 1997).

The kaolinite probably originates from strongly weathered local sediments whereas the smectite was probably transported from Mesozoic marls or the flysch in the Alpine foothills. The association of Ti and kaolinite in the pre-Alpine sediments is consistent with a local, sediment source which has experienced severe enough weathering to yield kaolinite. The source rock can tentatively be identified as the rutile-bearing Triassic sandstones on both sides of the Rijn Graben

(Van An del, 1950; Zorn-province). It is unlikely that the rutile is a weathering product, as its morphology is not consistent with secondary Ti-minerals as described by Hutton et al. (1978), Milnes and Fitzpatrick (1989) and Poppe et al., (1991) which are much finer-grained. Therefore it is more likely that Ti-minerals were concentrated in kaolinitic weathering profiles in the source area through residual enrichment.

As the extreme Ti-enrichment in the BTAB section beneath the lower organic layer coincides with a kaolinite-peak, it could be interpreted as a result of a temporary increase in input of a strongly weathered sediment source. However, it is also possible that it represents a placer-like concentration of fine silt-sized minerals as a result of extreme winnowing and sorting in the fluvial system, coinciding with a reworking phase during a temporary halt of the aggradation. The concentration of kaolinite can be explained by the larger grain size ("pseudo-silt") of kaolinite compared to the other clay minerals, which makes it more susceptible to concentration by winnowing and sorting along with fine silt-sized minerals.

If we compare the Ti-Al data from BTAB with the data presented in Huisman et al. (1996), it becomes clear that the Ti/Al ratio in the top of BTAB is low even compared with the Tegelen formation. Furthermore, the Ti-enrichment through sorting processes falls in the range of Ti-contents that were found in Brunssumian deposits. This suggests that these Ti-enrichments have the same origin as the ones in BTAB, and that the interpretation that they originate from weathering processes in a (sub)tropical climate (cf. Fig. 3.2.2) as posed by Huisman et al (1996) and Van Os et al. (1996) is not correct. The BTAB K/Al ratios are in general similar to the Reuver samples from these studies or slightly lower. It also becomes clear that K-loss through weathering of illite can result in K/Al ratios as found in the Brunssum section of Huisman et al. (1996).

Diagenetic processes The contents of Fe are highly variable with peaks occurring throughout the section. Fe is at least partly present as detrital phyllosilicates. As a rule of thumb, detrital Fe_2O_3 -contents in siliclastic sediments can be estimated as $0.25 \cdot \text{Al}_2\text{O}_3$ (Dellwig et al., 1996; Chapter 3.1). In our clay layers this would indicate a detrital Fe_2O_3 -content around 5%. The Fe in the peaks exceeding this background is probably present as oxides, carbonates or sulfides: Fe-peaks in the lower part of the section (0-400 cm), with bulk Fe_2O_3 -contents up to 32% represent Fe-oxide rich bands which were identified in the field by their tell-tale orange color. In the Fe-peaks above 400 cm, no such color was observed, so here the Fe probably occurs mainly as siderite (Fe-carbonate) or pyrite (Fe-sulfide).

S-contents are elevated in all three organic layers, but low S-enrichments occur also lower in the profile. It is unlikely that sulfides or sulfates are transported and deposited in a fluvial system, so the S is probably present as secondary minerals like sulfides (pyrite). Pollen assemblages indicate that there the sediments was deposited in a fresh-water system (cf. e.g. Zagwijn, 1960), but the S-contents are unusually high for continental deposits as usually only in brackish or saline water enough S is available for the formation of pyrite. However, similarly high S contents are reported from Late-Weichselien river fens in oxbow lakes as a result of breakdown of organic matter by methanogenesis (Chapter 4.1). The sedimentary setting of BTAB, however, is hardly comparable to these extremely organic-rich Late Weichselien river fens. Moreover, the micromorphological observations indicate that in BTAB the presence of high S-contents are caused by the deposits having been in contact with brackish or saline water after deposition.

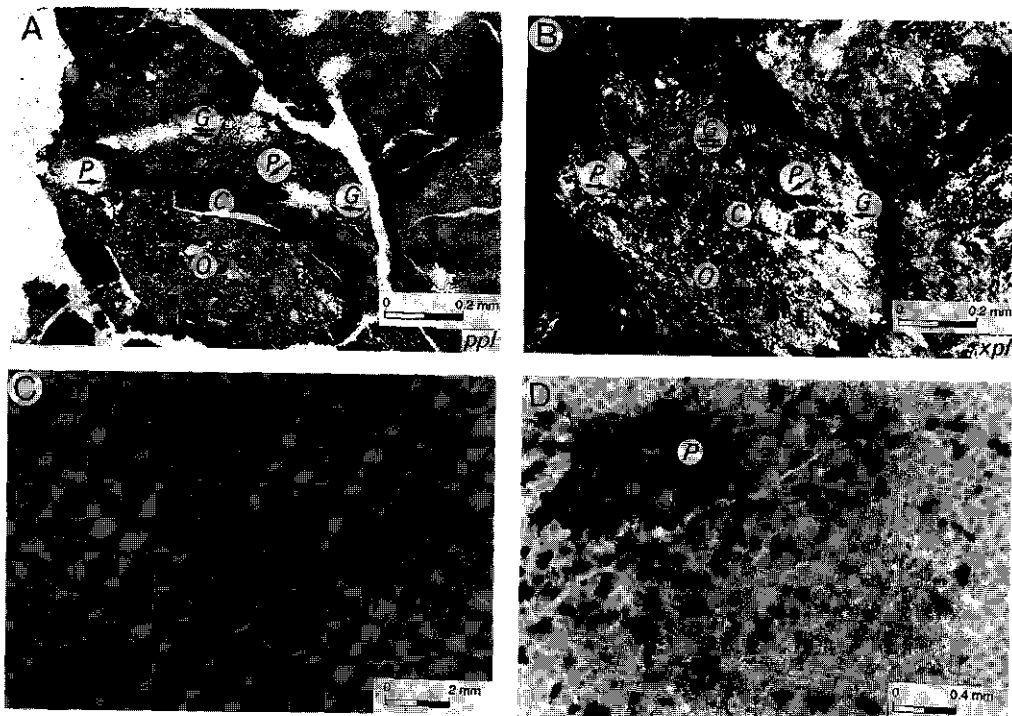


Figure 3.2.10 Photos of thin sections from section BTAB. See Fig. 3.2.5 for position of thin sections. PPL=plain polarized light; XPL=crossed polarized light. **A and B:** Original groundmass (O) with domains of oriented clay (C). Pyrite (P) and Gypsum (G) associated with these domains. (Thin section 4). **C:** Oxidized siderite nodules scattered throughout the groundmass (Thin section 1). **D:** Oxidized siderite in groundmass and pyrite associated with cracks (Thin section 1).

Micromorphological study showed that pyrite occurs as *framboids* (10-50 μ) or irregular concentrations (up to 5 mm) throughout the section, but that large amounts are concentrated in the organic layers (Fig. 3.2.8). They are either associated with organic matter or as loose or complete infillings in cracks. Pyrite and gypsum were also observed in domains of clayey infillings or coatings that are present in vertical or horizontal cracks, often accompanied by well preserved, predominantly horizontally oriented organic remains (Fig. 3.2.10 a,b). Such clay coatings are formed by downward physical clay illuviation (Bullock et al., 1985). The combination of the clay coatings, a microstructure that consists of moderate to strong coalesced aggregates and observations of B-fabrics dominantly parallel to cracks suggests that the clayey sediment has been

subject to repeated desiccation and subsequent flooding after deposition: Coalescence of micro aggregates in the groundmass is the result of desiccation of the clay after its deposition whereas B-fabrics parallel to cracks indicates swelling and shrinking of the clay as a result of repeated drying and wetting (Brewer, 1964; Fitzpatrick, 1980). The clay coatings are most probably formed when a brackish water flooded sediment was exposed to the influence of fresh rain water: In such conditions structural collapse easily takes place, giving rise to dispersion of clay and formation of clay coatings (Miedema, 1987). The pyrite in the organic-rich layers therefore probably formed during saline or brackish incursions over these organic-rich continental deposits. The gypsum is probably formed by oxidation of pyrite. The timing of this oxidation is uncertain; it could be related to a drying-out phase before burial by new sediment, but oxidation could also have taken place fairly recently through contact with oxic groundwater or during excavation of the clay pit.

In the deepest of the thin sections (nr.1), star-shaped or angular brown to red colored nodules occur randomly distributed throughout the groundmass (Fig. 3.2.10c). Similar nodules are also found in clusters, or as coatings in voids, whereas pyrite is scarce and only present in cracks, associated with organic matter (Fig. 3.2.10d). The morphology star- and angular shaped nodules is similar to siderite-occurrences (A.G. Jongmans, pers. comm.), which suggest an initial formation of siderite crystals which were subsequently oxidized to Fe-compounds under improved drainage conditions. Their random distribution through the groundmass suggests that they were formed by precipitation from siderite-oversaturated ground water, probably during or shortly after deposition of the sediment. Oxidation of the siderite may have taken place during the same desiccation phase responsible for the cracks and aggregated structure. Because pyrite does not show any trace of oxidation, it must have been formed by downward percolating saline or brackish water after the formation and subsequent oxidation of the siderite crystals, in a reduced environment.

The sequence of events of the studied section can be reconstructed as follows (see Fig. 3.2.11):

- 1 Deposition of clay and organic matter in a fluvial environment.
Formation of siderite in the lower part of the deposit.
- 2 Repeated drying and wetting of the deposits: cracks form, siderite oxidizes to Fe-oxides.
Swelling and shrinking processes result in structure formation and form B-fabrics along fissures.
- 3 Different phases of inundation by saline or brackish water: Alternation in formation of pyrite and clay coatings as a result of alternation in brackish and fresh conditions.
- 4 Burial by new sediment

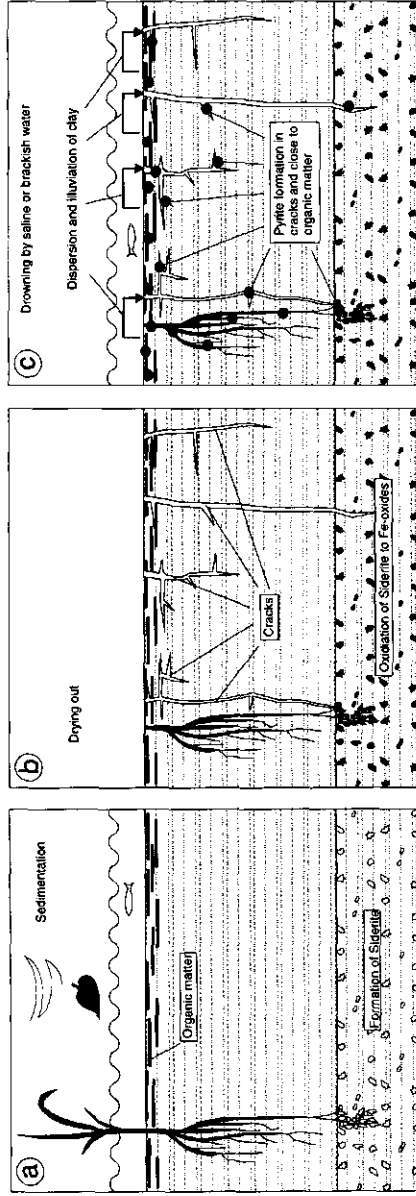


Figure 3.2.11 Reconstruction of deposition history of the organic layers in section BTAB. During the first stage (A), organic-rich sediments are deposited in a fresh-water environment, and small siderite nodules are formed. In the second stage (B), the sediments dry out, cracks form, and the siderite is oxidized to form Fe(hydr)oxides. In the third stage, one or more short-termed incursions by brackish or saline water cause dispersion and illuviation of clay, and the formation of pyrite in cracks and close to organic matter.

Overall geochemical data of Tegelen, Reuver and Brunssum clays:

In order to assess to what extent the variation in geochemistry as found in BTAB and by Huisman et al. (1996) is consistent within the Brunssum, Reuver and Tegelen Clays, we compare here the geochemical variation in a series of 5 sections with the BTAB-section. The data presented in Huisman et al. (1996) is included in this series (sections Brunssum and part of Maalbeek2).

Ti and Al show a similar positive correlation as found in BTAB (Fig. 3.2.12). Several samples show anomalously high Ti-contents similar to the one in BTAB. These anomalously high Ti-contents occur in layers of several dm thickness scattered throughout the Reuver and Brunssum sections, but they are absent in the Tegelen sections. In the Reuver sections they are restricted to the sediments with a local instead of Alpine sediment provenance. They are interpreted as representing local concentrations of small-sized heavy minerals in placer-like deposits. The absence of these in the sediments with Alpine provenance suggests that silt-sized heavy minerals in the Alpine-derived sediments are dominated by other minerals (e.g. epidote).

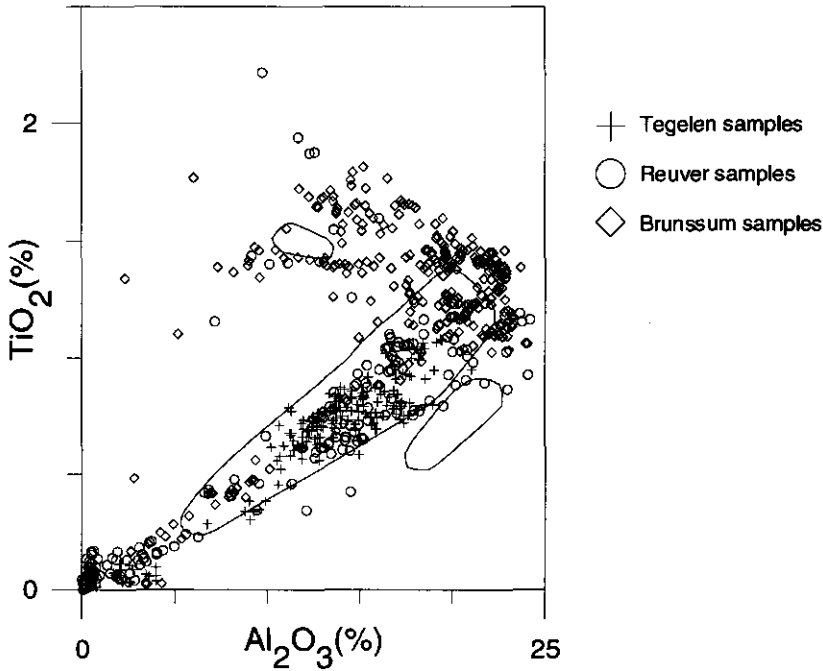


Figure 3.2.12 Scatterplot of TiO_2 versus Al_2O_3 for the sections Maalbeek 1+2, Hoher Stahl, Schalbruch and Brunssum. Ovals delineate the BTAB-groups as presented in Fig. 3.2.5.

In section BTAB, the shift from local to Alpine sediment provenance as was found in the heavy-mineral composition by Boenigk (1970) appeared to be reflected by a drop in Ti/Al and kaolinite, and an increase in smectite contents (see above). In Fig. 3.2.12 however, it becomes clear that this shift is not consistent; Most of the Tegelen samples show similar Ti/Al ratios as the lower part of BTAB, and most of the other Reuver and Brunssum deposits. The only samples that are comparable in Ti/Al to the top of the BTAB-section are the Reuver and some of the Tegelen samples from Hoher Stahl. A possible explanation for this is that the Reuver samples from Hoher Stahl and the top of the BTAB-section represent an almost pure Alpine source, whereas most of the Tegelen sediments consist of a mixture of Alpine- and locally derived sediments. However, localized Ti-concentrations as a result of the concentrations of fine silt-sized heavy minerals were not found in any of the Reuverian and Tiglian sections with an Alpine or a mixed Alpine-local sediment provenance, and were also absent in the Tegelen deposits in Brabant (west of the research area) (Chapter 3.1).

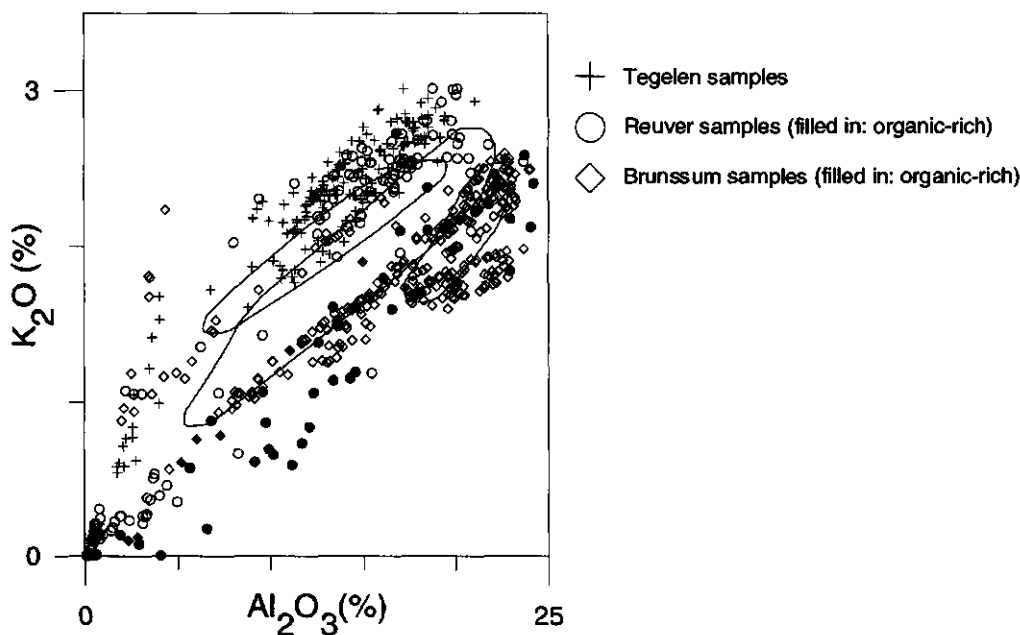


Figure 3.2.13 Scatterplot of K_2O versus Al_2O_3 for the sections Maalbeek 1+2, Hoher Stahl, Schalbruch and Brunssum. Ovals delineate the BTAB-groups as presented in Fig. 3.2.8. Organic-rich samples are indicated.

K and Al There is a general positive correlation between K and Al (Fig. 3.2.13) but there is a large variation in the K/Al ratios. As most of the low-K samples are from organic-rich sections, a large part of the variation can be explained by the postsedimentary depletion of K by weathering of illite by organic acids. In some of the samples with low Al-contents (below 8%), originating from Tegelen and Reuver as well as Brunssum sediments, strongly elevated K-contents occur. These sediments have low clay contents, as can be seen from the relatively low Al-contents, so the minerals responsible for the increased K-values must be present in the silt or sand fraction. As the bulk K/Al-ratio of these samples fall in the range of illite/muscovite, it is likely that high contents of muscovite are responsible for these high K-values. Because of the concentration of K-rich minerals like feldspars and micas in sandy material, K/Al ratios of these sands can become anomalously high. When comparing K/Al-ratios it is better therefore to concentrate on high-Al samples.

Neglecting the organic-rich and the low-Al samples, the Reuver and Brunssum sediments show a large variation in K/Al ratios, and generally lower values than in the Tegelen sediments. This suggests that the Tegelen clays have in general a higher content of illite and/or muscovite.

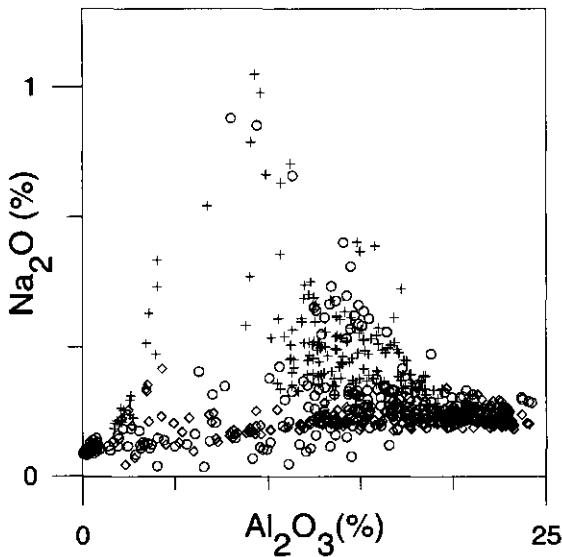


Figure 3.2.14 Scatterplot of Na₂O versus Al₂O₃ for all sections. Legend as 3.2.13. Samples from the Tegelen formation show elevated Na₂O-contents. Reuver and Brunssum samples usually have low Na₂O-contents, except for the Reuver samples from Hoher Stahl.

General discussion and Conclusions

Provenance shift

The change in Rijn sediment provenance and the increased tectonic uplift rates, the overall regression and the deterioration of the climate at the Plio-Pleistocene transition would theoretically all have had their effect on the sediment composition. It is difficult to assess the magnitude of the separate effects of each of these changes: both increase of the uplift rates and deterioration of the climate can cause a shift towards a less weathered sediment composition, and both of these are hard to distinguish from a provenance change towards a less weathered source area.

Climatic deterioration and increased tectonic uplift would result in a slow change in sediment composition (cf. Bestland et al, 1997), whereas provenance shifts would show a more abrupt change. Moreover, climate effects on sediment composition would first be recognizable and in the clays, whereas provenance shifts would affect all grain sizes. Therefore, the suddenness of the shift in Ti/Al ratios and kaolinite-contents in the BTAB-section the sudden increase in unstable heavy minerals (Boenigk, 1970) and the fact that the shift can be found in both sand and clay mineralogy indicates that the change in sand and clay mineralogy at the Pliocene-Pleistocene transition can for the major part be attributed to provenance shifts. The relapse to higher Ti/Al-contents in the Tegelen sediments, which show by virtue of their elevated Na-contents to be Alpine-derived, suggests that the influence of the Alpine source area is regionally diluted.

The change in K-contents is less abrupt than the change in Ti/Al in BTAB, and it shows an overall much larger variation. This could indicate that this variation is more climate-related, with lower rates of weathering of illite and muscovite during cooler climatic conditions. If this is the case, the large variation in K/Al may represent some of the smaller-scale climatic fluctuations superimposed on the overall cooling from Pliocene to Pleistocene. However, given the magnitude of K-depletion in organic layers (cf. Chapter 3.1), it is more probable that K/Al-ratios are more related to this organic-related weathering and less climate controlled. Low K/Al ratios in organic-poor sediments could very well be the result of the sediment being derived from reworked weathering profiles.

Overall, it can be concluded that detrital geochemical variation in the Brunssumian, Reuverian and Tiglian sediments are mostly controlled by sediment source and hence the large-scale tectonic setting, whereas climatic controls seem limited. This holds true for the variations in Na and Ti, and partly for K.

Depositional environment

The Pliocene and Early Pleistocene deposits form a sequence from deltaic fluvial to more estuarine with decreasing marine influence in time. This sequence may reflect delta progradation due to increased (Alpine) sediment supply or, less likely, an increased river gradient due to increased tectonics and sediment flux. It is unlikely that shorter-term sea level fluctuations are recorded. Sporadic contact between sea water and fluvial organic-rich deposits during

spring tides and storm floods may have caused the marine geochemical imprinting on fluvial organic-rich deposits.

4 Specific diagenetic processes

4.1 Siderite, syn- or postdepositional? A comparison of Early and Late Pleistocene deposits in the Netherlands

R.H. Smittenberg
D.J. Huisman
A. Veldkamp
A.G. Jongmans
B.J.H. van Os

Abstract

Siderite (FeCO_3) in sediments is often used as an indicator for the depositional environment, as it can only be formed under restricted geochemical conditions. However, postdepositional formation of siderite is usually neglected. This study investigates whether siderite in Early and Late Pleistocene deposits was formed syndepositionally, or postdepositionally under different circumstances. Within the Early Pleistocene Tegelen Formation, siderite is found as coatings around detrital dolomite grains, together with partially dissolved detrital calcite grains. Siderite also occurs as single nodules and mixed homogeneously through the groundmass. Micromorphological observations and thermodynamic calculations suggest that siderite precipitated at the expense of calcite, and that this process is still going on under present-day conditions. Siderite formation in Late Pleistocene river fens is syndepositional and associated with both calcite and vivianite. Therefore, though siderite may be an indicator for the depositional environment, formation in a later diagenetic environment can not be ruled out.

Introduction

Siderite (FeCO_3) formation in sediments occurs under restricted geochemical conditions. It requires a low dissolved sulfide content, high HCO_3^- activity or total CO_2 concentration, near neutral pH, low Eh and a $\text{Ca}^{2+}/\text{Fe}^{2+}$ ratio smaller than 20 (Berner, 1971; Appelo and Postma, 1994). Because of these restrictions on its formation, the occurrence of siderite in sediments is often used as an indicator for the depositional environment. As siderite formation is only possible at low S-levels, and fresh-water deposits are usually considered S-poor (Casagrande, 1998; Cohen et al., 1984; Postma, 1982), the presence of siderite in sediments is often regarded as a fresh water indicator (Curtis, 1967, Postma, 1982; Pye et al., 1990). However, siderite formation is also known from S-limited, Fe-rich pelagic settings, especially in zones of methanogenesis, and from direct precipitation from the water column in the bottom water of depositional basins like the Black Sea (Rajan et al., 1996). According to Mozley (1989) and Mozley and Carothers (1992), siderite formed in a continental setting is characterized by low amounts of Mg and Ca substituting Fe, and higher $\delta^{13}\text{C}$ -values when compared to marine siderites.

When using siderite as paleoenvironment indicator, it is important, however, not to rule out the possibility that it was formed long after deposition, and under different conditions than prevailed during sedimentation. Katsumoto and Iijima (1981) and Mozley and Carothers (1992) show that changes in pore-water chemistry during (deep) burial can cause precipitation of siderite. On a Quaternary time-scale, especially in low-gradient deltas of large river systems, sedimentary settings change continuously as a result of fluvial dynamics, tectonics and climate-induced sea level fluctuations. One can expect that

as a result the groundwater composition will vary accordingly, and reflect shifts between sea-, river-, meteoric water as source. Such changes can result in precipitation of minerals (like siderite) that are at odds with the original sedimentary environment of the deposits. In this study, we use “syndimentary” for diagenetic processes that are related to the depositional environment. For processes that occur after the sedimentary settings have changed, and therefore are not related to the original depositional environment, we use “postsedimentary”.

In the current chapter we study two different siderite-rich deposits from the Pleistocene Rijn-Maas delta. We compare the geochemical composition and mineralogical features in order to study whether the siderite was formed syndepositionally, i.e. in an unchanged depositional environment, or postdepositionally under altered circumstances. We studied the composition and morphology of siderite and other diagenetic minerals using micromorphological and (sub)microscopical techniques, X-Ray Fluorescence (XRF), X-Ray Diffraction (XRD).

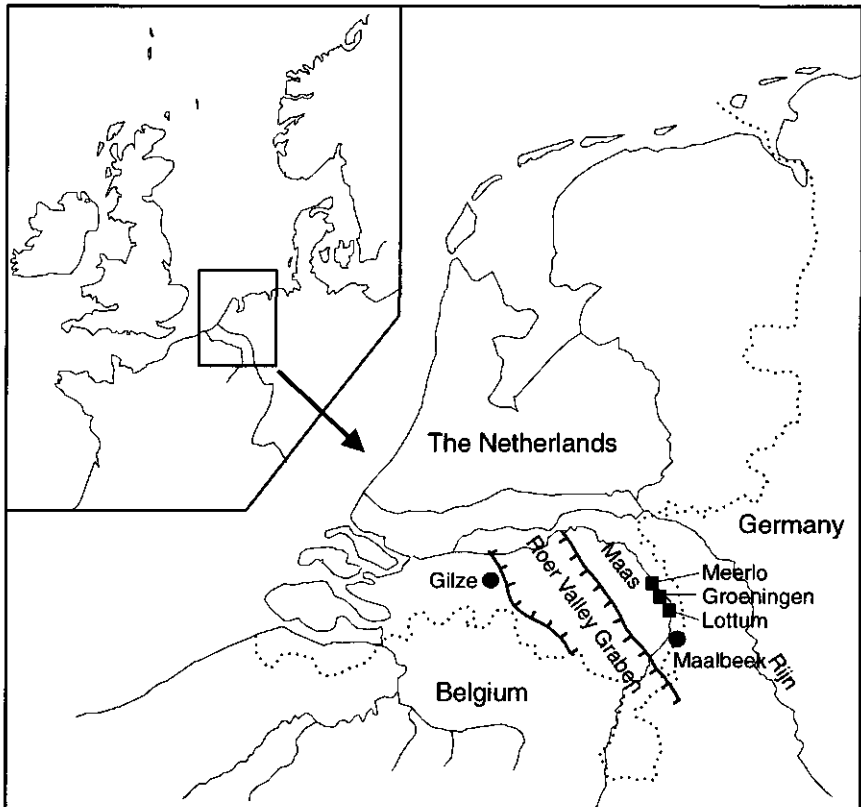


Figure 4.1.1 Map of the Netherlands with sampling sites indicated. Dots are Early and squares are Late Pleistocene sampling sites. The Tegelen formation lies in the Southern part of the Netherlands and stretches further into Germany and Belgium.

Materials and methods

Geological site conditions

Sediments from the Early Pleistocene Tegelen formation were studied at the Gilze and Maalbeek sites (see Fig. 4.1.1.) The Tegelen formation is characterized by thick (> 10m), often finely laminated clay layers, separated by coarse sand layers. In the east of the Netherlands it consists mainly of fluvial deposits, whereas in the west it consists of deposits from inshore, landward, fresh to brackish micro- to mesotidal environment (Zagwijn and Van Staaldunin, 1975; Kasse, 1988; Westerhoff and Cleveringa, 1996). The Tegelen sediments are derived from the Rijn system, just after its headward extension into the Alps during the onset of the first major Pleistocene glaciations and increased tectonic activity. (Chapters 3.1 and 3.2; Kasse, 1988; Boenigk, 1970). The present position of the sediments of the Tegelen formation is determined by tectonic movements related to the Roer Valley Graben system (see Fig. 4.1.1): In the Roer Valley Graben, the top of the Tegelen formation is found at a depth of 100-150 m. East of the Graben, in the vicinity of the Gilze site, the Tegelen sediments are close to the surface, overlain by at most 10-15 m of Middle Pleistocene fluvial sand and gravel. The clay is mined in a series of clay pits in the Netherlands-Germany border area. The clay from the Maalbeek clay pit tends to be soft when excavated, but hardens rapidly upon exposure. The Maalbeek section studied in this chapter is obtained from a core from the vicinity of the Maalbeek quarry face (58E284; see Chapter 3.2). The Tegelen section in this core consists of a sand/silt-laminated clay layer of about 12 m thickness. West of the Graben, Tegelen sediments crop out south of the Netherlands-Belgian border, where the clay is also mined, and dips towards the north (Kasse, 1988). At Gilze, the Tegelen sediments are overlain by 9 m of younger Early Pleistocene fluvial sediments. In the Gilze core, the Tegelen section consist of a series of 13 m of laminated sand and loam.

The Tegelen sediments are in general characterized by the frequent occurrence of high contents of Fe, Ca and Mg-carbonates. Only in the area west and southwest of Gilze they are poor in siderite and locally pyrite-bearing (Kasse, 1988; Chapter 3.1). The Tegelen deposits at Maalbeek and Gilze are poor in organic remains, but in other locations peat layers are often found in the top of the clay layers (Zagwijn and Van Staaldunin, 1975).

Because of the permeability of the overlying deposits, the present-day formation water in the Tegelen formation at Gilze and Maalbeek is probably of a fairly recent meteoric origin. Studies by the Netherlands Institute of Applied Geosciences/Geological Survey of the Netherlands (NITG-TNO) indicate that even the groundwater that is currently present in the deepest part of the Tegelen formation in the Roer Valley Graben is mostly younger than around 10,000 years old, i.e. of fairly recent origin (Nolte, 1996).

The sediments at the Meerlo, Lottum and Groeningen study sites are of Late Pleistocene (Late Weichselien) age. They consist of the infillings that accumulated during the Allerød and Young Dryas in abandoned channels of the river Maas (Tebbens et al., 1997). They are presently in use as pastureland, with groundwater tables a few cm below the surface. The infillings consist mainly of organic rich material (peat and gyttja) interchanging with thin clay layers. The fens are situated in a low position, on

the edge of the present-day Maas floodplain, and close to older, elevated, river terraces. As a result of this, they are susceptible to influence of lateral and upward groundwater movement. Orange-colored hydromorphic Fe-hydroxides precipitates are abundant in ditches in the surroundings of the Meerlo site, which suggest that upward moving groundwater provides large amounts of Fe to the Meerlo area. Tebbens et al. (1997) measured high amounts of iron, calcium, phosphorous and carbonates in the fens, and attributed this to diagenetic processes. The presence of abundant vivianite (Fe-phosphate) was clear from the typical bright-blue color on the samples after exposure to air.

Methods

The Tegelen sections (Gilze and Maalbeek) were sampled for XRF from 10cm diameter cores of the Geological survey of the Netherlands (boring codes: (Maalbeek: 58E284 and Gilze: 50E368)). See Chapter 2 for standard sampling practice and analytical methods for XRF-analyses. Additionally, we took 8x8 cm undisturbed subsamples in cardboard boxes, four from the Maalbeek core (8.74-8.81m; 12.40-12.47m; 14.80-14.87m; 17.23-17.30m) and two from Gilze (14.28-14.36m; 18.65-18.70m) for micromorphological research (Figs. 4.1.3 and 4.1.4). Sample depths were chosen in such a way that a wide range of iron, magnesium, calcium and sulfur contents were covered, based on the XRF measurements. Uncovered thin sections and fresh surfaces of undisturbed, freeze-dried samples were also studied with SEM-EDAX.

The Late Pleistocene samples for XRF-analyses were collected with a hand core with a diameter of 2.7cm with 10 cm intervals, or whenever changes in color, lithology or grain size occurred. No thin sections were made of the Late Pleistocene deposits because they were very soft, organic material rich and water saturated which made preparation difficult. Rough surfaces of undisturbed pieces were studied by SEM-EDAX.

Additional samples for mineralogical analyses were taken from all sections. They were studied by XRD, Thermo-Gravitational Analyses (TGA) and by studying the CO₂-release of the samples at specific temperatures. As the results of the methods were similar, we will present them combined as "mineralogical analyses".

Data treatment

For this Chapter, the interpretation of the XRF analyses is focused on some specific elements. Al₂O₃ reflects the clay content, SiO₂ the amount of sand (Chapter 3.1); MnO, P₂O₅ and S are often related to iron containing minerals subject to redox reactions like vivianite and pyrite. CaO, MgO and Fe₂O₃ are related to carbonates, but Fe and Mg occur also in significant amounts in clay minerals. In order to determine the contents of Fe, Ca and Mg in carbonates, they have to be corrected for the amounts of these elements that are present in the clay. In Chapter 3.1 we found that the contents of Fe₂O₃ and MgO clay can be estimated on the basis of the Al₂O₃-content according to:

$$\text{MgO}(\text{clay}) = \text{Al}_2\text{O}_3/10$$

$$\text{Fe}_2\text{O}_3(\text{clay}) = \text{Al}_2\text{O}_3/4$$

As a result, the contents of MgO and Fe₂O₃ in carbonates can be estimated as the difference between their total and their clay-related contents according to:

$$\text{MgO(carb.)} = \text{MgO (tot)} - \text{Al}_2\text{O}_3/10$$

$$\text{Fe}_2\text{O}_3(\text{carb.}) = \text{Fe}_2\text{O}_3(\text{tot}) - \text{Al}_2\text{O}_3/4$$

MgO(carb), Fe₂O₃(carb.) and CaO and were plotted against each other in ternary graphs to investigate possible relationships between the different carbonate fractions. Similar procedures were performed with Fe₂O₃, CaO and P₂O₅ to establish possible relationships between siderite, calcite and vivianite.

Results

Tegelen Formation

Geochemistry The ternary graph of CaO, MgO(carb) and Fe₂O₃(carb) (Fig. 4.1.2) demonstrates a constant MgO(carb) percentage in the Maalbeek record, indicating a uniform dolomite content. Fe₂O₃(carb) and CaO display considerable variations, suggesting varying amounts of siderite

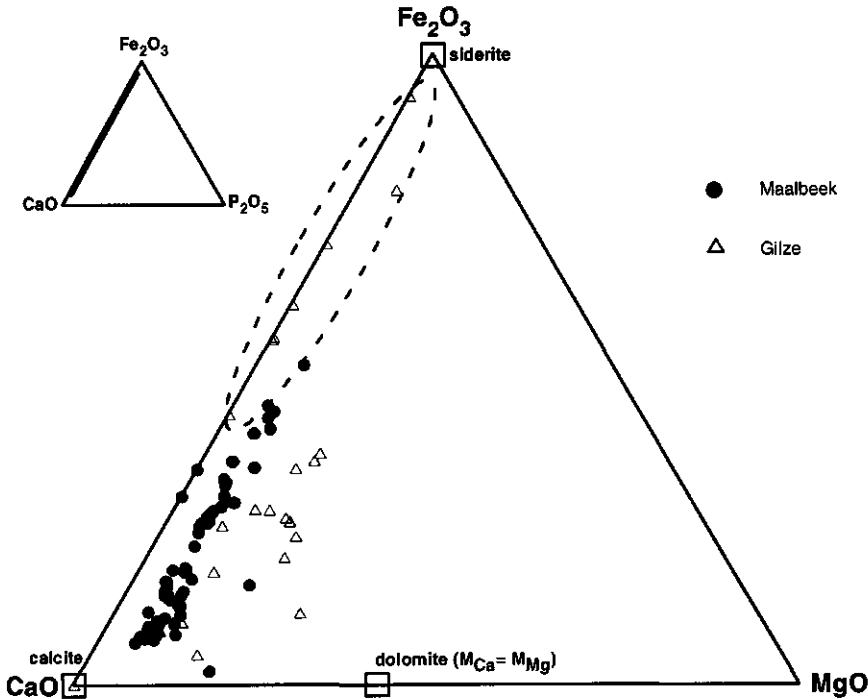


Figure 4.1.2 Ternary graph of Fe₂O₃(carb), CaO and MgO(carb). The locations of ideal calcite, siderite and dolomite are indicated. Data from Gilze part i are encircled (see text). In the upper left corner is a ternary graph of Fe₂O₃(carb), CaO and P₂O₅.

and calcite. Within the Gilze core, the MgO(carb) percentages are higher and more variable, whereas the Fe₂O₃(carb) and CaO percentages are comparable to the Maalbeek record. An exception is the upper part of the Gilze core, where MgO(carb) estimate is nil and CaO and Fe₂O₃(carb) contents are low (Figures 4.1.3 and 4.1.4).

Depth profiles of the chemical composition in the Maalbeek core (Fig. 4.1.3) show that high contents of MgO, Fe₂O₃ and CaO are restricted to the clay layer, which is characterized by relatively high Al₂O₃ and low SiO₂ contents. In this layer, the contents of MgO are high but more or less constant. The contents of Fe₂O₃ and CaO, however, show more variation, as well as MnO and P₂O₅. The pattern of a high background with superimposed peaks indicates the overall presence of Fe- and Ca-bearing minerals with additional locally concentrated MnO and P₂O₅. The XRD-measurements confirm that the Ca, Fe, and Mg-bearing minerals present in this section can be identified as calcite, siderite and dolomite (Fig. 4.1.3). The S-levels gradually increase with depth, but are still low.

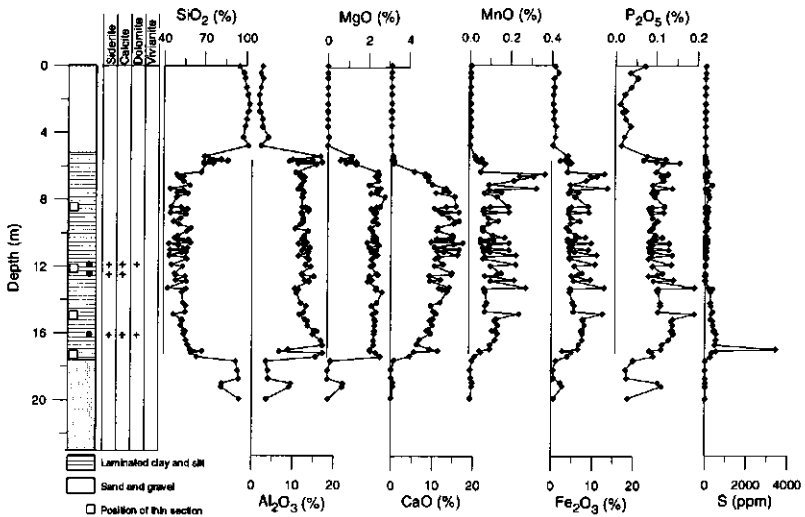


Figure 4.1.3 XRF data from the Maalbeek section. Dots in the lithological column indicate sample depths for mineralogical analyses. The presence of specific minerals, determined by mineralogical analyses, are indicated by crosses. Thin section sample depths are indicated by boxes.

In the Gilze core (Fig. 4.1.4), high SiO₂ and lower and more variable Al₂O₃ contents reflect a lower and variable clay content which decreases with depth. Within the profile, three different parts can be distinguished with respect to MgO, CaO, Fe₂O₃, P₂O₅ and Al₂O₃ concentrations:

i) 9-13.5 m: MgO, CaO, P₂O₅ and Fe₂O₃-contents are low, and more or less follow the Al₂O₃-content. This is the area delineated in Fig. 4.1.2 with no Mg(carb) and low Fe(carb) and Ca(carb), so apparently no or few carbonate minerals are present. A sudden increase in P₂O₅ marks the transition to ii.

- ii) 14-20m: MnO and Fe₂O₃ show a peak at 13.5 m., after which the concentrations remain higher through the rest of section ii. MgO-and P₂O₅-contents are also elevated, but do not show a clear spatial pattern. CaO-content increases steadily with depth. Two S-peaks can be identified, but the overall S-contents remain low.
- iii) 18-22m: The CaO content decreases steadily. The contents of MgO, MnO, Fe₂O₃ and P₂O₅ are also lower than in part ii.

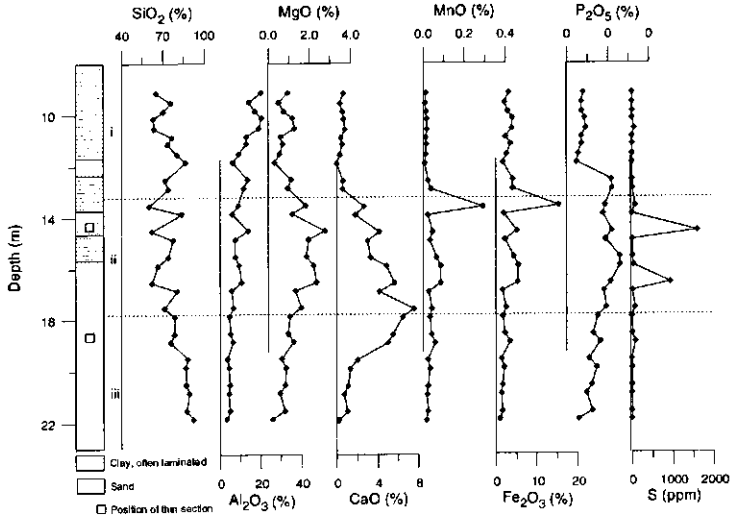


Figure 4.1.4 XRF data from Gilze section. Parts i,ii and iii (see text) area separated by broken lines. Boxes indicate thin section sample depths.

Micromorphological observations and submicroscopical data. All thin sections show well sorted horizontal laminated structures and poorly sorted, complex layered structures, with parallel oriented micas, lath shaped tissue remnants and organic fibers. Grain size ranges from clay to fine sand, microstructure is close porphyric. Dominant minerals, in addition to carbonates, are quartz, feldspar and micas. Based on their rounded shape, size and distribution they are interpreted as detrital particles. In all thin sections few pyrite framboids (10 to 50 μm in diameter) occur, sometimes associated with organic matter.

Varying amounts of carbonate minerals showing considerable morphological variation were observed in the thin sections. Using SEM-EDAX, they could be identified as dolomite, calcite and siderite. The following morphological types were observed (Figs. 4.1.5 and 4.1.6):

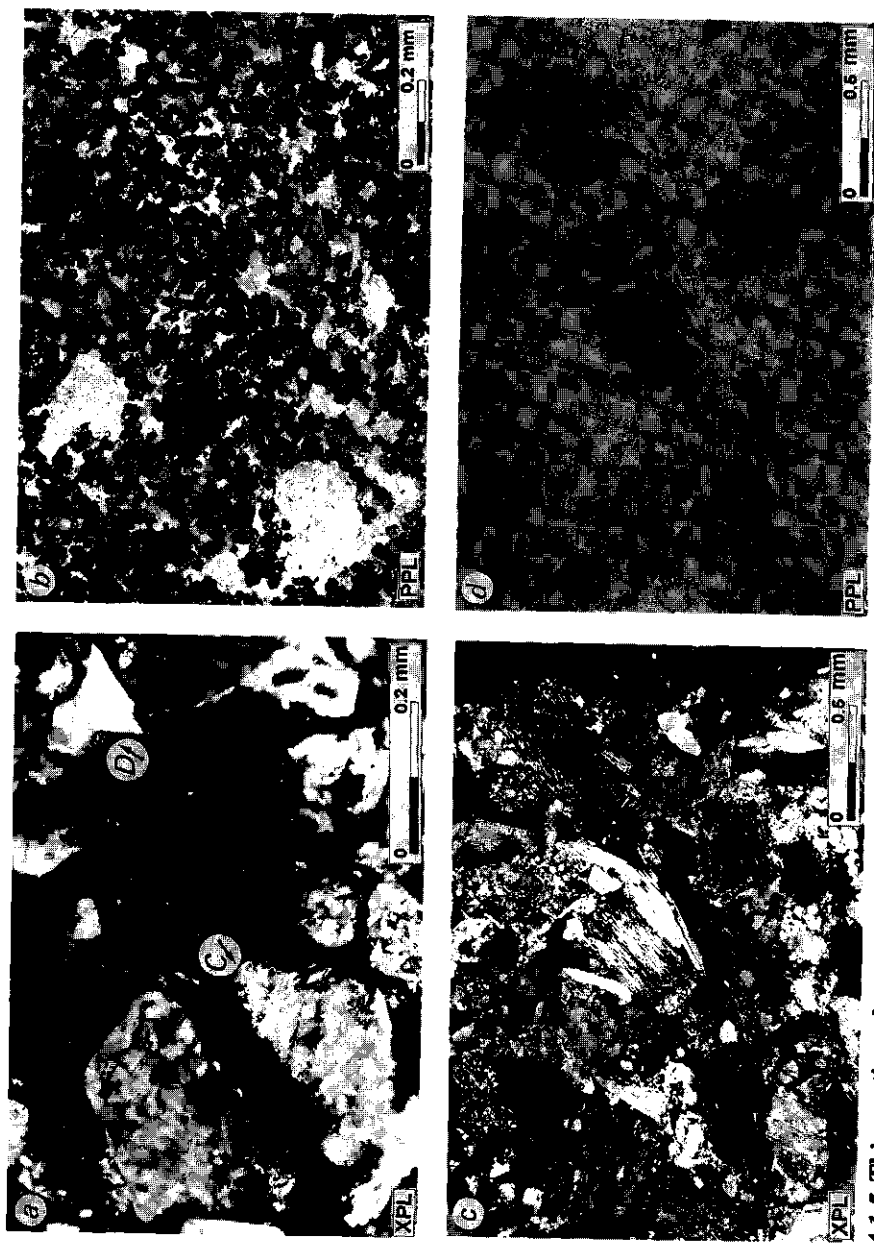


Figure 4.1.5 Thin section photomicrographs taken under a petrographic microscope. **A.** Within the lower left corner (**C**) a calcite grain is shown (type i). The denticulated border and the holes within the grain indicate dissolution of the mineral. In the upper right corner a dolomite grain (**D**) coated with siderite can be seen (type ii). **B.** Equidimensional siderite grains (type iv). **C.** Siderite grains between the platelets of micas. The mica platelets show high interference colors, while the siderite is visible as dark dots. Left of the middle mica a siderite dolomite grain can be seen. **D.** PPL of **C.**, showing the abundant amount of siderite nodules within the micas.

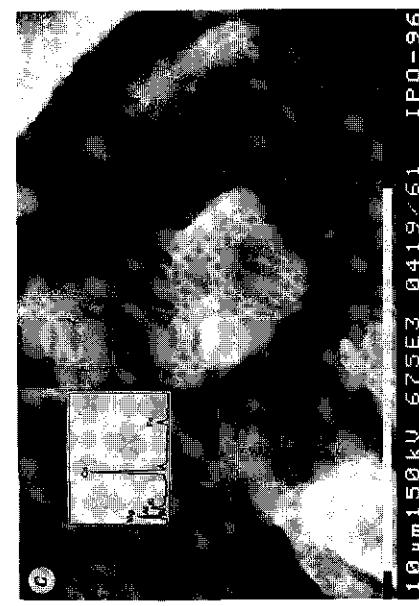
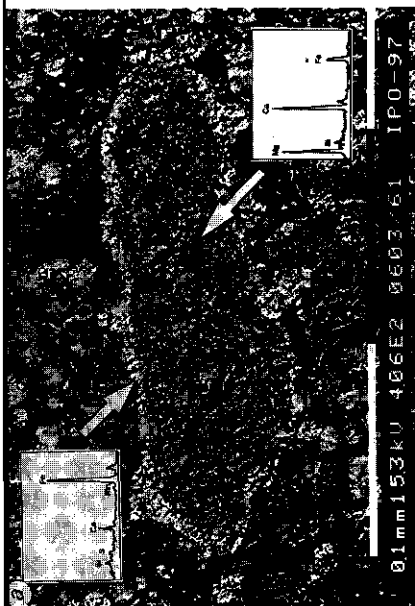
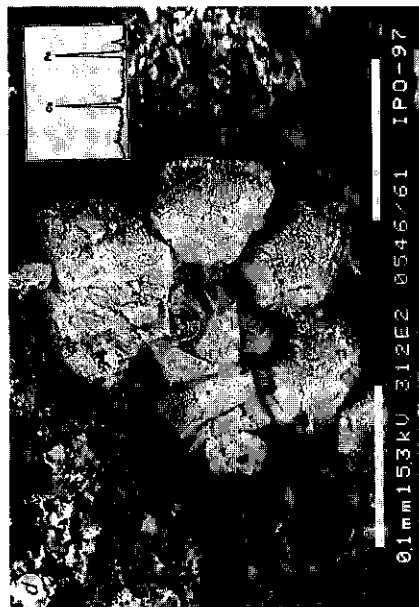
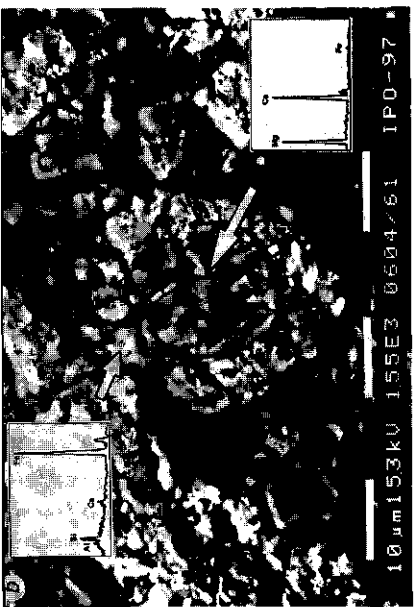


Figure 4.1.6 SEM photographs (backscatter). Results of EDAX measurements of different locations are shown in the enclosed graphs. A.¹ Dolomite grain coated with siderite (type ii). Around the grain siderite nodules (type iv) can be seen (bright dots). B.¹ Siderite nodule with a nucleus of dolomite (type ii). C.² In the center a euhedral grain is shown with a botryoidal shaped surface. The chemical composition points towards dolomite with a siderite coating (type ii). D.² A concretion of subangular concentric nodules, probably consisting of a mixture of calcite and dolomite. EDAX measurements on different locations on the nodules showed some variation of the Fe and Ca content. ¹ photo from thin section. ² photo from rough surface.

- i) Coarse-crystalline to micritic calcite grains have a similar size as detrital minerals. In Gilze thin sections, such grains often have a denticulated surface and display holes within the grain as a result of dissolution processes (Fig. 4.1.5a).
- ii) Dolomite grains of the same size and crystallinity as (i) are coated with calcium-rich siderite (Figures 4.1.5a and 4.1.6a). Few grains also show dissolution features.
- iii) Sand to silt sized carbonate concretions with Ca, Mg and Fe in varying ratios, occur as subrounded grains.
- iv) Equidimensional single nodules of calcium-rich microcrystalline siderite (2 to 40 μ m in diameter) are often fused together to botryoidal grains (Fig. 4.1.5b). The centers of these nodules occasionally consist of dolomite (type ii) (Fig. 4.1.6b). In silt to clay bands parallel to the stratification, small (<1 μ m) crystals of probably siderite and calcite occur homogeneously mixed through the groundmass. Due to the small size, the mineralogy of these grains could not be determined. However, bulk XRF data from these depths show elevated contents of Fe and Ca.
- v) A cementing agent of calcite occurs between sediment grains. Sometimes siderite nodules (iv) were observed within the calcite cement.

Frequently, exfoliated micas bear abundant distinct siderite nodules of type (iii) (2 to 25 μ m in diameter) inside cleavage cracks (Figure 4.1.5c and 4.1.5d).

SEM-EDAX study of the rough surfaces of undisturbed samples from the Maalbeek core showed the presence of euhedral grains with a botryoidal surface coating (Fig. 4.1.6c). They contained Ca and Mg as well as Fe, suggesting that they consist of dolomite grains coated with siderite, similar to type ii described above. Apart from that, smooth surfaced euhedral calcite grains were observed.

Late Pleistocene Maas deposits

Geochemistry A Fe_2O_3 - CaO - P_2O_5 ternary graph of all Late Pleistocene samples (Fig. 4.1.7) show a wide variation with respect to CaO and Fe_2O_3 contents, suggesting that siderite and calcite are present in varying amounts. Lottum samples have high contents of P_2O_5 which was confirmed by the presence of abundant vivianite as deduced from the bright blue colors observed after oxidation of some of the Lottum samples.

In the depth profiles of the Late Pleistocene sites (Figures 4.1.8-4.1.10), Al_2O_3 and SiO_2 contents reflect the presence of mineral material and these values are negatively correlated with organic matter. The $\text{MgO}/\text{Al}_2\text{O}_3$ ratio is close to 10, suggesting that all magnesium is incorporated in clay minerals (see equation 1). This is confirmed by the XRD-measurements. Depth profiles of Lottum and Meerlo show CaO values of 20% and Fe_2O_3 contents over 40%, whereas Groeningen shows lower CaO (up to 3 %) and comparable Fe_2O_3 contents (Figs. 4.1.8-4.1.10). XRD-measurements confirm that calcite occurs at Lottum and Meerlo, whereas it is absent in Groeningen. Siderite occurs at all sites. The highest contents of CaO and Fe_2O_3 are present in the gyttja-layers, whereas peat layers have lower contents. The same is true for the contents of P_2O_5 and MnO in all three sites. S contents on the other hand are highest in the peat layers. The S-contents reach as high as 1.5%. The elevated Fe_2O_3 , MnO, P_2O_5 and CaO in the gyttja layers contents indicate high contents of calcite, Mn-bearing siderite and vivianite in the gyttja layers. The elevated S-contents in the peat suggest the presence of pyrite or

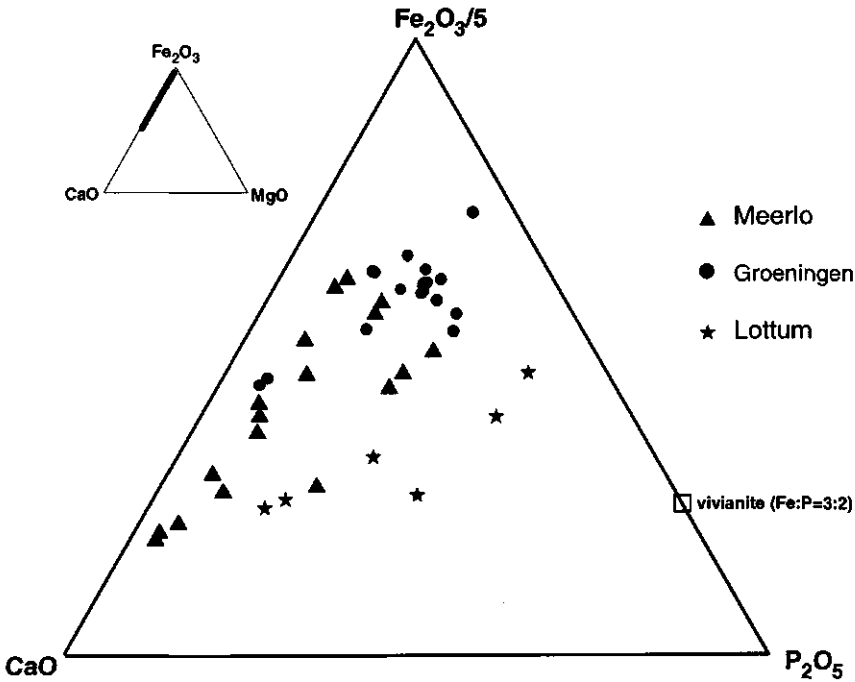


Figure 4.1.7 Ternary graph of $\text{Fe}_2\text{O}_3(\text{carb})/5$, CaO and P_2O_5 . The ideal composition of vivianite is indicated. In the upper left corner is a ternary graph of $\text{Fe}_2\text{O}_3(\text{carb})$, CaO and $\text{MgO}(\text{carb})$.

organically bound sulfur. XRD-measurements confirmed the presence of vivianite only in one sample from Meerlo, probably because it was oxidized quickly after sampling. At the Groeningen and Lottum sites, the highest contents of CaO , Fe_2O_3 , MnO and P_2O_5 occur in the lowest gytja layers.

Submicroscopical data. SEM-EDAX analysis of undisturbed rough surfaces of a Meerlo sample displayed subangular concentric nodules (50-100 μm in diameter). They contained Fe and Ca in varying ratios, with locally some P (Fig. 4.1.6d). Since only siderite and calcite were determined with XRD, these nodules probably consist of thoroughly mixed siderite and calcite. In a Groeningen sample nodules were found with Fe and P contents comparable to the Meerlo nodules, but with less Ca and occasionally with some Mn and S. These nodules may represent an association of phosphate and carbonate minerals.

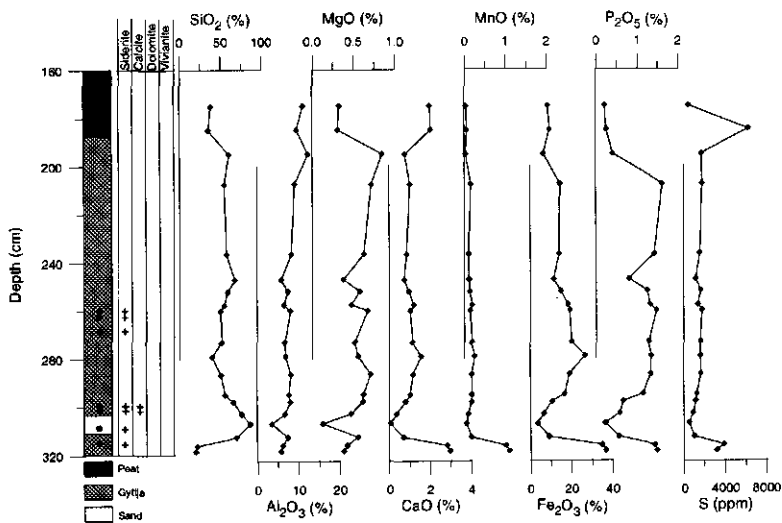


Figure 4.1.8 XRF data of the Groeningen site. Dots in the lithological column indicate sample depths for mineralogical analyses. The presence of specific minerals, determined by mineralogical analyses, are indicated by crosses.

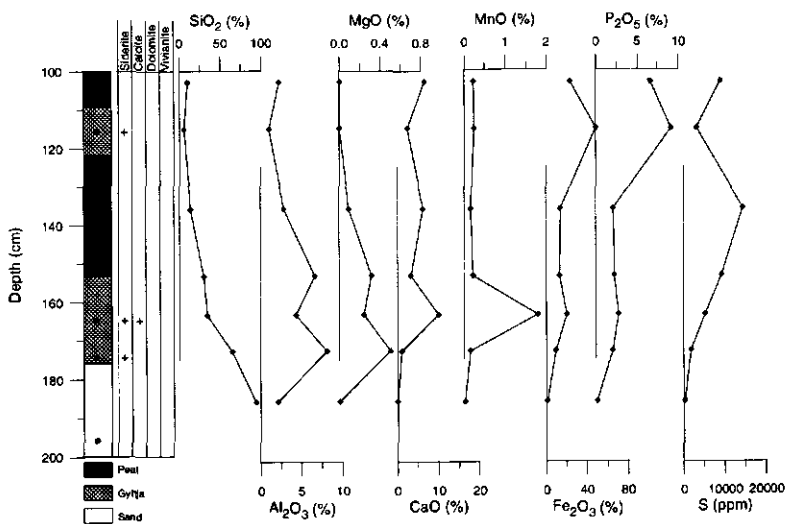


Figure 4.1.9 XRF data of the Lottum site. Dots in the lithological column indicate sample depths for mineralogical analyses. The presence of specific minerals, determined by mineralogical analyses, are indicated by crosses.

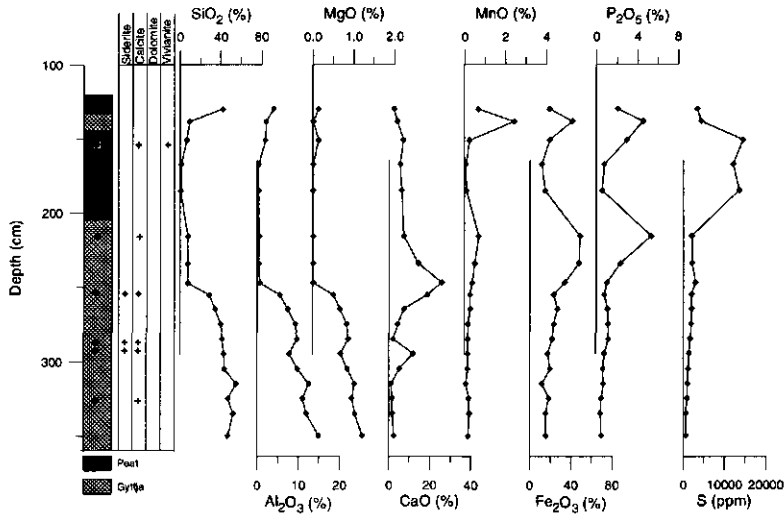


Figure 4.1.10 XRF data of the Meerlo site. Dots in the lithological column indicate sample depths for mineralogical analyses. The presence of specific minerals, determined by mineralogical analyses, are indicated by crosses.

Discussion

Siderite formation in the Tegelen Formation

The occurrence of calcite and dolomite grains type i and ii (see results and Figs. 4.1.5a and 4.1.6b) with similar size as detrital minerals like quartz, indicates a fluvial detrital origin of these carbonates. They originate most probably from the Mesozoic dolomitic limestones in which the Rijn started to incise during the Early Pleistocene (Hoselmann, 1996; Walther and Zitzmann, 1981). The constant Mg concentration throughout the Maalbeek section supports detrital genesis of the dolomite since a uniform distribution is not likely to be related to a local diagenetic origin (cf. Behrens and Land, 1972). Dissolution of calcite grains and reprecipitation of calcite cement (type iv) explains the larger variation of the CaO content through the profile, compared to the Mg content.

Given the fluvial (Maalbeek) or fresh-water estuarine (Gilze) depositional environment as determined by Zagwijn (1960) Kasse (1988) and Westerhoff and Cleveringa (1996) on the basis of sedimentological and palynological research, one would at first conclude that the siderite present in these sections was formed syndepositionally in these environments. However, the occurrence of microcrystalline siderite as small, botryoidal grains (type iii) within coarser-grained sediments, between mica platelets, as overgrowths on dolomite grains, and the occurrence in bands throughout the clay layers (type iv) all indicate that siderite was formed postdepositionally *in situ*.

The observed hardening on exposure of the Tegelen clay in the Maalbeek excavation probably results partly from oxidation of this type-iii microcrystalline siderite to cementing Fe-(hydr)oxides. The encountered concretions of Ca, Mg and Fe carbonate (type iii) are most probably formed by precipitation of siderite on a detrital dolomite/calcite concretion, or by precipitation of both siderite and calcite on an altered (*in situ* weathered) dolomite grain. The preference of siderite to accumulate around dolomite grains can be explained by the similarity of the crystal lattice. A possible formation process of the siderite nodules between exfoliated mica platelets could be the reaction of available CO_3^{2-} with Fe^{2+} out of the weathering mica, forming a siderite nucleus between the platelets. This nucleus would then form a kernel where siderite would preferentially precipitate from Fe^{2+} and CO_3^{2-} from outside.

Summarizing, calcite and dolomite have a detrital origin, whereas siderite is formed after deposition. Calcite is dissolving and may locally precipitate. Meeting the earlier mentioned constraints on siderite formation, dissolution of calcite is thermodynamically possible while dolomite and siderite remain stable (Figure 4.1.11). When ferrous iron-rich water intrudes a system where Ca^{2+} , Mg^{2+} and CO_3^{2-} are in equilibrium with calcite and dolomite, siderite will precipitate and the CO_3^{2-} concentration will decrease, implying that both calcite and dolomite will become unsaturated. Calcite will predominantly dissolve, because it is the least stable carbonate, though dolomite may also dissolve at the same time depending on the Mg^{2+} concentration, the Total Inorganic Carbon (TIC) concentration and pH. The process will raise the CO_3^{2-} concentration again, stimulating more siderite precipitation. With a continuous supply of ferrous iron and a discharge of calcium with groundwater flow, a steady state will be reached with dissolving calcite and precipitating siderite until all calcite is dissolved. These processes of siderite could have taken place shortly after deposition. However, the current composition of the groundwater in the vicinity of the Gilze study site (Saager, 1996) shows that presently calcite and dolomite are in equilibrium with the solution, while the solution is super-saturated with respect to siderite (Fig. 4.1.11). The process of precipitation of siderite at the expense of calcite is therefore

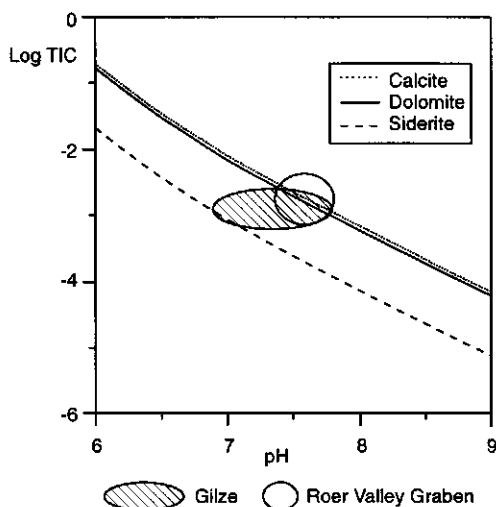


Figure 4.1.11 pH-TIC (Total Inorganic Carbon) stability diagram of calcite, siderite and dolomite calculated with thermodynamic data of Appelo and Postma (1994). Equilibrium lines are calculated with $[\text{Ca}] = [\text{Mg}] = 10^{-3}$ M and $[\text{Fe}] = 10^{-4}$ M. Taken a low Eh value and sulfur content, siderite is the most stable carbonate, while dolomite is slightly more stable than calcite. pH and TIC prevailing in the Tegelen sediments in the Gilze area (Saager, 1996) and in the Roer Valley Graben (Nolte, 1996) are indicated.

an ongoing process. A comparison with groundwater data from the Tegelen formation in the Roer Valley Graben (1996) shows that there similar conditions prevail, and that there too siderite precipitates at the expense of calcite. (Fig. 4.1.11).

Siderite formation in Late Pleistocene river fens

In the Late Pleistocene sites, the higher concentrations of Ca, Fe, P and Mn in gyttja layers when compared to peat indicates that the calcite, siderite and vivianite were specifically formed in the gyttja layers. The joint formation of calcite and siderite requires a high bicarbonate concentration, whereas the presence of vivianite indicates high phosphorus availability. The most likely source for the bicarbonate needed to form the carbonate minerals is decomposition of organic matter during methanogenesis. Fe, Ca and Mn are probably supplied by upward or lateral moving groundwater from elsewhere. This is supported by the observation of hydromorphic Fe(hydr)oxides around the Meerlo site. The large amounts of P probably originate from organic matter that has been decomposed during methanogenesis. The same may be true for the high S concentrations. The cause for the differentiation between P (highest in gyttja) and S (highest in peat) is not clear.

Conclusions

The siderite occurring in the Tegelen formation as well as the siderite of the Late Pleistocene river fens are formed under a large influence of groundwater. However, the Early Pleistocene siderite is formed postdepositionally under waterlogged conditions with carbonate originating from dissolution of calcite, reacting with ferrous iron supplied by groundwater and micas. Calcite and dolomite have a detrital origin. In contrast, the Late Pleistocene siderite is formed syndepositionally during methanogenesis under Fe-rich reducing circumstances, which also favor formation of iron phosphate minerals. Ca rich carbonates occurring within the same setting are most probable also authigenic. In both settings, the groundwater composition plays a crucial role in supplying especially Fe to form siderite. However, whereas in the Late Pleistocene deposits the groundwater composition and movement is directly related to the depositional environment of organic-rich river fens, the siderite occurring within the Tegelen formation is related to a groundwater composition that has no relation to the original depositional environment. It is difficult to estimate for how long these siderite-forming processes have been active in the Tegelen sediments. Given the age of the sediments (1.5-2 Million years), and the amount of calcite still present, the siderite-forming episodes have probably been relatively short.

Our results demonstrate that siderite is not necessarily an indicator for the environment during deposition, because it may also reflect younger diagenetic environments. This is especially the case in large-scale-deltaic settings, like the Rijn-Maas delta, where fluvial dynamics, tectonics and repeated re- and transgressions through climate-induced sea-level fluctuations can cause a multiple or even cyclic changes in the groundwater composition after deposition. Syndepositional siderite formed by methanogenesis can be recognized, however, by its association with large amounts of (vivianite-) P and the presence of appreciable amounts of S. If siderite is associated with other carbonates and organic

matter contents are low, it may have been formed postdepositionally through interaction with groundwater.

4.2 Trace element and REE anomalies in Quaternary organic-rich deltaic deposits

D.J. Huisman
B.J.H. van Os
J. Voncken
A.C.M. Clerkx

Abstract

During the formation of low-gradient deltas of large river systems, multiple cycles of interchanging of fresh and saline water and oxic and reduced diagenetic environments occur, driven by the glacial- to interglacial climatic cycle. Because of the potential reactivity of organic matter, the geochemical characteristics of organic-rich sediments can be strongly affected by these changing diagenetic environments.

In the geochemical/sedimentary record of the Pliocene and Early Pleistocene Rijn -Maas delta, organic-rich layers display anomalous enrichments of trace elements, heavy metals and rare earth elements (REE). These enrichments are driven by the sea-level fluctuations linked to the cyclic glacial-interglacial. During marine highstands, high groundwater levels cause Fe,Mn-hydroxides to become reduced, thus releasing Fe and associated trace elements into the groundwater. At the same time, transgressions of saline water over organic surface layers and saline groundwater intrusions cause the formation of pyrite and other sulfides that may contain elevated levels of As and Mo and, depending on the Fe-source, Co, Ni, Pb and Zn. Associated with the pyrite-forming reduced environment, Y, REE, Cr, V and U are immobilized and accumulate. During lowstands, lower groundwater levels cause part of the sulfides to oxidize, except for those that are present in reduced islands formed by the organic layers. Fe-oxides form, and trace elements like As, Co, Ni, Pb, Zn, Y and REE are incorporated, only to form a source for Fe and trace elements during the next reduced phase.

Introduction

The low-gradient deltas of large river systems form extensive interfaces between fresh and saline water systems. Re- and transgressions over such delta plains do not only cause interfingerings of fluvial and marine sediments, but also alternating marine and continental diagenetic environments over large areas. Moreover, changes in ground water regime through fluctuations in sea level or river dynamics may result in variations in the redox-state of sediments, and thus cause additional diagenetic processes. Because of the large differences in chemical environment between continental and marine settings, one can expect that at this dynamic saline-fresh interface a large variation of geochemical processes occur. Some indications that this is the case was reported by Leckie et al. (1990) and Middelburg (1990), who describe accumulations of

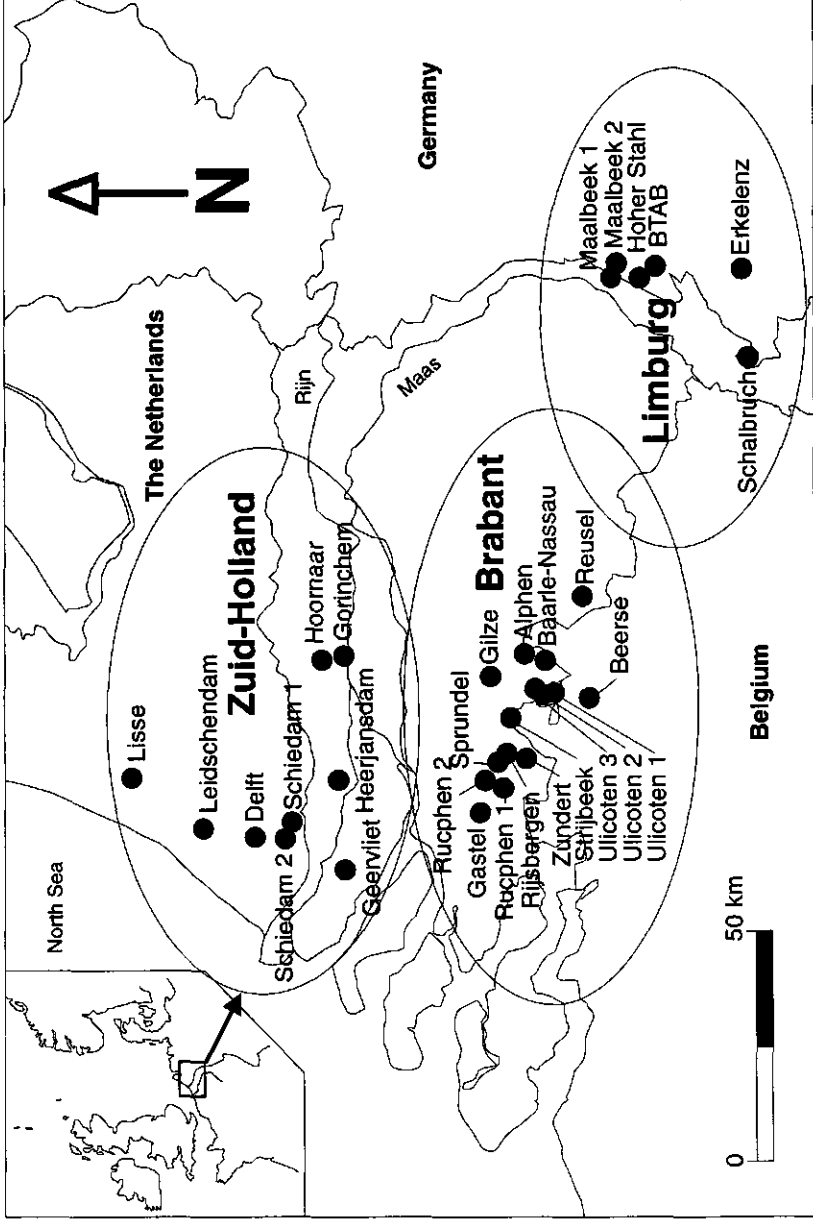


Figure 4.2.1 Sample areas and locations.

elements like V, Mo and U in littoral or drowned continental deposits. Because of their relatively high reactivity, organic deposits present in a deltaic sediment body are the most likely places for such processes to occur. These organic deposits include peat from laterally extensive coastal marshes, and peat, gyttja and organic-rich clays from local basins, river fens and paleosols. Studying such deposits therefore would indicate the net effects of changing diagenetic environments and identify the most important processes. Knowledge of these processes is important for assessing the role of large-scale deltas in global element budgets.

Present-day diagenetic-geochemical research is mainly focused either on pelagic and marine settings like the Pacific, the Mediterranean and the Black sea, or on evaporitic basins like Baffin bay. These settings provide the means to accurately study specific processes in a uniform environment. The geochemical processes in a deltaic environment appear to be underreported, despite the fact that this is a highly dynamic geochemical environment.

In order to investigate the diagenetic processes in large-scale delta systems we made a series of geochemical observations from the Rijn -Maas Schelde delta in the Southern Netherlands. We investigated the mineral phases associated with heavy metal, As, V, U, Y and REE enrichments and we propose a diagenetic model to describe the processes and interactions leading to the formation of these enrichments.

Geological setting

We present data from a series of borings in the Early Pleistocene Kedichem and Tegelen formations and the Reuver clay from the Pliocene Kiezeloëliet formation which form a continuous series of deposits in the Rijn-Maas-Schelde delta in the south of the Netherlands (see Fig. 4.2.1) (stratigraphy by Zagwijn and Van Staalduinen, 1975 and Kasse, 1988). The deposits consist mainly of interchanging clay and sand layers, deposited in a fluvial environment (Fig. 4.2.2). In the Tegelen formation thick, finely laminated organic-poor silty clay layers occur which are deposited in a fresh to brackish tidal environment. These layers often contain siderite. The siderite is probably still being formed at the expense of calcite through interaction with groundwater (Nolte, 1996 and Chapter 4.1). Locally pyrite-rich estuarine clays are found (see Kasse, 1988).

In general there are more or less continuous browncoal, peat or organic-rich clay layers at the top of the Reuver clay in Limburg, the Tegelen formation in Brabant and the Kedichem formation in Zuid-Holland. Additionally, thin layers of organic-rich clays, gyttja, peat and browncoals occur throughout the formations except in the laminated tidal clays of the Tegelen formation. Despite the fluvial origin of the deposits, S-contents are locally high (up to 5% in Brabant and Limburg, 12% in Zuid Holland) in a large number of the organic layers. Correlated with the S, As contents may reach levels up to 900 ppm. Micromorphological studies in the Limburg area indicate that the high S-contents are caused by the presence of vast amounts of pyrite that originated from saline incursions over organic-rich fresh-water deposits before burial (see Chapter 3.2). Indeed, paleogeographical reconstructions show that the fluvial sediments investigated were deposited relatively close to marine the sea (see Fig. 4.2.2). In the Tegelen deposits at Beerse, a series of three organic-rich paleosols with large pyrite nodules (Beerse member) are found in a sand layer that is under- and overlain by pyrite-rich tidal laminated clays (Rijkvorsel and Turnhout members) (see also Kasse, 1988).

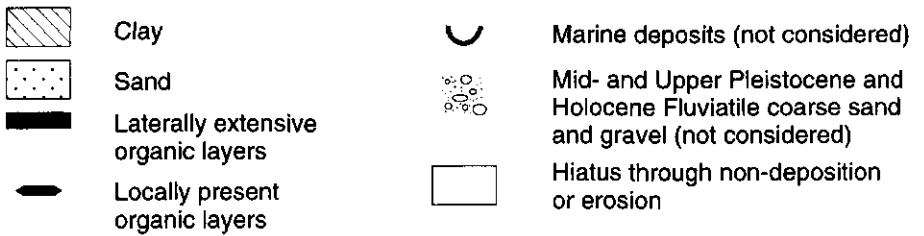
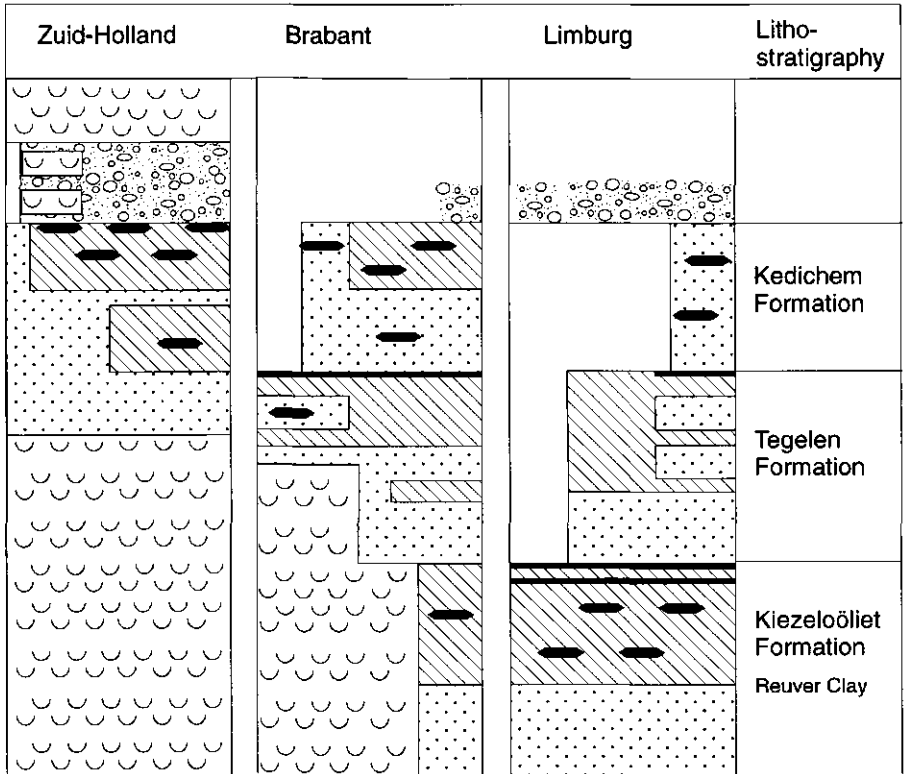


Figure 4.2.2 Schematic stratigraphy of the Pliocene and Early Pleistocene deposits in the research areas.

In the Limburg Area, the Pliocene and Early Pleistocene deposits are overlain by at least five to ten meters of fluvial gravel of the Sterksel formation. Deposits younger than Early Pleistocene are scarce in the Brabant area. The only exceptions are a few meters of Middle Pleistocene gravels (Sterksel formation) in the east of the area and a thin cover of Late Pleistocene cover sands. In the Zuid-Holland area, the Early Pleistocene fluvial deposits are overlain by Middle to Late Pleistocene gravel and coarse sand (Sterksel, Urk and Kreftenheye formations) and Holocene marine peat and clay (Westland formation). All sediments studied here are presently below groundwater.

Materials and methods

Sampling and analytical techniques

All borings from Brabant and Zuid Holland were performed in the framework of geological mapping programs of the Geological Survey of the Netherlands (presently NITG-TNO). Borings Maalbeek 1 and 2 were done to study the lithostratigraphy of Pliocene and Lower Pleistocene deposits in the Tegelen-Reuver area. Borings Schalbruch (KB 1/92, TK 25, 4901) and Erkelenz (KB 4903/10) were provided by the Geological Survey of Nordrhein-Westphalen. Hoher Stahl, Brunssum, BTAB and Beerse are clay pits. XRF was used as standard analysis. See Chapter 2 for sampling from cores and quarry faces. Subsamples were taken from selected organic-rich layers from the Brabant area for ICP-MS analyses, in order to measure the contents of those elements that could not be measured by XRF (Mo, REE). Additionally, pyrite nodules from the Beerse pit and the Erkelenz boring were analyzed. Undisturbed samples were taken in cardboard boxes for micromorphological research from organic layers in sections BTAB (7), Ulicoten 1 (4) and Sprundel (1). See Chapter 2 for analytical techniques.

Distinguishing anomalies from background

In the sediments under consideration, the bulk contents of Co, Cr, Cu, Ni, Pb, V, Y and Zn have in general a positive linear correlation with Al_2O_3 , which indicates that their detrital composition is mainly determined by the content of clay minerals and other phyllosilicates. The Ba-content is correlated with K_2O due to Ba substitution for K in K-bearing minerals (see Chapter 5). To identify and quantify enrichments, we define the background (detrital) contents of the elements on the basis of their relation with Al_2O_3 :

$$(1) \quad Me = b Al_2O_3 + a$$

Where Me is the concentration of a specific trace element in ppm, Al_2O_3 the concentration of Al in oxide-%, and a and b are the regression parameters. Subsequently, we can define enrichments or depletions as deviations from the detrital background according to:

$$(2) \quad Me^* = Me - (b Al_2O_3 + a)$$

With Me^* representing the enrichment or depletion in ppm relative to the detrital background. In the case of enrichments, Me^* will be positive, whereas Me^* will be negative in case of depletion.

We prefer to use this calculation of Me^* over Al-normalization as a measure for enrichment and depletion because when using Al-normalization, the levels of enrichment are exaggerated at low Al-contents and underestimated at high Al-contents.

The Al_2O_3 - corrected background values for Co, Cr, Cu, Ni, Pb and Zn were taken from Chapter 5. They are based on data from the Brabant borings. The Ba- K_2O regression line is used as estimation of the background as its correlation is better than the Ba- Al_2O_3 correlation. We calculated the parameters for the relation between Al_2O_3 and V and Y using the same data.

	N	R^2
Co = $0.59 Al_2O_3 + 4.49$	265	0.39
Cr = $7.51 Al_2O_3 + 21.7$	803	0.78
Cu = $1.15 Al_2O_3 + 0.54$	545	0.56
Ni = $2.29 Al_2O_3 - 1.23$	766	0.72
Pb = $1.17 Al_2O_3 + 3.53$	790	0.81
Zn = $3.78 Al_2O_3 + 6.84$	526	0.62
Ba = $20.0 Al_2O_3 + 97.9$	788	0.82
Ba = $130.25 K_2O + 51.50$	788	0.91
V = $7.64 Al_2O_3 - 9.17$	773	0.80
Y = $2.04 Al_2O_3 + 5.88$	787	0.76

U-contents are usually below the detection limit for XRF-analyses, so no relation with Al could be calculated. The coefficient of determination (R^2) is low for Cu and especially Co. This is probably partly due to smaller datasets and measurements close to the detection limit.

As-contents do not show a correlation with Al, but are generally directly correlated with the S-content according to:

	N	R^2
As = $0.0042 S + 2.83$ (As and S in ppm)	712	0.71

Because of the lack of correlation between As and Al, we cannot determine a detrital background of As, indicating that As is mainly dependent on secondary enrichment..

Results and discussion

Trace element contents in organic layers

S and As have higher concentrations in virtually all organic layers compared to the sand and clay layers. In 80 % of the organic-rich layers (36 out of 45) from all over the research area, enrichments occur of various combinations of the elements Co, Cr, Cu, Ni, Pb, V, Y and Zn (see Figs 4.2.3, 4.2.4, 4.2.5). In several of the organic-rich layers, U-contents were enriched to levels above the XRF detection limits. There is no overall correlation between the element enrichments and the contents of Corg- or S. Furthermore, some of the strongest enrichments of especially Ni

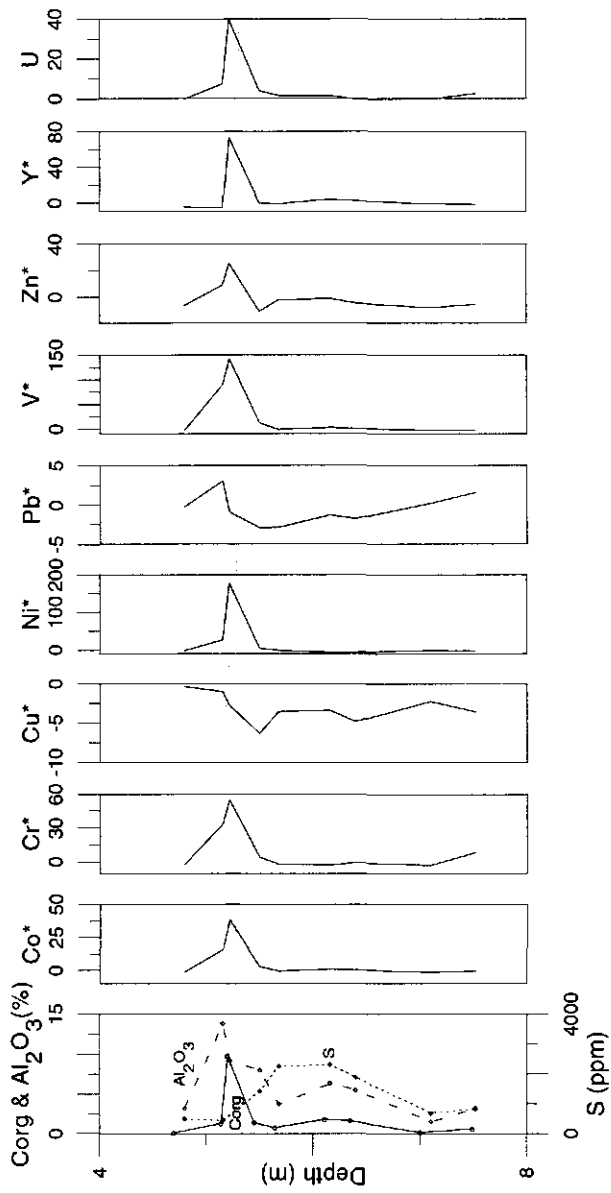


Figure 4.2.3 Depth profile of trace element concentrations, corrected for Al, in a part of section Sprundel. The shaded band indicates an organic-rich clay layer. In this layer, the contents of Co, Cr, Ni, V, Zn, Y and U are elevated.

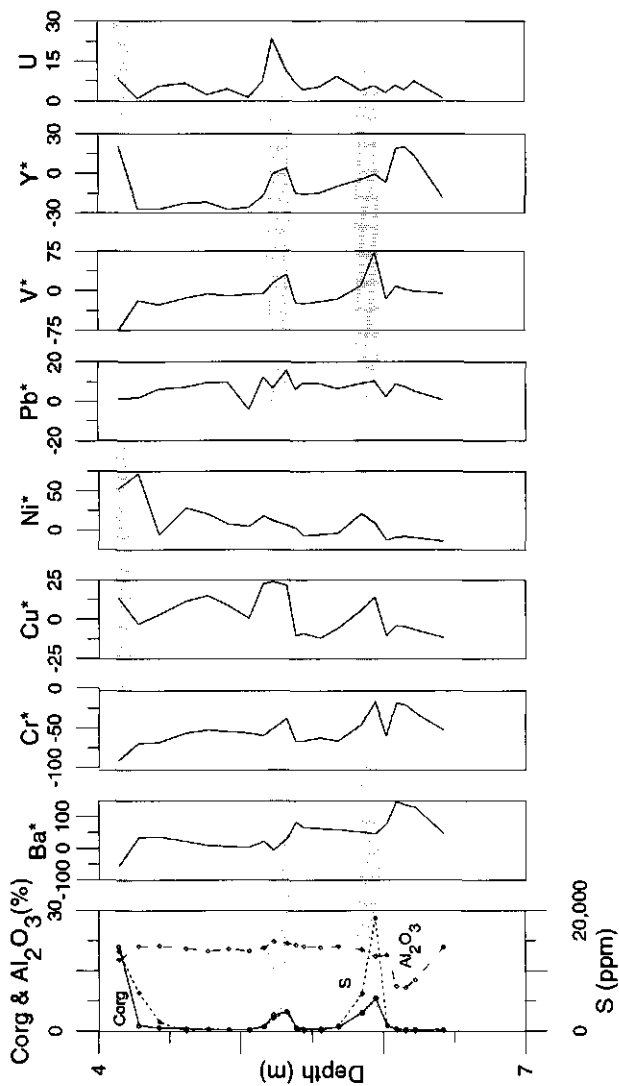


Figure 4.2.4 Depth profile of trace element concentrations corrected for Al in a part of section BTAB. The shaded bands indicate organic-rich layers. Each of the organic layers shows elevated contents of several of the elements Cr, Cu, Ni, V, Y and U. Note that the Ni-enrichments associated with the upper two organic layers is just at the edge, of the layers. Ba, Cr and V are depleted in the upper organic-rich layer.

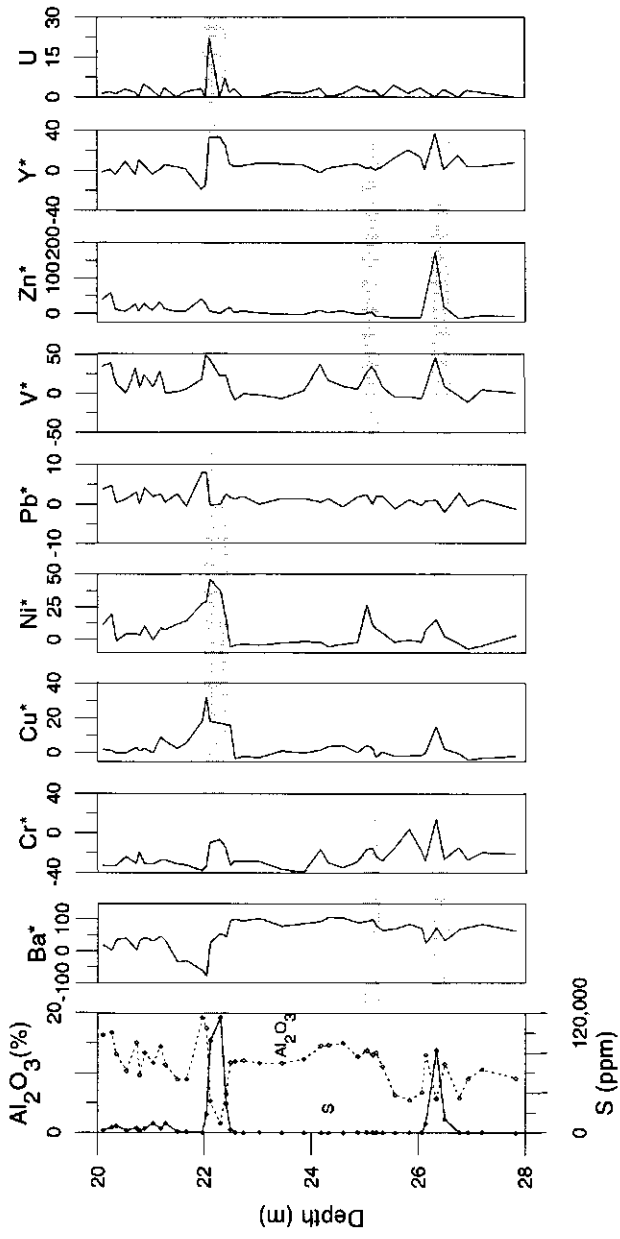


Figure 4.2.5 Depth profile of trace element concentrations corrected for Al in a part of section Heerjansdam. The shaded bands indicate organic-rich layers. Each of the organic layers shows elevated contents of several of the elements Cr, Cu, Ni, Pb, V, Zn, Y and U. Ba is depleted in the upper organic layer.

and to a lesser extent Cu and V do not coincide with the highest Corg-peaks but can be found at the boundaries between the organic layers and the under- or overlying sediment.(cf. Fig. 4.2.5 and 4.2.6). The organic layers that were analyzed by ICP-MS showed, apart from above mentioned elements, numerous cases of elevated Mo and REE contents. The chondrite-normalized REE-patterns from these enrichments are similar to the patterns of the non-organic sediments, but they do show an additional positive Ce-anomaly (Fig. 4.2.7). Apart from enrichments, some of the peat and browncoal layers show depletions of Ba and, less frequently, Cr and V (cf. Fig. 4.2.5).

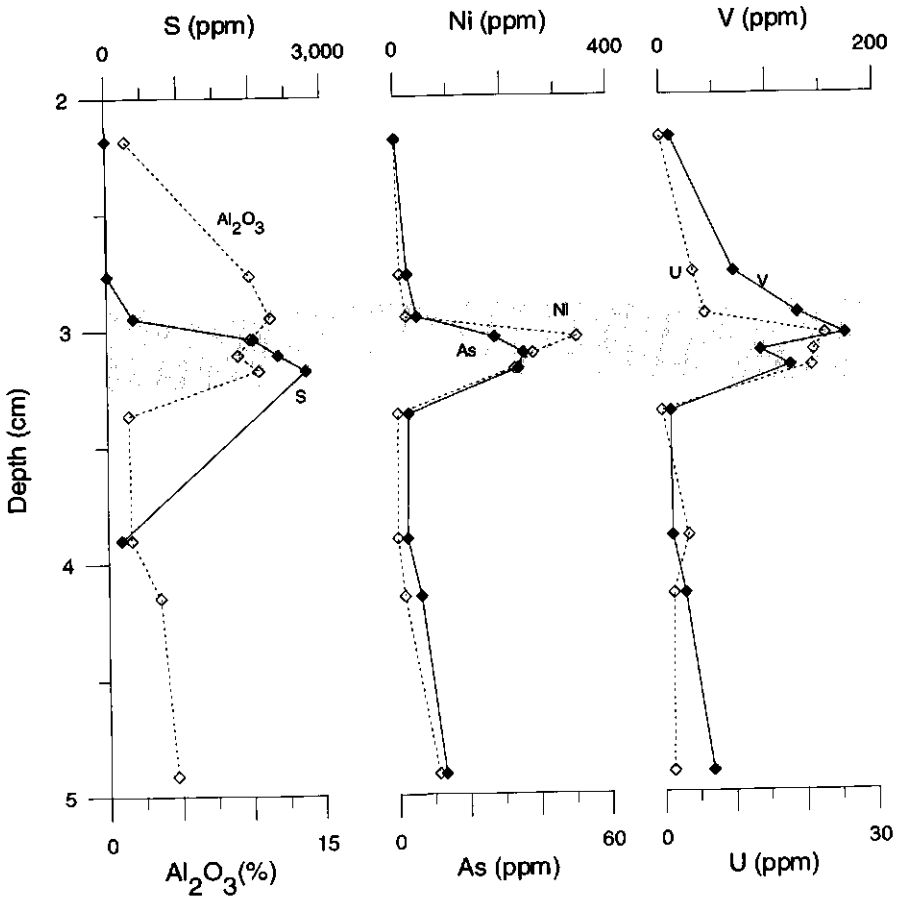


Figure 4.2.6 Depth profiles of Al, S, As, Ni, V and U; section Ulicoten 1. The shaded area is a (pyrite) S-bearing organic-rich clay layer, in which As, Ni, U and V are enriched. Note that the highest enrichments of Ni, V and U are at the upper boundary of the S-bearing section, and do not coincide with the highest S-values.

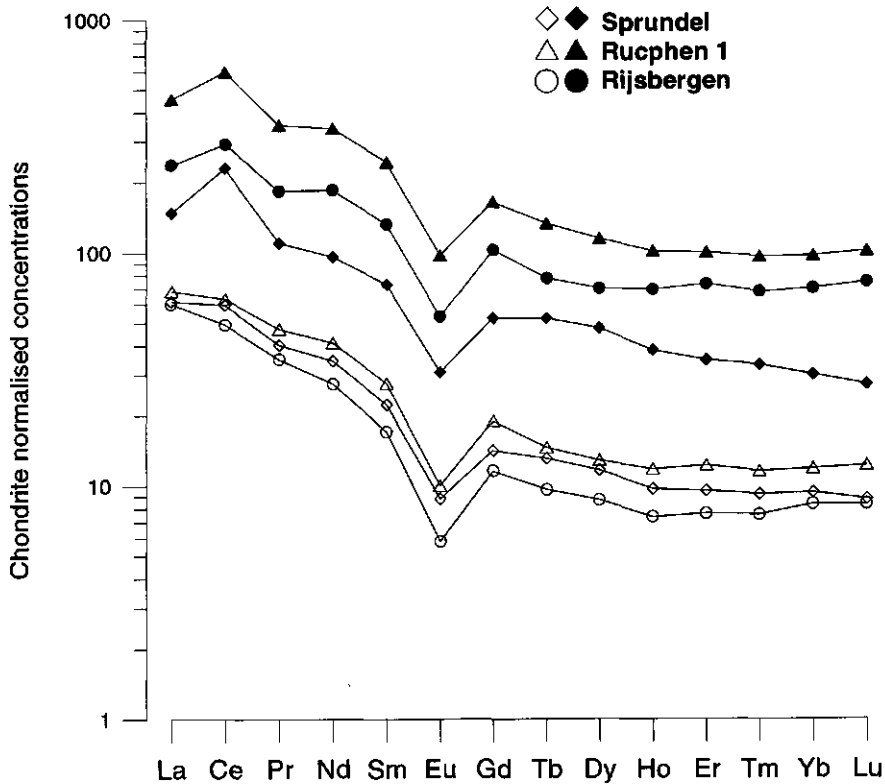


Figure 4.2.7 Chondrite-normalized REE-patterns of organic-rich (closed) and equivalent organic poor (open) sediments from three cores. The organic-rich samples show higher REE-contents and a positive Ce-anomaly.

Speciation of the enriched elements

Important processes that are known to cause immobilization and accumulation of trace elements and that are applicable to our low-temperature, organic-rich settings include the formation of sulfides, sulfates, phosphates and Fe/Mn-(hydr)oxides, adsorption by organic matter and immobilization by reducing. We tried to determine the mineralogical form of the enriched elements by micromorphological and submicroscopical techniques. The samples originated from the sections BTAB and Erkelenz in the Limburg area, and Beerse, Ulicoten 1, Rijsbergen and Sprundel in the Brabant area. Cores from the Zuid-Holland area appeared to be oxidized, so the original speciation could not be determined.

Sulfides. Pyrite framboids were found in all samples studied. In the BTAB-section, pyrite occurs also as massive infillings of cracks and always associated with organic matter (Chapter 3.2). In Ulicoten 1, Beerse and Erkelenz, large pyrite nodules (0.5-2 cm diameter) were found that typically consist of a kernel of well-crystalline pyrite with high reflectance surrounded by a thick rim of less crystalline pyrite with low reflectance which often incorporates detrital quartz grains from the surrounding sediment (Fig. 4.2.8). In the Beerse section, three organic layers, situated directly underneath pyrite-rich estuarine clay, contain a large number of plant remains that are fossilized by pyrite with high reflectance, which has replaced the original cell walls (Fig. 4.2.9a). In the upper layer these plant remains have a rim of blackish pyrite, similar to the rims of the pyrite nodules described above. This rim consists of botryoidal-shaped massive pyrite (Fig. 4.2.9b). In one of the rims, a separate euhedral galena (PbS) crystal was found (Fig. 4.2.9c). No such rims were present in the lower organic layers.

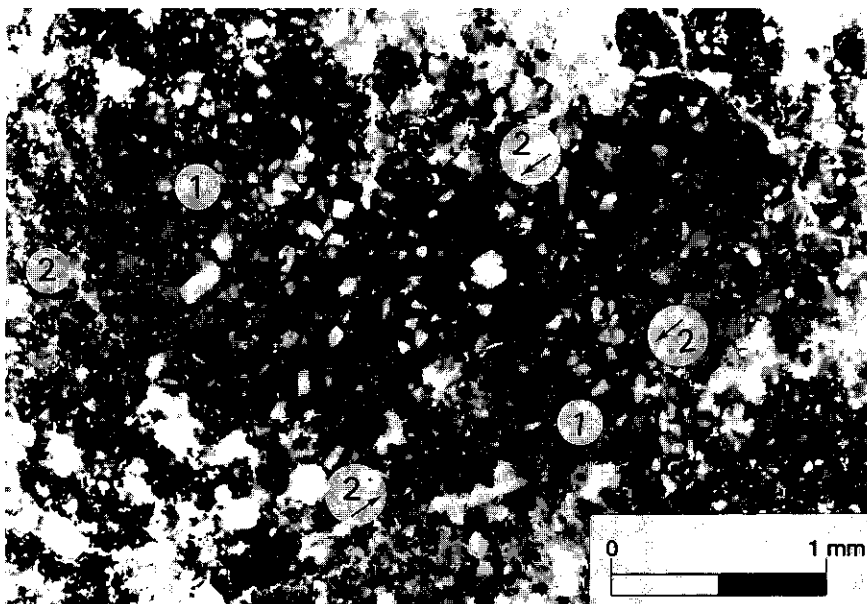


Figure 4.2.8 Rimmed pyrite in thin section from organic layer in Ulicoten 1; incident light. "1" indicates the brightly reflecting pyrite core of the nodule, "2" indicates parts of the less reflecting, dark outer rim.

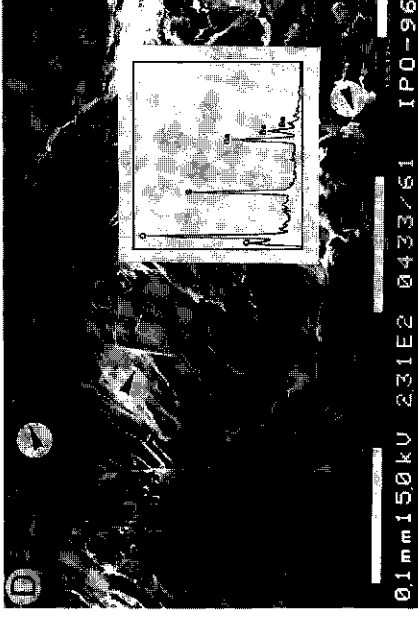
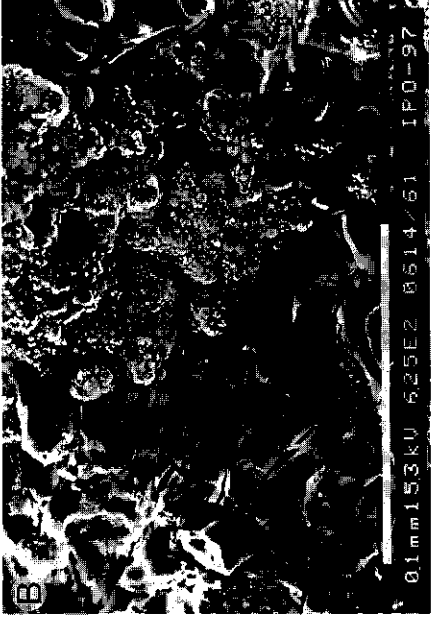
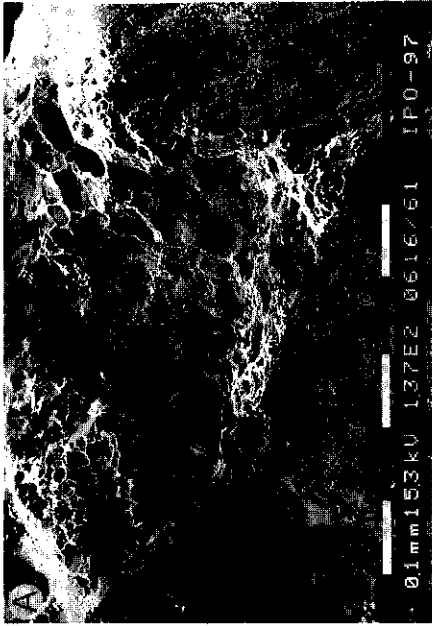


Figure 4.2.9 SEM photos of **A.** Pyritized cell walls of plant; Beerse. **B.** Pyrite from rim of rimmed plant fossil (Beerse). **C.** Galena crystal from the rim of a plant fossil (Beerse). **D.** Barite crystals (see arrow) in peat (Rijsbergen) with EDAX-scan.

The pyrites present in the organic layers studied appears to have a large variation in trace element contents. SEM-WDAX analyses of pyrite framboids from the Ulicoten1 core show that the most abundant framboids (5-30 μm) have no significant contents of any trace element (Fig. 4.2.10). Next to those, however, smaller-sized (3-10 μm) framboid-like clusters occur which are less crystalline, sometimes elongated and contain appreciable amounts of Ni and Co.

Analyses of rimmed pyrite nodules from Beerse and Erkelenz, presented in table 4.2.1, show that there is a large variation in the trace element contents of the rimmed pyrites.

Table 4.2.1: Analyses of "rimmed pyrites" from Beerse and Erkelenz. "-" = below detection limit; "ND" = not determined. All concentrations in ppm. :

Name	Type pyrite nodule	Type analyses	As	Co	Cr	Cu	Ni	Pb	Y	Zn	Mo
Erkelenz 1	Rimmed amorphous	ICP-MS	2831	1	8	1	23	1.3	1.3	20	91
Erkelenz 2	Rimmed amorphous	ICP-MS	2873	1	5	1	15	0.3	1.3	9	88
Beerse 1	Rimmed plant fossil	ICP-MS	696	872	10	0.87	1384	137	7.3	145	7.0
Beerse 2	Rimmed plant fossil	ICP-MS	733	52	6	0.69	97	71	1.5	13	10.8
Beerse 3	Rimmed plant fossil	ICP-MS	595	45	7	0.59	91	67	1.7	11	7.5
Beerse 4	Plant fossil	ICP-MS	1034	91	4	3.76	353	40	4.1	16	5.5
Beerse 5	Plant fossil	ICP-MS	985	67	6	4.48	278	40	5.9	16	7.4
Beerse 6	Rimmed amorphous	XRF	3739	2409	32	5	2719	666	ND	100	ND

The Erkelenz-nodules only shows elevated contents of As and Mo, whereas the Beerse nodules have lower contents of Mo and are enriched in As, Co, Ni, Pb and sometimes Zn in variable amounts. The REE-contents of the Erkelenz-nodules are low and show patterns comparable to shale (Fig. 4.2.11). Therefore it is likely that the REE in those nodules are not incorporated in the pyrite, but represent minor amounts of detrital material that were incorporated into the nodules. Some of the Beerse nodules however, do show elevated REE-contents. It may be noted that the samples with elevated REE-contents (Beerse 1, 4 and 5) also show elevated Y-concentrations. Still, as significant amounts of these elements are usually not present in sulfides, it is likely that they occur in another (diagenetic?) mineral phase that is present within the pyrite nodule.

From the above observations it may be concluded that at least part of the enrichments of As, Co, Ni, Pb, Zn and Mo can be explained by the presence of sulfides with varying contents of these elements. Raiswell and Plant (1980) link the contents of trace elements in pyrites to the source of the iron, with pyrite formed with local, oxide-derived iron having higher trace elements contents (especially Co, Cu, Ni, Zn) than pyrite formed with iron from external sources, i.e.

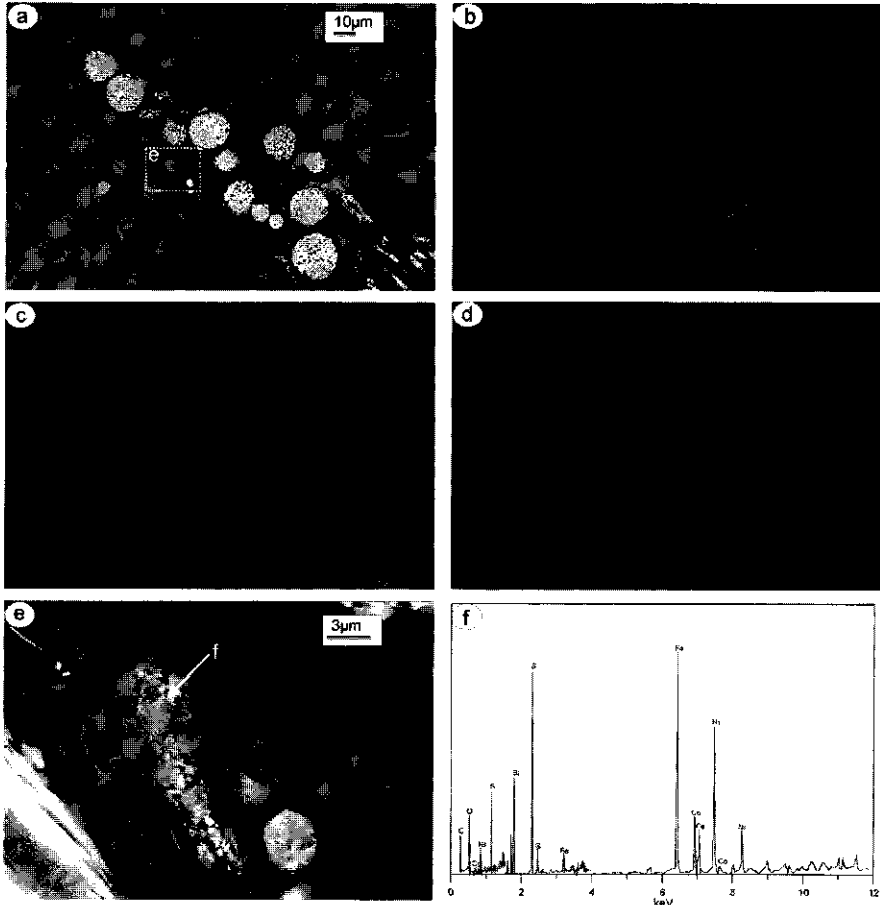


Figure 4.2.10 SEM-WDAX analyses of pyrites from Ulicoten 1. **A.** Pyrite framboids in organic material. Stippled square delineates the enlargements in **E.** **B.** S X-ray map of **A.** **C.** -Fe X-ray map of **A.** **D.** Ni X-ray map of **A.** Note that the Ni occurs only in a cluster of small framboid-like pyrites. **E.** Ni-rich framboids; detail of **A.** Note that the pyrite is less well crystallized than the Ni-poor framboids. Arrow "P" indicates WDAX-measurement presented in **F.** **F.** WDAX-measurement (composite) of framboid in **E.**

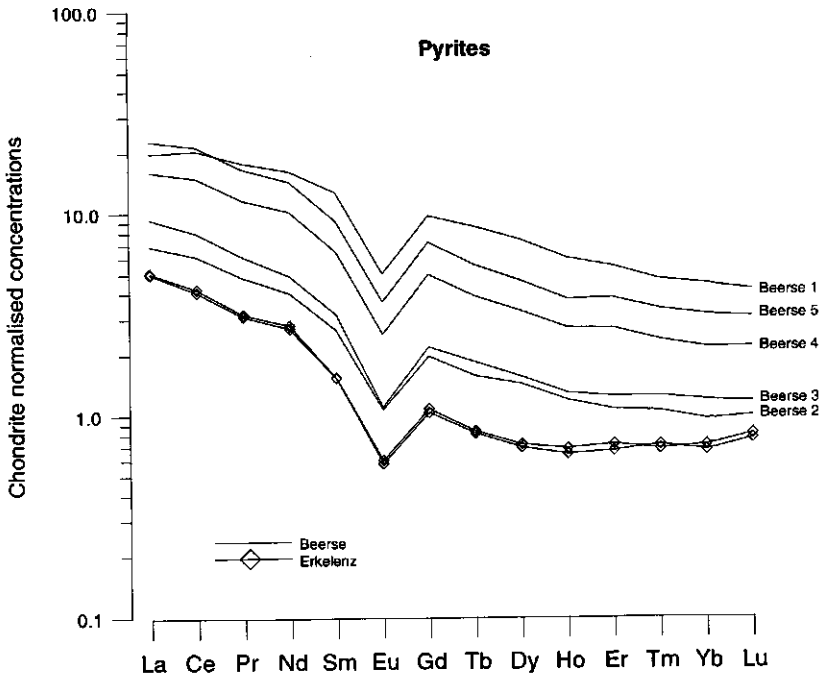


Figure 4.2.11 Chondrite-normalized REE-patterns of pyrite-framboids from Beerse and Erkelenz (see also table 4.2.1).

transported with groundwater. They claim furthermore that As and Mo contents in Fe-oxides are too low to explain the elevated contents of As and Mo in the pyrite, and they assume an external Fe-source. In contrast, we found high As-contents in hydromorphic Fe-oxides in the Brabant research area (see Chapter 5). Brinkman (1976) found Ni,Co-rich gel-like Fe-sulfides in nodules of pyrite and marcasite (a dimorph of pyrite; Deer et al., 1992) nodules associated with plant remains in Pliocene browncoal deposits south-east of the Limburg area. According to that study, the sulfur was derived from oxidizing (brown)coal elsewhere. Furthermore, Huerta-Diaz and Morse (1992) show that As and Mo are preferentially incorporated into the pyrite structure, causing an enrichment of these elements in comparison to Fe during pyrite formation. From the above discussion it is most likely that the high contents of As, Co, Mo, Ni, Pb and Zn are caused by preconcentration of these elements in (hydromorphic) Fe/Mn-oxides in a terrestrial environment. In a later phase, the elements were released into groundwater when these Fe/Mn-oxides were reduced, and subsequently they were immobilized in pyrite or as separate sulfides.

An additional process that may cause enrichment of trace elements relative to Fe (if Fe is derived from groundwater) is the formation of siderite. In Chapter 4.1 it was demonstrated that siderite formation is still taking place in the calcite-rich clays of the Tegelen formation. We found

that siderite is very poor in trace elements (except Sr). Therefore, during siderite formation Fe is depleted in the groundwater whereas the trace metals are becoming relatively enriched.

The occurrence of rimmed pyrite, the variations in trace metal concentrations in the nodules, and the occurrence of "clean" pyrite framboids next to Co- and Ni-enriched ones in Ulicoten 1 indicates that there have been several stages of sulfide formation, with different Fe-sources in each stage:

- Stage 0 Fluvial deposition; formation of organic layers and pre-enrichments in Fe, Mn-hydroxides.
- Stage 1 Transgression and drowning by saline water:
 - a Formation of primary pyrite.
 - b Dissolution of pre-enriched Fe, Mn-hydroxides.
 - c Local formation of secondary pyrite in (organic-rich) buried deposits with enriched groundwater.
- Stage 2 Regression:
 - a Pyrite oxidation; release of metals.
 - b Enrichments in Fe, Mn-hydroxides.
 - c Local formation of secondary pyrite with enriched groundwater (organic layers).

On a Quaternary timescale, phase 1 and 2 would interchange along with the glacial-interglacial cycle. Brinkman (1976) found pyrite framboids that were surrounded by a rim of alternating Fe-hydroxides and marcasite in Pliocene deposits South-East of the Limburg area. As Fe-hydroxide is only formed in oxic, and marcasite, like pyrite, only in reduced environments, this observation indicates that the groundwater at this site was alternatingly oxic and reduced. This supports the cyclic nature of the changes in groundwater composition.

Sulfates. Micromorphological observations on samples from BTAB, gypsum minerals were observed next to the pyrite. Barite crystals were observed by SEM in the borings Ulicoten 1 and Rijsbergen (Fig. 4.2.9d). A possible source for the SO_4^{2-} needed for the formation of these minerals is sea water (stage 1), but it is more likely that it is derived from pyrite-oxidation during an oxidation phase (stage 2).

Phosphates. Several studies describe the authigenic formation of secondary REE and Y phosphates: Rasmussen and Glover (1994) and Rasmussen (1996) describe authigenic overgrowths of phosphates with REE and Y as major or minor constituents in Australian marine sandstones. According to Rasmussen (1996) Y- and REE-phosphates are formed during early diagenesis with the decomposition of organic matter during sulfate- or Fe-reduction as main phosphate-source and Y and REE released from Fe- and Mn-oxides by anoxic reduction. Nicaise et al. (1996) found secondary REE, Y-phosphates formed during soil formation in a karst area. Ce is the only one of the REE that shows fractionation as a result of low-temperature redox processes, occurring both as Ce^{3+} and as Ce^{4+} . As Ce^{4+} , i.e. under oxic conditions, it is preferentially incorporated in Fe/Mn-oxides in oxic conditions (cf. German et al., 1991; Koons, 1980; Koppi et al., 1996; Morey and Setterholm, 1997). The positive Ce-anomaly in encountered

in our sediments indicates that Fe- and Mn- oxides are the most likely source for the REE encountered. Although we have not observed any Y, REE-mineral, it is likely that the REE were first immobilized and enriched in Fe/Mn-oxides in an oxidizing environments (stage 0 and 2). Subsequent reduction of these oxides and the onset of sulfidization caused the immobilization of Y and REE as phosphates (stage 1; cf. German et al., 1991 and Rasmussen, 1996).

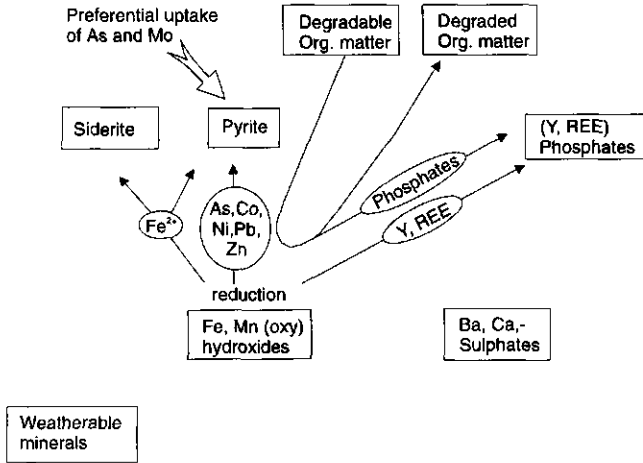
Other immobilization processes. Because of the reducing effects of organic matter and its role as a substrate for Fe- and S- reducing bacteria, elements that are mobile in oxic environments and immobile in reducing (Cr, V, U) tend to reach organic layers through diffusion or groundwater transport and accumulate there (stage 2). Often it remains unclear to what extent these elements are present as separate mineral phases or adsorbed on the organic matter (Bonatti et al., 1971; Colley et al., 1984; Huerta-Diaz and Morse, 1992; Langmuir, 1978; Middelburg et al., 1997; Shaw et al., 1990).

Depletion of Ba, Cr, V. Most of the lignite layers on top of the Reuver clay and the peats of Zuid-Holland and Brabant show relative depletions in Ba, and sometimes of Cr and V too (e.g. Ba, Cr and V in BTAB in Fig. 4.2.4). The general correlation between Cr, V and Ba on the one and Al and K-contents on the other hand indicates that these elements are present primarily in phyllosilicates. Therefore, the observed depletion of Ba, Cr and V suggests that these elements were actively removed from these minerals. Chapters 3.1 and 3.2 show that illite clay weathered after deposition to form smectite in organic layers under the influence of organic acids, and that thereby the bulk K-contents decrease. Therefore, it is likely that the depletion of Cr, V and Ba as found in several organic layers, including those in BTAB, is the result of similar *in situ* weathering processes.

Figure 4.2.12 (Next page) Schematic overview of the effects of changing diagenetic environment on the formation and dissolution of Fe and S minerals, and on the related trace element accumulations. **A.** During saline transgressions or intrusions, Fe,Mn-hydroxides and sulfates are reduced to form pyrite, while organic matter is degraded. Trace elements present in the Fe,Mn-hydroxides are taken up into pyrite or other sulfides, or (in the case of Y and REE), become immobilized by phosphates that are released during the degradation of organic matter. As and Mo may be preferentially enriched due to preferential uptake into sulfides. **B.** During oxic episodes, pyrite and possibly other sulfides oxidize. This causes a decrease in pH, as a result of which weatherable minerals may be attacked. Fe,Mn-hydroxides are formed, and may take up trace elements that were present in the sulfides, or released by weathering. Moreover, elements like As, Co, Ni, Zn, Y and REE may be enriched due to preferential uptake. The sulfate released during sulfide-oxidation forms gypsum and barite.

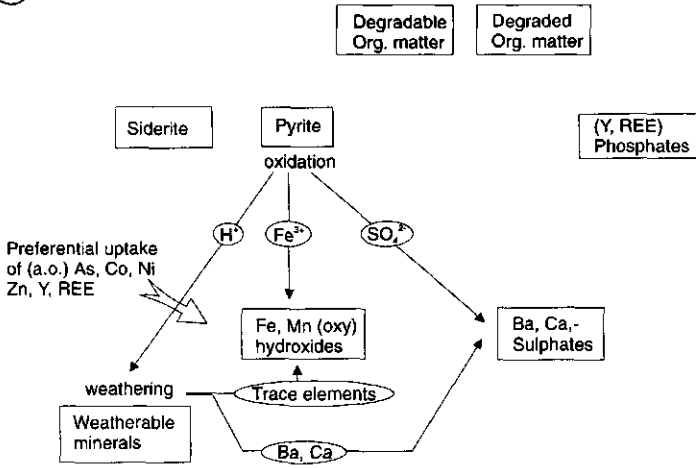
(A)

Processes during saline transgressions or intrusions



(B)

Processes during oxic episodes



Diagenetic interactions

From the above it can be concluded that anomalies of As, Co, Cu, Ni, Pb, Zn and Mo are related to pyrite and specific sulfides that were formed in several stages. Part of the sulfidization formation took place before burial during marine transgressions over continental organic deposits, with sulfate derived from sea water and Fe from local, continental sources. Minor amounts of pyrite-S may also originate from destruction of organic matter (e.g. methanogenesis) in fens or bogs (see Chapter 4.1). Because of the low gradient of the delta and the relative proximity of equivalent marine deposits such transgressions could be as short-termed as spring tides or storm floods. After burial, pyrite formation in organic layers probably continued whenever marine transgressions caused saline groundwater intrusions, causing downward percolation of SO_4^{2-} -rich water. Moreover, fluctuations in groundwater level as a result of episodic or cyclic changes in sea level or river regime can cause changes from a reduced to an oxic diagenetic environment. During such oxic periods the oxidation of pyrite may have several consequences (see Fig. 4.2.12). Firstly, Fe(hydr)oxides will be formed as long as the pH does not drop too much. These oxides will incorporate part of the trace elements from the pyrite, and may concentrate and take up additional trace elements, including Y and REE, from groundwater. Secondly, the decrease in pH associated with sulfide oxidation will promote weathering of primary minerals. As a result of these weathering processes major and trace elements, including Ba, Cr and V are released. Thirdly, the elevated SO_4^{2-} -levels may cause Ba and Ca to precipitate as barite and gypsum respectively. Sulfide-formation is promoted in reduced organic-rich layers which come into contact with water having elevated contents of Fe and SO_4^{2-} derived from pyrite oxidation in overlying deposits. Reducing conditions could persevere during the subsequent regression phase in the peat or organic layers whereas other parts of the sediment body become oxidized. As U, Cr and V are mobile under oxidized conditions and immobile under reduced, the presence of Cr, V and U-enrichments in part of the layers indicates that at least one episode occurred in which this organic layer remained reduced while the surrounding sediment was oxic or suboxic. Additional evidence that such conditions existed is given by the Ni-enrichments in pyrite found at the outside of the organic-rich layers (cf. Figs. 4.2.5 and 4.2.6). As the organic layers remained sulfate reducing during an oxic phase, Ni, released from Fe-hydroxides was subsequently sulfidized. Sulfidization of Ni occurred mainly at the outside of the organic layer as soon as the sulfide concentration allowed the formation of Ni-rich pyrite or even the precipitation of NiS. Associated with the pyrite formation, REE and Y may be immobilized by the phosphates that are released from decomposing organic matter.

Conclusions

The enrichments of As, Co, Cr, Cu, Ni, Pb, V, Zn, Ba, Y, Mo and REE in organic-rich layers in the Early Pleistocene Rijn-Maas Schelde delta are caused by a series of interconnected and alternating diagenetic processes. The most important of these are driven by the effects of interchanging fresh and saline water, and oxic and reducing conditions in ground water on the formation and oxidation of sulfides. Especially periodic fluctuations in ground water redox state, e.g. related to glacial-interglacial sea level fluctuations, may cause multiple stages of

preconcentration of trace elements in iron oxides, as a result of which second- or later-generation sulfides can be expected to obtain locally extremely high trace element contents.

The suites of trace elements enriched in these organic layers is very typical, as it contains elements that can be mobile under oxic conditions and immobilize during reduction, as well as elements that are mobile under reduced conditions and immobilize during oxidation. Moreover, it contains elements that are specifically immobilized by sulfides as well as sulfates, phosphates and organic matter-binding. The processes involved in accumulating and immobilizing these elements can be coupled to the mondial Quaternary glacial-interglacial cycles. Therefore, this type of element enrichments in organic-rich sedimentary sections may be diagnostic for all large-scale deltaic environments.

5 A geological interpretation of heavy metal concentrations in soils and sediments in the southern Netherlands

D.J. Huisman
F.J.M. Vermeulen
J. Baker
A. Veldkamp
S.B. Kroonenberg
G.Th. Klaver

Abstract

The natural variation in heavy metal contents of subsurface sediments in the Southern Netherlands is described, based on a series of 820 bulk geochemical analyses. The detrital heavy metal contents of these sediments show linear correlations with Al as a result of their joint occurrence in phyllosilicates. Anomalous enrichments occur as a result of the presence of glauconite (As, Cr, Ni, Pb, Zn), pyrite (As) or Fe-oxides (As, Ba, Ni, Zn), due to the interaction of organic-rich subsurface material with groundwater (Co, Ni, Zn) or as a result of anthropogenic pollution in topsoils (Cu, Pb, Zn). The contents of Al, Fe, K and S are well suited to determine background values, and to identify the cause for anomalous accumulations of heavy metals.

Introduction

The increasing use of the subsurface as a source for drinking water and for large infrastructural projects (roads, railways, tunnels, subsurface storage facilities etc.) requires detailed knowledge about the chemical properties of its sediments. As subsurface sediments can act both as a source and as a sink for heavy metals, it is important to know their chemical characteristics in order to evaluate heavy metal behavior and the results of pollution on the quality of drinking water. For large infrastructural projects, the disposal of soil material may be problematic if the heavy metal content is too high. Moreover, the effects of lowering of the groundwater table can only be evaluated if enough geochemical data are available.

Apart from that, as the chemical composition of most soils in the Netherlands is influenced by anthropogenic activities, subsurface sediment composition may be used as a proxy for natural background values for heavy metals. In recent geochemical mapping campaigns, preindustrial sediments were regarded as pristine, without anthropogenic influences (Hindel et al., 1996; De Vos et al., 1996). The background values for heavy metals that are in use now for legislative purposes however, are based on samples from topsoils (cf. Edelman, 1984) which in the Netherlands almost by definition have anthropogenic influence. The use of subsurface sediments as a proxy for natural background values of topsoils however, neglects possible heavy metal accumulation by geochemical cycling processes (leaching, organic decay, plant growth).

The natural background concentration of heavy metals in siliclastic sediments is a function of (1) the mineralogy of the original sediment source, (2) the grain size and (3) diagenetic processes (Moura and Kroonenberg, 1990; Hakstege et al., 1993, Chapter 3.1). In this paper we

study the way these factors influence the heavy metal contents in soils and especially subsurface sediments, using data gathered during an extensive geochemical mapping program in the South of

Table 5.1: Geological setting and sediment characteristics

Geological Time	Deposits (formation name)
Late Pleistocene and Holocene	Coversand (Nueneen group)
Early Pleistocene	Fluviatile fine sand and clay, locally organic rich (Kedichem formation)
	Estuarine sand and clays, locally siderite-rich (Tegelen formation)
Pliocene	Fluviatile sand and clay, organic rich (Kiezeloöliet formation)
	Marine shell-bearing coarse sand and clay with shell-layers (Oosterhout formation)
Miocene	Marine coarse glauconite-rich sand (Breda formation)

the Netherlands. Table 5.1 shows that the sediments studied show considerable variation in grain size (coarse sand to clay), lithology (sand, clay, peat, shells), and diagenetic environment (marine, estuarine, fluviatile, eolian) (Chapter 3.1).

Our aim is to describe and explain the basic heavy metal geochemistry of the Dutch subsurface sediments. First we will focus on grain size effects, using Al as a proxy for clay content (cf. Kumar et al., 1996). We use Al as the correlation between heavy metals and Al is more straightforward due to their joint occurrence in phyllosilicates whereas the correlation with clay content is the result of the concentration of phyllosilicates in the finer fractions. Moreover, the analysis of Al content is more reliable and uniform than that of grain size, and there are no problems with sample inhomogenities as both Al and heavy metal contents can be measured in one run or, after destruction, in the same solution (XRF, ICP, AAS, NAA). Secondly, the effects of specific mineralogy, diagenetic processes and anthropogenic pollution on the heavy metal contents will be discussed. Discussion will be on the nature of diagenetic processes affecting heavy metal contents and the use of major element contents for the identification and evaluation of heavy metal enrichments.

Materials and methods

In this Chapter we use data from a series of borings that were carried out in the framework of the completion of the geological map of sheet 50 (Breda-Tilburg) by the Geological Survey of the Netherlands (presently NITG-TNO) (Fig. 5.1). Boring Ulvenhout was made as a part of the "Overbank-project" for geochemical characterization of Holocene sediments (*unpublished research*). See Chapter 2 for a description of the boring methods, the sampling practice and the method for XRF-measurement techniques. Linear regression was performed using the software package GRAPHER.

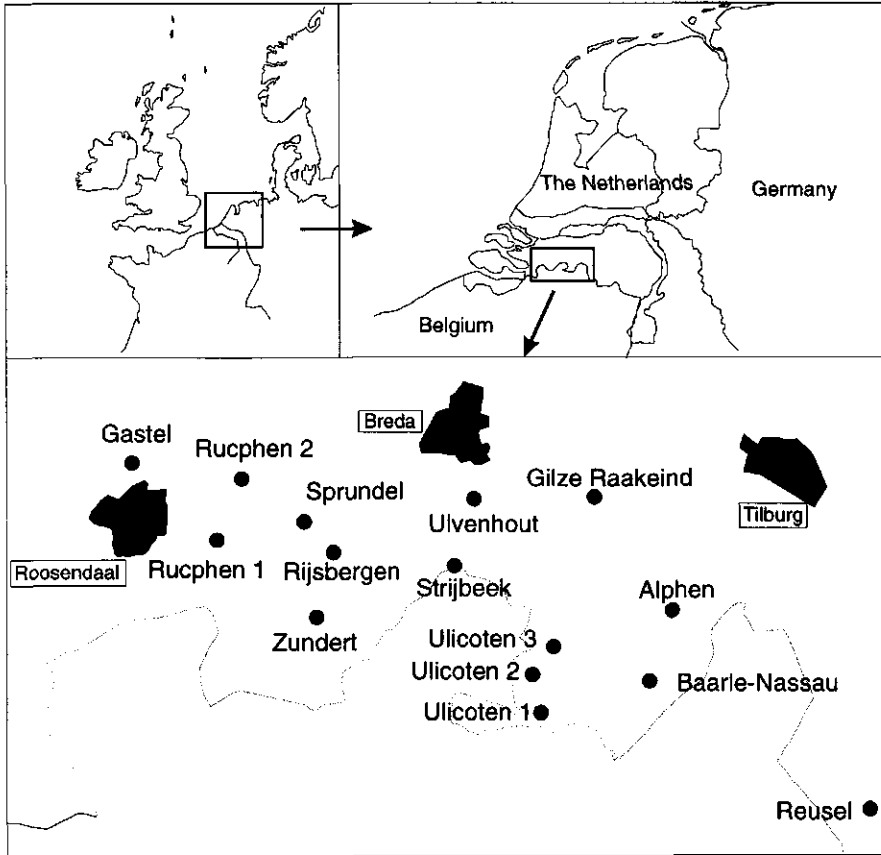


Figure 5.1 Research area and position of borings.

Results and Discussion

The scatterplots in Figure 5.2 illustrate that there is a general overall correlation between most of the heavy metals and Al, except for As which shows no correlation at all with Al. However, in all the plots varying numbers of samples deviate considerably from the overall heavy metal-Al correlation, and the R^2 for the correlation between Al and the heavy metals is thus generally low:

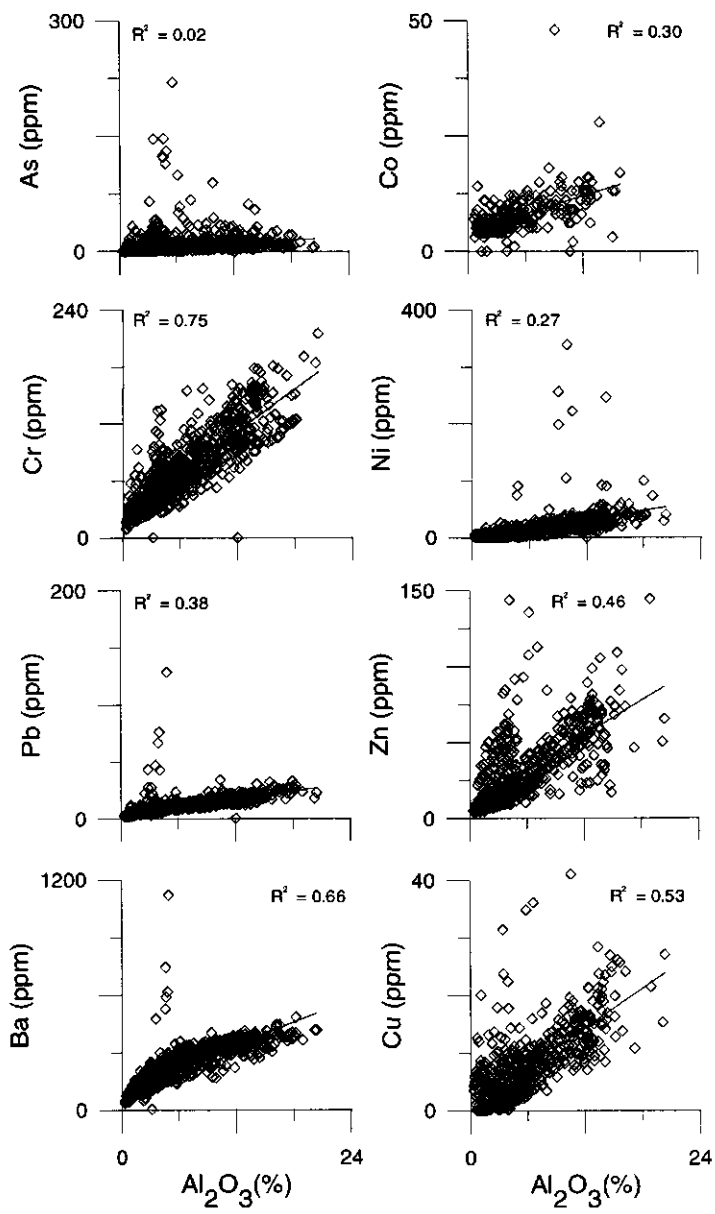


Figure 5.2 Scatterplots of heavy metal versus Al content.

<u>Regression model</u>	<u>Model fit</u>	<u># Observations</u>
As = 0.51 * Al ₂ O ₃ + 6.03	R ² = 0.02	(n= 820)
Co = 0.64 * Al ₂ O ₃ + 4.28	R ² = 0.30	(n= 283)
Cr = 7.41 * Al ₂ O ₃ + 23.0	R ² = 0.75	(n= 820)
Cu = 1.14 * Al ₂ O ₃ + 0.64	R ² = 0.53	(n= 571)
Ni = 2.74 * Al ₂ O ₃ - 1.82	R ² = 0.27	(n= 820)
Pb = 1.10 * Al ₂ O ₃ + 4.53	R ² = 0.38	(n= 820)
Zn = 3.78 * Al ₂ O ₃ + 9.61	R ² = 0.46	(n= 571)
Ba = 19.6 * Al ₂ O ₃ + 104	R ² = 0.66	(n= 820)

In theory, we would expect a good correlation between heavy metal and Al contents in siliclastic sediment as a result of their joint occurrence in phyllosilicates. Deviating heavy metal concentrations would be the result of other, not grain size related processes like diagenesis or anthropogenic pollution. The low R² for the correlation between most of the heavy metals and Al in our dataset appears to be the result of a relatively small number of high outliers (Fig. 5.2). A closer examination of these outliers revealed that most of them belong to either of the following groups:

- Sediments from Miocene age
- Samples with high S-concentrations
- Samples with high contents of Fe-oxides
- Samples from organic-rich subsurface layers
- Topsoils

The reasons for these outliers are discussed below.

Miocene deposits

One of the main characteristic properties of the Miocene deposits is that they contain relatively large amounts of the mineral glauconite (Zagwijn and Van Staaldin, 1975). Glauconite is a K- and Fe-rich and Al-poor mica of marine biogene origin (Deer et al., 1992) which form sand-sized aggregations in the sediments under consideration. Given the high content of K and the low Al-concentrations in glauconite (Deer et al., 1992) and the low Al-concentrations in the samples under consideration, we can use the K content as a proxy for glauconite content. In Figure 5.3, As, Cr, Ni and Pb show a close correlation with K for the Miocene glauconite-rich samples from boring Reusel which indicates that in these sediments glauconite is the major source for these elements. Because of the low Al-concentration in glauconite, the samples plot above the Al-heavy metal regression line in Figure 5.2. A similar correlation can be seen for Zn, but some high-Zn outliers remain unexplained. The poor correlation between Ba and K indicates that no Ba is present in glauconite (see Chapter 3.1). The lack of correlation between K and Co may indicate a lack of Co in glauconite, but it may also be the result of measurement uncertainties as the Co contents are close to the detection limit.

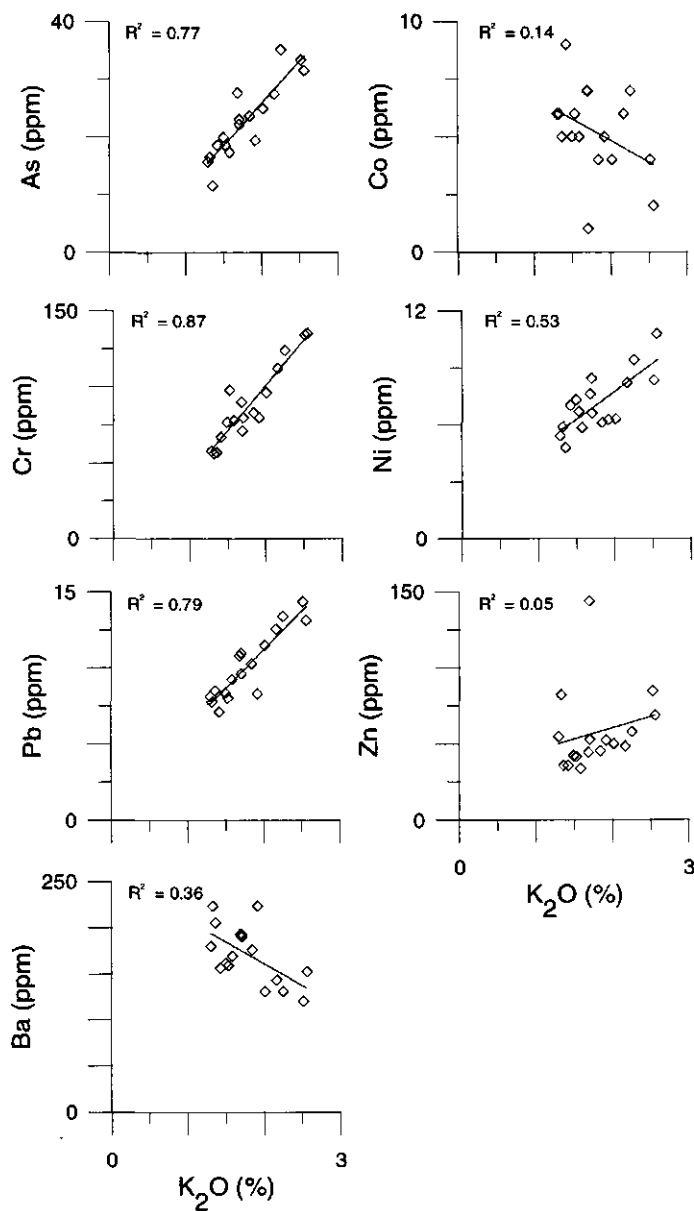


Figure 5.3 Scatterplot of heavy metal versus K content. Glauconite-rich samples (Boring Reusel)

S-rich samples

S-rich samples, which are frequently but not exclusively organic-rich, have generally high As-contents (Fig. 5.4; boring Rucphen 2).

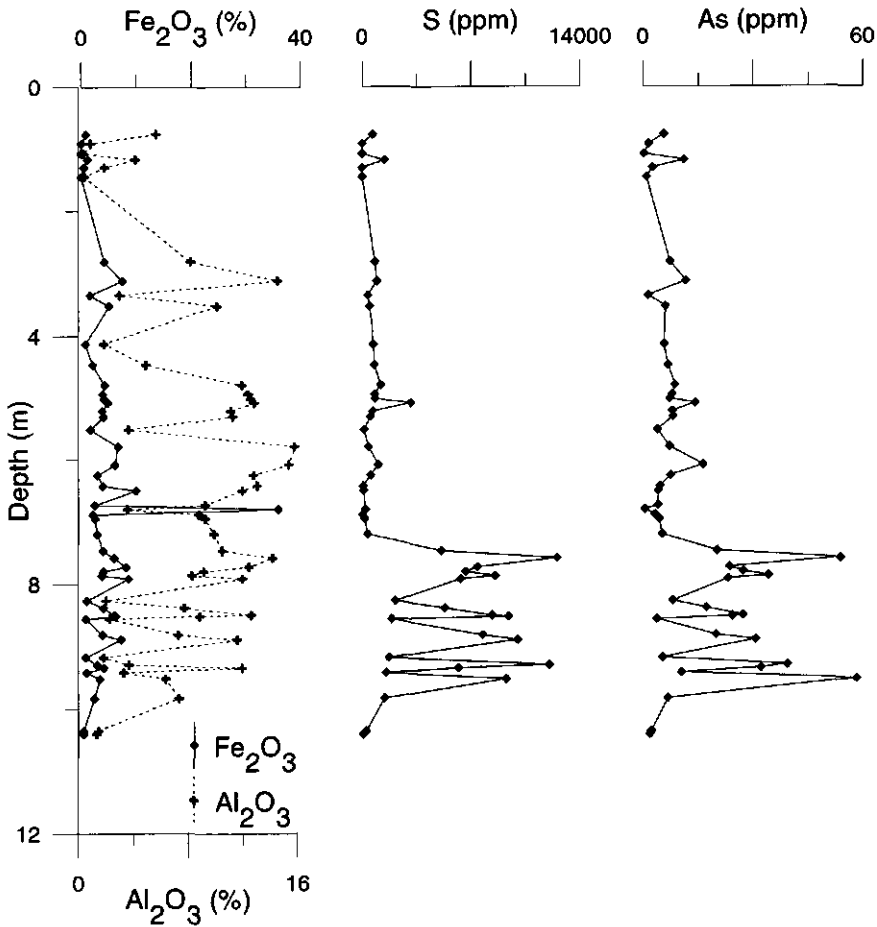


Figure 5.4 Depth profile of Al, Fe, As and S, boring Rucphen 2. A localized Fe-peak at 6.80 m depth reflects the presence of a thin siderite-band. Below 7 m, elevated As-contents follow the elevated S-contents due to the presence of pyrite.

A possible overall good linear correlation between As and S contents in all glauconite-poor sediments (Fig. 5.5) is disturbed by several outliers, particularly with low S contents:

<u>Regression model</u>	<u>Model fit</u>	<u># Observations</u>
As = 0.0023 * S + 6.63	R ² = 0.12	(n= 744)

The most common S-bearing minerals in the sediments under consideration are probably pyrite and gypsum. Since As is a common substitution for S in pyrite (Deer et al., 1992), the correlation between As and S contents indicates that pyrite could be the major As-bearing mineral.

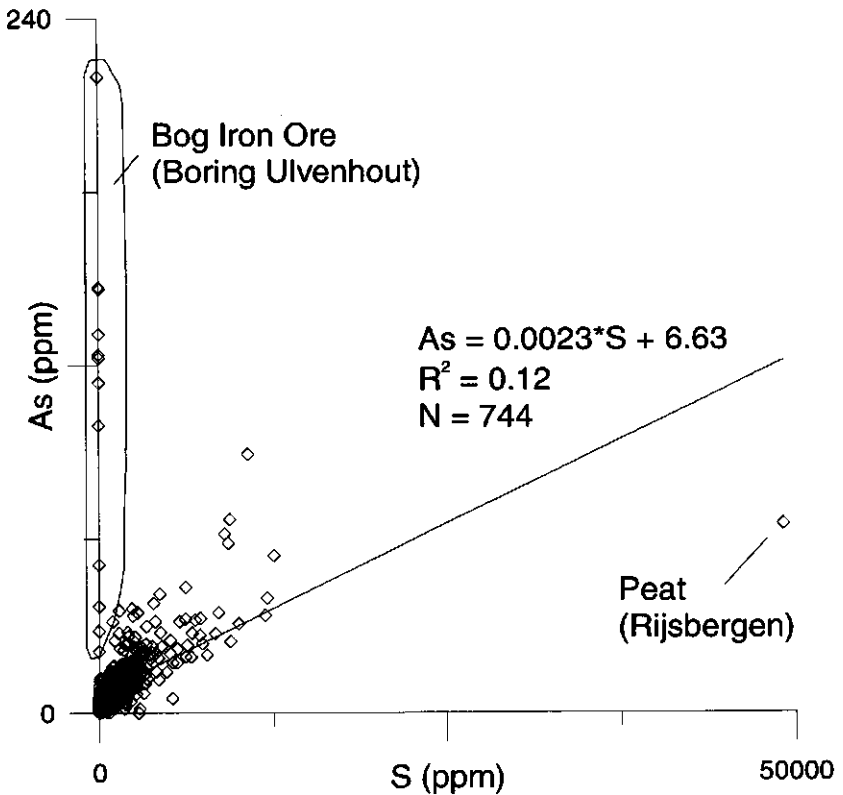


Figure 5.5 Scatterplot of As versus S and the regression line. All samples.

There are two distinct (groups of) outliers in Figure 5.5. A high-As, low S group is discussed below ("Bog iron ore"). The second outlier, the only peat sample in the dataset, shows a very high S content ($\pm 5\%$), but a relatively low As/S ratio, which is probably the result of the presence of additional gypsum-S over the pyrite. By omitting these outliers, the As-S correlation is much improved:

Correlation As-S without glauconitic and bog iron ore samples:

<u>Regression model</u>	<u>Model fit</u>	<u># Observations</u>
As = 0.0026 * S + 4.45	$R^2 = 0.55$	(n= 713)

Correlation As-S without glauconitic, bog iron ore and peat samples:

<u>Regression model</u>	<u>Model fit</u>	<u># Observations</u>
As = 0.0042 * S + 2.83	$R^2 = 0.71$	(n= 712)

Bog iron ore

A number of the outlying samples in the scatterplots of Ba, Ni and Zn versus Al and As versus S (Fig. 5.2 and 5.5) originate from a layer with hydromorphic accumulations of Fe-oxides ("bog iron ore") in boring Ulvenhout (Fig. 5.6). The depth distribution of these heavy metals in the zone of iron accumulation does not correspond with the distribution of Fe; Ba shows a strong accumulation in its center and Ni and Zn show a steady increase downward. Only As shows a more or less similar behavior to Fe, i.e. a more or less constant concentration throughout the accumulation zone.

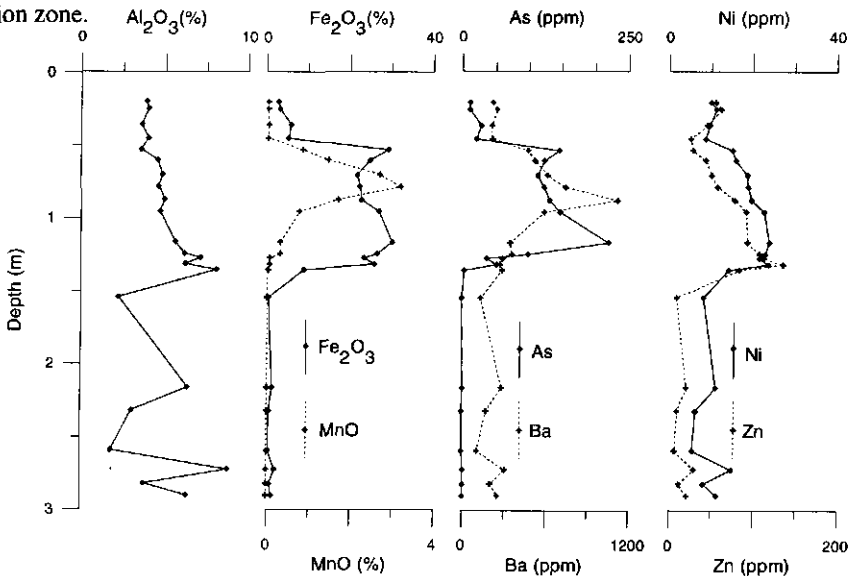


Figure 5.6 Depth profile of Al, Fe, Mn, As, Ba, Zn and Ni, boring Ulvenhout. Between 0.50 and 1.50 m, the presence of hydromorphic Fe, Mn(hydr)oxides causes elevated Fe and Mn contents. Associated with this are elevated contents of As, Ba, Ni and Zn.

Iron oxides, especially bog iron ore have been known to contain strong accumulations of several heavy metals and often of As (Pruissen and Zuurdeeg, 1988; Moura and Kroonenberg, 1990, Chapter 4.2). The strong enrichments of As, Ba and, to a lesser extent, Ni and Zn in association with bog iron ore indicates that these elements accumulate during hydromorphic iron accumulation. The correlation between As and Fe suggests that As is built into the Fe-oxide crystal lattice in a constant ratio to Fe. The irregular accumulation of Ba, Zn and Ni in the Fe accumulation zone and the lack of correlation with the Fe content indicates that these elements are either present as separate mineral phases, or that they are built into the Fe-oxide structure in varying ratios to Fe.

In contrast to Fe-oxide, Fe-carbonate (siderite) does not show any accumulation of heavy metals.

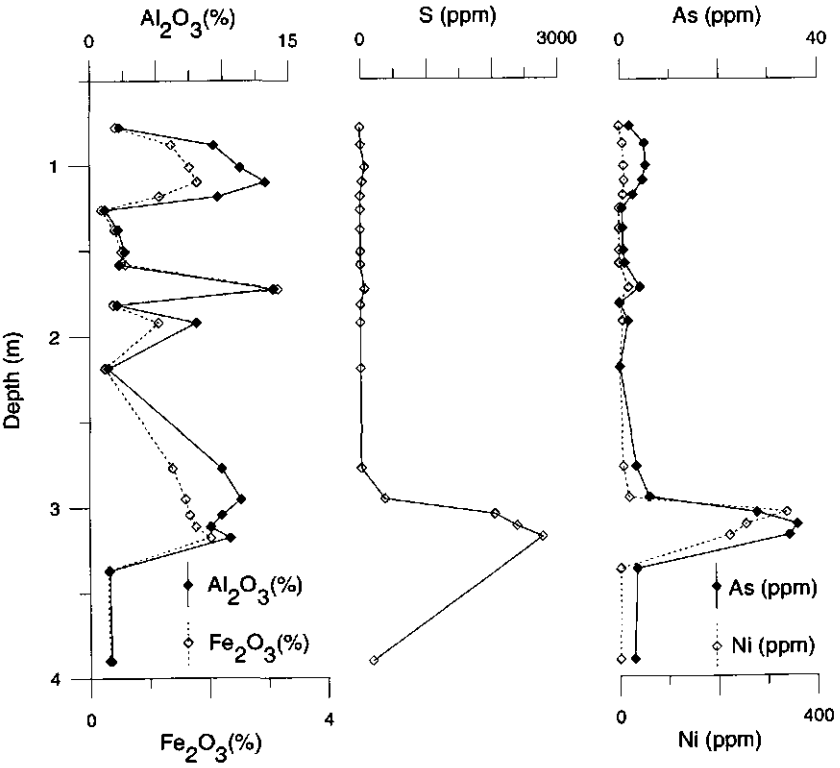


Figure 5.7 Depth profile of Al, Fe, S, As and Ni, boring Ulicoten 1 (see also Fig. 4.2.6). Enrichment of As and Ni in a organic-rich layer.

Organic-rich subsurface layers

With the exception of the bog-iron ore samples, all Ni-outliers are from organic rich subsurface layers, often in association with Co and/or Zn accumulations (Fig. 5.7 and 5.8; boring Ulicoten 1 and Sprundel). Although frequently As and S-accumulations occur in the same organic layers, there is no correlation between Ni on the one hand and As and S on the other. This type of accumulation involving Ni, Co and Zn occurs in all sampled subsurface organic-rich layers with the exception of the one peat sample, but the concentrations of the elements involved vary considerably (cf. Hakstege et al., 1993). The nature and origin of this type of enrichment is described in more detail in Chapter 4.2.

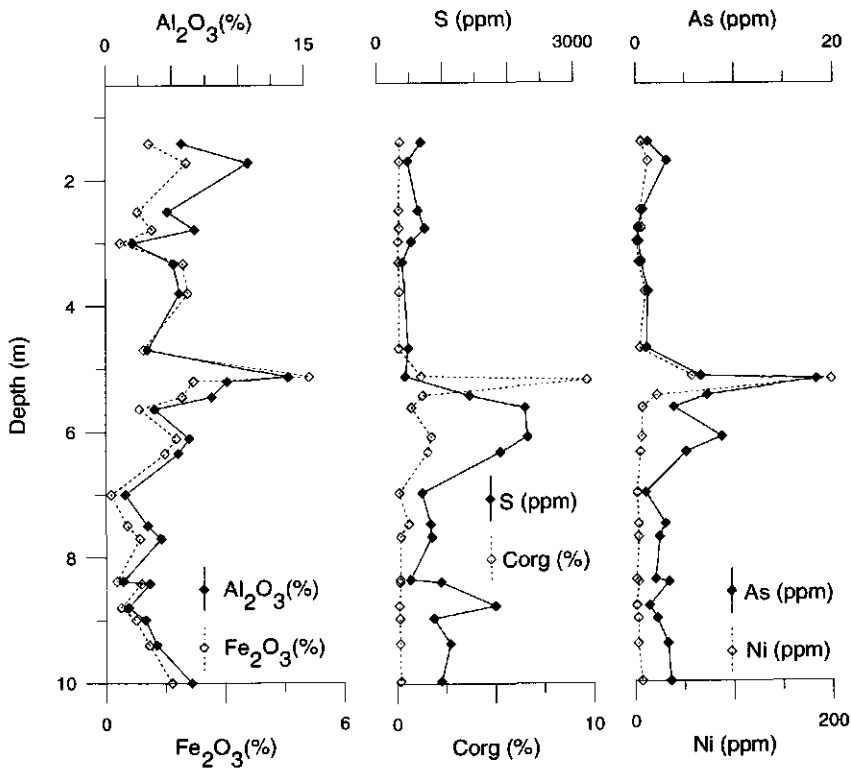


Figure 5.8 Depth profile of Al, Fe, S, Corg, As and Ni, boring Sprundel (see also Fig. 4.2.3). Enrichment of As and Ni in organic-rich layer.

Top soils

All samples from topsoils show increased contents of Pb. Often Cu and Zn are enriched also (Fig. 5.9 and 5.10; boring Ulicoten 3 and Baarle Nassau). Because all topsoil samples show Pb-accumulation, it is likely that there has been anthropogenic input to the surface soil materials. The source of the Pb is most probably atmospheric deposition from automobile emissions of leaded petrol. The less frequent enrichments of Cu and Zn in topsoils suggests that the anthropogenic sources of these elements are likely to be more local. Possible sources are pig manure (Cu) and the Campine Zinc industry (Zn). Increased surface concentrations of metals may, however, also be related to natural biogeochemical cycles.

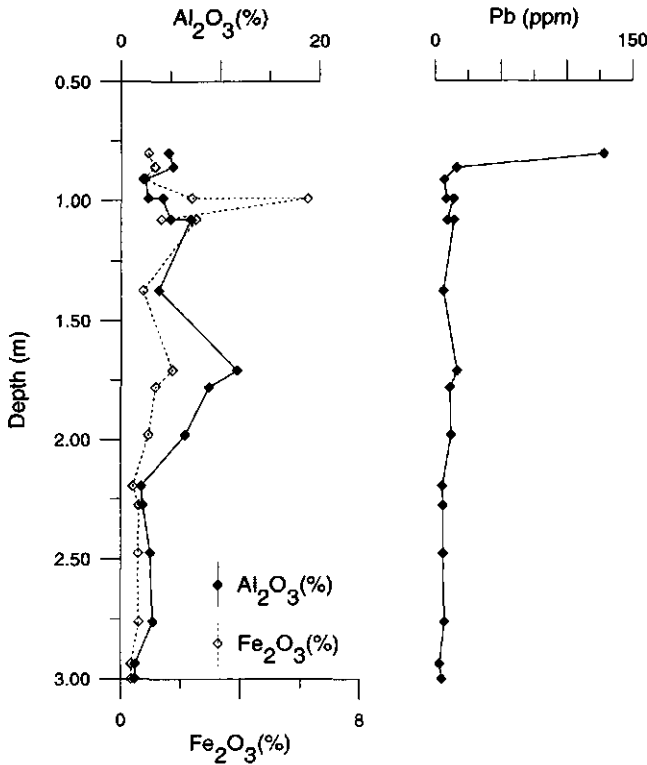


Figure 5.9 Depth profile of Al, Fe and Pb, boring Ulicoten 3. The Pb-contents are elevated in the topsoil.

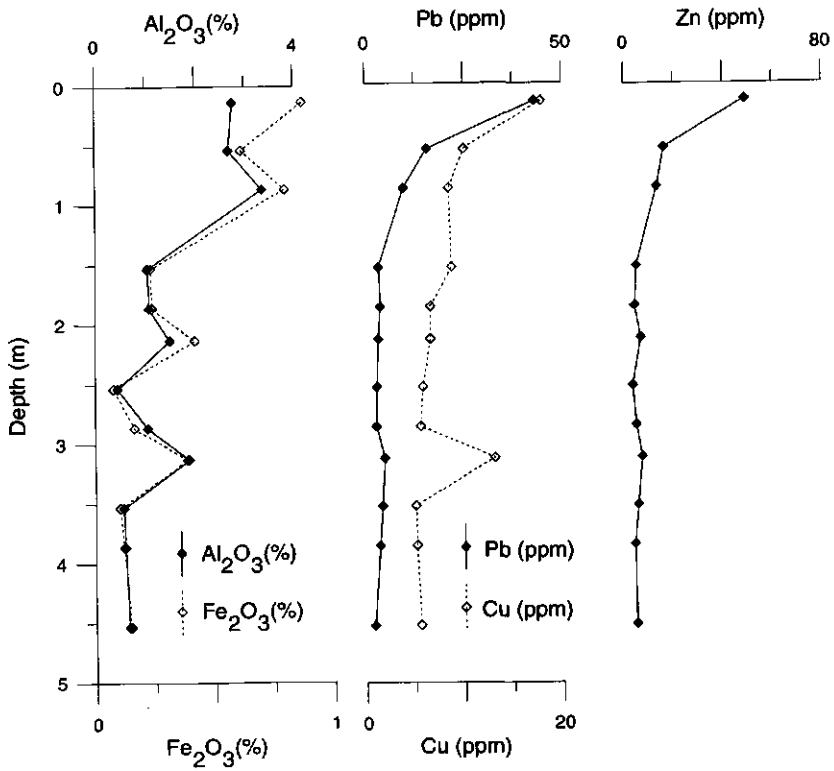


Figure 5.10 Depth profile of Al, Fe, Pb, Cu and Zn, boring Baarle Nassau. The Pb-, Cu-, and Zn-contents are elevated in the topsoil.

Relation between heavy metals and major elements

Regression analysis leaving out the samples influenced by glauconite, iron oxide, organic matter-related accumulations or anthropogenic influence results in a much better correlation between Ba, Co, Cr, Cu, Ni, Pb and Zn concentrations and Al content (see also Fig. 5.11):

<u>Regression model</u>	<u>Model fit</u>	<u># Observations</u>
As = 0.64 * Al ₂ O ₃ + 3.43	R ² = 0.11	(n= 789)
Co = 0.59 * Al ₂ O ₃ + 4.49	R ² = 0.39	(n= 265)
Cr = 7.51 * Al ₂ O ₃ + 21.7	R ² = 0.78	(n= 803)
Cu = 1.15 * Al ₂ O ₃ + 0.54	R ² = 0.56	(n= 545)
Ni = 2.29 * Al ₂ O ₃ - 1.23	R ² = 0.72	(n= 766)
Pb = 1.17 * Al ₂ O ₃ + 3.53	R ² = 0.81	(n= 790)
Zn = 3.78 * Al ₂ O ₃ + 6.84	R ² = 0.62	(n= 526)
Ba = 20.0 * Al ₂ O ₃ + 97.9	R ² = 0.82	(n= 788)

Only some outliers in Cu and Zn that unexplained. In a similar way, the correlation As-S is very good after leaving out the peat and the glauconite and iron oxide influenced samples (see also Fig. 5.5 and 5.12).

The correlation Ba-K is even better than Ba-Al, probably because Ba substitutes directly for K in the crystal lattices of most K-bearing minerals (including the phyllosilicates) while the other heavy metals substitute mainly for Al and Si in phyllosilicates (see Fig. 5.13) (Newman and Brown, 1987; Deer et al., 1992):

Relation Ba-K whole dataset:

<u>Regression model</u>	<u>Model fit</u>	<u># Observations</u>
Ba = 121.61 * K ₂ O + 65.66	R ² = 0.67	(n= 820)

Relation Ba-K without glauconitic and diagenetically or anthropogenically enriched samples

<u>Regression model</u>	<u>Model fit</u>	<u># Observations</u>
Ba = 130.25 * K ₂ O + 51.50	R ² = 0.91	(n= 788)

In Chapter 3.1, variations in Ba/K ratio resulting from K-uptake by clay minerals in marine environments are described for the Reusel and Sprundel. In the non-glauconitic sediments, these variations, albeit significant, are small enough to not disturb the regression model presented above.

Because of the good correlations between heavy metals and major element contents, the detrital heavy metal concentration in non-glauconitic siliclastic sediments can be described as a function of the contents of Al and K. Heavy metal enrichments as a result of the presence of glauconite, diagenetic accumulations or anthropogenic influence are apparent from the increased ratios to Al or K. Information about the nature of the accumulation can be obtained by comparison

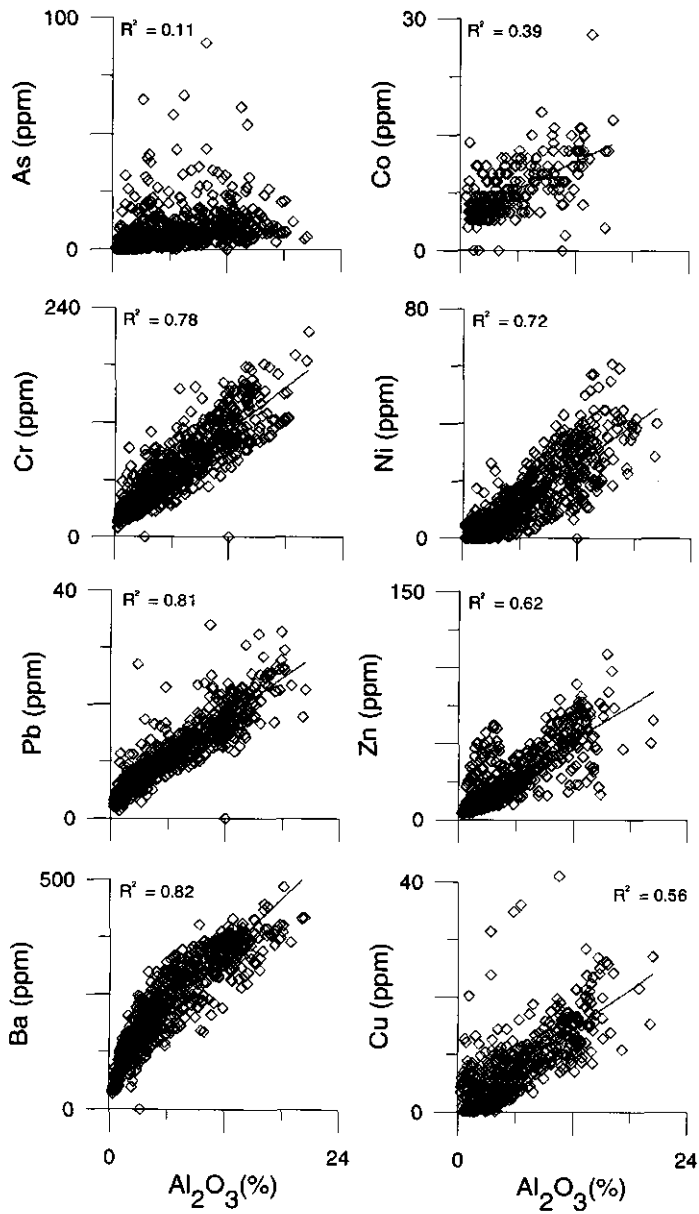


Figure 5.11 Scatterplots of heavy metal versus Al content. Diagenetically enriched, glauconite-rich and topsoil samples left out.

to the contents of K (glaucinite), Fe (iron oxide) and S (pyrite). These elements and the presence of organic matter are indicative of natural causes of heavy metal enrichment, and can be useful in distinguishing natural accumulations from anthropogenic pollution.

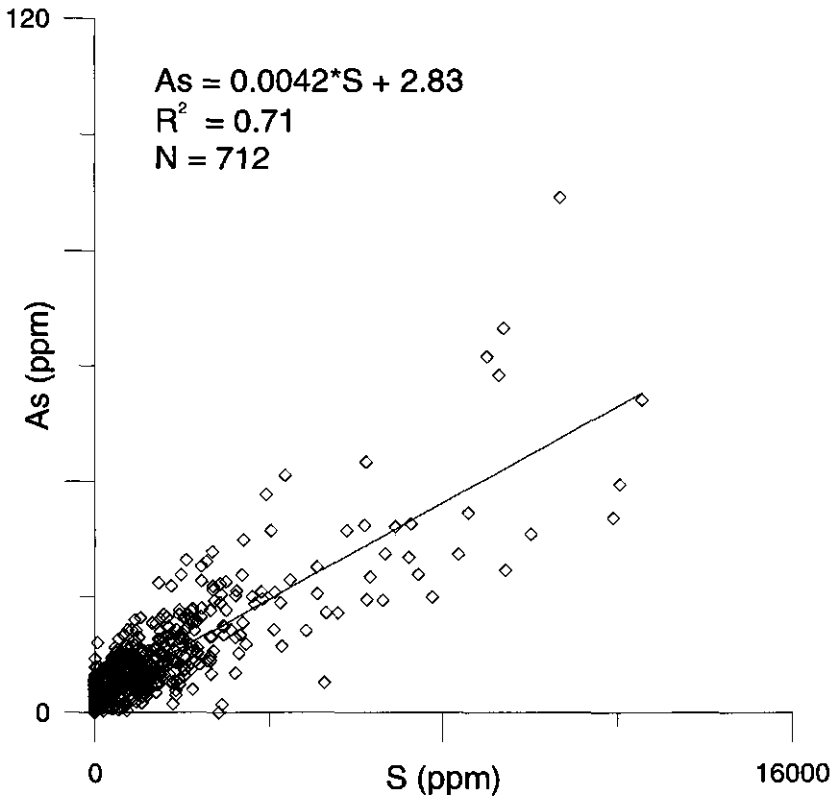


Figure 5.12 Scatterplot of As versus S with regression line. Glaucinite-bearing, peat and bog iron ore samples left out.

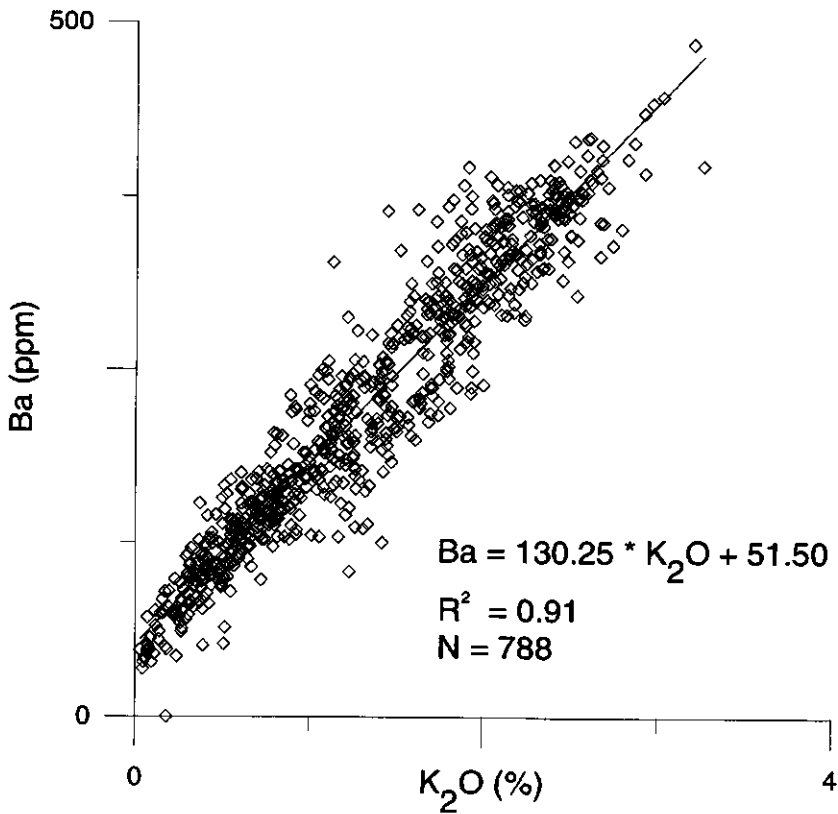


Figure 5.13 Scatterplot of Ba versus K content with regression line. Diagenetically enriched and glauconite-rich samples left out

Conclusions

There is an overall good correlation between the contents of heavy metals and Al and K in the siliclastic sediments of the Southern Netherlands. Sediments influenced by pollution, diagenetic heavy metal accumulation or the presence of glauconite show distinct deviations from the overall correlation of heavy metal contents with Al and K.

Observed natural causes for heavy metal accumulation are the presence of glauconite (As, Cr, Cu, Ni, Pb) the formation of pyrite (As) or bog iron ore (As, Ni, Zn) and interaction between groundwater and subsurface organic matter (Ni, Co, Zn). Anthropogenic contamination causes an overall increase in Pb in topsoils, and locally may have increased Cu and Zn contents. This indicates that in industrialized areas like the Netherlands, topsoil samples are in general unsuitable

to determine natural background values for Pb and in local areas for other heavy metals such as Cu and Zn.

Al, K, Fe and S contents form a suitable tool for the evaluation of heavy metal concentrations in soils and sediments in environmental research. Al and K can be used to determine whether heavy metal contents exceed background values and by how much. K, Fe and S contents provide means to determine the nature of heavy metal enrichments and to distinguish natural enrichments from anthropogenic pollution.

6 Spatial prediction of the geochemical variability of Early Pleistocene subsurface sediments in the Netherlands

D.J. Huisman
J. P. Weijers
L. Dijkshoorn
A. Veldkamp

Abstract

In order to meet the demand for more information about subsurface sediment composition, we started a geochemical mapping campaign in an Early Pleistocene fluvial formation (Kedichem) in the Netherlands. We first determined the spatial extension and thickness of the sediment body. Subsequently, we used Fuzzy clustering techniques on approximately 2000 heavy-mineral counts from the NITG-TNO database to map the spatial extension of the Schelde, Rijn and Baltic sediment provenance within the formation.

Geochemical data were collected during a sampling campaign in which about 600 samples from the Kedichem formation were analyzed. We used factor analysis to determine the major factors that determine the geochemical composition. These factors include clay content, presence of carbonates, pyrites and Fe,Mn-hydroxides, sodic plagioclase and zircon, and organic-matter-related diagenetic processes. We tested which of the available lithological data from the NITG-TNO boring database correlate with the geochemical composition in order to make a geochemical prediction model on the basis of the lithological data. We found that the database classes Sand, Clay + Gyttja and Peat are geochemically significantly different and therefore can be used to predict the contents of Si, Ti, Al, Fe, Mn, Mg, Ca, Cr, Cu, Pb, V, Zn, Ba, Ga, Nb, Rb, Sr and Y. For the elements As, Ni, U and S, the classes Organic-poor Clay, Sand+Peat and Gyttja+Organic-rich Clay are significantly different. For Na and K, a division can be made into Mica-rich Clay, Mica-poor Clay, Mica-rich Sand, Mica-poor Sand and Peat + Gyttja. By classifying the lithological data from the NITG-TNO core description, we made a geochemical model to predict the geochemical composition in the Kedichem formation

We visualized this model by calculating and interpolating the average composition of 5 m horizontal slices of the Kedichem formation. The model performance is fairly good, although it has a tendency to underestimate extreme values.

Introduction

In the previous chapters it was shown that the geochemical properties of Dutch subsurface sediments are mainly related to a limited number of sediment properties: grain size, sediment provenance-related mineralogy, and several syn- and post-depositional diagenesis processes. Consequently, geochemical characteristics can be statistically predicted based on lithological and mineralogical properties of the sediment. Such sedimentological data of the Dutch subsurface are recorded in the boring- and heavy-mineral- databases of NITG-TNO (formerly the Geological Survey of the Netherlands). Each boring is spatially specifically logged, offering the means to build

a spatial model of the geochemical variation in subsurface sediments based on existing sedimentary data.

In this Chapter we have linked the geochemical composition of the Kedichem formation and its lithological characteristics, and applied it to a spatial model of the geochemical composition. We limited this model-study to one geological formation only. We chose the Kedichem formation as there are large variations in lithology and sediment provenance that (can) have impact on the geochemical composition of the sediment. Furthermore, part of the formation has been studied already in Chapter 3.1, so there was already sufficient geochemical data available. In contrast to the process-oriented approach of Chapter 3.1, 3.2, 4.1 and 4.2, we use a statistical approach, as this is the most objective way to provide a link between core descriptions and geochemistry that can serve as input for spatial modeling of geochemical data.

We first studied the spatial distribution of the Kedichem formation, by analyzing the upper- and lower boundaries and the thickness distribution. Subsequently the spatial patterns of the heavy-mineral suites were studied in order to determine the sediment provenance. We used factor analysis (SPSS) to assess which factors that are most important for the geochemical variation. Subsequently, the geochemical data was linked to the lithological codes in order to test which codes are significantly different from each other, and what their average geochemical properties are. Finally, we made a geochemical distribution model, based on the correlation between lithological parameters and geochemistry, and made maps that predict the contents of some representative key elements (Al, Ni and Na). As an approximation of the 3-D variation, slices were used of the average composition of 5 m or, if not enough data is available, a larger thickness.

Geological Setting

The Kedichem formation consists of a series of Early Pleistocene fluvial fine sands and clays with localized peat in the central and southern Netherlands (Fig. 6.1) (stratigraphy according to Zagwijn and Van Staaldunin, 1975). Several Maas terrace deposits that are also incorporated in the Kedichem formation are not considered in this study. Sediment provenance is from the Rijn in the central Netherlands and from the Maas and Schelde river systems in the south. Rijn-derived sediments are generally mica-rich, and have an unstable heavy-mineral composition. Early Pleistocene Maas- and Schelde-derived sediments are characterized by low mica contents and a stable heavy-mineral composition.

The Kedichem formation overlies the Early-Pleistocene Tegelen and Harderwijk formations which have a Rijn and a Baltic provenance respectively. It is overlain by Middle- to Late Pleistocene coarse-grained Rijn deposits that belong to the Sterksel, Urk and Kreftenheye formations. To the North it is lateral equivalent to and interfingers with the Baltic-derived coarser grained Enschede formation (see Zagwijn and Van Staaldunin, 1975).

In Zuid Holland, both the Kedichem and the underlying Tegelen formation have a Rijn provenance, and are therefore mica-rich and have an unstable heavy-mineralogy. Furthermore they consist both of fine sands and clays and are both deposited in a coast-near fluvial facies, so it is difficult to distinguish them (Van Staaldunin, 1979). The Tiglian and the Upper Pliocene Reuver deposits in the southern part of the Roer Valley Graben (to the south of Eindhoven) have a Schelde/Maas-provenance, which makes them hard to distinguish from the Kedichem formation. A large number of NITG-TNO boring classifications show here a sudden increase in the thickness of

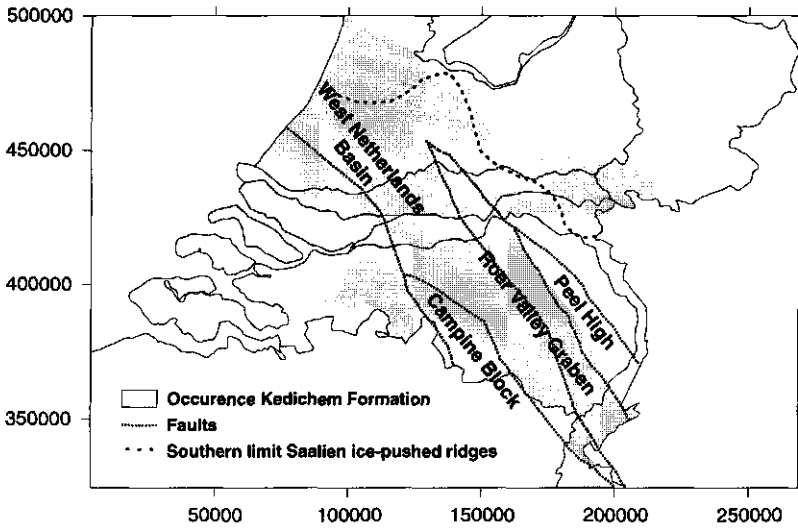


Figure 6.1 Occurrence of the Kedichem formation in the Southern Netherlands, with fault pattern used in this study (from Van den Berg, 1996 and pers. comm.) and the maximum extent of the Saalien ice sheet (Zagwijn and Van Staaldunin, 1975)

the Kedichem formation from 20 to 80 m which is caused by the incorporation of Tiglian and Reuverian deposits into the Kedichem formation. This is contrary to the definition of Zagwijn and Van Staaldunin (1975) who state that the Kedichem formation was deposited after the Tegelen formation, but it is a reflection of the similarity of the sediment composition.

Materials and Methods

Data Sources

Stratigraphical and lithological data: Lithological and stratigraphical data were obtained from the so-called REGIS-database. This is a collection of core descriptions from the main NITG-TNO boring database, that were selected for nation-wide coverage and good quality to serve as a basis for the NITG-TNO aquifer model REGIS (see Broers et al. (1992) for information on REGIS). For this purpose, the core descriptions were checked for errors and when needed a new stratigraphic classification was added (Weijers, 1995). The borings are coded according to the recently introduced standard core description, developed as a standard method for the macroscopical description of borings. This coding is based on the standard coding for sedimentary samples of the Dutch Normalization Institute (Nederlands Normalisatie Instituut, 1989).

Lithological descriptions distinguish the main lithological classes sand, clay, gravel, peat and loam, which we grouped together into larger classes (table 6.1).

Table 6.1: RUNSTER-equivalents of used codes:

Main lithological codes and their equivalents:		
Sand:	110,111,112	(Fine sand)
	120,121,122	(Middle fine sand)
	130,131,132	(Coarse sand)
Clay	210	(Clay)
	211, 212, 213, 214	(Silty clay)
	215, 216, 217	(Sandy clay)
Peat	410	(Peat)
	420, 421, 422	(Clayey peat)
	440	(Browncoal)
Gyttja	450	(Gyttja)
Loam <not used>	220, 221, 222	(Loam)
Gravel <not used>	310, 320, 330	(Gravel)
Additional lithological codes and their equivalents:		
Humus-rich	214	(Contains peat)
	414, 415	(Humus-bearing to humus-rich)
	442, 443	(Contains peat-lumps)
	450	(Contains gyttja)
Humus-poor	413	(Humus-poor)
	441	(Traces of peat lumps)
	No mention	
Mica-rich	683, 682	(Mica-bearing to mica-rich)
Mica- poor	681	(Mica-poor)
	No mention	

Additional properties include contents of humus or plant remains, micas, shells, clay lumps, etc. Note that these descriptions are based on macroscopically visible properties, and that they are meant to describe good-quality cores as well as bad-quality flush samples.

The database contains for each boring an ID, X- and Y-coordinates, height relative to sea level (NAP), date of boring, depth reached and a quality-label. For each lithological unit, the upper- and lower depth, the lithological code and where present and applicable estimations of clay content, median of the grain size and carbonate content are recorded. Additionally, for each boring a stratigraphic classification is given, with the upper and lower boundaries of each formation within the boring. As the Limburg area was not incorporated in the REGIS-database, additional stratigraphic data were obtained from the mapping program for geological map 60 (M. van den Berg, pers. comm.).

Heavy-mineral data: The heavy-mineral data were extracted from the NITG-TNO heavy-mineral database. This contains which contains all heavy-mineral counts that were performed by NITG-TNO on samples from the Netherlands and the surrounding areas for lithostratigraphic research. These heavy-mineral counts were done by optical determination of the transparent grains of the 63-500 μm sand fraction with a density $>2.87 \text{ g/cm}^3$, after treatment with HCl and HNO_3 to remove carbonates, Fe-(hydr)oxides and humus. Typical heavy minerals in the Kedichem formation include the so-called unstable (among others garnet, epidote, saussurite, alterite, hornblende) and stable minerals (among others zircon, rutile, staurolite and tourmaline). The database contains in total approximately 40.000 analyses. The heavy-mineral database was extended with the heavy-mineral data of Kasse (1988).

Geochemical data: For our sampling program, we selected borings to give a large spatial covering. Apart from that, we only took cores and no Bailer- and flush samples, as in our experience Bailer- and flush borings do not allow dense enough sampling to characterize the effects of diagenetic processes. Unfortunately, no good-quality cores were available from the Roer Valley Graben and from the North-East of the Kedichem area, so our data is restricted to the Brabant and Zuid-Holland areas. Some of the cores were often already several years old, and had been exposed to air before sampling. For sampling and analytical details, see Chapter 2.

Data treatment

From the REGIS database those lithological units were selected that were classified as belonging to the Kedichem formation, including uncertain classifications (e.g. classified as either "Kedichem or Harderwijk formation"). We filtered out incomplete records and wrong classifications interactively. These included a series of borings where the Kedichem formation had a thickness of 0 to 50 cm, borings outside the Kedichem area (e.g. on the Peel high), Kedichem sections in ice-pushed ridges, and sections that, because of the lack of correlation with the surrounding borings, were clearly erroneously classified as Kedichem. In this way, about ten percent of the borings was discarded. Because of the problems discerning the Kedichem from the underlying Tegelen formation, the lower boundary of the Kedichem formation in the REGIS-cores showed a large variation in parts of the Zuid Holland area. As in those areas the top of the Tegelen formation was not encountered above 75 m depth, we decided that in those areas the maximum

Kedichem depth is 75 m. below NAP; sections below 75 m. were regarded as representing Tegelen material.

In order to determine the upper- and lower boundaries of the formation, we used the moving average module of the ILWIS-package without linear prediction, with a limiting distance of 10km and weight method of $(1/d^2)^{-1}$, and with the data stratified according to the tectonic units. The position of the faults for this stratification was based on Van den Berg (1996, pers. comm.) (see Fig. 6.1).

We selected the Kedichem samples from the heavy-mineral database either by directly selecting the Kedichem sections from the borings that were also incorporated in the REGIS-database, or, if no stratigraphic data was available, by interpolation the upper- and lower boundaries of the Kedichem formation between neighboring borings. As heavy-mineral samples are often taken as samples mixed over a considerable core length, a sample was regarded as belonging to the Kedichem formation when even a small part of this sample range fell into a Kedichem-section. Samples that were composites of over 7.50 m were discarded. Apart from that, a series of samples were discarded that clearly were wrongly classified, as according to their high content of volcanic minerals they should be attributed to Middle to Late Pleistocene formations. About 2000 heavy-mineral counts remained for further analyses.

Heavy-mineral counts are conventionally used for stratigraphic research, in which they are an aid in determining lithostratigraphic boundaries in (a series of) cores. In this respect, the datasets are small, usually only some tens of analyses at the most for one core, and the results can be interpreted in great detail. However, such an approach is not suitable for our purpose because we study larger-scale variations, so we need less detail, and because of the large size of the dataset. For our purpose it is necessary to search for homogeneous groups in this complex dataset, and to investigate whether they provide useful information for stratigraphy, mineralogy and geochemistry. One way to do this is to apply cluster analysis, a multivariate statistical technique used for classification of numerical data by grouping the observations which are most alike into clusters. From the many clustering techniques that exist (see Davis, 1986, for an overview), we chose to use fuzzy C-means cluster analysis to make an objective classification of the heavy-mineral suites. Standard (non-fuzzy) C-means clustering simply assigns observations to a certain cluster. Fuzzy clustering, however, describe the likeliness of a sample to a cluster in a membership function that varies between 0 (not alike to the cluster) to 1 (almost identical to the cluster). Because of this, it is most appropriate to use fuzzy clustering in datasets where one can expect large compositional overlaps (cf. Frapporti, 1994). This is the case in our dataset because of the possible mixing of sediments from different sources. The FUZZY program of S.P. Vriend (Utrecht University) was used; technical and theoretical information can be found in Vriend et al. (1988). As the heavy-mineral composition in the Kedichem formation is determined by the relative contribution of three sediment sources (Rijn, Baltic, Schelde), we started clustering towards three clusters. Increasing the number of clusters gave a more interpretable subdivision.

The lithological codes of the borings which were analyzed geochemically were extracted from the central borings-database of NITG-TNO, and coded using the RUNSTER-4 program in order to make them compatible with the standard core descriptions as used in REGIS (see Weijers, 1995). We investigated which of the lithological codes could be used as base of the geochemical model by testing (student's t-test) which of them would divide the geochemical

dataset into significantly different groups. Subsequently, for each element the average composition in each of these groups was calculated. Finally, we used these averaged contents per lithological unit as a model to predict the geochemical composition of subsurface sediments in the Kedichem formation.

Visualization

We made visualizations of the spatial distribution of the heavy-mineral clusters and the geochemical model result for three key elements (Al, Na, Ni). As a 2-D approach to the 3-D spatial variation, we made maps that each represent a "slice" of 5 m thickness of the Kedichem formation. If not enough data was available, the slices were made thicker. The maps of the heavy-mineral clusters give for each sample that falls (completely or partially) within the slice the membership with each of the three clusters.

For the geochemical model, we first calculated the average composition of the sediments in each observation point by taking the weighted average of the model values for each lithological unit present in the slice. Maps were made of the interpolated predicted geochemical values with the Kriging-module of the SURFER software package.

Results and Discussion

Spatial characteristics of the Kedichem formation

In Fig. 6.2 we give the interpolated maps of the upper- and lower boundaries of the Kedichem formation, and its thickness. The shape of the Kedichem-body appears to be determined primarily by tectonic processes; this accounts for its deep position in the fastest subsiding part of the Roer valley graben, its limited thickness in western Brabant, where it lies on the rift shoulders of the Brabant massif, and in Gelderland, where it lies close to the Northern edge of the Peel high, and its absence on the Peel high where it was either never deposited, or eroded later. However, the map of the formation thickness is for a large part dominated by the large thickness in the southern Roer Valley Graben that represents the incorporation of Tegelen and Reuver sediments into the formation because of definition problems (see above). The increased thickness of the formation between the present Rijn and Maas river courses may represent a Northwestern extension of the Graben, but could also be the result of incorporating some of the underlying Tegelen sediments. Moreover, it is unclear to what extent the observations in the Arnhem-Nijmegen area are from the ice-pushed ridges.

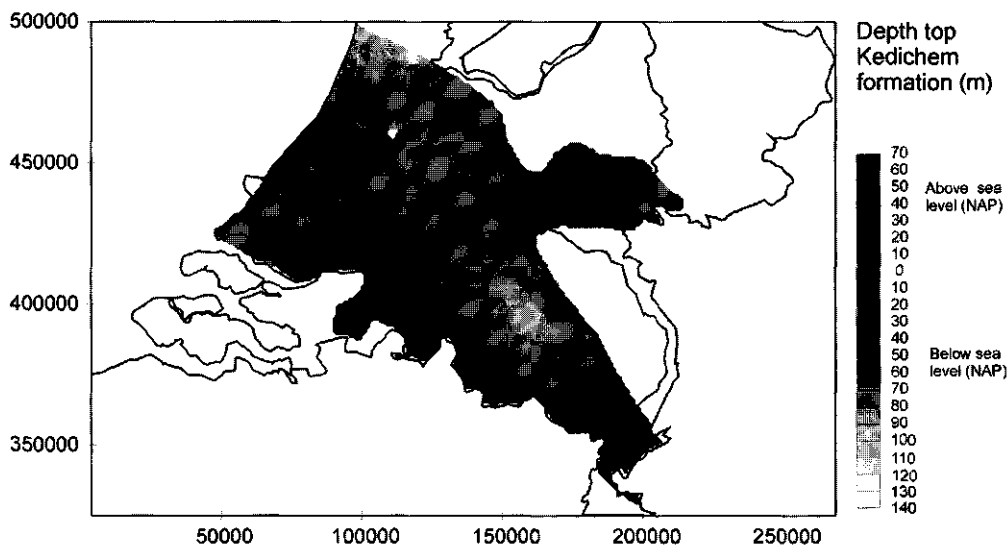


Figure 6.2 A Upper boundaries of the Kedichem formation.

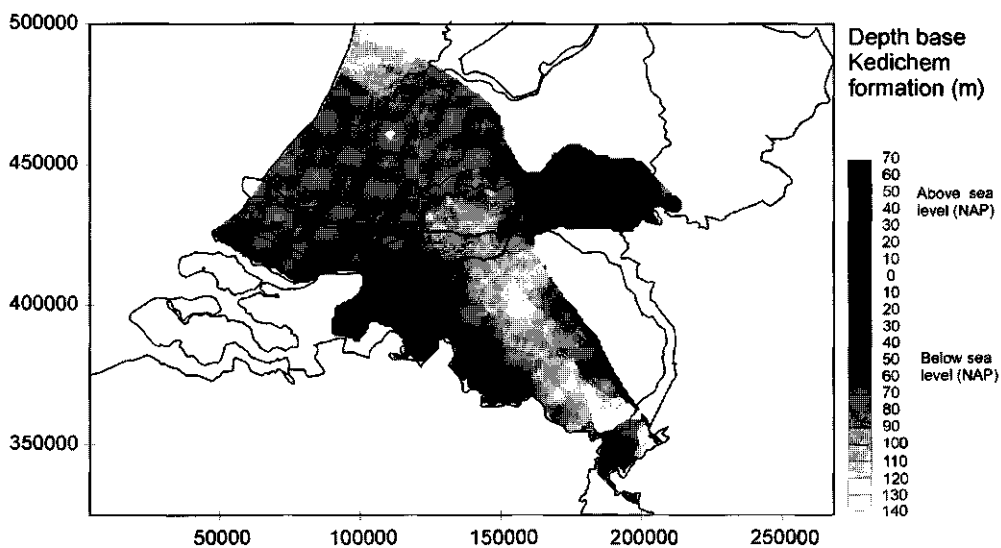


Figure 6.2 B Lower boundaries of the Kedichem formation

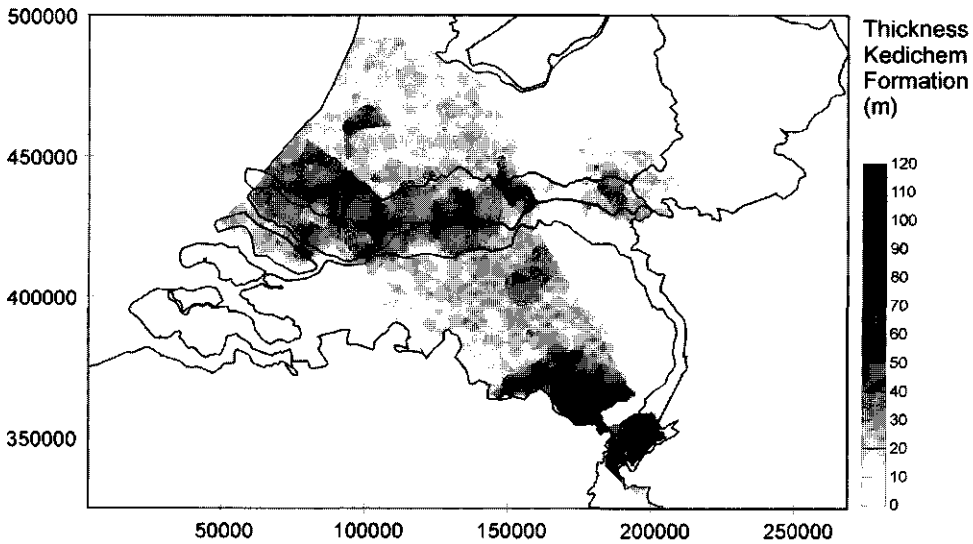


Figure 6.2 C Thickness of the Kedichem formation.

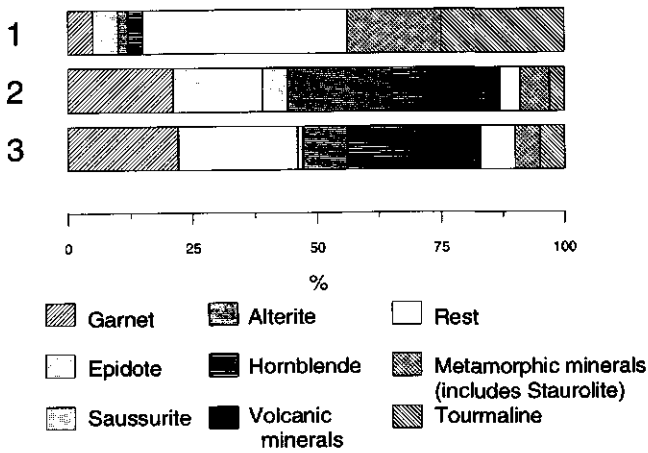


Figure 6.3 Heavy-mineral clusters as determined by fuzzy clustering.

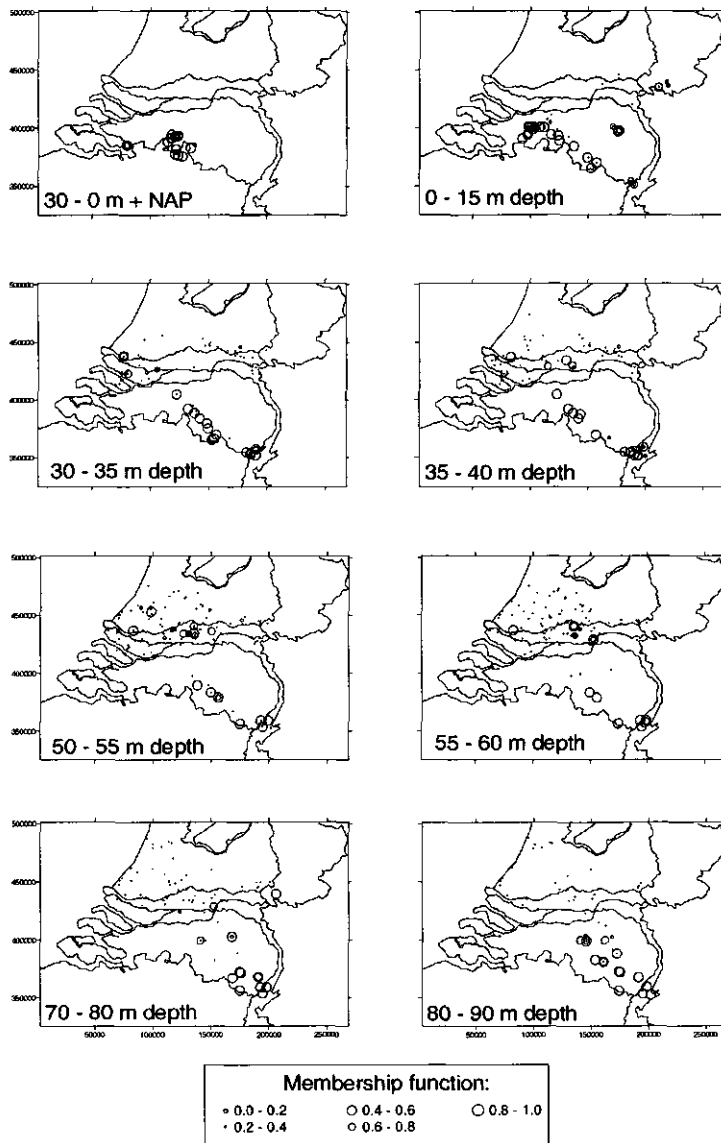
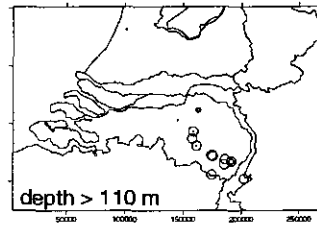
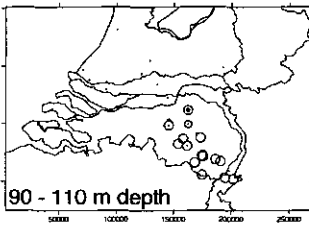
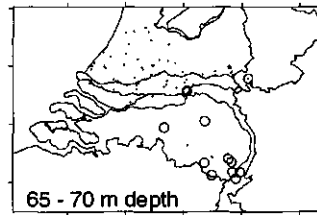
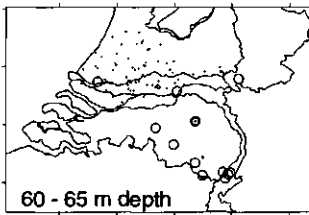
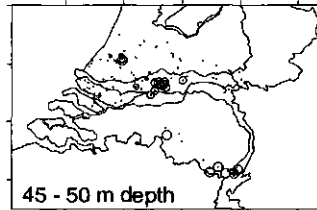
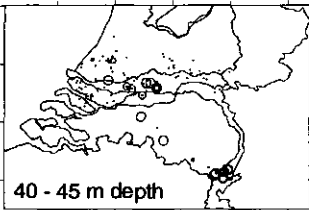
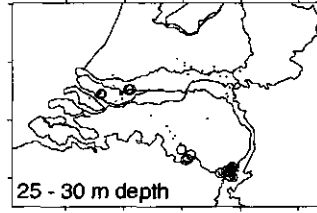
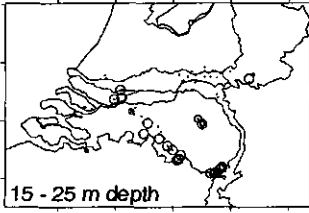


Figure 6.4 (Including next page) Spatial patterns of heavy-mineral cluster 1. Point size indicates membership function.



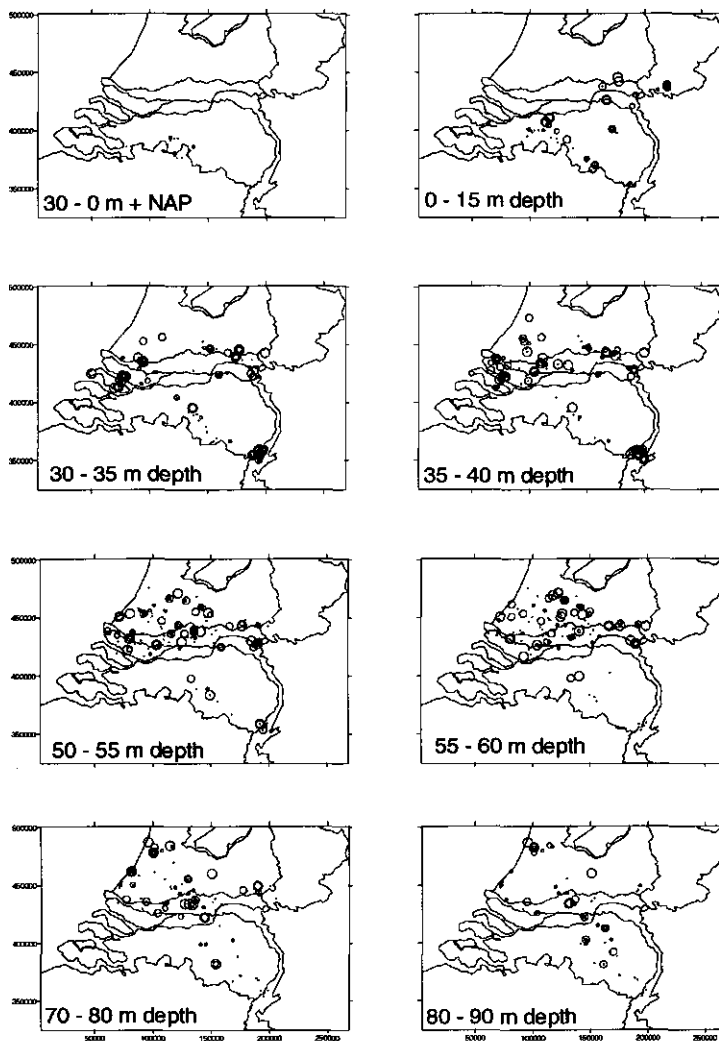
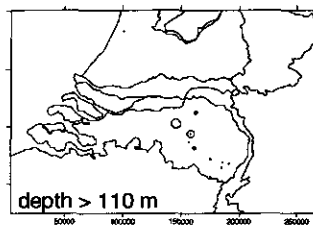
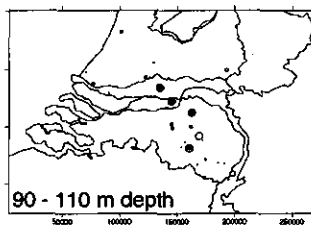
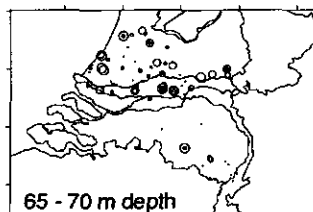
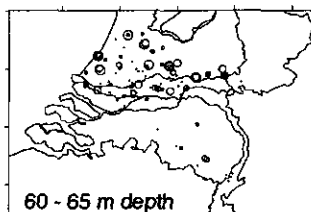
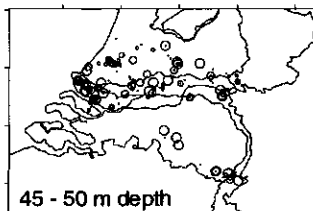
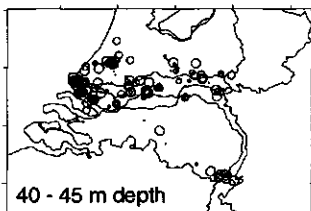
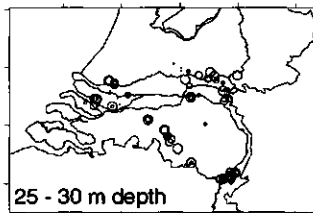
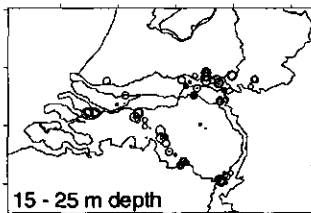


Figure 6.5 (Including next page) Spatial patterns of heavy-mineral cluster 2. Point size indicates membership function as in 6.4.



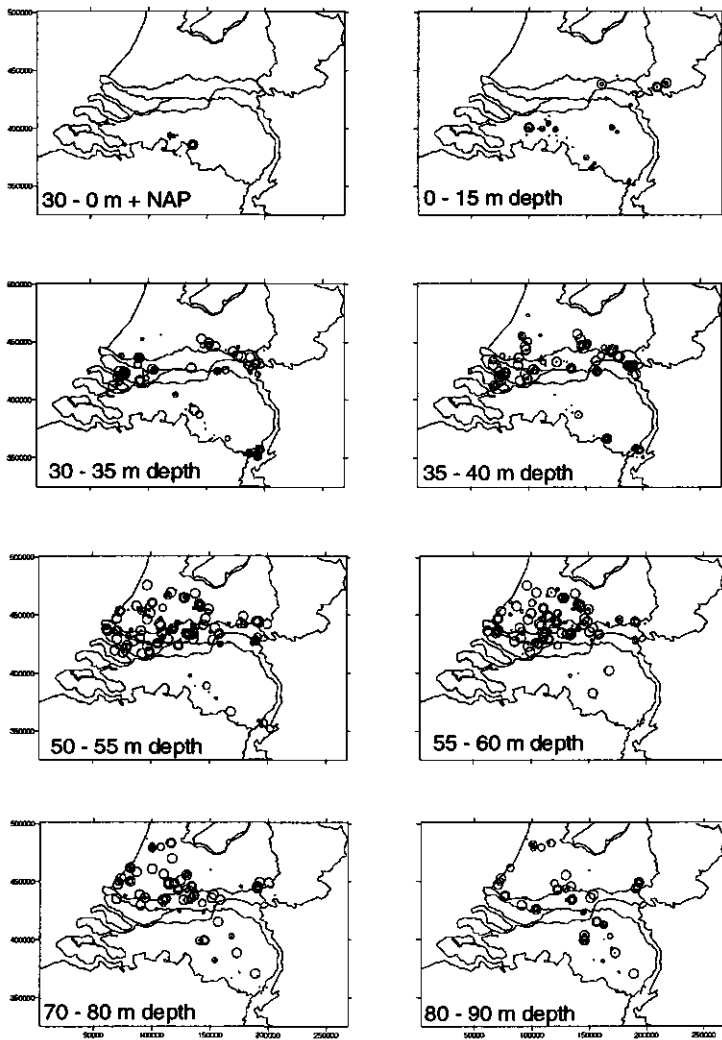
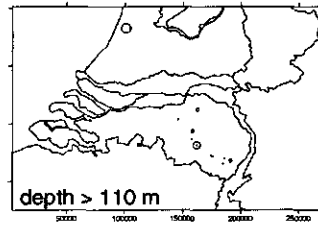
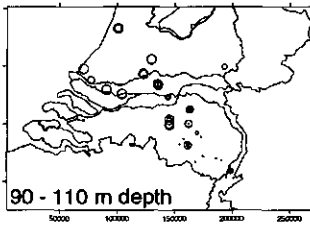
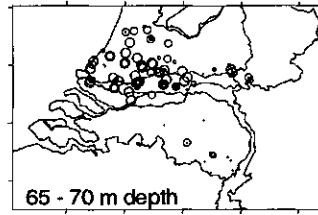
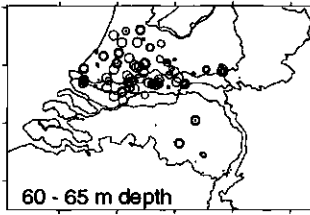
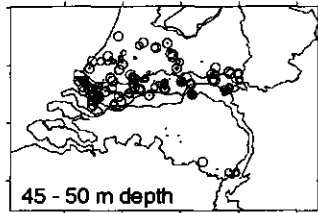
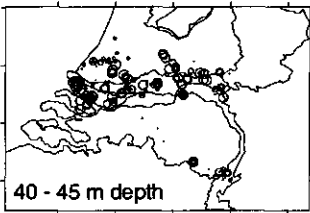
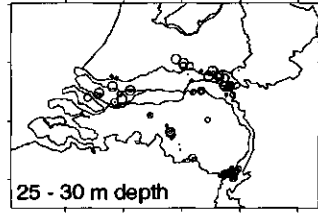
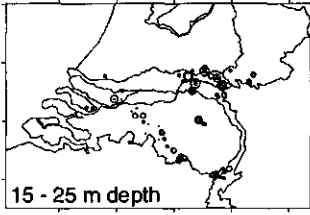


Figure 6.6 (Including next page) Spatial patterns of heavy-mineral cluster 3. Point size indicates membership function as in 6.4.



Heavy minerals

In Fig. 6.3, the composition of each of the three heavy-mineral clusters is presented. The first cluster consists of fully stable heavy minerals (tourmaline and the metamorphic and rest groups), and is similar to the heavy-mineral suites usually found in sediments derived from the Schelde drainage area and in Pliocene Rijn sediments (cf. Kasse, 1988). The other two clusters show an unstable heavy-mineral association with garnet, epidote, alterite, saussurite and hornblende. The main difference between the two is that cluster 2 has higher alterite contents, whereas cluster 3 shows higher contents of epidote and hornblende. They probably represent two types of Rijn- and Baltic-derived sediments (cf. Zagwijn and Van Staalduinen, 1975).

The maps of the cluster memberships (Figs. 6.4, 6.5, 6.6) show that the stable cluster is mainly restricted to the South of the area. Therefore it can be identified as Schelde-derived material. Its occurrence in the deeper parts of the Southern Roer Valley Graben may also be a reflection of the incorporation of the Pliocene Reuver sediments into the Kedichem formation (see above). The two unstable clusters occur mainly in the North of the area, and do not show a large difference in their distribution. Probably both clusters represent a mixture of Rijn and Baltic sediments, with the main difference based on the contents of hornblende. The distribution indicates that the methods we used to discern provenance is not able to distinguish between sediments from Baltic and from Rijn provenance. This may be caused by a limited Baltic influence in our dataset, but it is more likely that the difference between the two sources is too small for these methods to detect.

Geochemical factors

We used factor analyses to determine the most important factors that influence the sediment geochemical composition. Factor analysis gave five factors that incorporated more than one element, and which explained in total 88 % of the total variation (see table 6.2). The first factor, which explains 50 % of the variation, comprises Al, K, Mg, Ti, Ba, Cr, Cu, Pb, V, Zn, Ga, Nb, Rb, Th and Y. It probably represents the content of clays and micas. The second factor includes Ca, Mg, P and Sr explains 14 % of total variation, and can be identified as representing carbonates. The presence of P may represent CaPO_4 , but it is more likely that it is related to vivianite in siderite-rich samples (see Chapter 4.1). This seems to be contradicted by the absence of Fe in this factor. However, this can be explained by the occurrence of Fe in other phases like oxides and pyrite where it does not correlate with these carbonate-related elements. Factor 3 comprises As and S, which show a negative correlation with Si. It explains 7 % of the total variance. It is probably related to the presence of pyrite in organic-rich layers with low contents of (quartz-) sand. The presence of SiO_2 in the organic factor instead of the clay factor indicates that the low contents of (quartz-) sand in peat cause such low SiO_2 -contents that the differences in SiO_2 -content between clay and sand are trivial in comparison. The fourth factor, which consists of Fe, Mn and P and represents 5 % of the variation, probably represents (hydromorphic?) Fe- and

Table 6.2: Varimax-rotated factor scores of factors 1-7; scores < 0.50 blanked out:

Element	1	2	3	4	5	6	7	Communality
Al	0.96	0.96
As	.	.	0.91	0.84
Ba	0.88	0.93
Ca	.	0.91	0.93
Cr	0.82	0.82
Cu	0.60	0.76
Fe	.	.	.	0.78	.	.	.	0.94
Ga	0.94	0.96
K	0.88	0.92
Mg	0.53	0.79	0.93
Mn	.	.	.	0.95	.	.	.	0.92
Na	0.67	0.86
Nb	0.90	0.95
Ni	0.82	.	.	0.82
P	.	0.53	.	0.63	.	.	.	0.85
Pb	0.74	0.61
Rb	0.93	0.96
S	.	.	0.94	0.92
Si	.	.	-0.57	0.88
Sr	.	0.86	0.95
Th	0.74	0.81
Ti	0.91	0.95
U	0.91	.	.	0.86
V	0.88	0.91
Y	0.56	0.76
Zn	0.66	0.71
Zr	0.93	.	0.96
explained variance	50%	14%	7%	5%	5%	4%	2%	

Mn-oxide enrichments in which P is present as accessory element. Factor 5, explaining 5% of the total variance, consists of Ni and U. It probably represents the enrichments of these elements in organic-rich subsurface layers (see Chapter 4.2). The elements Na (2%) and Zr (4%) are each included in a separate factor, indicating that their contents do not show a linear correlation with any of the other elements. This can be explained by the fact that they both occur in a single mineral phase (Na in sodic plagioclase; Zr in zircon) that is sorted independently from the clay- or coarse sand fraction.

A problem of the factor analysis is that it does not account for the non-linear interrelations that exist between some of the elements (cf. Chapter 3.1 and 3.2). The most important of these are Na-Al and (to a lesser extent) K-Al (see Figs 6.7 and 6.8). Na-Al scatterplots show overall low Na-contents, irrespective of Al, for some deposits. In other deposits however, Na contents show a positive correlation with Al in the range of 0 up to 8% Al₂O₃, and a negative correlation with Al above 8% Al₂O₃. This is caused by the concentration of sodic plagioclase in the fine-sand and silt

fractions (see Chapter 3.1 and 3.2 for a more thorough discussion about this phenomenon). In a similar way, variations in the muscovite-contents in the fine sand fraction may cause differences in the K/Al-ratio in especially low-Al samples.

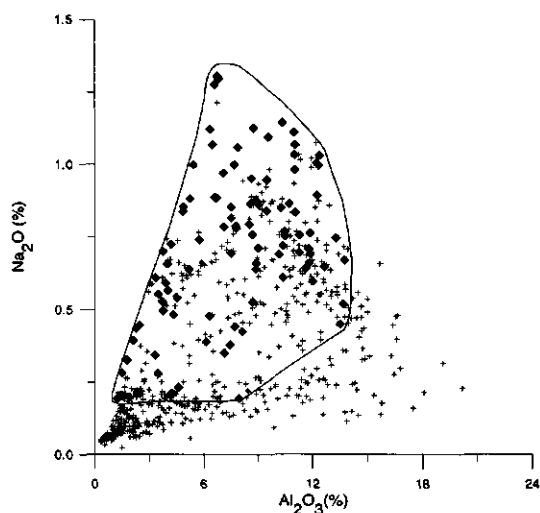


Figure 6.7 Scatterplot of Na_2O versus Al_2O_3 . Diamonds represent mica-rich, crosses mica-poor samples. Mica-rich samples have generally high Na_2O -contents.

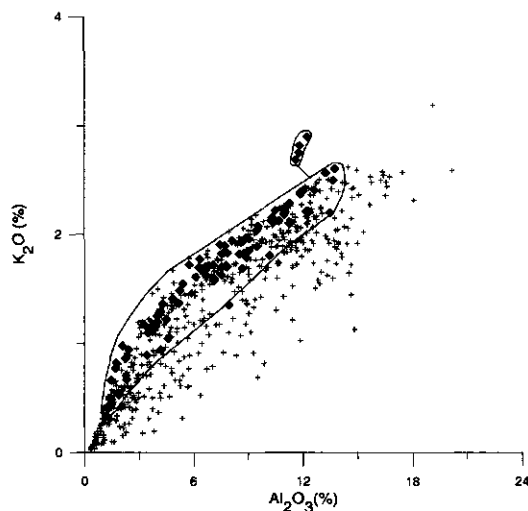


Figure 6.8 Scatterplot of K_2O versus Al_2O_3 . Diamonds represent mica-rich, crosses mica-poor samples. Mica-poor samples have in general a lower $\text{K}_2\text{O}/\text{Al}_2\text{O}_3$ -ratio.

Geochemical modeling

After coupling the geochemical data to the lithological codes (tables 6.3, 6.4 and 6.5), we found that the clay, sand and peat classes are significantly different for virtually all elements. The only exceptions are P, Th and Zr. For the elements that are mostly related to clay and carbonate contents (Si, Ti, Al, Fe, Mn, Mg, Ca, Cr, Cu, Pb, V, Zn, Ba, Ga, Nb, Rb, Sr and Y), gytija is not significantly different from clay, so these two can be grouped together.

Table 6.3: Average concentrations, standard deviations and number of samples (N) for clay-content dominated elements:

Element	Clay and Gytija			Peat			Sand		
	Conc.	Std. Dev.	N	Conc.	Std. Dev.	N	Conc.	Std. Dev.	N
SiO ₂ (%)	68.99	12.31	286	24.16	25.37	23	88.15	10.99	281
TiO ₂ (%)	0.60	0.15	286	0.28	0.22	23	0.19	0.15	281
Al ₂ O ₃ (%)	10.53	3.13	286	6.08	3.86	23	3.72	2.71	281
Fe ₂ O ₃ (%)	4.36	2.77	286	9.93	6.09	23	1.47	3.29	281
MnO (%)	0.04	0.06	286	0.06	0.05	23	0.03	0.18	281
MgO (%)	0.96	0.75	286	0.77	0.47	23	0.20	0.43	281
CaO (%)	2.60	4.26	286	7.19	5.59	23	0.56	1.59	281
Cr (ppm)	88	28	286	52	31	23	48	29	281
Cu (ppm)	15	7	220	19	10	23	7	6	183
Pb (ppm)	17	5	286	11	5	23	8	8	281
V (ppm)	79	33	286	52	45	23	21	21	281
Zn (ppm)	54	26	220	58	53	23	18	17	183
Ba (ppm)	325	56	286	213	103	17	173	81	281
Ga (ppm)	10	5	286	7	5	17	2	3	281
Nb (ppm)	14	3	286	8	4	17	6	3	281
Rb (ppm)	87	31	286	52	37	17	28	23	281
Sr (ppm)	96	63	286	105	47	17	33	33	281
Y (ppm)	31	9	286	43	34	17	14	8	281

This probably reflects the relatively high clay contents that can be found in gytija, but it may also relate to the difficulty in distinguishing gytija from organic-rich clay macroscopically. There were only a few loam-samples (6) and they were not significantly different from any other lithological class. Therefore loam is not incorporated in our model. For the elements that are most related to pyrite and organic-related accumulation (As, S, Ni and U), significant differences occur not only between clay and sand, but organic-rich material (gytija, peat and organic-rich clay) forms a separate group with increased contents of these elements.

Table 6.4: Average concentrations, standard deviations and number of samples (N) for organic matter dominated elements:

Element	Organic-poor Clay			Peat, Gytija and Organic-rich clay			Sand		
	Conc.	Std. Dev.	N	Conc.	Std. Dev.	N	Conc.	Std. Dev.	N
As (ppm)	7	7	184	41	95	125	4	6	281
Ni (ppm)	24	13	184	40	51	125	9	11	281
U (ppm)	2	2	184	4	6	119	1	1	281
S (ppm)	965	2144	181	11577	22543	119	574	1237	250

The main lithological groups can be further subdivided according to the mica contents to distinguish between the differences in the relation of Na and K with Al. This is most pronounced for Na; high Na-contents occur in mica-bearing samples (Fig. 6.7). It can be explained by mica-rich sediments being derived from the Rijn system, which also transported Alpine sodic plagioclase, whereas low-mica sediments were derived from the Schelde system, which transported material poor in sodic plagioclase (cf. Chapter 3.1 and 3.2). The higher K/Al-ratios in mica-rich sediments can be linked directly to mica as one of the major K-sources in the sediment (Fig. 6.8).

Table 6.5: Average concentrations, standard deviations and number of samples (N) for mica-related elements:

Element	Mica-poor clay			Mica-Rich Clay		
	Conc.	Std. Dev.	N	Conc.	Std. Dev.	N
K ₂ O (%)	1.84	0.42	238	2.12	0.38	38
Na ₂ O (%)	0.53	0.23	238	0.75	0.14	38
Element	Mica-poor sand			Mica-rich sand		
	Conc.	Std. Dev.	N	Conc.	Std. Dev.	N
K ₂ O (%)	0.73	0.48	222	1.70	0.40	17
Na ₂ O (%)	0.18	0.14	222	0.87	0.35	17
Element	Peat and Gytija					
	Conc.	Std. Dev.	N			
K ₂ O (%)	1.17	0.81	33			
Na ₂ O (%)	0.36	0.29	33			

A further subdivision of the main lithological classes proved to be of little use for geochemical differentiation. Additional lithological codes (thin clay layers; clay lumps, etc.) did not provide significant differences either.

We made a geochemical model based on the data above to predict the contents of Al, Na and Ni as characteristic elements of each of the three element groups. In order to make slice-maps, we calculated the concentrations of Al, Ni and Na on the basis of the average composition of each core within each slice according to:

$$(1) \quad \text{Al}_2\text{O}_3 = 10.53 * \text{C} + 6.08 * \text{P} + 3.72 * \text{S}$$

Al_2O_3 : percentage of Al_2O_3

C: Relative amount of clay and gyttja (m/m).

P: Relative amount of peat (m/m).

S: Relative amount of sand (m/m).

$$(2) \quad \text{Ni} = 24 * \text{Cn} + 40 * \text{H} + 9 * \text{S}$$

Ni: amount of Ni (in ppm)

Cn: Relative amount of organic-poor clay (m/m).

H: Relative amount of peat, gyttja and organic-rich clay (m/m).

S: Relative amount of sand (m/m).

$$(3) \quad \text{Na}_2\text{O} = 0.53 * \text{Cp} + 0.75 * \text{Cm} + 0.18 * \text{Sp} + 0.87 * \text{Sm} + 0.36 * \text{Pg}$$

Na_2O : percentage of Na_2O

Cp: Relative amount of mica-poor clay (m/m).

Cm: Relative amount of mica-rich clay (m/m).

Sp: Relative amount of mica-poor sand (m/m).

Sm: Relative amount of mica-rich sand (m/m).

Pg: Relative amount of peat, gyttja and organic-rich clay (m/m).

For the last formula, we decided to classify all sediments in a slice of a boring as mica-rich when it contained least one mica-rich section.

Model Performance

The performance of the model can best be demonstrated by comparing the model outcomes with the actually measured geochemical composition in a core. In Fig. 6.9a, such a comparison is made for boring Rucphen 2 (see also Figs. 3.1.11c, 3.1.13 and 5.4). The overall performance of the model is quite good for Al and Ni: the modeled values for each lithological unit follow the measured values of Al and Ni, but the extremes of the measured values are higher than the model due to the averaging procedure. This means that for these elements the variation in the model values follows the variation in real element contents, but that the real absolute contents are more extreme. The model performance is less for the Na-model. The main problem here is probably that in the original lithological data the presence of micas is not always mentioned. Therefore the Na-contents of low-mica sediments in our geochemical model are in fact an average of mica-rich and mica-poor material, which results in an overestimation of the Na-contents. In some sections, there is no modeled value because there was no model value for the lithological code ("Loam" at 3 and 9.5 m depth; "Siderite" at 7 m depth). The data from this boring has been part of the dataset that was used to make the model, so the overall model performance for boring

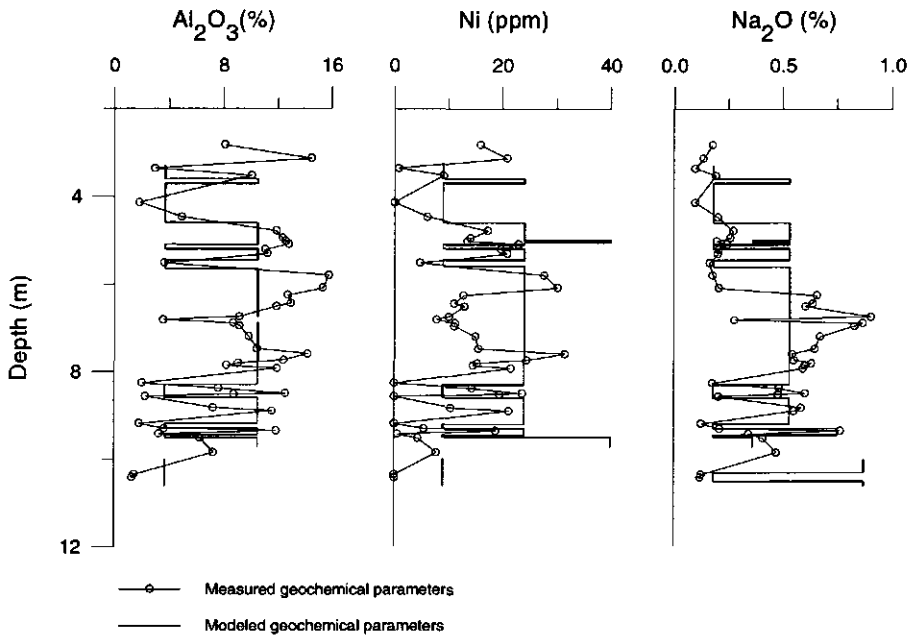


Figure 6.9 A Comparison between measured and modeled geochemical parameters for boring Rucphen 2.

Rucphen 2 is probably overestimated. Furthermore the good quality of this boring is not representative for the borings in the NITG-TNO boring database, as they include a large number of (counter-)flush borings.

Fig. 6.9b also demonstrates the effects of averaging the modeled geochemical values for the slice maps. It is clear that a large part of the variation is lost during this preparation for visualization. Furthermore, in the top one can see that only a short length of observations (approx. 30 cm) become representative for the total 5 m of sediments because there are no other observations. A comparison of the average modeled with the average measured geochemical parameters shows that they have large differences. This is probably for a large part related to our way of sampling, which tends to emphasize thin layers of clay or organic rich material at the expense of more homogeneous sand units.

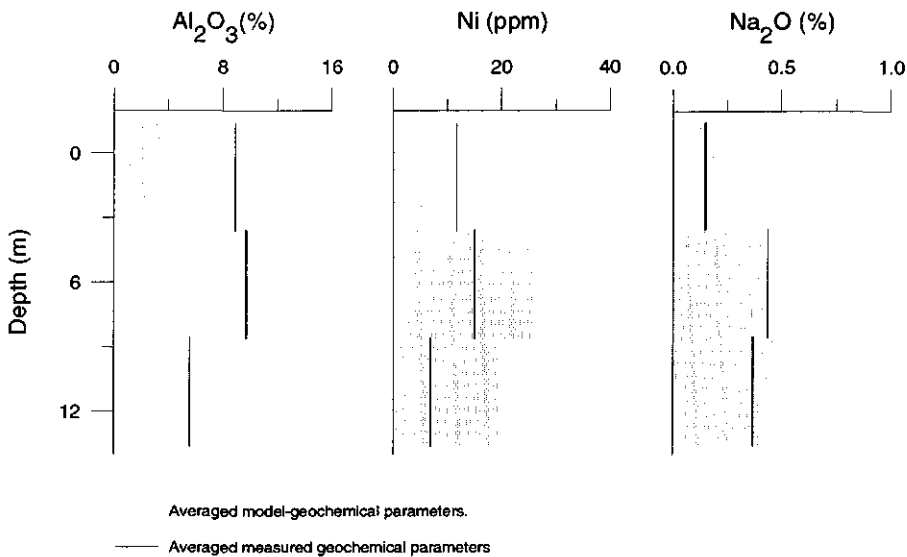


Figure 6.9 B Measured and modeled parameters after averaging into slice-maps.

Spatial characteristics of the geochemical model

The patterns that emerge from the maps of the modeled Al-contents (Fig. 6.10) clearly differ between the various slices: The slices from +30 m to -40 m show low Al-contents in the south, and higher contents in the North, which indicates higher sand contents in the south. Furthermore, the patterns are patchy and show little overall patterns, indicating that the spatial patterns are on a smaller scale than can be studied with our sample densities. In the deeper slices, especially below 60 m, the Al-contents in the Zuid Holland area decrease significantly, reflecting an overall large-scale fining-upward sequence which might be related to a regression. The Roer Valley Graben displays high Al-contents, which continue in a northwestern direction. The occurrence of high Al-contents, i.e. significant amounts of clay, in the areas where the top of the Kedichem formation lies deepest (Roer Valley Graben; Amsterdam/ IJmuiden area) indicates that the distribution of clay-rich deposits is determined at least partially by tectonic processes. Moreover, the distribution of Al-rich areas in e.g. the 65-70 m slice suggests that the main tectonic system which was active during the deposition of the Kedichem formation is associated with the Roer Valley Graben subsidence, whereas the West Netherlands Basin fault system which has a more westerly direction (Geluk et al., 1994) was of less importance.

The slice-maps of the modeled Ni-distribution (Fig. 6.11) show similar patterns as the Al-maps. This can be attributed partly to the influence of the contents of clays and other phyllosilicates on the Ni-contents. However, the association of Ni with organic-rich material is more important as it has the most extreme values (see averages table 6.4; Ni(sand) = 9 ppm, Ni(clay) = 24 ppm, Ni(org.) = 40 ppm). The comparability of the Al- and the Ni-patterns therefore

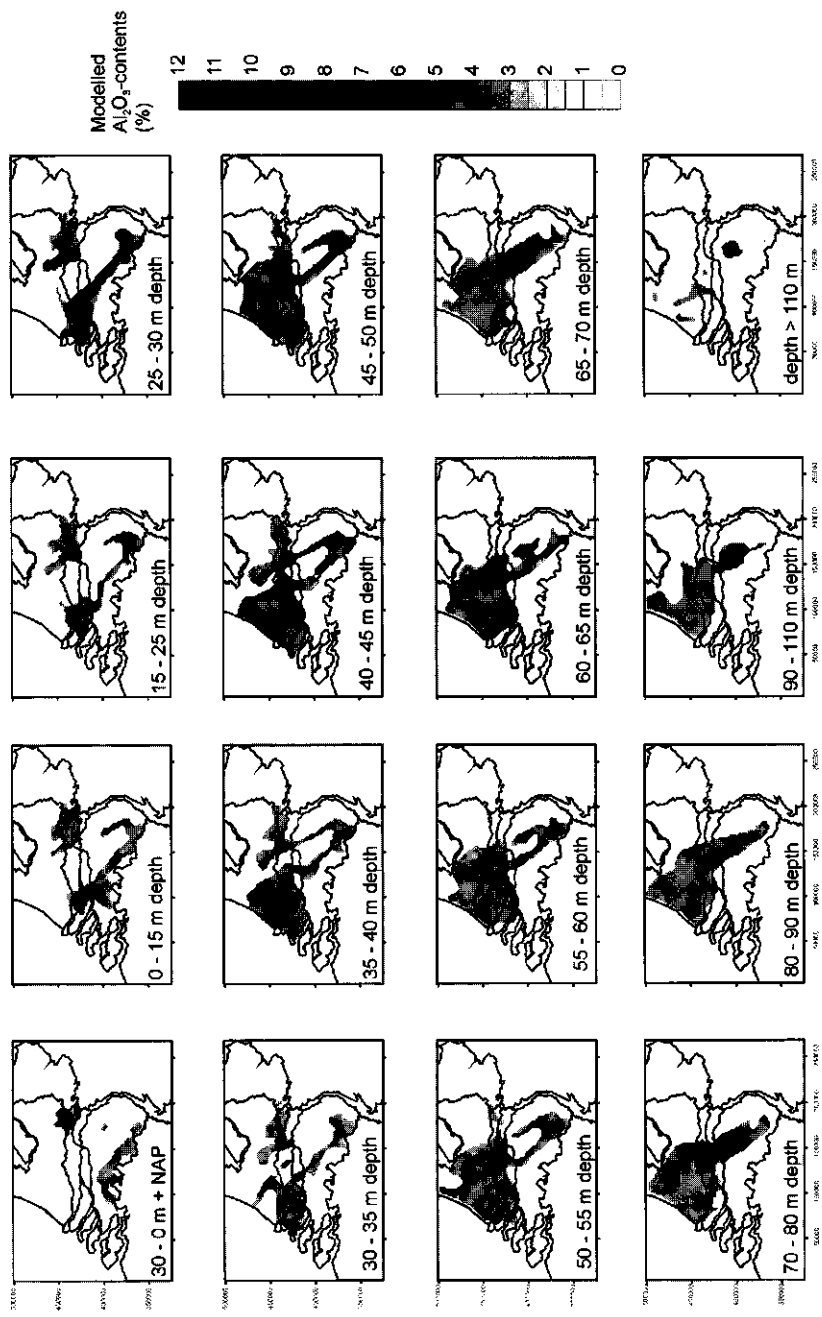


Figure 6.10 Spatial geochemical model of Al_2O_3 for the Kedichem formation.

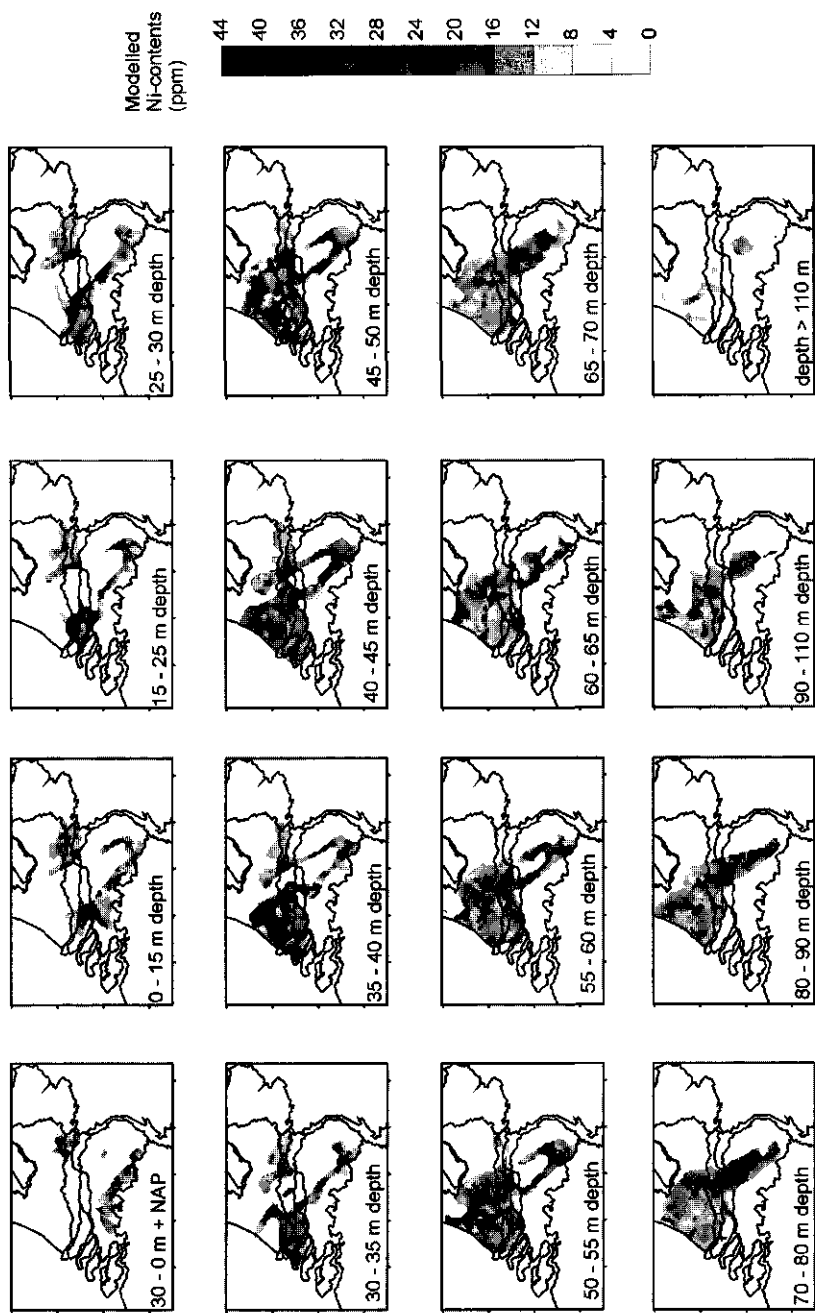


Figure 6.11 Spatial geochemical model of Ni for the Kedichem formation.

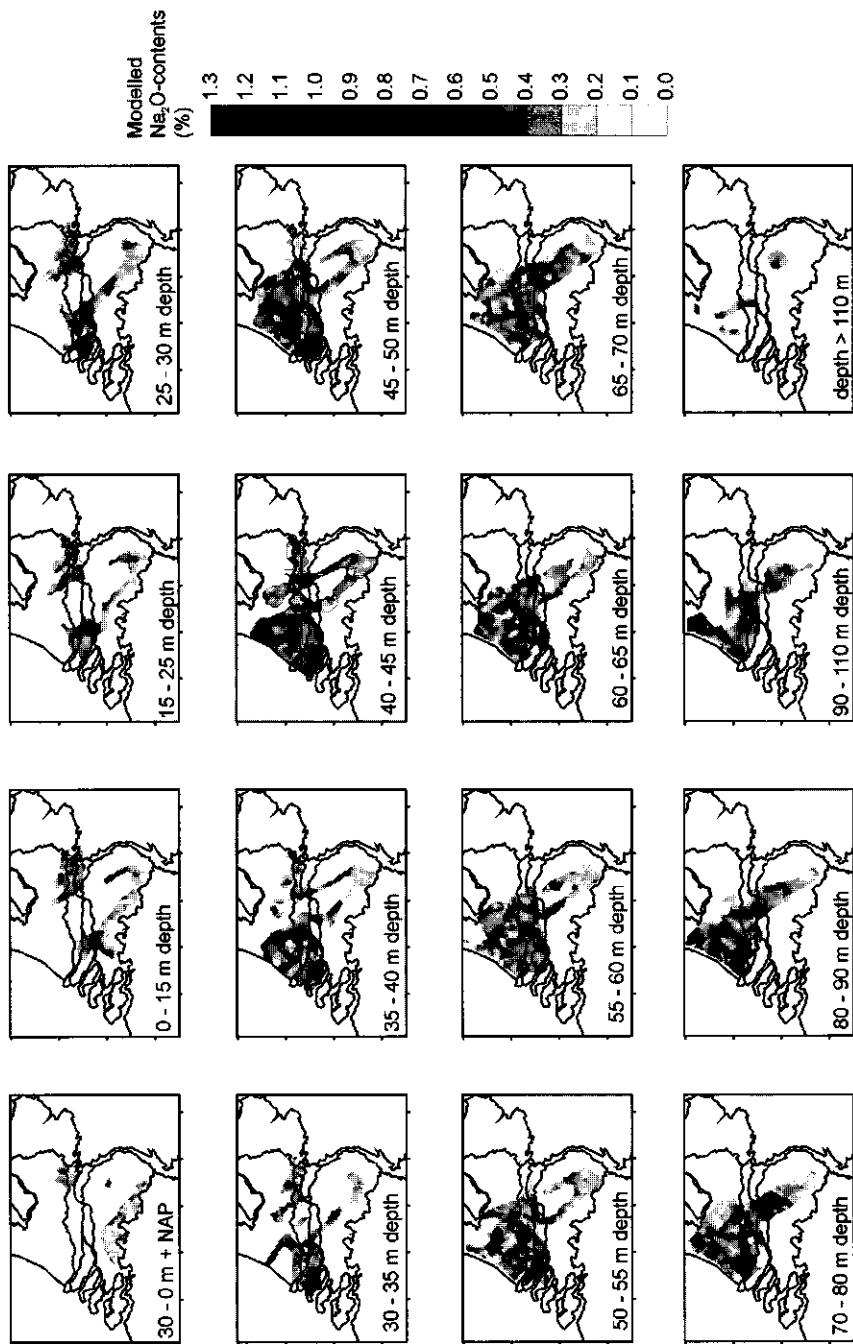


Figure 6.12 Spatial geochemical model of Na_2O for the Kedichem formation.

must be attributed also to the occurrence of relatively abundant organic-rich sections in clay layers. This is consistent with an interpretation that the clay layers represent basin clays and oxbow lake infillings, of meandering to anastomosing systems, as they often include peat and organic-rich horizons (cf. Einsele, 1992). The presence and position of the most important organic-rich deposits appear to be determined by tectonic processes (subsidence), which is another indication that subsidence was active during the deposition of the Kedichem formation.

The modeled Na-contents (Fig. 6.12) show in general low Na-contents in the south, and variable Na-contents in the north of the area. This can be compared directly to the heavy-mineral clusters, which show high memberships for the stable heavy-mineral cluster in the south (see Fig. 6.4), and represents the influence of the Schelde river system on the composition of the Kedichem sediments. There is a clear boundary between high Na contents in the northern and low Na contents in the southern part the Roer Valley Graben (see e.g. the 50-55m slice-map). This boundary coincides neatly with the increase in thickness of the Kedichem formation in the south of the Graben. This supports our interpretation that this increase in thickness is caused by the classification of Tiglian and older sediments with a stable mineralogy into the Kedichem formation (see above). The lack of easily interpretable patterns in the modeled Na-contents in the north of the area (esp. Zuid-Holland) is probably caused by an interaction between lithological differences, differences in sediments sources (local occurrences of Schelde-derived sediments), and the inconsistencies in the observations on the mica content in part of the core descriptions.

Conclusions

In this paper we presented a method to characterize the geochemical composition of subsurface sediments with a relatively small amount of analyses. The contents of all elements, except P, Th and Zr, could be linked to lithological codes from the NITG-TNO boring database to make predictions of geochemical properties in places where no geochemical data are available. The results show that the variation in the Kedichem formation is not large, but that still spatial patterns can be discerned. Furthermore, it appears that a major part of the geochemical variation in the Kedichem formation can be related to tectonic processes.

The spatial modeling of key-elements demonstrates that it is possible to make predictions about variations of the contents of these elements in Dutch subsurface sediments. The method of linking geochemical to lithological data by averaging is crude, but it is probably still the best way to proceed with a geochemical characterization of the Dutch subsurface. However, it must be noted that the range of modeled values is in the same order of magnitude as the range of element concentrations that one can find within one lithological unit. This indicated that the absolute values of the predictions should not be taken at face-value, but more as a general indication. An extensive sensitivity analysis is recommended for future geochemical subsurface modeling. The patterns that emerge from the spatial modeling of lithological parameters that influence the geochemical composition, however, can be useful for geochemical as well as geohydrological and stratigraphic research.

The use of formation boundaries as *a priori* stratification for geochemical research would be unwise, as it is likely that a large number of the formation boundaries are insignificant for the geochemical composition. Future geochemical characterization programs would be served better

by studying sediments without *a priori* division in formations. Differences in sediment provenance can be taken along as a factor that is based on sediment-petrological characteristics like heavy-mineral composition and mica content. It must be stressed that it is not possible to directly link the geochemical composition of sediments with the heavy-mineral content. One reason for this is that the heavy minerals represent only a small fraction (a few percent at the most) of the total sediment. Moreover, heavy-mineral counts, in which each mineral is expressed as a percentage of the total amount of grains, do not relate to the actual content of the mineral but rather to the abundance relative to the other heavy minerals. For example, the contents of Zr, which in the sediments studied occurs only in the mineral zircon, do not differ significantly between the Schelde-derived and the Rijn-derived sediments in the Kedichem Formation. Still, heavy-mineral counts from Schelde-derived sediments show high zircon contents (often >50%), whereas heavy-mineral counts from Rijn sediments show only a few percent of zircon. This reflects the higher contents of heavy minerals that is present in Rijn sediment when compared to Schelde material.

This study illustrates the relative importance of organic layers for the subsurface heavy metal geochemistry. However, it may be more important to understand the processes that are involved in diagenetic element enrichments and know the chance that enrichments in e.g. Ni occur than to exactly predict the content in each specific organic layer.

For a nation-wide geochemical characterization, more effort is needed to accurately describe, study and present the spatial patterns presented here; the slice maps used are relatively easy to make and to use, but it is a crude 2-D approximation of truly 3-D variation patterns. In the center of the Roer Valley Graben, e.g., inhomogeneous subsidence rates probably caused layers that were originally more or less horizontal to become bowl-shaped. Such layers would appear dissected and divided amongst a large number of slices, whereas their shape could be described more accurately and useful in a true 3-D description of the sediment body.

7 Synthesis and conclusions

Introduction

The purpose of the GEOBON-project was to determine which factors influence the geochemical composition of the Dutch subsurface sediments, and to characterize the spatial variation of these factors. We found that the main factors that determine the subsurface sediment geochemistry are the contents of clay mineral and micas, of carbonates, of pyrite, of Fe,Mn-hydroxides and diagenetic enrichments in organic-rich layers. In the Kedichem formation, these factors explained in total 81% of the total geochemical variation (see Chapter 6). Sediment properties and processes influencing these factors include grain size, sediment provenance, specific sorting processes and syn-or postdepositional weathering or neoformation of specific minerals. The data presented in this thesis, the first systematic geochemical mapping of these sediments, do not only provide new insight in the genesis and the build-up of the Netherlands' subsurface, but also provide new tools for future research. Moreover, it and gives information that can be used to study, predict and evaluate human activities on surface and subsurface sediments. In the following we evaluate the methods used and give an overview of implications and possible future applications.

Methods used

Our experience is that the method for geochemical characterization used in this study (a large number of bulk XRF-analyses, supported with additional ICP-MS, XRD, micromorphological and SEM-data) is suitable for determining and explaining the geochemical variation, as well as the speciation of the elements. From this data, information about the reactivity and conditional stability of the various phases can be deduced. XRF-analyses should form the backbone of any geochemical mapping campaign because it is cheap and quick. Other methods should only be used to measure specific elements that cannot be done with XRF (ICP-MS) or to answer specific questions about speciation (XRD, mineral counts), small-scale distribution (micromorphology, SEM) or conditional availability or reactivity (sequential extraction schemes). A geochemical study of diagenetic processes and the associated minerals, like in Chapter 4.1 and 4.2, is impossible to do without micromorphological and submicroscopical data. In order to study reactivity of subsurface sediments, e.g. with respect to natural attenuation of organic pollutants and the buffering of nitrate, it is important to have detailed information about geochemical factors like the contents Corg, S, pyrite and carbonates. Therefore it is recommended to include these analyses in the standard core description of the NITG-TNO.

Despite the possibility to measure large amounts of samples using XRF, characterization of the geochemical composition of the Dutch subsurface sediments with standard mapping techniques would be too time and cost intensive. Therefore such a program would need to be performed on the basis of analyses from a relatively small amount of borings, and furthermore on data already available. We demonstrated that the geochemical data can be used to make "geochemical transfer functions" to translate data from the NITG-TNO boring database into a geochemical spatial prediction model. Such a model would, however, probably be best served by making an *a priori*

subdivision only according to sediment source based on heavy minerals instead of a subdivision into various geological formations. As the organic-rich sediments are important from an environmental as well as a scientific point of view, their occurrences and composition should be one of the main foci during a geochemical characterization program. Organic-rich layers can only be sampled with enough detail and accuracy if good quality cores are available. They should preferably be fresh, as otherwise additional micromorphological or SEM-analyses become impossible because of oxidation of sulfides and organic matter. Bailer-bore samples may be used for stratigraphic research if no good-quality cores are available. They are, however, unsuitable for the study of organic-related element accumulations. Samples from flush borings should not be used at all for geochemical research because of the possible loss of micas and clay minerals during the boring procedure.

Our method of spatial modeling and visualization is relatively crude, but it demonstrates the possibilities for spatial modeling of geochemical properties. 2-D slice maps like the ones we used to visualize 3-D sediment bodies can be useful as an easy access to the composition of subsurface deposits, and could also be applied different fields like geohydrology, facies analysis and stratigraphy. However, in order to describe, study and understand underground structures, a true 3-D approach, like the ones used in petroleum geology, is necessary.

Geochemistry as stratigraphic tool

Because of the large influence of provenance on the contents of specific elements (Na, Ti, Ca, Mg) and the sand and clay mineralogy, study of the geochemistry supported with mineralogical analyses can yield abundant information about the sedimentation history of the Dutch subsurface. Moreover, such studies can provide important new stratigraphic tools. Heavy-mineral stratigraphy, the present-day standard practice, has the disadvantage that it only represents a small part of the sand fraction. Geochemical tools have the advantage that they represent the bulk sediment composition. Moreover, bulk geochemical tools, if necessary supported by clay mineralogical analyses, are applicable to both sands and clays, and are therefore more universal applicable. Because bulk geochemistry reflects the composition of the total sediment, bulk geochemical data may also be used to estimate relative proportions of different sediment sources in a certain deposit, which may provide data needed for process-based modeling of the genesis of the Rijn-Maas-Schelde delta.

In order to link geochemistry to the heavy-mineral stratigraphy, the geochemical characteristics of the most important heavy-mineral zones and of the transitions between these zones should be determined by analyzing key sections. It may also be necessary to study in more detail the chemical composition of major mineral phases (feldspars, micas, heavy minerals). When a link is made between the heavy-mineral stratigraphy and the bulk geochemistry, bulk geochemical analyses can become a valuable contribution to the stratigraphic toolbox, next to heavy-mineral counts and pollen analysis. It can probably not completely replace the heavy-mineral stratigraphy as is in use now, especially since the NITG-TNO database with a large amount of heavy-mineral analyses done in the past serves as a stratigraphic reference. Still, it can give new insights in sediment source characteristics, and it can provide data to quantify the relative contribution of each sediment source which, in turn, can be used for process-based modeling of the genesis of the Rijn-Maas-Schelde-Baltic delta.

In this study, it is shown that especially the organic-rich layers show geochemical fingerprints of past redox conditions and groundwater composition. Therefore, a detailed study of organic-rich layers, applying geochemical, mineralogical and (sub)microscopical techniques, would provide information on epidepositional facies changes as well as post-burial variation in groundwater composition. Events that can be traced in this way include past saline water transgressions or intrusions, oxidation phases and possibly past groundwater sources.

Implications for human activities

Natural background values heavy metals

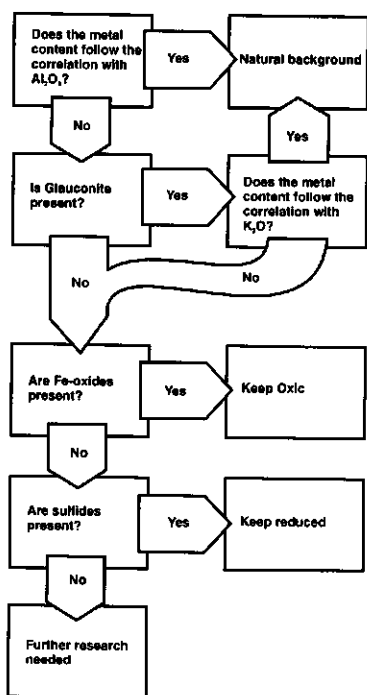


Figure 7.1 Guideline to identify heavy metal anomalies, and to prevent those metals to be released to groundwater

The geochemical composition of subsurface sediments can be regarded as an indication of the natural background of most elements. In chapter 5 we showed that the background of the elements that are of interest from the point of view of environmental protection (esp. heavy metals) can be described in their relation to Al, K and S. We also argued that this method of determining the background is better, both theoretical and practical, than the relation with clay and organic matter content that is used in present-day environmental legislation.

On the basis of our results, we can propose a series of steps that can be used as a guideline to identify heavy metal anomalies in soils and subsurface sediments, and to prevent those metals to be released to groundwater (Fig. 7.1):

- Step 1: Determine whether higher contents of heavy metals are present than would be expected on the basis of the Al- and possibly K- contents. If no significantly elevated contents occur there is no problem. Otherwise step 2.
- Step 2: Check whether glauconite may be present in the material studied. For surface material, this is probably only relevant in some restricted areas in Twente, De Achterhoek, where Miocene greensands occur in the ice-pushed ridges (Zagwijn and Van Staalduinen, 1975), and in glauconite-bearing

limestones and marls in Zuid-Limburg. If glauconite is present and the elevated heavy metal and As-contents correlate with K, the major part of the heavy metals are present in the crystal lattices of the glauconite, and therefore virtually immobile and unavailable. However, it may be possible that prolonged exposure to air, e.g. as a result of changes in groundwater table or building activities causes the glauconite to oxidize, as a result of which the heavy metals and As become available or are stored in a less stable form (Fe-hydroxides). In order to evaluate these risks, more research is needed on the speed and effects of oxidation processes and weathering on glauconite. If no glauconite is present, step 3.

Step 3: Determine whether heavy metals and/or As may be present as naturally occurring Fe(oxy) hydroxides or as sulfides. The presence of Fe-hydroxides can be deduced easily from the tell-tale orange-rust colors, but it may need to be confirmed by chemical analyses for legal purposes. If heavy metals and/or As are present in these natural Fe-compounds, they are immobile, unavailable and therefore not harmful as long as the diagenetic environment remains oxic, and the pH does not become too low. Restrictions may be put on land use to prevent release of the harmful components due to reduction processes or acidification.

The presence of organic matter may be an indication that heavy metals and/or As are present a naturally occurring sulfides. However, this certainly needs to be confirmed by determining the sulfur contents. It must be noted however, that in organic-rich layers high contents of especially Ni may occur in combination with low S-contents as a result of the presence of high-Ni pyrites. If such enrichments are related to the presence of sulfides, the elements are immobile as long as the diagenetic environment remains reduced. Evaluation of possible future land use therefore should take into account that not only lowering of groundwater tables and nitrate pollution, but also building and subsurface activities can cause oxidation of the sulfides, as a result of which harmful heavy metals and/or As can become available, and groundwater pH may drop.

If a heavy metal and/or As enrichments are not related to Fe-hydroxides or sulfides, they are most likely anthropogenic in origin.

It must be stressed, that these guidelines are based on Early Pleistocene fluvial subsurface sediments. More research is needed to test whether the same guidelines are also applicable for marine deposits and topsoils. In this respect it is also recommended to study the heavy metal contents of phosphorite nodules, and the effect of the presence of phosphorite on the quality of groundwater or soils.

Effects of subsurface anthropogenic activities

Our study shows that subsurface sediments and groundwater in The Netherlands form a dynamic environment. The various anthropogenic subsurface activities can disturb this system. Increasing use of the subsurface without proper precautions therefore could seriously endanger our future drinking water sources. It must be stressed that not only lowering of groundwater tables and increased nitrate leaching to groundwater, but also large infrastructural projects and preparations for the storage of waste and carbon dioxide will cause reduced sediments to come

into contact with the atmosphere or with oxic water. If reduced phases like sulfides are present in these subsurface sediments, they may oxidize which in its turn may result in increased contents of As, Co, Ni, Pb and Zn, associated with a lowering of the pH in groundwater and, potentially, drinking water. Moreover, sediment removed from the subsurface during e.g. subsurface tunneling may be harmful if it contains such reactive phases. Therefore it is important to assess prior to starting such projects whether organic layers occur, and what element enrichments in what phases can be encountered. In such situations, the possible presence of such localized reactive element concentrations, and the exact mineralogy is of larger importance than the average composition of the sediment.

Summary

Traditionally, the Netherlands' subsurface is mainly used to obtain good quality drinking and industrial waters from the different aquifers. Due to the lack of space on the surface, increasing environmental problems and demand for energy, the subsurface will be used increasingly for other activities, including large underground infrastructural projects, underground storage of waste and greenhousegasses and underground storage capacity for the energy sector. In order to evaluate the effects of the underground activities, detailed knowledge about the subsurface sediments is required. The geochemical composition of the subsurface sediments and the associated mineralogy forms an important part of the information needed to make decisions where and under what restrictions the different activities in the subsurface can best be planned.

This thesis is a result of the GEOBON-project, which was started in order to meet this information need. The project studied the chemical composition of subsurface sediments by sampling and analyzing cores that were made by the Geological Survey of the Netherlands as is described concisely in Chapter 2.

Chapter 3 present results from two study areas, Brabant and Limburg, which show how sediment source, sorting processes, depositional environment, grain size, weathering and syn- and post-sedimentary diagenesis affects the geochemical composition of Miocene, Pliocene and Lower Pleistocene sediments in the Southern Netherlands:

Chapter 3.1 contains the results of a sediment geochemical study that was performed in unconsolidated Upper Cenozoic sediments from the South of the Netherlands. Glauconite-rich sediments (Breda Formation) show anomalously high K contents and low Ba/K ratios. Major shifts in sediment composition as a result of changes in the Rijn system and shifts between Rijn and Schelde provenance as known from heavy-mineral studies are recorded in changes in the grain size dependent variations between Al, Na and K: Pleistocene Rijn sediments (Tegelen Formation) show higher Na contents than Pliocene Rijn sediments (Oosterhout and Kiezeloëliet Formations) and Schelde-derived material (Kedichem Formation), probably as a result of larger contents of sodic plagioclase. Schelde-derived sediments show low K/Al ratios as result of a smectite-dominated clay mineralogy and low contents of micas, whereas Rijn-derived sediments have high K/Al ratios which reflect an illite-kaolinite dominated clay mineralogy and higher contents of muscovite.

The presence of siderite causes high Fe-contents in the Tegelen formation in the east of the study area. Increased Mg contents in the siderite-bearing sections from the Tegelen formation and in parts of the Oosterhout and Kiezeloëliet Formation are probably caused by the presence of minor amounts of dolomite. Localized high (pyrite-) S-concentrations are not only found in the marine-estuarine Oosterhout and Tegelen Formations but also in the fluvatile Kiezeloëliet and Kedichem Formations, which indicates at least minor marine transgressions during their deposition.

Chapter 3.2 studies the change from a stable to an unstable heavy mineralogy in the composition of Rijn-derived sediments at the Pliocene-Pleistocene transition. This change has previously been attributed to a decrease in weathering intensity due to climatic cooling, and to a change in the Rijn sediment provenance from local to Alpine-derived. We studied the

geochemistry of several sections with Pliocene and Early Pleistocene Rijn deposits, and one section (BTAB) in more detail using clay mineralogical and micromorphological techniques to study the exact nature and the cause of this change, and associated changes in sedimentary setting. We found a general increase in Na_2O - contents at the local to Alpine provenance shift, which can be attributed to the Alpine source supplying fresh, sodic plagioclase-rich material instead of the local, strongly weathered sediments. There is a general trend of increasing $\text{K}_2\text{O}/\text{Al}_2\text{O}_3$ from the Pliocene to the Early Pleistocene that can be attributed to a similar decrease in degree of weathering. However, this trend is disturbed by the loss of K from clay minerals during post-depositional *in situ* weathering in organic-rich layers. In the Upper Pliocene BTAB section, we found a clear transition from kaolinite and high $\text{TiO}_2/\text{Al}_2\text{O}_3$ -ratios to smectite-rich material with lower $\text{TiO}_2/\text{Al}_2\text{O}_3$ that coincides with the local to Alpine provenance shift. However, Early Pleistocene sediments have $\text{TiO}_2/\text{Al}_2\text{O}_3$ -ratios that are similar to the ones before the transition so this effect is not consistent. Local high TiO_2 -anomalies, caused by preferential sorting and concentration of especially rutile in placer-like deposits occur in most Pliocene sections, but they are absent in the Upper Pliocene and Lower Pleistocene Alpine-derived deposits. Overall, the detrital geochemical variation in these deposits are primarily controlled by the source of the sediment, and hence the large-scale tectonic setting, whereas climatic control is limited.

The Pliocene organic-rich layers were originally formed in a fresh-water fluvial environment. Nevertheless they show high concentrations of S due the presence of abundant pyrite as a result of inundation by saline water during short-termed flooding events like spring tides or storm floods, after or alternating with one or more desiccation phases.

Chapter 4 focuses on the effects of specific diagenetic geochemical processes that cause enrichments or depletions of certain chemical elements:

Chapter 4.1 describes the formation of siderite (FeCO_3), which is often used as an indicator for the depositional environment of sediments, as it can only be formed under restricted geochemical conditions. By doing so, the possibility that siderite was formed later, under altered circumstances is often neglected. In this study, siderite in Early and Late Pleistocene deposits is investigated to establish whether it was formed syndepositional, or postdepositional under different circumstances. Within the Early Pleistocene Tegelen Formation, siderite is found as coatings around detrital dolomite grains, together with partially dissolved detrital calcite grains. Siderite also occurs as single nodules and homogeneously mixed through the groundmass. Siderite precipitation at the expense of calcite is proposed, which is likely to be an actual process as the current groundwater composition agrees well with the thermodynamics necessary for this process. Siderite formation in Late Pleistocene river fens is syndepositional and associated to both calcite and vivianite.

A comparison between these two settings shows that siderite may be an indicator for the environment during deposition, but the presence of siderite in sediments may also be the result of interaction with groundwater under diagenetically altered circumstances.

In chapter 4.2, we focus on the effects of multiple cycles of interchanging of fresh and saline water and oxic and reduced diagenetic environments that occur during the formation of low-gradient deltas of large river systems, driven by the glacial- to interglacial climatic cycle. Because

of the reactivity of organic matter, the geochemical characteristics of organic-rich sediments can be strongly affected by these changing diagenetic environments.

In the geochemical/sedimentary record of the Pliocene and Early Pleistocene Rijn-Maas delta, organic-rich layers display anomalous enrichments of trace elements, heavy metals and rare earth elements (REE). During marine highstands, high groundwater levels cause Fe-hydroxides to become reduced, thus releasing Fe and associated trace elements into the groundwater. At the same time, transgressions of saline water over organic surface layers and saline groundwater intrusions cause the formation of pyrite and other sulfides that may contain elevated levels of As and Mo and, depending on the Fe-source, Co, Ni, Pb and Zn. Associated with the pyrite-forming reduced environment, Y, REE, Cr, V and U are immobilized and accumulate. During lowstands, lower groundwater levels cause part of the sulfides to oxidize, except for those that are present in the organic layers, where they are protected from oxidation. Fe-oxides form, and trace elements like As, Co, Ni, Pb, Zn, Y and REE are incorporated, only to form a source for Fe and trace elements during the next reduced phase.

Chapter 5 describes the natural variation in heavy metal contents of subsurface sediments in the Southern Netherlands. The detrital heavy metal contents of these sediments show linear correlations with Al as a result of their joint occurrence in phyllosilicates. Anomalous enrichments occur as a result of the presence of glauconite (As, Cr, Ni, Pb, Zn), pyrite (As) or Fe-oxides (As, Ba, Ni, Zn), due to the interaction of organic-rich subsurface material with groundwater (Co, Ni, Zn) or as a result of anthropogenic pollution in topsoils (Cu, Pb, Zn). The contents of Al, Fe, K and S are well suited to determine background values, and to identify the cause for anomalous accumulations of heavy metals.

Chapter 6 describes the result of a geochemical mapping campaign in an Early Pleistocene fluvial formation (Kedichem) in the Netherlands. This is the first step towards a nation-wide geochemical database that can be used to meet the demand for information about the composition of subsurface sediments. We first determined the spatial extension and thickness of the sediment body. Subsequently, we used Fuzzy clustering techniques on approximately 2000 heavy-mineral counts from the NITG-TNO database to map the spatial extension of the Schelde, Rijn and Baltic sediment provenances within the formation.

Geochemical data was collected during a sampling campaign in which about 600 samples from the Kedichem formation were analyzed. We used factor analysis to determine the major factors that determine the geochemical composition. These factors include clay content, presence of carbonates, pyrites and Fe,Mn-hydroxides, sodic plagioclase and zircon, and organic-matter-related diagenetic processes. We tested which lithological data from the NITG-TNO boring database is correlated the geochemical composition and therefore can be used to make a geochemical prediction model. We found that the classes Sand, Clay + Gytja and Peat are significantly different and therefore can be used to predict the contents of Si, Ti, Al, Fe, Mn, Mg, Ca, Cr, Cu, Pb, V, Zn, Ba, Ga, Nb, Rb, Sr and Y. For the elements As, Ni, U and S, the classes Organic-poor Clay, Sand+Peat, Gytja+Organic-rich Clay are significantly different. For Na and K, a division can be made into Mica-rich Clay, Mica-poor Clay, Mica-rich Sand, Mica-poor Sand

and Peat + Gyttja. By classifying the lithological data from the NITG-TNO core description, we made a geochemical model to predict the geochemical composition in the Kedichem formation. We visualized this model by calculating and interpolating the average composition of 5 m horizontal slices of the Kedichem formation. The model performance is fairly good, although it has a tendency to underestimate extreme values.

The results of our study demonstrate that geochemical characterization of sediments can be performed by doing a large number of low-cost XRF analyses, supported with a limited amount of XRD-, ICP-MS, SEM and micromorphological analyses. The geochemical variation can be determined and the speciation and hence the reactivity and conditionally availability of harmful elements can be deduced. The geochemical methods employed in this study can not only be used to study sedimentation history and stratigraphy, but they can also yield important information about the composition and reactivity of subsurface sediments which can be used for ground water quality management and evaluation of underground activities.

Samenvatting

De Nederlandse ondergrond wordt meer en meer gebruikt voor allerlei menselijke activiteiten, waaronder de winning van drinkwater, grote infrastructurele projecten en in de toekomst mogelijk de opslag van (nucleair) afval en kooldioxyde. Om de schadelijke effecten van dergelijke activiteiten te kunnen beperken en de aquifers te behouden als bron van schoon drinkwater, is informatie nodig over de samenstelling van de ondergrond en wat menselijke activiteiten daarop voor effect kunnen hebben. Een belangrijk onderdeel van deze benodigde informatie is de geochemische samenstelling van de in de ondergrond aanwezige sedimenten. In dit proefschrift staan resultaten van het zogenaamde GEOBON-project, dat is opgezet om aan deze informatiebehoefte een bijdrage te leveren.

In het kader van het GEOBON-project werd de chemische samenstelling van de ondergrond bestudeerd door bemonstering en chemische analyse van boorkernen van de Rijks Geologische Dienst (RGD; tegenwoordig NITG-TNO). De gebruikte methoden staan kort aangegeven in hoofdstuk 2.

In hoofdstuk 3 staan de resultaten van twee regionale geochemische studies in Brabant en Limburg. Hieruit blijkt hoe de geochemische samenstelling van Mioceen, Pliocene en Onder-Pleistocene afzettingen in Zuid-Nederland wordt beïnvloed door factoren als de bron van het sediment, sortering, afzettingsmilieu, korrelgrootte, verwerking en nieuwvorming van mineralen.

Hoofdstuk 3.1 bevat de resultaten van een sediment-geochemische studie die is uitgevoerd op ongeconsolideerde Boven-Cenozoïsche sedimenten uit Brabant. Glauconietrijke afzettingen (Formatie van Breda) vertonen uitzonderlijk hoge K-gehalten en lage Ba/K ratio. Belangrijke veranderingen in de samenstelling van het sediment als gevolg van veranderingen in het Rijn systeem en verschuivingen in sediment herkomst tussen Rijn en Schelde zijn weergegeven in veranderingen in de korrelgrootte-afhankelijke variaties tussen Al-, Na- en K-gehalten. Zo vertonen Pleistocene Rijn sedimenten (Formatie van Tegelen) hogere Na-gehalten dan Pliocene Rijn sedimenten (Oosterhout en Kiezeloëliet Formaties) en Schelde sedimenten (Formatie van Kedichem), waarschijnlijk als gevolg van hogere gehalten aan natriumhoudende plagioklazen. Schelde sedimenten vertonen lage K/Al ratio's doordat de kleimineralen vooral uit smectiet bestaan en weinig mica's aanwezig zijn. Rijn sedimenten vertonen hoge K/Al verhoudingen door de hogere gehalten aan illiet en muscoviet.

De aanwezigheid van sideriet veroorzaakt hoge gehalten aan Fe in de Tegelen formatie in het oosten van het studiegebied. Verhoogde Mg-gehalten in de sideriet-houdende delen van de Tegelen formatie en in delen van de Oosterhout en Kiezeloëliet formaties worden waarschijnlijk veroorzaakt door de aanwezigheid van kleine hoeveelheden dolomiet. Plaatselijke verhoogde (pyriet-) zwavel concentraties komen niet alleen voor in de mariene en estuariene afzettingen van de Tegelen en Oosterhout formaties, maar ook in de fluviale Kedichem en Kiezeloëliet formaties, wat er op duidt dat er kleinschalige mariene transgressies hebben plaatsgevonden tijdens hun vorming.

Hoofdstuk 3.2 beschrijft het geochemische equivalent van de verandering van een stabiele naar een instabiele zware mineralen-associatie in Rijn sedimenten rond de overgang van het Pliocene naar het Pleistoceen. Deze verandering is in het verleden toegeschreven aan afnemende verwerking door afkoeling van het klimaat, en aan een verandering van het

brongebied de Rijn van lokaal naar Alpen op deze grens. Wij bestudeerden de geochemie van verschillende secties met Pliocene en Vroeg-Pleistocene afzettingen. Eén van deze secties, BTAB, bestudeerde we gedetailleerd met kleimineralogische en micromorfologische technieken om de oorzaak van deze verandering en de geassocieerde veranderingen in het afzettingsmilieu te bestuderen. We vonden dat de Na-gehalten in het algemeen toenemen bij de overgang van lokale naar Alpine sedimentbronnen, wat kan worden verklaard met het feit dat de Alpen vers, Na-plagioklaas-rijk materiaal leverden in plaats van het lokale sterk verweerde sediment. Er is een algemene trend van toenemende K/Al-ratio's van het Pliocéen naar het Pleistoceen, die kan worden toegeschreven aan een vergelijkbaar verschil in verweringsgraad. Deze trend wordt echter verstoord doordat bij *in situ* verwerking van kleimineralen in organisch-rijke lagen K verloren gaat. We vonden in de Boven-Pliocene BTAB-sectie een duidelijke overgang van kaoliniet-rijk materiaal met hoge Ti/Al ratio's naar smectiet-rijk materiaal met lage Ti/Al-ratio's. Deze overgang valt samen met de verandering van lokale naar Alpine mineralogie. Dit effect is echter niet consequent. Lokale Ti-anomalieën, veroorzaakt door het uitsorteren en concentreren van met name rutiel in placerachtige afzettingen komen voor in de meeste Pliocene afzettingen, maar ze zijn afwezig in de Boven-Pliocene en de Onder-Pleistocene afzettingen van Alpine herkomst. In het algemeen blijkt de detritische geochemische variatie in deze afzettingen vooral te worden bepaald door de herkomst van het sediment en de grootschalige tectonische setting, terwijl de invloed van het klimaat gering is.

De organische lagen in de Pliocene secties werden oorspronkelijk gevormd in een fluviatiel milieu. Desondanks vertonen ze toch hoge zwavel-concentraties door de aanwezigheid van grote hoeveelheden pyriet. Dit is veroorzaakt doordat door springvloeden en/of stormen het landoppervlak voor korte periodes werd geïnundeerd door sulfaat-houdend zee water. De aanwezigheid van sideriet in plaats van pyriet in de Onder-Pleistocene afzettingen reflecteert een algemene lange-termijn regressie, die gecorreleerd met een dalende zeespiegel aan het begin van de eerste ijstijden.

Hoofdstuk 4 richt zich op de effecten van specifieke diagenetische processen waardoor bepaalde chemische elementen aanrijken of uitspoelen.

Hoofdstuk 4.1 beschrijft de formatie van sideriet (FeCO_3). De aanwezigheid van sideriet is vaak gebruikt als indicator voor het afzettingsmilieu waarin sediment is afgezet, aangezien het alleen onder specifieke geochemische condities gevormd kan worden. De mogelijkheid dat sideriet is gevormd ná afzetting wordt vaak genegeerd. In dit hoofdstuk wordt de sideriet die voorkomt in Vroeg en Laat-Pleistocene afzettingen bestudeerd, om vast te stellen of het syndepositioneel werd gevormd, of later toen de geochemische omstandigheden waren veranderd. Sideriet komt in de Vroeg-Pleistocene Formatie van Tegelen voor als coatings rondom detritische dolomiet korrels, samen met deels opgeloste calciet. Sideriet komt ook voor als concreties en is soms homogeen gemengd door de grondmassa. Wij nemen aan dat de sideriet neerslaat ten koste van de kalk. Dit proces is waarschijnlijk nog steeds actief, aangezien de huidige grondwater samenstelling overeenkomt met de thermodynamica die voor dit proces nodig is. In Laat-Pleistocene rivier moerassen is de sideriet syndepositioneel gevormd, in associatie met kalk en vivianiet. Hieruit blijkt dat sideriet inderdaad een indicator kan zijn voor het afzettingsmilieu, maar dat siderietvorming na afzetting onder veranderde geochemische condities niet kan worden uitgesloten.

In hoofdstuk 4.2 richten wij ons op de effecten van opeenvolgende cycli van afwisselend zoet en zout water en van oxische en gereduceerde omstandigheden in

grootschalige rivierdelta's met lage gradiënten, die worden veroorzaakt door de glaciaal-interglaciaal-cycli. Als gevolg van de reactiviteit van organische stof kan de geochemische karakteristiek van organisch-rijke sedimenten sterk worden beïnvloed door dit soort veranderingen.

In de geochemie en sedimentologie van afzettingen van de Pliocene en Vroeg-Pleistocene Rijn-Maas delta vertonen organisch-rijke lagen aanrijkingen van sporenelementen, zware metalen en zeldzame aardmetalen (REE). In periodes met hoge zeespiegelstanden raken Fe(hydr)oxyden gereduceerd door verhoogde grondwaterstanden, waardoor Fe en geassocieerde sporenelementen vrijkomen in het grondwater. Tegelijkertijd veroorzaken overstromingen met zeewater over oppervlakkige organische lagen en zeewater-intrusies de vorming van pyriet en andere sulfiden, waarin As, Mo en, afhankelijk van de Fe-bron, Co, Ni, Pb, en Zn in hoge gehalten kunnen worden opgenomen. Geassocieerd met het gereduceerde milieu worden ook Y, REE, Cr, V en U geïmmobiliseerd, waardoor ze aanrijken. Tijdens lage zeespiegelstanden zorgen verlaagde grondwaterstanden ervoor dat een deel van de sulfiden oxydeert, behalve diegene die worden beschermd door het gereduceerde milieu in organische lagen. Fe-hydroxydes ontstaan, en sporenelementen als As, Co, Ni, Pb, Zn, Y en REE worden daarin opgenomen. Deze hydroxydes kunnen dan weer een bron voor Fe en sporenelementen vormen tijdens de volgende gereduceerde fase.

Hoofdstuk 5 beschrijft de natuurlijke variatie in zware metalen-gehalten van ondergrondse sedimenten in het zuiden van Nederland. Detritische zware metalen gehalten vertonen een lineaire correlatie met Al-gehalten als gevolg van het feit dat ze beiden voorkomen in phyllosilicaten. Aanrijkingen boven de detritische samenstelling komen voor als gevolg van de aanwezigheid van glauconiet (As, Cr, Ni, Pb, Zn), pyriet (As), Fe-oxydes (As, Ba, Ni, Zn), als gevolg van interactie van grondwater met organisch-rijke lagen (Co, Ni, Zn), of als gevolg van antropogene vervuiling in bovengronden (Cu, Pb, Zn). De gehalten aan Al, Fe, K en S kunnen worden gebruikt om de detritische achtergrondgehalten te bepalen, en om de oorzaken van aanrijkingen vast te stellen.

Hoofdstuk 6 beschrijft de resultaten van een geochemische kartering in een Vroeg-Pleistocene fluviatile formatie (Kedichem) in Nederland. Dit is een eerste stap naar een landelijke geochemische ruimtelijke database die kan worden gebruikt als bron van informatie over de samenstelling van de ondergrond. Eerst bepaalden we het ruimtelijk voorkomen en de dikte van het sedimentlichaam. Vervolgens gebruikten we fuzzy clustering op ongeveer 2000 zware-mineraal-tellingen van de NITG-TNO database om de ruimtelijke verdeling van sediment uit de Schelde, Rijn en uit het Baltische riviersysteem binnen de Kedichem formatie te bepalen.

Geochemische data werd verzameld gedurende een campagne waarin ongeveer 600 monsters uit de formatie van Kedichem werden geanalyseerd. We gebruikten factoranalyse om de belangrijkste bronnen van geochemische variatie te bepalen. Deze factoren bleken kleigehalte, aanwezigheid van carbonaten, pyriet, Fe en Mn (hydr)oxydes, Na-plagioklaas en zirkoon en organische stof gerelateerde diagenetische processen te zijn. We testten welke data uit de boringen-database van NITG-TNO gecorreleerd is met de geochemische compositie, en dus gebruikt kan worden om een voorspellend geochemisch model te maken. We vonden dat een indeling in Zand, Klei + Gytta en Veen significant verschillende klassen oplevert, en dus gebruikt kan worden voor de voorspelling van de gehalten aan Si, Ti, Al, Fe, Mn, Mg, Ca, Cr,

Cu, Pb, V, Zn, Ba, Ga, Nb, Rb, Sr en Y. Voor de elementen As, Ni, U en S zijn de klassen Organisch-arme klei, Zand en Organisch-rijke klei + Gyttja + Veen significant verschillend. Voor Na en K kan een verdeling gemaakt worden in Mica-rijke klei, Mica-arme klei, Mica-rijk zand, Mica-arm zand en Veen + Gyttja. Wij maakten een geochemisch model voor het voorspellen van de geochemische samenstelling van de Kedichem formatie door de lithologische data uit het NITG-TNO boringen-archief te classificeren volgens deze indeling. We visualiseerden dit model door de gemiddelde samenstelling te berekenen en te interpoleren voor horizontale plakken van 5 meter dikte van de Kedichem formatie. Onze ervaring is, dat het model een redelijke voorspelling geeft over de chemische samenstelling van de ondergrond, maar dat het de neiging heeft extreme waardes te onderschatten.

Literature Cited

- Aller, R. and Michalopoulos, P., 1996, Controls on Fe diagenesis and authigenic mineral formation in terrigenous, nearshore environments, *in*, Bottrell, Proceedings of the 4th international symposium in the geochemistry of the earth's surface, 22-28 July 1996, University of Leeds, p. 15-18
- Appelo, C.A.J. and Postma, D., 1994, Geochemistry, groundwater and pollution, Rotterdam, A.A. Balkema, 536 p.
- Argast, S. and Donnelley, Th.W., 1987, The Chemical Discrimination of Clastic Sedimentary Components: *Jour. Sed. Petrology* 57: 813-823
- Barnhisel, R.I. and Bertsch, P.M., 1989, Chlorites and Hydroxy-Interlayered Vermiculite and Smectite, *in*, J.B. Dixon and S.B. Weed, Minerals in Soil Environments 2nd ed., SSSA, Madison, USA, p.729-788
- Behrens, E.W. and Land, L.S., 1972, Subtidal Holocene dolomite, Baffin Bay, Texas: *Jour. Sed. Petr.* 42: 155-161.
- Berner, R.A., 1971, Principles of Chemical Sedimentology, New York, McGraw-Hill, 240 p.
- Bestland, E.A., Retallack, G.J. and Swisher III, C.C., 1997, Stepwise climatic change recorded in Eocene-Oligocene paleosol sequences from Central Oregon, *Journ. Geol.* 105: 153-172
- Bhatia, M.R., 1983, Plate tectonics and geochemical composition of sandstones: *Jour. Geol.*, 91: 611-627
- Boenigk, W., 1970, Zur Kenntnis des Altquartärs bei Brüggem, Köln, Geologisches Institutes der Universität Köln, 143 p.
- Bonatti, E., Fisher, D.E., Joensuu, O. and Rydell, H.S., 1971, Postdepositional mobility of some transition elements, phosphorus, uranium and thorium in deep sea sediments, *Geoch. Cosmoch. Acta* 35: 189-201
- Brewer, R., 1964, Fabric and mineral analysis of soils, J. Wiley, New York, 470 p.
- Brinkman, K., 1976, Zur Geochemie und Genese der Eisensulfide in jungtertiären Sedimenten der Niederrheinischen Bucht, Universität Köln (PhD-thesis), 134 p.
- Broers, H.P., Hoogendoorn, J.H., and Houtman, H., 1992, Opbouw van het geohydrologische lagenmodel van Regis/digitale grondwaterkaart, TNO-GG, rapport OS 92-01-A, Delft, 76 p.

- Bullock, P., Federoff, N., Jongerius, A., Stoops, G. and Tursina, T., 1985, Handbook for soil thin section description, Wayne Res. Pub. Albrighton, England, 152 p.
- Burger, A.W., 1997, Sedimentpetrologisch onderzoek aan twee boringen ten zuiden van Tegelen, Rapport NITG-TNO 97-70-C, SP-rapport 1033, 11 p.
- Buurman, P., 1972, Paleopedology and stratigraphy on the Condrusian peneplain (Belgium) (PhD thesis), Wageningen, Pudoc, 67 p.
- Casagrande, D. J., 1987, Sulphur in peat and coal, *in*, Scott, A.C. (ed.) Coal and coal-bearing strata: Recent advances, Geological Society Special Publication 32: 87-105
- Cohen, A.D., Spackman, W. and Dolsen, P., 1984, Occurrence and distribution of sulfur in peat-forming environments of southern Florida, *Int. Journ. of Coal Geol.* 4: 73-96
- Colley, S., Thomson, J., Wilson, T.R.S. and Higgs, N.C., 1984, Post-depositional migration of elements during diagenesis in brown clay and turbidite sequences in the North East Atlantic, *Geoch. Cosmoch. Acta* 48: 1223-1235
- Cox, R., Lowe, D.R., and Cullers, R.L., 1995, The influence of sediment recycling on evolution of mudrock chemistry in the south-western United States: *Geoch. Cosmoch. Acta* 59: 2919-2940
- Curtis, C.D., 1967, Diagenetic iron minerals in some Carboniferous sediments, *Geoch. Cosmoch. Acta* 31: 2109-2123
- Davis, J.C., 1986, Statistics and data analysis in geology (2nd edition), John Wiley and Sons, New York, 646 p.
- De Vos, W., Ebbing, J., Hindel, R., Schalich, J., Swennen, R. and Van Keer, I., 1996, Geochemical mapping based on overbank sediments in the heavily industrialised border area of Belgium, Germany and the Netherlands, *Journ. Geoch. Expl.* 56: 91-104
- Deer, W.A., Howie, R.A., and Zussman J., 1992, An introduction to the rock-forming minerals 2nd edition: Harlow, Longman, 696 p.
- Dellwig, O., Brumsack, H.J. and Böttcher, M. 1996, Geochemical characterisation of a Holocene sedimentary sequence from the NW German coastal area, *in*, Bottrell, Proceedings of the 4th international symposium in the geochemistry of the earth's surface, 22-28 July, 1996, University of Leeds, p. 43-46
- Edelman, Th., 1984, Achtergrondgehalten van stoffen in de bodem - Reeks Bodembescherming 34, Staatsuitgeverij, (Den Haag)

Einsele, 1992, *Sedimentary basins*, Springer-Verlag, Berlin, 628 p.

Fitzpatrick, E.A., 1970, A technique for the preparation of large thin sections of soils and consolidated materials, *in*, D.A. Osmond and P.Bullock (eds) *Micromorphological techniques and applications*, Techn. Monograph 2. Soil Survey of England and Wales, Rothamstead Exp. Stu. Harpenden U.K.

Fitzpatrick, E.A., 1980, *Micromorphology of soils*, Chapman and Hall, London, 433 p.

Frapporti, G., 1994, *Geochemical and statistical interpretation of the Dutch national ground water quality monitoring network (PhD-thesis)*, Rijks Universiteit Utrecht, 121 p.

Geluk, M.C., Duin, E.J.Th., Duser, M., Rijkers, R.H.B., Van den Berg, M.W. and Van Rooijen, P., 1994, Stratigraphy and tectonics of the Roer Valley Graben, *Geologie en Mijnbouw* 73: 129-141

German, C.R., Holliday, B.P. and Elderfield, H., 1991, Redox cycling of rare earth elements in the suboxic zone of the Black Sea, *Geoch. Cosmoch. Acta* 55: 3553-3558

Gibbard, P.L., 1988, The history of the great Northwest European rivers during the past three million years: *Phil. Trans. R. Soc. Lond. B* 318: 559-602

Haese, R.R, Wallman, K, Dahmke, A., Kretzman, U., Müller, P.J. and Schulz, H.D., 1997, Iron species determination to investigate early diagenetic reactivity in marine sediments, *Geoch. Cosmoch. Acta* 61: 63-72

Hakstege, A.L., Kroonenberg, S.B. and Van Wijck, H, 1993, Geochemistry of Holocene clays of the Rhine and Meuse rivers in the central-eastern Netherlands: *Geologie en Mijnbouw* 71: 301-315

Hillier, S., 1995, *Erosion, Sedimentation and Sedimentary Origin of Clays*, *in* ,Velde, B, *Origin and Mineralogy of Clays*, Springer, Berlin, p. 162-219

Hindel, R., Schalich J., De Vos, W., Ebbing, J., Swennen, R. and Van Keer, I., , 1996, Vertical distribution of elements in overbank sediment profiles from Belgium, Germany and the Netherlands, *Journ. Geoch. Expl.* 56: 105-122

Hoselmann, C., 1996, Der Hauptterrassen-komplex am unteren Mittelrhein: *Z. dt. geol. Ges.* 147/4, Stuttgart, p. 481-497.

Huerta-Diaz, M.A. and Morse, J.W., 1992, Pyritization of trace metals in anoxic marine sediments. *Geoch. Cosmoch. Acta* 56: 2681-2702

Huisman, D.J., Van Os, B.J.H., and Klaver, G.Th., 1996, The geochemical record of climate-induced changes in weathering intensity during the Pliocene and Early Pleistocene, *in* Bottrell, S.H. (ed.), Proceedings of the fourth international symposium on the geochemistry of the earth's surface 22-28 July, 1996, University of Leeds, Leeds p.194 -196

Hutton, J.T., Twidale, C.R. and Milnes, A.R., 1978, Characteristics and origin of some Australian silcretes, *in*, T.L. Smith (ed.), Silcrete in Australia, Dept. of Geography, University of New England, 304 p.

Johnsson, M.J., 1993, The system controlling the composition of clastic sediments, *in*, Johnson, M.J. and A. Basu (eds.), Processes controlling the composition of clastic sediments: Boulder, Colorado, Geological Society of America Special Paper 284 p.1-19

Kasse, C., 1988, Early Pleistocene tidal and fluvial environments in the Southern Netherlands and Northern Belgium, Amsterdam, Free University Press 190 p.

Katsumoto, R., and Iijima, A., 1981, Origin and diagenetic evolution of Ca-Mg-Fe carbonates in some coalfields of Japan, *Sedimentology* 28: 239-259

Klosterman, J., 1992, Das Quartär der Niederrheinischen Bucht, Geologisches Landseamt Nordrhein-Westfalen, Krefeld, 200 p.

Koons, R.D., Helmke, P.A. and Jackson, M.L., 1980, Association of trace metals with iron oxides during rock weathering, *Soil Sc. Soc. Am. J.* 44: 155-159

Koppi, A.J., Edis, R., Field, D.J., Geering, H.R., Klessa, D.A. and Cockayne, D.J.H., 1996, Rare earth element trends and cerium-uranium-manganese associations in weathered rock from Koongarra, Northern Territory, Australia, *Geoch. Cosmoch. Acta* 60: 1695-1707

Kroonenberg, S.B., 1992, Effect of provenance, sorting and weathering on the geochemistry of fluvial sands from different tectonic and climatic environments, *in*, Proceedings of the 29th International Geological Congress (Kyoto, Japan) Part A, p. 69-81

Kumar, N., Anderson, R.F. and Biscaye, P.E., 1996, Remineralization of particulate authigenic trace metals in the Middle Atlantic Bight: Implications for proxies of export production, *Geoch et Cosmoch Acta* 60: 3383-3397

Langmuir, D., 1978, Uranium solution-mineral equilibria at low temperatures with applications to sedimentary ore deposits, *Geoch. Cosmoch. Acta* 42: 547-569

Leckie, A.D., Chaitanya, S., Fariborz, G. and Wall, J.H., 1990, Organic-rich, radioactive marine shale: a case study of a shallow-water condensed section, Cretaceous Shaftsbury formation, Alberta, Canada, *Jour. Sed. Petr.* 60: 101-117

- Middelburg, J.B.M., 1990, Early diagenesis and authigenic mineral formation in anoxic sediments of Kau Bay, Indonesia, Rijks Universiteit Utrecht, 177 p. (PhD-thesis)
- Middelburg, J.J., van der Nat, J.F.W.A. and Van Os, B.J.H., 1997, Oxidation in the rhizosphere of macrophytes: consequences for elemental cycles (*in prep.*)
- Miedema, R., 1987, Soil formation, microstructure and physical behaviour of Late Weichselien and Holocene Rhine deposits in the Netherlands, Wageningen Agricultural University, 339 p. (PhD-thesis)
- Milnes, A.R. and Fitzpatrick, R.W., 1989, Titanium and Zirconium minerals, *in*, J.B. Dixon and S.B. Weed, Minerals in Soil Environments 2nd ed., SSSA, Madison, USA, p. 1131-1205
- Morey, G.B. and Setterholm, D.R., 1997, Rare earth elements in weathering profiles and sediments of Minnesota: implications for provenance studies, *Journ. Sed. Res.* 67: 105-115
- Moura, M.L. and Kroonenberg, S.B., 1990, Geochemistry of fluvial and eolian sediments in the south-eastern Netherlands: *Geologie en Mijnbouw* 69: 359-373
- Mozley, P.S., 1989, Relation between depositional environment and the elemental composition of early diagenetic siderite: *Geology*, 17: 704-706.
- Mozley, P.S. and Carothers, W.W., 1992, Elemental and isotopic composition of siderite in the Kuparuk Formation, Alaska: Effect of microbial activity and water/sediment interaction on early pore-water chemistry: *Jour. Sed. Petr.* 62: 681-692.
- Nederlands Normalisatie Instituut, 1989, Geotechniek Classificatie van onverharde grondmonsters, NNI, NEN 5105, 23 p.
- Nesbitt, H.W., Fedo, C.M. and Young, G.M., 1997, Quartz and feldspar stability, steady and non-steady state weathering, and petrogenesis of siliclastic sands and muds, *Journ. Geol.* 105: 173-191
- Nesbitt, H.W., and Young, G.M., 1996, Petrogenesis of sediments in the absence of chemical weathering: effects of abrasion and sorting on bulk composition and mineralogy, *Sedimentology* 43: 341-358
- Nesbitt, H.W., Young, G.M., McLennan, S.M. and Keays, R.R., 1996, Effects of chemical weathering and sorting on the petrogenesis of siliclastic sediments, with implications for provenance studies, *Journ. Geol.* 104: 525-542
- Newman, A.C.D. and Brown, G., 1987, The chemical constitution of clays, *in*, Newman, A.C.D. (ed), Chemistry of clays and clay minerals, Harlow, Longman: 1-129

Nicaise, D., De Putter, Th., André, L., Jedwab, J. and Dupuis, C., 1996, Néof ormation de phosphates nanométriques de terres rares en altération acide de basse température: implications pour le piégeage des terres rares, de l'uranium et du thorium, C.R. Acad. Sci. Paris. t. 323, série IIa: 113-120

Nieuwenhuize, J., Maas, Y.E.M., and Middelburg, J.J., 1994, Rapid analysis of organic carbon and nitrogen in particulate materials, *Marine Chemistry*, 45: 217-224

Nolte, A., 1996, Hydrogeochemie van de Centrale Roerdal Slenk en het optreden van diepe kwel, TNO Rapport GG 96-90 (B), Delft, NITG-TNO, 105 p.

Poppe, L.J., Commeau, J.A., and Valentine, P.C., 1991, Mineralogy of the silt fraction in surficial sediments from the outer continental shelf off Southeastern New England, *Jour. Sed. Petr* 61: 54-64

Porrenga, D.H., 1967, Clay mineralogy and geochemistry of recent marine sediments in tropical areas, (PhD thesis) University of Amsterdam 145 p.

Postma, D., 1977, The occurrence and chemical composition of recent Fe-rich mixed carbonates in a river bog: *Jour. Sed. Petr.* 47: 1089-1098.

Postma, D., 1982, Pyrite and siderite formation in brackish and freshwater swamp sediment: *Am. Journ. Sci.*, 282: 1151-1183

Pruissen, F.G.M. and Zuurdeeg, B.W., 1988, Hoge metaalgehalten in ijzeroerknollen in de Nederlandse bodem, *Milieutechniek* 3: 84-91

Pye, K., Dickson, J.A.D., Schavion, N., Coleman, M.L. and Cox, M., 1990, Formation of siderite-Mg-calcite-iron sulphide concretions in intertidal marsh and sandflat sediments, north Norfolk, England: *Sedimentology* 37: 325-343.

Raiswell, R. and Plant, J., 1980, The incorporation of trace elements into pyrite during diagenesis of black shales, Yorkshire, England, *Econ. Geol.* 75: 684-699

Rajan, S., Mackenzie, F.T. and Glenn, C.R., 1996, A thermodynamic model for water column precipitation of siderite in the Plio-Pleistocene Black Sea: *Am. Journ. Sci.* 296: 506-548.

Rasmussen, B., 1996, Early-diagenetic REE-phosphate minerals (Florencite, Gorceixite, Crandallite, and Xenotime) in marine sandstones: a major sink for oceanic phosphorus, *Am. Journ. of Sci.* 296: 601-632

Rasmussen, B. and Glover, J.E., 1994, Diagenesis of low-mobility elements (Ti, REEs, Th) and solid bitumen envelopes in permian Kennedy Group sandstone, Western Australia, *Journ. Sed. Res.* 64: 572-583

Righi, D. and Meunier, A., 1995, Origin of Clays by Rock Weathering and Soil Formation, *in*, Velde, B, Origin and Mineralogy of Clays, Springer, Berlin, p. 43-157

Roser, B.P. and Korsch, R.J., 1986, Determination of tectonic setting of sandstone-mudstone suites using SiO₂ content and K₂O/Na₂O ratio: *Jour. Geol.* 94: 635-650

Saager, P.M., 1996, Onderzoek naar de bedreiging van waterwinputten van de WNWB door diffuse verontreiniging, Grontmij, De Bilt, 78p.

Shaw, T.J., Gieskes, J.M. and Jahnke, R.A., 1990, Early diagenesis in differing depositional environments: The response of transition metals in pore water, *Geoch. Cosmoch. Acta* 54: 1233-1246

Stritzke, R., 1997, Ergebnis der pollenanalytischer Untersuchung der Kernbohrung KB 1/92 Schalbruch, TK25, Blatt 4901 Selfkant, Internal report GLANW (Geol. Survey Nordrhein-Westfalen) Krefeld, Germany, 3p.

Tebbens, L.A., Kroonenberg, S.B. and Van den Berg, M.W., 1995, Compositional variation of detrital garnets in Quaternary Rhine, Meuse and Baltic River sediments in the Netherlands, *Geologie en Mijnbouw* 74: 213-224

Tebbens, L.A., Veldkamp, A. and Kroonenberg, S.B., 1996, The onset of post-glacial soil formation recorded in late Weichselian and Early Holocene Meuse river sediments, *in* Bottrell, S.H. (ed.), Proceedings of the fourth international symposium on the geochemistry of the earth's surface 22-28 July, 1996, University of Leeds, Leeds p. 225 - 228

Tebbens, L.A., Veldkamp, A., and Kroonenberg, S.B., 1997, Bulk geochemistry of fluvial overbank sediments as a paleoclimatic indicator: the Late Weichselian and Early Holocene Meuse river sediments (the Netherlands), (*submitted*)

Van Andel, Tj.H., 1950, Provenance, transport and deposition of Rhine sediments (PhD-thesis), Veenman, Wageningen, 129 p.

Van Andel, Tj.H., 1958, A defense of the term Alterite (Discussion), *Journ. Sed. Petr.* 28: 234-235

Van Baren, F.A., 1934, Het voorkomen en de betekenis van kali-houdende mineralen in Nederlandse gronden (PhD thesis), Wageningen, Veenman, 118 p.

- Van den Berg, M.W., 1996, Fluvial sequences of the Maas (PhD thesis), University Wageningen 181 p.
- Van den Berg, M.W. and Veldkamp, A., 1993, Three-dimensional modelling of Quaternary fluvial dynamics in a climo-tectonic dependent system. A case study of the Maas record (Maastricht, The Netherlands), *Global and Planetary Change* 8: 203-218
- Van Os, B.J.H., Huisman, D.J., Klaver, G.Th., Van den Berg, M.W., and Westerhoff, W.E., 1996, Climate induced geochemical variations in Dutch overbank deposits during the Lower Pleistocene and Pliocene, *Journal of Conference Abstracts* 1: 635
- Van Santvoort, P.J.M. and De Lange, G.J., 1996, The process of oxidation of sapropels in eastern Mediterranean sediments, and its implications for paleoclimatic interpretations, *in*, *Proceedings 3e Nederlands Aardwetenschappelijk Congres*, 2/3 May 1996, Veldhoven
- Van Staalduin, 1979, Toelichting bij de geologische kaart van Nederland 1: 50.000, blad Rotterdam West (37W), Rijks Geologische Dienst, Haarlem, 140 p.
- Veldkamp, A. and Kroonenberg, S.B., 1993, Application of bulk sand geochemistry in mineral exploration and Quaternary research: a methodological study of the Allier and Dore terrace sand, Limagne rift valley, France, *Appl. Geoch.* 8: 177-187
- Vriend, S.P., Van Gaans, P.F.M., Middelburg, J. and Nijs, A., 1988, The application of fuzzy c-means cluster analysis and non-linear mapping to geochemical datasets: examples from Portugal, *Appl. Geoch.* 3: 213-224
- Walther, H.W. and Zitzmann, A., 1981, Geologische karte der Bundesrepublik Deutschland und benachbarter gebiete 1:1.000.000, Bundesanstalt für Bodenforschung, Hannover
- Weijers, J.P., 1995, Standaard Boor Beschrijvingsmethode, Rijks Geologische Dienst rapport GB2463, Haarlem, 76 p.
- Wefels, U., 1995, Schwermineralanalysen aus der Bohrung KB 1/92 Schallbruch, TK25:4901 Selfkant, Internal report GLANW (Geol. Survey Nordrhein-Westfalen) Krefeld, Germany, 8p.
- Westerhoff, W., and Cleveringa, P., 1996, Excursion Guide to the Upper Pliocene and Lower Pleistocene deposits in the Dutch-German border area near Tegelen and Reuver, INQUA-SEQS symposium 16-21 June 1996 Kerkrade, The Netherlands
- Wright, V.P., Vanstone, S.D. and Marshall, J.D., 1997, Contrasting flooding histories of Mississippian carbonate platforms revealed by marine alteration effects in paleosols, *Sedimentology* 44: 825-842

Zagwijn, W.H., 1960, Aspects of the Pliocene and Early Pleistocene vegetation in the Netherlands: (PhD thesis) Leiden, Mededelingen Geologische Stichting Serie C-III-1 Vol. 6, 78 p.

Zagwijn, W.H., 1989, The Netherlands during the Tertiary and the Quaternary: a case history of coastal lowland evolution: *Geologie en Mijnbouw* 68: 107-120

Zagwijn, W.H. and Doppert, J.W.C., 1978, Upper Cenozoic of the southern North Sea Basin: paleoclimatic and paleogeographic evolution: *Geologie en Mijnbouw* 57: 577-588

Zagwijn, W.H. and Van Staaldouin, C.J., 1975, Toelichting bij geologische overzichtskarten van Nederland, Haarlem, Geological Survey of the Netherlands, 134 p.

Curriculum Vitae

Dirk Johannes Huisman werd op 2 december 1967 in Wageningen geboren. Van 1979 tot 1986 volgde hij de ongedeelde VWO-opleiding aan het Christelijk Streek Lyceum in Ede. In 1987 begon hij aan de studie Bodemkunde aan de Landbouwniversiteit in Wageningen. Hij studeerde af in 1993 met de afstudeervakken Bodeminventarisatie en Landevaluatie, Geologie en Mineralogie en Geografische Informatie Systemen. Direct na zijn afstuderen begon hij als Assistent in Opleiding (AIO) bij de vakgroep Bodemkunde en Geologie te werken aan het GEOBON-project. Dit proefschrift is een weergave van de resultaten van dit werk. Sinds januari 1998 werkt hij bij het NITG-TNO (voorheen de Rijks Geologische Dienst) aan het toepassen van geochemische en mineralogische onderzoekstechnieken voor de geologische kartering van Nederland.

ERRATUM

**GEOCHEMICAL CHARACTERIZATION OF SUBSURFACE
SEDIMENTS IN THE NETHERLANDS**

D.J. HUISMAN

ISBN 90-54858613